

6

LEVEL II

14 B S
NORDA 31

11

Environmental Report of the Northwest Pacific for the Marine Seismic System (MSS).

AD A099820

10 James A./Green
Peter/Fleischer

Sea Floor Division
Ocean Science and Technology Laboratory

11 Dec [REDACTED] 80

12 279

DTIC
ELECTE
S JUN 08 1981
D
E

9 FILE COPY

Rept for
1 Dec 78 - 31 Sep 80



15 WARPA Order-3693

DISTRIBUTION STATEMENT A
Approved for public release
Distribution Unlimited

Naval Ocean Research and Development Activity

NSTL Station, Mississippi 39529

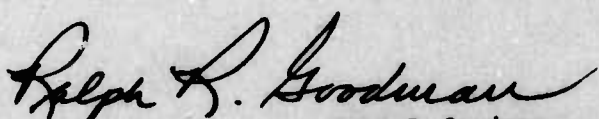
392 773

81 6 08 001

mt

Foreword

This report, commissioned by Defense Applied Research Projects Agency, Nuclear Monitoring Research Office, supplies environmental data compilations of the Northwest Pacific Ocean for reference and selection of potential sites for installation of the Marine Seismic System (MSS). The report is intended to aid scientists and engineers working on various aspects of the MSS and to address possible environmental questions which might arise.



Ralph R. Goodman
Technical Director
NORDA

A.R.P.A. Order Number 3693
Sea Floor Division, Code 360
Novel Ocean Research and Development Activity, NSTL Station, MS 39529
1 December 1978 to 31 September 1980
Principal Investigator: James A. Green (601-688-4620)
Northwest Pacific Environment Report for the Marine Seismic System

DISCLAIMER NOTICE

THIS DOCUMENT IS THE BEST
QUALITY AVAILABLE.

COPY FURNISHED CONTAINED
A SIGNIFICANT NUMBER OF
PAGES WHICH DO NOT
REPRODUCE LEGIBLY.

Executive Summary

This report presents data compilations to aid in planning and site selection for the Marine Seismic System (MSS). Data are compiled for two geographic areas: the Northwest Pacific (40° - 56° N, 145° - 170° E) and the Kuril-Kamchatka earthquake region. Included for the Northwest Pacific are cultural, meteorological, oceanographic, geological, geophysical and seismological data to define the environment in which the potential MSS will operate. Kuril-Kamchatka earthquake zone data consist of seismic velocity structure of the crust and upper mantle and earthquake hypocenters.

Northwest Pacific cultural data (political geography and ship traffic) favor MSS sites in areas of the east central Northwest Pacific. The 200 mile limit from Soviet territory forms a northwestern boundary. Merchant shipping and fishing density are lowest toward the northeast.

Severest meteorological and oceanographic conditions exist during winter and are concentrated in the northern areas. Current speeds are probably greatest in the eastward-flowing Kuroshio current to the south of the Northwest Pacific and in the southwestward-flowing Kamchatka current to the northwest. On the basis of meteorology and oceanography, potential MSS sites should be located as far south as possible without being in the Kuroshio current.

The Northwest Pacific seafloor is a province of abyssal hills bordered on the west by the Kuril-Kamchatka Trench and on the east by the Emperor Seamounts. Unconsolidated sediments in the area are generally post-Oligocene and vary from 0-600 m in thickness. These sediments are primarily siliceous clays interspersed with ash

layers and characterized by low rigidity. Beneath the unconsolidated sediments, a smooth acoustic basement is probably composed of cherty deposits in southern Northwest Pacific areas, and of secondary volcanics in eastern areas. Acoustic basement may be true oceanic basement where seamounts outcrop or in areas where the basement is rough.

The Kuril-Kamchatka earthquake region has complex geology. Seismic velocity structure, heat flow, and gravity all vary considerably. Earthquakes generally decrease in activity and deepen to the northwest; however, this trend is marked by local exceptions. For example, earthquakes are absent under the Kuril Basin; deepest earthquakes (greater than 300 km) are shallower in the southern region near Sakhalin than in the north under the Sea of Okhotsk; and shallow earthquakes are densest east of the Southern Kurils.

Two MSS site areas are proposed primarily for their advantageous local geology. Site area 1 is located east of the Southern Kurils. This location is favorable for most environmental parameters except ship traffic, fishing and major current speeds, all of which create ambient acoustic noise. Site area 2 is located centrally opposite the Kuril-Kamchatka earthquake region. Major environmental problems at this site consist of harsher weather conditions than at site area 1.

Both site areas fall into a seismic "shadow zone" as evaluated by Hart et al. (1980). This concurrence could require major revision in site selection. Three additional sites (3-5) were designated outside the "shadow zone", but the authors feel that these sites are inferior to sites 1 and 2.

Acknowledgements

The authors wish to thank those persons who performed specific tasks leading to the completion of this report. Marion Litchlier (CSC), Steve Madosik (NORDA) and Lou Hemler (NORDA) processed much of the geophysical data. Renee Edman (NORDA) drew most of the maps and illustrations. Linda McRaney (NORDA) edited the text and Vicki Spiers (NORDA) completed the word processing.

The authors also acknowledge the assistance of those contributing both ideas and data. Valuable advice was given by T. Kinder (NORDA), J. A. Ballard (NORDA), W. Ludwig (LDGO), P. Lonsdale (SIO), D. Scholl (USGS), G. Greene (USGS), A. Lowrie (NAVOCEANO), S. Trowell (NORDA), D. Handschumacher (NORDA), R. Jacobson (NORDA) and G. L. Maynard (NORDA). Particulary helpful in data gathering were B. Keville (NAVOCEANO), S. Smith (SIO), and T. Chase (USGS).

Accession For	
NTIS GRA&I	<input checked="" type="checkbox"/>
DTIC TAB	<input type="checkbox"/>
Unannounced	<input type="checkbox"/>
Justification	
By	
Distribution/	
Availability Codes	
Dist	Avail and/or Special
A	

Contents

LIST OF ILLUSTRATIONS	v	C. Surface Sediments	8
LIST OF TABLES	vi	1. Grain Size of Sediments	9
LIST OF MAPS	vi	2. Clay Minerals	10
I. INTRODUCTION	1	3. Coarse Fraction	10
II. CULTURAL FEATURES	1	D. DSDP Cores	10
A. Political Geography	1	1. Time Correlation	11
B. Ship Traffic	1	2. Sedimentation Rates	11
1. Merchant Ships	1	3. Physical Properties	12
2. Fishing Ships	1	E. Acoustic Stratigraphy	12
3. Composite Traffic	2	1. Transparent Layer	13
III. METEOROLOGY AND OCEANOGRAPHY	2	2. Sediment Thickness Map	13
A. Storms	2	3. Acoustic Basement	14
B. Winds	2	4. Basement Roughness Map	15
C. Icing	2	5. Structure Contour Map of the Acoustic Basement	15
D. Wave Heights	3	6. Representative Seismic Reflection Profiles	15
E. Surface Water Temperature	3	F. Geologic History	16
F. Surface Currents	3	1. Magnetics	16
G. Current Speeds	3	2. Plate Rotations	17
H. Sound Speed	4	3. Sedimentary History	17
I. Biological Fouling	4	G. Seismic Activity	18
IV. GEOLOGY AND GEOPHYSICS	4	1. Seismic Studies	18
A. Regional Setting	5	2. Earthquake Epicenters	19
1. Kuril-Kamchatka Earthquake Region	5	H. Deep Seismic Velocity Structure	20
2. Western Aleutian Earthquake Region	5	1. Deep Structure Beneath and East of the Focal Zone	20
3. Emperor Seamounts	5	2. Velocities in the Focal Zone	21
4. Hokkaido Rise	6	3. Velocities West of and Above the Focal Zone	22
5. Hokkaido Trough	6	I. Gravity and Heat Flow	23
6. Basin Between Southern Hokkaido Rise and Shatsky Rise	7	V. DISCUSSION AND SITE SELECTION	23
7. Shatsky Rise	7	VI. RECOMMENDATIONS	25
8. Provinces Adjacent to the Emperor Seamounts	7		
B. Bottom Roughness	8		

VII. REFERENCES	25
Bibliography I	30
Bibliography II	40

Illustrations, Tables, and Maps

Illustrations

Figure 1. North Pacific base map	59
Figure 2. Northwest Pacific base map 1	61
Figure 3. Merchant shipping density	63
Figure 4. Fishing density	65
Figure 5. Surface currents in winter	67
Figure 6. Surface currents in summer	69
Figure 7. Composite fishing and shipping density	71
Figure 8. Storms	73
Figure 9. Winds	75
Figure 10. Sea surface air temperatures below 0°C	77
Figure 11. Sea surface air temperatures below -8°C	79
Figure 12. Greatest waves	81
Figure 13. Surface water temperature (February) and annual variation in temperature	83
Figure 14. Depth and value of the February temperature maximum	85
Figure 15. Surface current speed distribution	87
Figure 16. Histogram of surface current speeds	89
Figure 17. Current speed model	91

Figure 18. Index for sound speed profiles	93
Figure 19. Sound speed profiles	95
Figure 20. February sound channel depth	97
Figure 21. August sound channel depth	99
Figure 22. Physiographic province map	101
Figure 23. Index to continuous seismic reflection profiles	103
Figure 24. Continuous seismic reflection profiles AA', BB', CC'	105
Figure 25. Continuous seismic reflection profiles DD', EE', FF', GG', HH'	107
Figure 26. Continuous seismic reflection profiles II', JJ'	109
Figure 27. Surface sediment size and type	111
Figure 28. Surface sediment type, components of Figure 23	113
Figure 29. Core index	115
Figure 30. Time columns for cored sediments and geological events	117
Figure 31. Sediment columns for retrieved cores	119
Figure 32. Summary of DSDP Site 303	121
Figure 33. Summary of DSDP Site 304	123

Figure 34. Summary of DSDP Site 192	125	Figure 52. Thickness of the upper sedimentary layer	161
Figure 35. Summary of DSDP Site 193	127	Figure 53. Thickness of the lower sedimentary layer	163
Figure 36. Shear velocity for DSDP 192, 193 sediments	129	Figure 54. Free-air gravity	165
Figure 37. Magnetic anomalies	131	Figure 55. Heat flow	167
Figure 38. Formation and migration of the Northwest Pacific crust	133	Tables	
Figure 39. Earthquake epicenters of 0-40 km	135	Table I. Surface sediment types	169
Figure 40. Earthquake epicenters of 40-70 km	137	Table II. Grain size of surface sediments by geologic province	169
Figure 41. Earthquake epicenters of 70-120 km	139	Table III. Northwest Pacific DSDP core data	170
Figure 42. Earthquake epicenters of 120-200 km	141	Table IV. Physical properties of Pacific Ocean sediments, terrigenous sediments and red clays.	171
Figure 43. Earthquake epicenters of 200-300 km	143	Table V. Physical properties of North Pacific cores	172
Figure 44. Earthquake epicenters of 300-400 km	145	Table VI. Grain size of DSDP sediments	173
Figure 45. Earthquake epicenters of greater than 400 km	147	Table VII. Density and porosity of DSDP sediments	174
Figure 46. Index to crustal profiles	149	Maps (in Pocket)	
Figure 47. Northwest Pacific oceanic crust sections	151	I. Bathymetry	
Figure 48. Crust and mantle velocity models for the Southern Kurils	153	II. Sediment isopach	
Figure 49. Crustal cross-sections of the Kuril-Kamchatka earthquake region	155	III. Structure contour to the acoustic basement	
Figure 50. Depth to Moho and velocities used to define the Moho	157	IV. Bottom roughness with bathymetry	
Figure 51. Depth to layer complex 2	159	V. Acoustic basement roughness with structure contour of the acoustic basement	
		VI. Sediment isopach, bathymetry and bottom roughness	
		VII. Structure contour to the acoustic basement and bathymetry	
		VIII. Sediment isopach, structure contour and basement roughness	

Environmental Report of the Northwest Pacific for the Marine Seismic System (MSS)

I. Introduction

This report is a compilation of environmental data that are critical to the selection of an installation site for the Marine Seismic System (MSS) in the Northwest Pacific. The area described in this report is the Northwest Pacific Ocean between 40°N and 56°N. It is bounded by the 170°E Meridian on the east and the Kuril-Kamchatka earthquake region on the west. Environmental parameters are grouped according to cultural, oceanographic/meteorologic and geological/geophysical topics. Data have been assembled from published literature and data banks of major oceanographic institutions. The mapped data are presented at a uniform page-size scale to allow maximum comparison of data parameters. Extensive bibliographies and large-scale geological/geophysical maps are also included.

II. Cultural Features

A. Political Geography

The area of study is bounded on the north and the west by the U.S.S.R., on the southwest by Japan, on the northeast by the U.S. and on the south and east by the Pacific Ocean (Fig. 1). The Kuril Islands, Kamchatka, and the Komandorskie Islands are territories of the U.S.S.R., Hokkaido is Japanese, and the Aleutians are American. The nearest accessible ports are on Hokkaido, Japan, and Adak, Alaska. Nationally claimed waters extend 200 nm from national territory. Soviet waters line the western and northern borders of the Northwest Pacific (Figs. 1, 2 and large-scale maps).

B. Ship Traffic

Ship traffic near potential MSS sites exposes instruments and cables in the

water to the threats of damage and vandalism, and to ambient noise generated by ship engines. Merchant ships are generally confined to great circle routes between major ports (Fig. 1); however, the Northwest Pacific routes vary with seasons and currents.

Merchant ships are potential noise sources, while fishing ships threaten potential MSS sites with damage and vandalism in addition to noise. Unpublished data from models of Planning Systems, Inc., were compiled to show the instantaneous number of ships distributed by one degree squares. Figures 3, 4, and 7 present distributions of merchant ships, fishing ships, and composite traffic, respectively.

1. Merchant Ships

Distribution of merchant ships is shown in Figure 3. The densest merchant shipping occurs in the southern areas adjacent to major great circle shipping routes (Fig. 1) and in the area traversed by the Kuroshio Current (Figs. 5 and 6). Merchant shipping shifts to the north in summer and to the south in winter in response to the same seasonal shifts of the Kuroshio. The lowest concentrations of merchant ships occur in winter when the instantaneous number exceeds 0.20 only in areas south of 43°N. Except in the southwest, spring through fall routes are generally contained north of 40°N. The dense area from the southwest corner to 45°N, 170°E reflects the overlapping spring, summer and fall route. The dense area between 40°N, 157°E and 43°N, 170°E is largely attributable to the overlap of winter routes with spring and fall routes.

2. Fishing Ships

Fishing ship density (Fig. 4) is greatest in areas where the Kuroshio

and Kamchatka currents converge (Figs. 5 and 6). The greatest density is generally northwest of the merchant shipping routes (Fig. 3). Summer fishing is more intense north of the western central regions, while winter fishing is densest in the southwest.

3. Composite Traffic

The composite traffic map (Fig. 7) combines the merchant ship and fishing ship instantaneous numbers, but the fishing value is doubled because of the greater problem that fishing ships present. Density of the composite traffic is greatest in the southwest and lowest in the north. Summer traffic is greatest from the southwest to about 45°N , 170°E . Winter traffic is mainly south of 43°N .

III. Meteorology and Oceanography

Topics covered in this section present the critical meteorologic/oceanographic constraints to the MSS. Due to a voluminous amount of data that are often irrelevant to a MSS installation, a complete picture of the meteorology/oceanography is not attempted. The reader is referred to the bibliography sections for more comprehensive information.

Both the air and the upper ocean of the Northwest Pacific are part of a dynamic system that is dependent to a large extent on geography and seasons. Summer anticyclonic air circulation is controlled by a high-pressure cell centered about 40°N , 150°W . Winter cyclonic movement is caused by a more local low-pressure cell centered at 50°N , 180°W (Fig. 1). These pressure cells trigger wind and surface currents. Wind directions are synonymous with the atmospheric circulation, whereas surface currents are the product of Ekman transport and geostrophic flow. Intermediate and deep-ocean circulation in the Northwest Pacific is poorly understood, and seasonal effects on circulation are likely to be insignificant below 1500 m.

A. *Storms*

Figure 8 is a condensation of monthly cyclone (low pressure area) maps showing cyclone paths and the percent of time an area is covered by cyclones (Gorshkov, 1974). Month abbreviations are plotted to represent the highest concentrations of cyclones for specific months. Storms occur most frequently during winter months and are more prevalent in the north adjacent to the major winter low pressure cell (Fig. 1). Paths for the low pressure fronts generally move from southwest to northeast, but their paths, which represent averages, do not necessarily coincide with major storm concentrations.

B. *Winds*

Compiled from Gorshkov (1974), Figure 9 is a synthesis based on monthly wind distributions and displays the percent of time that winds are greater than 16 m/sec (31 kn). The figure shows this percentage for the months with the highest winds, November through March; the month abbreviations are centered at areas with maximum monthly winds. Strong winds (greater than 16 m/sec) are more prevalent in the west, southeast and northeast. The average direction of winter winds is northeasterly in the north and northwesterly in the south. While winter winds are cyclonic and are generated by a major low-pressure cell, summer winds are anti-cyclonic and generated by a major high pressure cell (Fig. 1). Summer winds are not as strong as winter winds, and are nearly opposite in direction.

C. *Icing*

Icing of equipment exposed to air can be a significant problem in the Northwest Pacific. Figures 10 and 11 show the number of months when sea surface temperatures drop below 0°C and -8°C , respectively (Gorshkov, 1974). The distribution of -8°C is presented to delineate the extent of extremely cold temperatures. The freezing temperatures, coupled with the intense winter

storm activity (Fig. 8), should produce icing in all areas of the Northwest Pacific. The least icing problem should occur in the southeast, the severest in the north and northwest.

D. Wave Heights

Wave heights in the Northwest Pacific can exceed 17.5 m (Fig. 12) and highest waves occur in non-summer months in the southeastern areas.

E. Surface Water Temperature

Surface water temperatures vary seasonally. Figure 13 shows the average water temperature for the coldest month (February), coupled with the annual variation in temperature of surface waters (Gorshkov, 1974). Warmest temperatures can be calculated by adding the annual variation to the February temperatures.

Winter cooling at surface waters produces a reversal in the temperature profile for the Northwest Pacific. The depth of the temperature maximum produced by this cooling and the temperature at the maximum are plotted in Figure 14 (Reid, 1973). The depth of the maximum indicates the extent of penetration of February or winter cold temperatures in the water column. Maximum warmest waters are present in the southern area where the Kuroshio Current is located.

F. Surface Currents

Surface current circulation in the Northwest Pacific consists of the eastward-flowing warm water of the Kuroshio Current at about 40°N and the southward-flowing cold water of the Kamchatka Current (also called Oyashio south of Kamchatka) that borders western land masses. In winter, the Kamchatka Current is squeezed westward and the Kuroshio is pushed southward as a result of seasonal Ekman transport caused by northerly winds (Fig. 5). In summer, the Kamchatka Current expands eastward and the Kuroshio northward due to prevailing southerly winds (Fig. 6).

G. Current Speeds

Maximum surface current speeds are to be expected within the major current areas, in the eddies adjacent to major currents, and during the winter when strongest winds occur. Figure 15 depicts surface current speeds that are based on reported ship drift for the months having the highest average value (U.S. Navy, 1977). The data show high speeds in a band on the west where the Kamchatka Current is constricted in winter and also in spotty areas in the path of the Kuroshio Current to the south. Since the data are averaged values, they are only useful to show general current speed distribution.

Figure 16 is a histogram of the highest monthly average surface current speed for one degree squares, the same data as that presented in Figure 15. Speeds are less than 0.8 kn for most one degree square locations; however, a fraction of the speeds exceeds 3.0 kn. Maximum surface current speeds will exceed these averaged measured speeds.

Figure 17 presents a maximum current speed profile based upon the model used by the Naval Oceanographic Office (NAVOCEANO) to evaluate current speeds for mooring design (Joseph Tamul, pers. comm.). The NAVOCEANO model states that maximum speed is at the sea surface and decreases linearly to one-third its original value at 400 m depth. From 400 m to the bottom, the speed decreases linearly to 0. The profile represented by a dashed line in Figure 17 depicts a maximum surface speed of 4 kn as observed in major ocean currents. This speed decreases linearly to 1.3 kn at 400 m and decreases linearly to 0.4 kn from 400 m to the bottom. The bottom speed is an assumed maximum bottom current speed based upon bottom photographs of the Northwest Pacific. Since bottom currents are evident in some areas of the Northwest Pacific, the zero bottom speed used in the NAVOCEANO model cannot be used as a maximum speed for the model in Figure 17.

To supplement the maximum current speed model, Figure 17 also shows measured current speeds. Current speeds derived from unpublished Ekman current meter measurements collected by NAVOCEANO (1930-1975) are plotted for the upper 500 m of the model. Eighty percent of these measurements have speeds represented by the darker shading, while the remaining 20% are represented by the lighter shading (Fig. 17). Although the measurements are biased because most data were collected in the calmer summer months, the slope of the current speed profile parallels the maximum speed model. Speeds at intermediate depth, as represented by solid black bars on Figure 17, are calculated from the geopotential anomaly maps of Reid et al. (1975). These values represent speeds averaged for large areas over long periods of time.

H. Sound Speed

Sound speed in the water column of the Northwest Pacific varies both seasonally and geographically. For stations plotted on Figure 18, Figure 19 shows sound speed profiles for the upper 1600 m of the water column (Senior, 1976, and NAVOCEANO, 1978). The profiles show that sound speed varies considerably in the upper 800 m of the water column. The April profiles (A and B) show that sound speed increases steadily with depth from a surface minimum, except in the region of the Kuroshio Current where surface sound speeds decrease to a minimum at about 500 m. The July profiles (C) display a thin, temperature-induced, high-velocity surface layer which grades into a velocity minimum at about 200 m.

The sound channel axis is defined as the depth of the sound velocity minimum. Figures 20 and 21, respectively, depict the winter and the summer sound channel depths. The maps are synthesized from upper water column sound velocity contour maps for discrete depths (Gorshkov, 1974). In winter, the sound channel is deepest in southeastern areas traversed by the Kuroshio Current. Figure 20 shows that

in winter two sound channels exist in the southeastern sections of the area. The sound channel is either poorly defined or absent in the remaining areas because the cold surface waters create a velocity minimum near the surface. The summer sound channel ranges from about 200 m to 500 m in depth and deepens toward the southeast.

I. Biological Fouling

Biological fouling of exposed MSS equipment should not be a problem in the Northwest Pacific (John DePalma, pers. comm.). The most intense fouling occurs in the upper 25 m with the accumulation of about one pound of barnacles per square foot of equipment surface per year. Algae will produce films on equipment in the upper 25 m and could only cause problems to light transmitting, transparent or movable parts. Bottom fouling should be insignificant. Cables, however, should be protected with Teredo shields for the surface 25 m and near the ocean bottom.

IV. Geology and Geophysics

Because the Geology/Geophysics section is long and complex, an organizational summary is offered. The section is introduced with a REGIONAL SETTING which outlines the geology of the Northwest Pacific and adjacent seas and continental areas. This section is followed by extensive geological compilations. The general subject trend of these compilations begins with the ocean bottom and proceeds through the sediment column, crustal rock and mantle. In BOTTOM ROUGHNESS, the topography of the ocean bottom is classified and mapped according to relief and slopes. Next, SURFACE SEDIMENTS presents the sedimentary characteristics of the ocean bottom.

The following sections deal with the sediment column. DSDP CORES presents extensive sediment data for the DSDP cores drilled in the area. Supplementing the DSDP CORES, ACOUSTIC STRATIGRAPHY offers mapped acoustic horizons

and sediment thickness. Finally, GEOLOGIC HISTORY explains crustal formation and past sedimentary environments of the Northwest Pacific. In addition to describing the occurrence of sediments found in DSDP cores, this section discusses the sediment column in poorly surveyed areas.

The remainder of the Geology/Geophysics section covers the geographic areas where seismic waves traverse to reach a potential MSS. In SEISMIC ACTIVITY, the seismic sources are located. DEEP SEISMIC VELOCITY STRUCTURE outlines velocity structure of the areas between the seismic sources and the potential MSS and presents generalized crust and mantle velocity profiles for the Kuril-Kamchatka region and the Northwest Pacific Ocean. The final section, GRAVITY AND HEAT FLOW, provides additional data about the deep structure of the area.

A. Regional Setting

The geographic scope of this section includes the Northwest Pacific, as well as adjacent seas and continental areas. The regional divisions in this section are used primarily to define these areas in discussion and do not represent absolute geological or seismological provinces. The Kuril-Kamchatka earthquake region, the Western Aleutian earthquake region and the Emperor Seamounts (Fig. 1) are discussed mainly as peripheral areas to the Northwest Pacific regions, which are mapped as physiographic subprovinces (Fig. 22). These subprovinces are the focus for most of the research presented in this report.

1. Kuril-Kamchatka Earthquake Region

From east to west the Kuril-Kamchatka earthquake region includes the Kuril-Kamchatka Trench, the Southern Kamchatka Peninsula, the Kuril Island Arc, and the Sea of Okhotsk. The trench reaches depths over 9000 m and marks a plate boundary where the Pacific oceanic lithosphere under-thrusts the Asian plate (see Seismic

Activity section). Parallel to and west of the trench is a line of volcanoes located on the Kuril Island Arc and Eastern Kamchatka. The Bussol Proliv is a submarine pass (Map 1) which transects the island arc at 47°N. It connects the Sea of Okhotsk to the Northwest Pacific at a depth of 2500 m. The Kuzenshterna Proliv is another pass, located at about 48.5°N, which connects the same water bodies at a depth of 1500 m. The passes serve as channels for cold water exchange between the Sea of Okhotsk and the Northwest Pacific Ocean. West of the Kuril island Arc, the Kuril Basin is the only deep ocean basin in the Sea of Okhotsk. The Basin has an average depth of 3200 m and connects with the Pacific Ocean through the Bussol Proliv.

2. Western Aleutian Earthquake Region

The western Aleutian earthquake region is a trench and island arc system; however, the tectonic mechanism of this region is strike-slip movement between the Pacific and North American Plates (Cormier, 1976). The western Aleutian trench averages 6500 m in depth and is generally shoaler than the Kuril-Kamchatka Trench. The Aleutian trench is floored with thick, ponded sediments, whereas the Kuril-Kamchatka Trench rarely contains ponded sediments. The two trenches connect in an inverted "V" south of the Kamchatka Strait. This strait has a depth of 3000 m and connects the Kamchatka Basin of the Bering Sea to the Pacific Ocean. Since the Kamchatka Basin also averages 3000 m, the Kamchatka Strait is an important area for water exchange, and acts as a conduit that channels Bering Sea sediment into the Northwest Pacific.

3. Emperor Seamounts

The Emperor Seamounts, located on the east of the Northwest Pacific abyssal hills province, have a northern limit just southward of the Kamchatka Strait and seaward of the Aleutian and Kamchatka Trenches. The northernmost

crest of the Emperor chain is Meiji Guyot (Map 1), an elongated plateau which has a minimum depth of about 3000 m and bears a thick sediment cover on its northeastern slopes. Meiji Guyot trends N45°W, whereas the remaining Emperor Seamounts trend N20°W as far south as 40°N.

The Emperors are thought to have formed as the Pacific plate moved to the northwest across a "hot spot" (Clague and Jarrard, 1973). This hypothesis would date Meiji as the oldest existing seamount and the bathymetric trend can be explained by contemporaneous plate movement. The seamounts decrease in age southward and generally have shoaler crests and sparser sediment cover to the south. The Emperor Seamounts are listed from north to south, with their corresponding minimum depth:

Meiji	2923 m
Detroit	2239 m
Tenchi	2349 m
Jimmu	1275 m
Suiko	1106 m
Nintoku	943 m

Deep latitudinal gaps traverse the Emperor Seamount chain. They are located in southern regions between Jimmu and Suiko, Suiko and Nintoku, and south of Nintoku. These gaps may be related to geologic trends in the adjacent Northwest Pacific abyssal hills province and they could serve as passes for deep water transport.

4. Hokkaido Rise

The Hokkaido Rise is a northeast/southwest-trending structure elevated 3000 m above the Kuril-Kamchatka Trench on the northwest and from 400-800 m above Pacific crust on the southeast (Fig. 22 and Map 1). The structure parallels the Kuril-Kamchatka Trench and trends perpendicularly to presumed present Pacific plate movement (Lancelot, 1978). Greatest topographic expression is present at 45-48°N where the average depth is about 4900 m. The Rise is transected by several

depressions. Located in the south are two depressions (40-41°N, 149°E) which may be northern sections of the proposed Nakwe Channel (Mammerickx, 1980).

Another depression transects the Rise at 44°N. A saddle located at 48-49°N has an average depth of 5500 m, which is up to 500 m deeper than the Rise to the south. This saddle and the southern depressions could be areas of deep water exchange between the trench area and the Northwest Pacific abyssal hills province. North of the saddle the Rise displays the northwest-southeast bathymetric trends that parallel the Emperor Seamounts south of Meiji.

Two anomalous structures cross the Hokkaido Rise between 44°N and 48°N. First, a trough which connects with the Hokkaido Trough appears to cut the eastern Hokkaido Rise with a relief of up to 400 m. The trough extends eastward from 155°E and trends roughly east-west. Second, a N30°W-trending line of seamounts crosses the Hokkaido Rise and the Hokkaido Trough (Map 1). These seamounts could extend south of the trough and east of the rise with a N40°W trend.

According to McAdoo et al. (1979), the rise is of secondary origin due to the buckling of an elastic lithosphere as it descends into the Kuril-Kamchatka Trench. Small-scale faulting that trends northeast-southwest is apparent on continuous seismic reflection profiles; however, detailed mapping of the faults is difficult due to lack of profile coverage. These faults tend to support the McAdoo et al. proposal.

5. Hokkaido Trough

This report contains the most comprehensive mapping of the Hokkaido Trough yet compiled (Map 1). The sinuous trough appears to trend roughly east-west from the Hokkaido Rise toward the Emperor Seamounts. The trough also appears to extend toward the Bussol Proliv of the Kuril Island chain to the

west and toward the gap between Suik and Jimmu of the Emperor Seamounts. From 161°E to 165°E the trough consists of a series of parallel ridges and troughs, suggesting a series of faulted blocks. At 161°E the trough bends slightly to the northwest. Farther west the trough branches into two troughs of lesser relief. One trough extends into the Hokkaido Rise and the other bends southwest-northeast, parallel to the Hokkaido Rise. Relief varies from as little as 100 m in speculative southwestern extensions of the trough to over 1400 m where ridges parallel the trough. Continuous seismic reflection profiles collected west of 160°E show that the trough contains a maximum thickness of 0.5 seconds (two-way travel time) of ponded sediment, while flanking ridges have almost no sediment (Fig. 24, CC'). No adequate explanations are available as to the origin of this feature. Magnetic data now being processed reveal large anomalies across the trough and parallel ridges. Further collection and analysis of magnetics, bathymetry, and seismic reflection profiles are needed.

6. Basin Between Southern Hokkaido Rise and Shatsky Rise

This region is characterized by broad parallel, small amplitude (200 m) northeast-southwest-trending ridges and depressions (Map 1). Typical depths are 5400 to 5700 m. Geological data coverage of the area is better than for other Northwest Pacific provinces. Magnetic anomalies mapped by Hilde (1975) show magnetic isochrons that are roughly parallel to the bathymetric trends. DSDP drill sites 303 and 304 are located in this province, and both drill holes penetrated basaltic basement of middle Cretaceous age. In the north, the province appears to be cut by the seamount chain mentioned in the Hokkaido Rise section as well as the Hokkaido Trough. North of the trough to about 47°N, the bottom apparently continues to have the same bathymetric character as the southern area; however, data coverage is sparse.

7. Northern Shatsky Rise

The northern extension of the Shatsky Rise is located in the southeastern corner of the survey area. The rise is elevated about 700 m above the surrounding ocean floor and has an average depth of 5000 m. The bathymetric trend of the Rise parallels the northeast-southwest trends of the surrounding basins and the Hokkaido Rise.

The Shatsky Rise is a north/south-trending feature which appears to extend from 30°N to 45°N; however, the major section of this feature is south of 40°N. Although sediment and acoustic velocity studies have been conducted in the major portion of the Rise, the northern extension remains largely unstudied. Speculations concerning the northern extension should not be based on knowledge of the southern section until more is known about the area.

8. Provinces Adjacent to the Emperor Seamounts

Bathymetric trends change from a northeast-southwest trend to a northwest-southeast orientation near the Emperor Seamounts (Map 1). This orientation, which parallels the Emperor Seamounts south of Meiji, is most prominent southwest of the Meiji Guyot, where parallel ridges and troughs with relief of 500 m to over 1000 m extend as far west as 162°E. The parallel ridges generally have thin sediment cover (0.2-0.4 sec), while the troughs have flat, ponded sediments as thick as 1.0 sec. One trough appears to extend southward from the Meiji area to 45°N. Agapova et al. (1973) describe their discovery of northwest-southeast parallel fracture zones as far west as 162°E in the region from 46-52°N. This area has poor bathymetric track coverage; moreover, the Russian data extracted from a small-scale illustration does not fit well with other available data. More data are needed to adequately map the morphology of this region.

B. Bottom Roughness

For this report, BOTTOM ROUGHNESS is a relative measure of slopes and relief of bottom topography as perceived from continuous seismic reflection records. Bathymetric contours (Map I) only show reliefs which exceed the contour interval (100 m). Slopes computed from these contours are generally averaged because they cannot measure the low amplitude short wavelength topography. Bottom roughness is a measure of this short wavelength topography, which, when superimposed upon the bathymetric contours (Map IV), will reflect the bottom topography in more detail.

Bottom roughness classifies all slopes and relief into three empirically-based groups which divide the Northwest Pacific into three relatively equal areas. The three roughness divisions by increasing relative roughness are:

- o Low roughness - relief less than 200 m in a 20 km span and/or slopes less than 3-4°.
- o Intermediate roughness - slopes of 3-10°. Intermediate roughness is intended as an overlap division.
- o Greatest roughness - relief differences greater than 200 m in a 20 km span and/or slopes greater than the 6-10° range.

The slopes of the bottom topography can vary somewhat, regardless of the relief. If an area has low relief, but a large amount of short wavelength topography, the slopes of the topography can be great. On the other hand, high relief areas may have broad gradual slopes. Usually high relief areas have greater roughness than low relief areas. For this reason, the high relief represented by bathymetric contours, which have more extensive track coverage than the bottom roughness, can be used to imply high roughness in areas with poor seismic reflection coverage.

For most purposes, low roughness areas are advantageous to the MSS and greatest roughness areas are to be

avoided. Major areas outside the 200 mile limit that have low roughness are located in a broad band east of the southern Hokkaido Rise, in a smaller area adjacent to the eastern flank of the Hokkaido Rise at about 47°N, and in troughs both adjacent and parallel to the Emperor Seamounts (Map V).

Roughest areas are the seamount provinces and faulted areas on the Hokkaido Rise and the Shatsky Rise. Areas adjacent to the Meiji Guyot and the Hokkaido Trough are assumed to be rough on the basis of high relief bathymetry. Figures 24-26 show seismic reflection profiles for lines indexed on Figure 23. Profiles A, E, F, G and I represent smooth bottom. Profile H shows intermediate bottom and profiles B, C, D and J show rough bottom.

C. Surface Sediments

Surface sediment types of the Northwest Pacific have been classified and mapped by Frazer et al. (1972). This classification is the outcome of a compilation of data, analyses, and sediment descriptions that are not always directly compatible. As a result, the classification contains ambiguities, but nevertheless serves as a useful summary of general sediment types. Surface sediments of the Northwest Pacific consist of combinations of six basic components:

- o Clay - fine grained (<4 μ m), <30% biogenic sediments.
- o Calcareous ooze - >30% biogenic carbonate.
- o Sand and silt - size of sediment particles predominantly 4 μ m to 2000 μ m, <30% biogenic sediments.
- o Mud - terrigenous deposits, generally fine grained, but containing significant components of sand and silt.
- o Siliceous ooze - <30% biogenic silica.
- o Volcanic sediment - containing detectable amounts of ash, glass shards, pumice or other volcanic materials.

Ideally, a sediment should be classified by size, source and composition; the Frazer et al. (1972) classification is based upon a partial combination of the three criteria. The clay and sand/silt components are size classifications, whereas mud, an undifferentiated mixture of predominantly clay with sand/silt, is classified by both size and source. The biogenic (organically derived silica or carbonate) and volcanic components are both compositional and source classifications, and may encompass all three size classes.

Adapted from the Frazer et al. map, Figures 27 and 28 show that most surface sediments are combinations of the six major types. Major combinations of sediment type on Figure 23 are listed in Table I.

Because volcanic constituents are usually present in small amounts, sediments containing them are named with the adjective "volcanic" to the far left, for example: volcanic siliceous mud. When sediments containing 10-30% biogenic material appear in combination with muds, clays, or sand and silt, they are no longer designated as oozes; rather the predominant biogenic material becomes an adjective modifier of the size term such as calcareous silt or siliceous clay.

Distribution patterns of surface sediment can indicate sediment sources. Sands and silts are generally found on the continental margins close to the terrigenous source. In the Meiji area, where sedimentation is dominated by currents carrying large amounts of terrigenous material, terrigenous muds extend seaward of the trenches (Scholl, et al., 1977). Clays are present in areas isolated from sources of terrigenous sediments. Calcareous oozes produced by planktonic foraminifera are present atop seamounts with depths shallower than the carbonate compensation depth. Siliceous components in sediments are ubiquitous because the Northwest Pacific is located within the

high latitude, diatom-producing zone. Volcanic materials appear throughout the area as a result of Kuril-Kamchatka volcanism. They are dispersed in small quantities in most sediments or are locally concentrated in thin ash layers.

1. Grain Size of Sediments

Soviet scientists have studied the grain size distribution of surface sediments in the Northwest Pacific more extensively than the American or Japanese scientists, particularly in the western areas. Unfortunately, the Soviets do not employ the Udden-Wentworth scale used by most western sedimentologists; therefore, their results are not directly comparable to other works. Instead, they use a grain size scale based on magnitudes of 10, the major divisions of which are sand, 100-1000 μm ; aleurite, 10-100 μm ; pelite, 1-10 μm ; and subcolloidal, $<1 \mu\text{m}$. This contrasts with the major Udden-Wentworth scale divisions of sand, 62-2000 μm ; silt, 4-62 μm ; and clay $<4 \mu\text{m}$. The two classifications are roughly equivalent and the Soviet system will be used only in this section.

Generalized grain size distributions of surface sediments extracted from Soviet maps of Kort (1970) are listed in Table II by size class for each of the physiographic provinces classified in this report.

Coarse sediments on the Emperor Seamounts and Meiji Guyot are probably due to a coarse carbonate fraction and volcanic material. On the Hokkaido Rise, sediment coarsens toward the Kuril-Kamchatka Trench due to increasing proximity to volcanic and terrigenous sources. Conversely, sediments become progressively finer on the southeastern side of the rise.

The mean diameter of surface sediment grains (Horn et al., 1970) is illustrated in Figure 27. With the exception of the Emperor Seamounts, mean diameter decreases southeastward, from

greater than 3 μm near the trench to less than 2 μm in the southeast. The Horn et al. study is based upon Lamont-Doherty Geological Observatory cores plotted on Figure 29. Additional LDGO cores collected since the Horn et al. study reveal similar grain size data (unpublished LDGO core descriptions). Surface sediments in the Northwest Pacific abyssal hills province are essentially clay size, with the coarsest material nearer to land or local volcanic sources.

Grain size analyses conducted by the Naval Oceanographic Office in the vicinity of Meiji Guyot (Loomis et al., 1972) (Fig. 29) show surface sediments there to be clays and silts. The sediments are coarser than basin sediments. Variation of grain size with depth in the sediment column is listed for DSDP cores in the Physical Properties section.

2. Clay Minerals

The mineralogy of clays suggests both the origin of sediment and the mechanism by which it was transported. Griffin et al. (1968) have mapped percentages of chlorite, montmorillonite, illite, and kaolinite for the less than 2 μm size fraction of surface sediments. The less than 2 μm size fraction is probably less than 50% of the sediments in the Northwest Pacific. In contrast, Griffin et al. (1968) assign typical Pacific pelagic sediment as 61% less than 2 μm , hence, Northwest Pacific sediments are coarser than the normal pelagic sediments.

Typical red clay provinces in the North Pacific have greater than 50% illite composition. The Northwest Pacific illite content varies from 20-50% and decreases northwesterly toward the Kuril Trench. The clay minerals which replace illite as major constituents are chlorite (20-30% and montmorillonite (30-50%). By comparison, typical North Pacific red clays contain 10-20% chlorite and 20-30% montmorillonite. The chlorite and montmorillonite contents increase northwesterly toward the trench. The higher content

of chlorite indicates low intensity weathering of terrigenous material and glacial transport; the higher montmorillonite indicates influx from a volcanic regime or in situ alteration of volcanic ash (Griffin et al., 1968).

3. Coarse Fraction

Coarse fraction sediments vary through time in response to glacial input, biogenic production, volcanism, and terrigenous weathering processes. The coarse fraction varies considerably within cores. Values as high as 90% or as low as 10% coarse material may be present in ash layers. Greatest abundances occur on Meiji Guyot and near land sources. Connolly et al. (1970) studied 20 m piston cores from the Northwest Pacific and found 50-80% of the coarse fraction to be of volcanic origin in the form of glass shards and pumice. Plagioclase, volcanic rock fragments, and ice-rafted detritus are important minor constituents which comprise less than 20% of the coarse fraction. These constituents are largely current-transported from terrigenous provenances. Pebbles greater than 5 mm are rare, and are assumed to be due to ice-rafting. Ice-rafted material in quantities greater than 1% of the coarse fraction are present north of 45°N with greatest concentrations in the vicinity of Meiji Guyot. Biogenic silica, which comprises 10-20% of Northwest Pacific surface sediments, contains a variable but high percentage of the coarse fraction.

D. DSDP Cores

DSDP core data for all sites in the immediate vicinity of the Northwest Pacific are listed in Table III. Only cores 192, 303, 304 and 436 have sediment sections representative of the Northwest Pacific abyssal hills province. Sites 192 and 436 have the best core recovery rates while sites 303 and 304 have inadequate recovery for Miocene and younger sediments.

Cores 303, 304, and 436 are all located in the southern area (Fig. 2). Cores 303 and 304 are located east of the Hokkaido Rise in the southern abyssal hills province where sediments are generally thin. Core 436 is situated on the Hokkaido Rise east of the northern Japan Trench and the core contains a thicker sediment column than 303 and 304. Cores 431, 432, and 433 are all located on the Emperor Seamounts where sediments are sparse (Maps I and II).

Core 193 contains only a short section of sediment and is incomplete for Pleistocene and older sediments. The reader should consult Figures 32-35 for general summaries of the data collected for cores 303, 304, 192 and 193.

Core 192, taken atop the sediment-capped Meiji Guyot, is the only available sample for sediments in the northern areas. This core is atypical because the sedimentary regime has always been above the Carbonate Compensation Depth and the Kamchatka Current is a likely transport agent for the bulk of Miocene and younger sediments (Scholl et al., 1977). As a result, sedimentation rates have been higher atop Meiji Guyot than on adjacent basin areas, largely due to the influx of current-transported terrigenous material. Abyssal hills areas are likely to have higher proportions of volcanically derived sediments due to the more dominant volcanic influx.

1. Time Correlation

Time correlation of DSDP lithologic units in Northwest Pacific cores reveals general depositional environments (Figs. 30 and 31). In Miocene and younger sediments, basic sediment components are pelagic clay, muds, biogenic silica and volcanic material. Older sediments include claystones, pelagic clays, cherts and carbonate sediments.

Pre-Miocene sediments show great geographic variation in lithology. Sediments immediately overlying basalt

basement were recovered at sites 303, 304, and 192. At sites 303 and 304, basal units of upper Cretaceous age consist of nanno ooze, chert and pelagic clays; Paleocene through Miocene sediments were not retrieved. At site 436, dark-brown, banded cherts of late Cretaceous age were cored. Paleocene through Middle Miocene sediments consist of 20 m of dark-brown, manganese-rich clay. In contrast, site 192, cored in younger Cretaceous crust, consists of late Cretaceous to lower Miocene chalks and claystones. The presence of carbonate sediments indicates deposition above the carbonate compensation depth.

The bulk of sediments in the Northwest Pacific are post-Oligocene. Miocene claystones are present at core 436, and core 192 contains early and middle Miocene claystones. Sediments at site 192 are late Miocene diatom-rich clays that grade into Pliocene diatom ooze, typical of Pliocene sediments in all cores. The ooze at site 192 contains more than 60% biogenic silica, while a similar unit at site 436 averages 30-40%. The short, incomplete, Pliocene sediment section recovered at site 303 is also diatom ooze. Pleistocene sediments at both sites 436 and 192 are generally siliceous volcanic clays interspersed with diatom oozes and ash layers; similar sediments are likely at sites 303 and 304, where only small portions of the Pleistocene section were recovered. The Pleistocene sediments at site 192 are probably current-derived terrigenous detritus (Scholl et al., 1977), while site 436 sediments are largely derived from volcanic ash from Japan and the Kuril Islands.

2. Sedimentation Rates

Sedimentation rates in the Northwest Pacific Basin vary with time and geography. Rates at DSDP core sites are labeled on the time columns (Fig. 30) and thickness columns (Fig. 31). Recent sedimentation rates have been calculated by Ninkovich (1975) from piston cores (Figs. 29-31). Rates are

higher nearest to land sources and lowest seaward. Ninkovich's rates vary from about 3.0 cm/1000 yrs near the Emperor Seamounts to greater than 6.0 cm/1000 yrs near the Kuril Trench. These rates are compatible with Pleistocene sedimentation rates measured in DSDP cores. At site 436, Pleistocene rates are presently at a maximum of 7.0 cm/1000 yrs and rates at site 192 average 6.0 cm/1000 yrs. Ninkovich proposed that the present sedimentation rate be projected for the total sediment column. In areas near DSDP cores this assumption is not valid. Site 436 has a present maximum rate which decreases with age due to increasing distance from volcanic sources. At site 192 rates increase with age into the Pliocene due to increased diatom productivity, while the general terrigenous component retains a steady rate from middle Miocene through the present. Rates of pre-Miocene sediments are less than 1.0 cm/1000 yrs at all DSDP sites. Due to low sediment retrieval at sites 303 and 304, only an average mid-Miocene to present rate of 1.6-1.7 cm/1000 yrs is proposed (Larson et al., 1975). Sedimentation here is probably similar to that at site 436 in that greater rates occur for younger sediment.

3. Physical Properties

Measurements of physical properties for Northwest Pacific sediments are scarce and unreliable. Related North Pacific studies (Richards, 1961; Moore, 1962; Keller, 1969; and Keller et al., 1970) consist of analyses of piston and gravity core sediments. Studies are extensive on DSDP cores 192 and 193 (Lee, 1973) and sparse on cores 303 and 304 (Larson et al., 1975). Because DSDP cores are disturbed by drilling, the ensuing laboratory tests could be in error. The reader should consult the references to evaluate the quality of the data.

Data on physical properties are extracted from various sources and listed in Tables IV-VII. Table IV (Keller et al., 1970) lists the mass

physical properties for Pacific sediments and averaged values for world ocean terrigenous and red clay sediments. Unfortunately Northwest Pacific sediments are not typical of any of the three groups, and pertinent values lie between the wide ranges listed. Table V (Moore, 1962) lists physical properties and calculated bearing capacities for North Pacific cores located east of the Emperor Seamounts. These sediments are similar in grain size and composition to Northwest Pacific sediments and may be representative physical properties at MSS sites.

DSDP data on physical properties are included for cores 303, 304, 192 and 193. Minimal data exist for cores 303 and 304 (Larson et al., 1975). Extensive data are available for cores 192 and 193; however, core 192 is not typical of the Northwest Pacific abyssal hills sediments, since it is located atop Meiji Guyot. Core 193 contains typical abyssal hills sediment, so physical properties measurements of this core are probably most representative of those to be encountered at an MSS site. Unfortunately, less than 100 m of sediment were retrieved at site 193.

Figures 32-35 present summaries of the DSDP core physical properties correlated to the depth in the core, sediment lithologies, and acoustic measurements. Tables VI and VII (Lee, 1973, and Larsen et al., 1975) list DSDP grain size and density/porosity data. Figure 36 shows measured vane shear strengths for DSDP 192 and 193 sediments plotted according to depth in the cores (Lee, 1973). In modeling for pore pressure, Lee estimated in situ vane shear strengths versus depth from his measured values (Fig. 36b). For a more thorough analysis of the methods and the results of this study, the reader should consult Lee (1973).

E. Acoustic Stratigraphy

The acoustic stratigraphy of the Northwest Pacific consists of acoustic

horizons that have been identified and mapped on the basis of visual inspection of continuous seismic reflection profiles. These data are supplemented by wide angle reflection, refraction and sediment data to allow estimates of seismic velocity and composition of the acoustic horizons.

Acoustic horizons for the Northwest Pacific have been identified in previous studies. Ewing et al. (1968) outlined the general acoustic stratigraphy for the Western Pacific. For the Northwest Pacific, they proposed an upper transparent layer underlain by either a smooth opaque layer or a rough layer believed to be oceanic basement. They also discovered a transparent layer beneath the opaque layer, generally in areas south of the Northwest Pacific. Houtz et al. (1979) achieved greater acoustic penetration on their continuous seismic profiles and discovered that the lower transparent layer is more widespread than proposed by Ewing et al. (1968). Houtz et al. (1979) combined the terms opaque layer and lower transparent layer into the term reverberant layer and mapped its presence on the southern Hokkaido Rise and on areas near the Emperor Seamounts and Shatsky Rise. Under most of the Northwest Pacific the acoustic stratigraphy consists of the upper transparent layer and an acoustic basement which is either the opaque layer, reverberant layer when smooth, or true ocean basement when rough.

The acoustic horizons are not readily correlated to the oceanic layer scheme, based on sediment and refraction data (Ludwig et al., 1970; Houtz et al., 1976). Corresponding to the depth range of the acoustic horizons are layer 1 (sediments) and layer 2 (true ocean basement). The upper transparent layer consists of low velocity material, probably unconsolidated sediments classified as layer 1A (Ludwig et al., 1970). The opaque layer and the reverberant layer are either consolidated sediments (layer 1B) or oceanic basalt, which is not necessarily true basement (layers 2 or 2A) (Houtz et al., 1976).

Rough acoustic basement might be true oceanic basement (layer 2).

1. Transparent Layer

The transparent layer corresponds to low velocity sediments. From wide angle reflection data, the transparent layer averages 1.74 km/sec for the Western Pacific (Houtz et al., 1979). This value is higher than the average velocity of 1.63 km/sec measured for Northwest Pacific DSDP sediments. Low velocity sediments are siliceous volcanic clays and muds, siliceous and calcareous oozes, and claystones predominantly of mid-Miocene and younger age. The base of the transparent layer is assumed to be where acoustic velocities increase suddenly to over 2.0 km/sec. In DSDP cores (Fig. 31), this interface coincides with chert layers in cores 436, 303 and 304. At 192, the interface could be true basement.

2. Sediment Thickness Map

Thickness of the transparent layer based upon digitized seismic reflection profiles is displayed on Map II. The map is more reliably interpreted in areas of dense track coverage. Comparisons with bathymetry, which has denser track coverage, allow sediment thickness interpretation where seismic profiles are scarce (Map VI).

The apparent thickness of the transparent layer varies from 0 to over 1.0 seconds of two-way travel time and averages about 0.4 to 0.5 seconds. Sediments generally thin southeastward away from the Kuril Trench. They thicken extensively over the Hokkaido Rise, particularly in the southwest, and thin on either side of the Rise. To the southeast, this thinning is due to the greater distance from volcanic and terrigenous sources. To the west of the Rise, the thinning may be due to slumping of sediments on the steep slope leading into the Kuril trench.

Kuril-Kamchatka Trench sediments are rarely turbidite-ponded. At one

isolated area, located about 51-52°N, 0.3-0.4 seconds of ponded sediments are apparent in the trench at the base of a large continental margin canyon (see Map I). Except for isolated locations within the trench, turbidites are absent in the Northwest Pacific.

Several areas of sediment ponding are probably due to local sedimentation. Near isolated seamounts, ponding generally occurs near the base. On a gentle western slope of the Shatsky Rise at about 41°N is a basin with over 0.5 seconds of sediment thickness that partially fills a bathymetric depression. A similar but larger sediment pond extends along the western side of the Emperor Seamount chain. Though seismic reflection coverage is poor, the Hokkaido Trough appears to be filled with flat-lying sediments in excess of 0.5 seconds. The trough is lined by seamounts, which could be a local source for the thick sediments.

Sediment distribution around the Meiji Guyot area, studied by Buffington (1973) and Scholl et al. (1973, 1977), has been updated in Map II. Sediment wedges are prominent in areas south of the Meiji area. The greatest sediment thicknesses are northeast of the Meiji Guyot crest although small wedges of thick sediment fill bathymetric lows which parallel the Emperor Seamounts south of Meiji Guyot.

3. Acoustic Basement

The acoustic basement seen on Northwest Pacific seismic reflection profiles can be one of three acoustic horizons. Smooth basement is either the opaque layer or the reverberant layer; rough basement is probably true oceanic basement.

Lying beneath the transparent layer, the opaque layer probably rests directly on true oceanic basement. The opaque layer is composed of either low velocity basalt or consolidated sediments. As revealed from refraction work (Houtz et al., 1976, 1979), the basaltic opaque layer (layer 2A) has an

average velocity of 2.43 km/sec. Since the low velocity basalt is suspected to exist most commonly near seamounts, it is probably secondary volcanic material and not ridge-crest basalt. Basal chert layers (layer 1B) found at DSDP sites 436, 303, and 304 produce the opaque layer in the southern regions and have acoustic velocities of 2.7 km/sec. The thickness of the chert layer at site 303 is about 30 m. Thickness of the opaque chert layer may be less at other Northwest Pacific locations because the crust is younger and has passed through less of the equatorial silica-producing zone (see Geologic History).

Consolidated carbonates are present in areas where sediments were deposited above the carbonate compensation depth. At site 192, for example, a carbonate basal layer lying on basalt has velocities of 2.2-3.5 km/sec. This carbonate layer, however, is not identified as the opaque layer. It lies directly on basalt and the basalt is identified as the acoustic basement. Similar carbonate layers are likely to be found on seamounts in the Northwest Pacific.

The reverberant layer is essentially a thick opaque layer and has similar origins and composition. The reverberant layer is generally thinner than 0.1 second north of 40°N, where it probably consists of banded cherts or secondary volcanic material at the base of seamounts. The reverberant layer is greater than 0.1 second in the southwest section of the study area (Houtz et al., 1979) and adjacent to the west slope of the Emperor Seamounts and northern Shatsky Rise (Fig. 25, EE'; FF').

True oceanic basement (layer 2) is composed of basalt and has acoustic velocities greater than 4.0 km/sec. True basement is assumed to be the rough acoustic basement in the Northwest Pacific because typical oceanic basement is rough. When acoustic basement is smooth, the true basement lies beneath and is not distinguishable from the lower velocity cover. True

basement as acoustic basement can be inferred from the basement roughness map (Map V).

4. Basement Roughness Map

Map V shows basement roughness with depth to acoustic basement superimposed. The smooth southern areas may correlate with the cherty acoustic basement. Smooth areas adjacent to the Emperor Seamounts could have secondary volcanic acoustic basements. Areas of rough basement, particularly on seamounts, appear to represent oceanic basement.

5. Structure Contour Map of the Acoustic Basement

The structure contour map (Map III), which was constructed from continuous seismic reflection records, presents the depth to the acoustic basement from the sea surface in two-way travel time. The contours represent the surface of the Northwest Pacific before the deposition of post-Oligocene transparent sediments.

Since much of the transparent layer sediment is draped, the general basement morphology is similar to that of the bathymetry map. Because data coverage is poor in most areas, recognition of structural features is nearly impossible. Small scale faulting, particularly on the Hokkaido Rise where coverage is good, apparently strikes northeast-southwest. In the Meiji Guyot area, the nature of the sediment-filled troughs is revealed on the structure contour map. One structural basin located northeast of Meiji Guyot is presently completely filled with over 1.0 second of sediment, while other basins generally have greater than 0.4 second of sediment.

6. Representative Seismic Reflection Profiles

Figures 24-26 show representative seismic reflection profiles which depict regional variation of bottom roughness, sediment thickness, and acoustic

basement. Figure 23 shows the locations where the profiles were collected.

Profile AA' (From R/V ROBERT CONRAD 12, 1968)

Typical of the southern abyssal hills subprovince, profile AA' shows smooth stratified sediments overlying a smooth acoustic basement. The acoustic basement is probably chert resting on true basement as revealed at the adjacent DSDP site 303.

Profile BB' (R/V ROBERT CONRAD 14, 1971)

Profile BB' depicts the faulted central Hokkaido Rise, which typically has rough bottom and acoustic basement with variable sediment thickness.

Profile CC' (R/V VEMA 21, 1965)

On profile CC', the Hokkaido Trough is depicted as a V-shaped feature in cross-section. The trough has steep, sediment-free walls and flat-lying sediments ponded in its deepest parts.

Profile DD' (from USNS BARTLETT, 1972)

Profile DD' illustrates the character of the Shatsky Rise in the Northwest Pacific. It is typically rough with thin or no sediment cover.

Profiles EE' (USNS BARTLETT, 1972) and FF' (R/V VEMA 20, 1965)

These profiles show the presence of the reverberant layer adjacent to the Emperor Seamounts (Houtz et al., 1979). The reverberant layer probably consists largely of secondary volcanics derived from the adjacent Emperor Seamounts and Shatsky Rise.

Profiles GG' (R/V VEMA 21, 1965) and HH' (R/V ROBERT CONRAD 14, 1971)

These profiles are typical of the Hokkaido Rise north of the rough central Rise and Hokkaido Trough. Both profiles have conformable sediments

resting on acoustic basement. Profile HH' has intermediate bottom and basement roughness, which is probably due to small scale faulting. Areas of smoother bottom and basement, as shown in profile GG', are located generally south of the areas with intermediate roughness.

Profile II' (R/V ROBERT CONRAD 14, 1971)

Profile II' transects the sediment-filled troughs and associated ridges to the southwest of Meiji Guyot. While the ridges have thin or no sediments resting upon rough basement, the troughs have thick, flat-lying sediments resting upon smooth acoustic basement. Acoustic basement may be true basement under the ridges, but the acoustic basement under the troughs is probably composed of secondary volcanics.

Profile JJ' (R/V VEMA 21, 1965)

The Meiji area is illustrated by profile JJ'. The south slope of Meiji Guyot generally has thin sediments, while thick sediments rest on the crest and northern slope of Meiji Guyot. In the south are the parallel ridges and the sediment-filled troughs shown in profile II'.

F. Geologic History

As the Northwest Pacific is underlain entirely by oceanic crust, a reconstruction of its evolution requires the application of the concepts of plate tectonics, magnetic anomaly patterns and the sedimentary record. Unfortunately, knowledge of magnetic anomalies in the Northwest Pacific is incomplete and plate movements are still hypothetical. However, the combination of magnetic data with DSDP stratigraphy produces a reasonably well-documented geologic history.

This section presents oceanic crustal ages based on magnetic isochrons, fossil plate rotations and sedimentary events based upon DSDP data. The

nature of sediments and basement in poorly surveyed areas can be inferred by an understanding of geologic history. The assumptions derived from the geological history will help to predict the nature of the materials that will be drilled for the MSS installation.

1. Magnetics

Mapping of magnetic anomalies helps establish crustal age and geologic structure and enables the projection of sea floor age to areas where the magnetics have not been deciphered. In an early study, Uyeda et al. (1967) demonstrated that magnetic anomalies trend generally northeast-southwest in the southern areas of the Northwest Pacific (Fig. 37). Solov'yeva et al. (1963) mapped aeromagnetic data in the northern areas and discovered low intensity anomalies that trend parallel to the Kuril Trench, a trend which is more northerly than that of Uyeda et al. Of interest is an anomaly located at about 45°N, 162°E (as mapped by Solov'yeva). It coincides with the position of the Hokkaido Trough. Though roughly parallel to the trend of Uyeda's anomalies to the south, this anomaly probably is caused by the structure of the trough and parallel ridges.

Hilde (1976) offers the most complete published study of seafloor spreading as based on magnetic anomalies (Fig. 37). Hilde shows that the crust ages toward the southeast. Mesozoic anomalies plotted on his map are displayed with respect to time in Figure 30. Anomalies south of about 45°N are large amplitude and their trends are well-documented (Fig. 37). The CL anomaly is the youngest identifiable Mesozoic anomaly and dates at about 109 mybp. The CL anomalies coincide with the newly mapped Hokkaido Trough and may actually represent structural anomalies at this location. North of the trough area, magnetic anomalies are not decipherable because of very low amplitude and poor coverage. This area may very well be the Cretaceous quiet

zone, which is late Mesozoic crust with low amplitude magnetic anomalies. One hypothesis is that the Hokkaido Trough represents a structural boundary and that crust of unknown age lies to the north (D. W. Handschumacher, pers. comm.).

Northwest Pacific magnetic data are presently being compiled by the first author to better define map trends in the south and to decipher the crust to the north. For this report, it is assumed that the northern area represents crust formed during the Cretaceous quiet zone as proposed by Hilde (1976).

2. Plate Rotations

Positioning of Northwest Pacific crust through geologic time is achieved by adjusting the plate rotations formulated by Lancelot (1978). Lancelot's plate rotations are based upon the apparent trends of Pacific island and seamount chains, and the rotations are compatible to formation paleolatitudes from magnetic signatures of DSDP basalts. The three rotations are:

- o 125 to 70 mybp: clockwise rotation around a pole at 30°N and 97°W at a rate of 0.69°/my. This pole is presently located in central Texas.
- o 70 to 40 mybp: clockwise rotation around a pole at 11°N and 89°W at a rate of 0.57°/my. This pole is presently located just west of Nicaragua and Costa Rica.
- o 40 my to present: clockwise rotation around a pole at 67°N and 45°W at a rate of 0.5°/my. This pole is presently located in southern Greenland.

The rotations have been adapted for the Northwest Pacific by the authors.

Figure 38a traces the movement of Northwest Pacific crust. Northwest Pacific oceanic crust was first produced in the Cretaceous from the Kula Ridge, an east/west-trending spreading ridge which was subducted into North Pacific trenches. This

crust formed the southern flank of the ridge and moved southward relative to it. However, the actual movement of Pacific crust was to the northeast, as indicated by Figure 38a. By 115 mybp, the M-3 magnetic isochron was forming at the ridge crest, and basalt at DSDP sites 303 and 304 had formed. The Cretaceous quiet zone crust or present crust north of about 45°N began forming at about 105 mybp and presumably had formed before 80 mybp. At 72 mybp, Meiji Guyot formed from a "hot spot" on previously formed oceanic crust, and Suiko Seamount followed at 58 mybp. Present plate movement began at 40 mybp when the collision of Pacific crust with Japan and Kamchatka was initiated. The subduction of the Kula spreading center into North Pacific trenches roughly coincides with this change in plate movement (Hilde, 1977). The present-day Northwest Pacific is a portion of the southern flank of the Kula Ridge.

3. Sedimentary History

The sedimentary history is compatible with the geographic constraints of the plate rotations. Figure 38b illustrates sedimentary environments of Northwest Pacific crust as it formed from the Kula Ridge and the "hot spot". Each of the four major sediment components is affected by either geography or water depth. Silica production is latitudinally controlled, whereas carbonate sedimentation occurs only above the carbonate compensation depth. Terrigenous and volcanic sediments are dependent on proximity to the sediment source. Figure 30, showing the time distribution of sediment types from DSDP cores, should be referred to in the following discussion.

Northwest Pacific crust traversed the equatorial silica biogenic zone between 5°N and 5°S up to 105 mybp (Fig. 38b). In the sediment record (Fig. 30) DSDP cores 303, 304, and 436 have prominent basal chert layers. More chert is present at the older site 304 than at site 303, probably because site 304 traversed a greater distance through

the biogenic zone. Consequently, basal chert should be either sparse or absent on crust younger than 105 mybp, such as that north of 45°N.

Northwest Pacific crust was formed by the subducted Kula Ridge up to about 80 mybp. Since ridge crests often have depths above the carbonate compensation depth (CCD), the initial crust formed on the Kula Ridge was likely to have carbonate sediments; however, as the initial crust moved away from the ridge crest, it fell below the CCD and subsequent carbonate sediment dissolved. This sequence is demonstrated at DSDP sites 303 and 304 where chalks and nanno ooze occur only as basal sediments, and carbonates are rare throughout the remaining column.

Typical deep-sea sediments were deposited from 105-15 mybp because Northwest Pacific crust was present north of the equatorial silica biogenic zone, was deeper than the CCD, and was far from terrigenous sediment sources. Sedimentation was slow and resulted in 20 m of manganeseiferous clays at site 436. Sites 303 and 304 have a sediment hiatus in this time period indicating low deposition rates and erosion.

A "hot spot" created Meiji Guyot about 72 mybp and Suiko about 58 mybp; the southern Emperor Seamounts are younger than 58 mybp. Deposits near the newly forming seamounts probably contained locally derived volcanic sediments. Carbonate sediments are common on seamounts that have depths above the CCD and where the carbonate sediments are not diluted by abundant terrigenous or volcanic sediments. Basal sediments atop Meiji Guyot (DSDP site 192) consist of nanno ooze and chalks and are mixed with claystone that is probably of altered volcanic and pelagic origin.

At about 15 mybp, sedimentation rates in the Northwest Pacific increased due to influx of biogenic silica and volcanic materials. Large quantities of biogenic silica were deposited as the Pacific Plate moved into the high

latitude biogenic silica zone. As the plate then moved westward, it neared the volcanic sources of the Kuril Islands, Kamchatka and Japan.

Ninkovich (1975), who attributes large quantities of sediments to Kuril-Kamchatka volcanism, states that a period of maximum explosive volcanism occurred at 10 mybp. Abundant deposition of volcanics and biogenic silica continues today.

G. Seismic Activity

The Kuril-Kamchatka earthquake region is characterized by a tabular block of earthquake foci dipping landward from the Kuril-Kamchatka Trench. Under Kamchatka, the dip of this block is 50-60° for earthquakes having focal depths of 220 km or less and 75° for deeper ones. The focal zone block measures 40-50 km in thickness (Fedotov, 1968). A line of active volcanoes parallels the Kuril-Kamchatka Trench at an average distance of 200-260 km northwest of the trench axis. Beneath the volcanic zone the depth of the earthquakes averages 100 km under Kamchatka and 120 km under the Southern Kuril Islands. Deeper earthquakes occur underneath the southern Kuril volcanoes than those under the northern Kuril volcanoes. Deepest earthquakes occur where the block dips beneath the Sea of Okhotsk, and all earthquake activity ends where the block apparently terminates under continental areas of Sakhalin and Siberia at depths in excess of 400 km.

1. Seismic Studies

The seismicity of the Kuril region is dramatic and has been studied by Russian, Japanese, and western scientists. By analyzing focal mechanisms and magnitudes of earthquakes, Averyanova (1965, 1975) has mapped areas of horizontal and vertical compression and tension in the crust and upper mantle, and has correlated the zones with the repetition rates of earthquakes. Fedotov (1968, 1963) postulates velocity structures in various regions of the earthquake

zones. He states that there is a ten-fold decrease in earthquakes from the upper 20 km to 125 km and from 125 km to 250 km. Tarakanov and Leviy (1968) plotted earthquake magnitude vs. depth for all recorded world earthquakes and found intervals where high magnitude earthquakes are absent. These zones of low magnitude earthquakes (60-90 km, 120-160 km, 220-300 km and 370-430 km) were suggested to be low velocity and strength zones in the upper mantle of the Kuril region. Kasahara and Harvey (1976) reported results from an ocean-bottom seismometer (OBS) installed in the southern region of the Kuril Trench; they give velocity data based upon earthquakes occurring in the Kuril and Japan earthquake systems. Veith (1974) modeled the velocity structure of the region based upon earthquake data. Ukawa (1979) also gives velocity models of the upper mantle under the Kuril-Japan Trench and refutes the idea of a continuous low velocity layer paralleling the down-going slab. Earthquake data are compiled by the National Earthquake Information Service (NEIS), Boulder, Colorado, and analyses of these data are given in this report.

2. Earthquake Epicenters

Somewhat at variance with the usual seismological conventions, earthquake epicenters are plotted here in discrete depth intervals of 0-40 km, 40-70 km, 70-120 km, 120-200 km, 200-300 km, 300-400 km, and greater than 400 km using 1965-1975 data compiled by NEIS. Earthquakes plotted have magnitudes of four or greater. The position of the depth bands of earthquakes is correlated with the geography and the geology of the Kuril-Kamchatka region to disclose the seismic trends and inhomogeneities. Plots are presented in Figures 39-45.

Shallow earthquakes form the upper boundary of the focal zone and they occur in scattered areas outside the focal zone (Fig. 39). For the purposes of this report, shallow earthquakes are defined as those occurring at a depth

of 0-40 km. Earthquake focal depths cannot be resolved in the 0-10 km depth range. Most "shallow" earthquakes occur west of the Kuril-Kamchatka trench. In the vicinity of the trench, focal mechanism solutions indicate that the earthquakes are caused mainly by dip slip fault displacement or tensional stress (Aver'yanova, 1965).

Other zones of shallow earthquakes are located along Sakhalin and in the Western Aleutian area. The Southern Kuril region has the highest concentration of shallow earthquakes, while the sparsest concentration is at about 50°N, coincident with the location of an upper mantle bulge to be discussed. The Bussol Proliv region (47°N) is aseismic.

The 40-70 km earthquakes form a narrower band than the shallower earthquakes (Fig. 40). Greatest concentrations are again located in the Southern Kuril region, while the smallest concentration is in and north of the Bussol Proliv area. The Western Aleutian earthquakes diminish in concentration, presumably because the mechanism responsible for the Western Aleutian earthquakes is a strike slip movement along the trench (Cormier, 1975) rather than an underthrusting as in the Kuril region. In this depth range, earthquake mechanisms change from the tensional stress and normal fault displacement to compressional stress and thrust faulting (Aver'yanova, 1965).

Intermediate depth earthquakes occurring between 70 and 120 km are shown in Figure 41. This compact earthquake band is centered over the Vityaz Ridge in the Southern Kuril area and lies just east of the volcanic belt in the Northern Kurils and Kamchatka. Concentrations are only slightly higher in the Southern Kurils.

The 120-200 km depth earthquake band (Fig. 42) underlies the volcanic belt in the Southern Kuril area and lies just west of the volcanic belt of the Northern Kurils and Kamchatka. In the

Southern Kurils, the earthquakes are also scattered near the trench. This may be due to errors of locating the epicenters (R. Jacobson, pers. comm.). Concentrations are lowest under Kamchatka.

As compared to earthquakes shallower than 0-200 km, earthquakes deeper than 200 km (Fig. 43) exhibit obviously different distributions and concentrations. The 200-300 km earthquakes are concentrated in two regions: west of Hokkaido and west of the Northern Kuril Islands, with a gap existing between the two in the Kuril Basin. In summarizing the works of Russian authors, Sykes et al. (1968) agree that normal faulting is occurring in these deeper earthquakes and along the outer wall of the focal zone, whereas the shallower earthquakes are largely accompanied by thrust faulting.

The 300-400 km zone of epicenters (Fig. 44) is also concentrated in two regions: west of the Southern Kurils adjacent to the area where the gap in the 200-300 km quakes occurs, and west of Kamchatka where earthquakes are sparser. Gaps in earthquake distribution are found west of Hokkaido, where the highest concentrations of 200-300 km earthquakes occurred, and in the region of 49°N.

Earthquakes with depths of 400 km or more (Fig. 45) are scattered sparsely in a continuous zone that trends northeast-southwest from about 47°N to 54°N. The southern end of the zone lies beneath Sakhalin. The deepest earthquakes appear to end about 600-700 km west of the trench axis.

H. Deep Seismic Velocity Structure

The layering and associated seismic velocities which constitute the deep structure are presented for the following three areas: the seismically active area or focal zone, the areas beneath, and east of, the focal zone; and the areas above, and west of, the focal zone (Fig. 53). These gross areas cover all possible paths that

seismic waves from the seismically active areas might travel in reaching an MSS at the candidate sites. Although nuclear testing is not likely to occur deeper than 10 km, earthquakes in the active region can occur at any depth to 500 km or more. While the primary concern of this report is to research shallow events, the deep structure may influence the propagation patterns of even the shallowest events. For this reason, it is necessary to concern oneself with the deep earthquakes whose ray paths would enter the same volumes within the earth.

In addition to the seismological overview, related geophysical parameters, namely, free-air gravity and heat flow, are included in this section. A series of maps are used to organize the large quantities of information into a convenient, easily comparable format.

1. Deep Velocity Structure Beneath and East of the Focal Zone

Since the proposed MSS will be moored in Northwest Pacific oceanic crust, extensive knowledge of the deep structure is required to reliably explain local effects on incoming seismic waves. Unfortunately, specific data needed for study is not available. Generally, only large scale models can be formulated from the available data. Works by Lamont-Doherty Geological Observatory give generalized information for overall Northwest Pacific crustal velocities that is based upon seismic reflection and refraction work with sonobuoys. Soviet crust and upper mantle studies based upon deep seismic sounding (DSS) data yield crustal layer models different from those of Lamont scientists. OBS studies by the Hawaii Institute of Geophysics and Japan have resulted in upper mantle velocity measurements and models of the southern Kuril Islands.

From seismic refraction and reflection studies (Den et al., 1969; Houtz et al., 1970; Shor et al., 1970; Houtz, 1976; Houtz et al., 1976; and Houtz et

al., 1979), crustal models have been proposed for regions of the Pacific Ocean. General crustal sections are located in Figure 46 and are depicted in Figure 47. The basic profile is divided into layers 1 through 3 with sublayers. Layer 1 is unconsolidated sediment with an average velocity of 1.74 km/s (Houtz, 1979). Layer 2A is oceanic basalt that is possibly capped by consolidated sediments (layer 1B) and/or volcanic material (Houtz, 1976). Layers 2B, 2C, and 3 are oceanic crustal materials. Average Pacific crustal velocities for layers 2A through 3 are: 2A, 3.6 km/s; 2B, 5.2; 2C, 6.1; 3, 6.9 (Houtz, 1976). The profiles reveal that boundaries between 2A, 2B, and 2C are often difficult to delineate. Layer 2A velocities may approach layer 2B velocities in older crust (Houtz, 1976). Profile D in Figure 47 shows the crustal model used by Kasahara et al. (1976) for their OBS study on the oceanic crust adjacent to Hokkaido. The model is based upon Den et al. (1969) and Ludwig et al. (1966).

Soviet models of oceanic crust, based upon deep seismic sounding (DSS), are presented in Profiles T and A, respectively (Tuyezov, 1970, and Zverev, 1977). These models differ from LDGO profiles by the omission of layer 2 and by deeper penetration in the Soviet models. Of note is that oceanic crust in Tuyezov's (1970) model is thicker than the surrounding profiles. Zverev's model of the Northwest Pacific introduces a deeper (9.0 km/sec) boundary at a depth of 29 km, which he calls the true crust-mantle boundary. Though obvious differences occur between American and Soviet crustal models, the isostatic equilibrium of the models is not in dispute. The Soviet 6.3 km/sec to 7.0 km/sec "oceanic" layer appears to be an average of the LDGO layers 2 and 3.

2. Velocities in the Focal Zone

In general, the focal zone is the seismically active region where the downgoing oceanic slab of the Pacific plate underthrusts the Kuril Islands of

the Asian plate. Specific seismic velocities are difficult to measure for the focal zone, and measurements presented in this section represent some kind of overlap with areas above and below the focal zone.

Upper mantle models for regions seaward of the Kuril focal zone are presented by Kasahara et al. (1976), and include results from the works of Ukawa (1979) and Fedotov (1965, 1968). Velocities of P waves from two Kuril earthquakes have been measured through the upper mantle seaward of the southern Kuril Islands by an OBS moored on oceanic crust off Hokkaido (Kasahara et al., 1976); for positions of the earthquakes see Figure 46. Assuming a homogeneous upper mantle, V_p velocities of 8.97 ± 0.34 km/s for a 137 km deep earthquake (Q-2) and 8.12 ± 0.28 km/s for a 0-60 km earthquake (Q-1) were obtained. Based upon the seismic waves arriving at the OBS from focal zone earthquakes, Kasahara et al. concluded that V_p increased with depth in the upper mantle and that the average velocity for the upper 230 km is greater than 8.5 km/sec. Fedotov (1965) measured velocities of 8.2-9.0 under oceanic crust east of the southern Kuril Islands. He states that mantle velocities under oceanic crust are consistently higher than mantle velocities under the Kuril Island arc and the Sea of Okhotsk. Ukawa (1979) proposes that the low velocity layer beneath the Kuril Trench is not parallel to the downgoing slab. He describes a low velocity layer at 90-200 km depth that has 1-5% lower P wave and 5-10% lower S wave velocities than those found immediately above the layer. Adjacent to the focal area the low velocity layer thins, and no velocity gradient exists down to 30 km beneath the high velocity downgoing lithospheric slab. Ukawa's velocity model NVL is to be contrasted with the Japanese Trench model ARC-TR of Fukao (1977). Figure 48B shows that earthquake waves converging upon the Hawaiian OBS of Kasahara et al. (1976) would have to originate at focal depths greater than 200 km in order to penetrate the anomalous low velocity

gradient layer or no-velocity gradient layer. For the proposed MSS sites, earthquakes shallower than 100 km would not penetrate the low-velocity or no-velocity gradient layers. This model is probably false, since we did not consider the effects of refraction through the medium.

Focal zone models are presented by Tarakanov et al. (1968) and Veith (1974). Tarakanov et al. (1968) plotted high-magnitude earthquakes against depth and found that, at the following four intervals of focal depth, earthquakes were sparse: 60-90 km; 120-160 km; 220-300 km; and 370-430 km. They suggest that these depth ranges have low seismic velocity and material strength. Veith's (1974) focal zone model, Figure 48A, shows that seismic velocities are consistently greater within the focal zone than at equivalent depths on either side of the focal zone.

3. Seismic Velocities West of and Above the Focal Zone

This section deals with seismic velocity structures located geographically west of Kuril Trench and above the downgoing slab. The velocity structures in this area are important because shallow earthquakes are often scattered outside the focal zone, and potential nuclear tests may occur on Kamchatka, near Sakhalin, or within the broad band of shallow earthquakes between the trench and volcanic regions. Seismic wave ray paths of earthquakes occurring in those regions must travel through the crust and mantle above, and landward of, the focal area before reaching the proposed MSS site; hence, the velocity structures should be known.

Most velocity studies of the crust and mantle above the Kuril-Kamchatka focal zone were conducted by Russian scientists using the "deep seismic sounding" (DSS) method. The DSS method is described in Kosminskaya et al. (1968), and early DSS data were compiled by Kosminskaya et al. (1964). Cross

sections of velocity layers, contour maps of thicknesses of velocity layers, velocities used to delineate layers, and depths of the layers are presented in Figures 49 through 53. The cross sections (Fig. 49) are based upon DSS interpretations of Weizman (1965), Zverev (1977), Tuyezov (1970), Tuyezov et al. (1968), Sychev (1977), and Gayanov (1968). Contour maps (Fig. 50-53) are based upon the same DSS data interpreted by Sergeev (1977).

The Russian scientists generally divide the crust into the following velocity layers: an upper 2.0 to 2.8 km/s unconsolidated sediment layer; a "granitic" layer or "layer complex₁" with velocities of 4.3 to 6.0 km/s; and an "oceanic" layer or "layer complex₂" with velocities of 6.0 to 6.9 km/s. The principally terrigenous source of the sediment layer explains the higher velocities as compared to the 2.0 km/s oceanic sediments, since terrigenous sediment is generally more consolidated than deep ocean sediments.

Scientists disagree on the nature of the "granitic" layer, which is thickest under continental type crust. Tuyezov et al. (1968) believe that the "granitic" layer of the Kuril Islands is actually a consolidated sediment layer. This explanation was adopted by Sergeev (1977), and this material is included in his estimate of the thickness of the lower sedimentary layer (Fig. 53). Markinin (1968) proposed that andesitic volcanics constitute much of this layer.

Whatever the true nature of the 5.5 km/s average velocity layer, its occurrence is thickest under the continental crust of Kamchatka and Sakhalin, with lesser thicknesses under the Sea of Okhotsk and Kuril Islands. The layer is absent from Russian profiles of oceanic crust and the suboceanic Kuril Basin. Layer complex₂, which has an average velocity of 6.6 km/s, is the thickest crustal layer except in continental crust. It is present in oceanic crust and is thickest under the region between the trench and island

arc. Under the suboceanic Kuril Basin layer 2 is thin, but it constitutes the total solid crust (Profile H-H", Fig. 49). For a more explicit description of thicknesses of the crustal layers and the velocities used to define them, consult Figures 49-53.

Crustal thickness varies over the Kuril-Kamchatka focal zone (Sergeyev, 1977) (shown as depth to Moho in Fig. 50). Moho depths of 35 km under North and South Kuril Islands and Sakhalin, 30 km under much of the Sea of Okhotsk, and 40 km under Kamchatka are representative of subcontinental and continental type crust. Lesser Moho depths of 15 km under the Kuril Basin and 20 km under much of the central Kuril Island arc region represent suboceanic type crust. A region of anomalous, shallow Moho depth near the Bussol Proliv (see Map 1), which connects to the Kuril Basin, represents a suboceanic type crust bridging the Northwest Pacific to the Kuril Basin. Profile FF' (Figs. 46 and 49) illustrates the shallow Moho depth and its oceanic velocity structure.

Upper mantle velocities defining the Moho and presenting the deeper mantle velocities described in the works of Fedotov (1963, 1968) appear in Figure 48. Generally, upper mantle velocities are greater under the Northwest Pacific than under the Kuril-Kamchatka focal zone; both regions are characterized by velocities greater than 8.0 km/sec. Above the focal zone, velocities are generally 8.0 km/s or less. An exception to this rule is shown in Profile AA' of Figure 49, where Kamchatka is shown to have 8.2-8.5 km/s upper mantle velocities. This profile represents continental crust on Kamchatka, but its location is actually north of the seismic zone. Fedotov (1963), referenced in Sykes et al. (1968), presents increasing upper mantle velocities of 7.6 to 8.1 in descending order beneath the southern Kuril volcanic belt (Fig. 48).

I. Gravity and Heat Flow

Free-air gravity anomalies (Watts, 1976) (Fig. 54) and heat flow (Uyeda et al., 1968) (Fig. 55) are related to velocity structures. Large positive gravity anomalies generally occur over regions of thick crust that is isostatically too heavy, as between the volcanic arc and trench where the crust has been thrust upward. Large negative anomalies are present over the trench areas in response to the underthrusting of the downgoing slab. In the Northwest Pacific another large positive anomaly is located over the Emperor Seamounts. This anomaly is probably due to the isostatic surplus of volcanic material deposited. The seamounts are flanked by large negative anomalies, representing edge effects of the Emperor Seamounts. The anomalies are probably due to downwarping of the lithosphere caused by the load of the seamounts. Minor positive anomalies exist over the Hokkaido Rise; isostatic surplus of crust here can be explained by the buckling of the oceanic crust before it descends into the trench. The Shatsky Rise exhibits only a slight gravity anomaly, an occurrence indicating that the rise may be isostatically equalized.

Northwest Pacific crust generally has low heat flow; however, west of the Kuril Trench, the heat flow increases. Based upon the flow and conductivity measurements of Langseth et al. (1970), calculated borehole temperatures should not exceed 40°C, assuming the borehole is in an area that has less than 500 m of unconsolidated sediment cover. Uyeda et al. (1968) (Fig. 55) show that areas of highest heat flow occur in the Kuril Basin in the Sea of Okhotsk. The regions of known higher heat flow are located west of the Kuril Trench.

V. Discussion and Site Selection

The purpose of this discussion is to evaluate environmental parameters and propose potential MSS sites. Because environmental parameters vary in their relative importance to the MSS they

should be weighted for the selection of the best site. Parameters can be weighted according to the extent that they vary geographically, as well as how critical they are to MSS planning. Some parameters vary geographically, while others are essentially constant throughout the study areas. Some parameters pose no special constraints upon MSS engineering, while others require special attention.

Some environmental parameters which have less impact upon MSS site selection are those that are not critical to present MSS specifications or those that do not geographically vary. In our opinion, neither fouling nor heat flow pose serious problems to MSS engineering in any Northwest Pacific location. On the other hand, surface sediment types and surface sediment physical properties do not vary geographically, but these parameters pose MSS bottom mooring problems throughout the study because of low sediment rigidity.

Geographically varying parameters influencing MSS site selection are those that: (1) threaten MSS equipment, (2) cause acoustic noise, (3) specify better local environment, and (4) specify better regional location.

A. Environment Threats to MSS Equipment

Severe or catastrophic environmental conditions most likely to threaten MSS equipment include weather, sea states, icing, currents and vandalism. Generally, the severest weather, sea states, and icing occur in northern areas of the Northwest Pacific during the winter. Conditions become less severe to the southeast.

Vandalism poses a threat in areas of densest fishing because of either intentional or inadvertant fouling of MSS cables and buoys by long lines. Because fishing activity is greatest in the west and least to the northeast, it is not a likely threat east of the territorial limits (approximately 370 km).

Both wind stress and geostrophic currents will impact MSS design and implantation techniques. Winter storms will generate excessive surface currents and severely ice surface exposed instrumentation. Thus, a submersible buoy design must be considered as a means of protecting the installation and de-icing surface equipment. Minimum wind speeds and maximum water temperature increase the viability of the de-icing procedure.

B. Acoustic Noise Sources

Acoustic noise is caused by ship engines and current flow past suspended and bottom-mounted instruments. Local low-level seismicity could also be defined as noise in the MSS context. Noise caused by shipping and currents is greatest in the southern Northwest Pacific where the Kuroshio current dominates. An MSS site should be north of about 42°N to avoid this region of greatest noise. Geomorphologically constricted areas should be avoided in site selection because of possible intensified bottom currents. Possible areas of low seismicity might be the Hokkaido Rise and toward the Kuril-Kamchatka Trench area.

C. Optimum Local Environment

Ideal local environmental parameters consist of low bottom roughness, sediment thickness greater than 200 m, and homogeneous geologic features. Because installation of the MSS involves drilling through sediment and installing a seismometer in crustal rock, the local environment should also have a predictable geologic column which will not create drilling problems. Two site areas were chosen on the basis of their ideal local geology (Fig. 2). Site area 1 is a well-surveyed area but probably has chert at the base of the unconsolidated sediment. Although site area 2 is not as well-surveyed, chert beds there are probably either thinner or missing. Since drilling chert poses difficulties, site 2 may be the better location.

D. Optimum Regional Location

The authors assumed that the best regional criteria for an MSS location were:

- o to stay outside the 200 mile limit of foreign territories.
- o to be as close as possible to the Kuril-Kamchatka earthquake region to limit reception of seismic waves from other major seismic areas.
- o to be centered geographically opposite the Kuril-Kamchatka region to best receive uniform seismicity coverage.
- o to compliment existing earthquake monitoring stations on Japan, the Aleutians and Hawaii.

Based upon these criteria, the site areas chosen are adequate for an MSS installation.

Hart et al. (1980) have evaluated seismic propagation paths and suggested that highest energy received from Kuril-Kamchatka seismic occurrences for all depths are generally greatest in eastern regions of the Northwest Pacific which are greater than 500 km from the Kuril-Kamchatka Trench axis. Areas less than about 500 km from the trench are likely to fall in a seismic shadow zone, which might be an unfavorable condition for an MSS site. Unfortunately areas outside the shadow zone are poorly surveyed and are geologically complex. These areas are the northern Shatsky Rise, the Emperor Seamounts, and adjacent western basins, all of which have unpredictable acoustic basement.

Three additional sites outside the shadow zone have been selected. They are site 3 (41°N , 162.5°E), site 4 (44.8°N , 168°E) and site 5 (47.2°N , 166.5°E). All three sites are located on smooth bottom with a reverberant layer acoustic basement. The locations were selected for areas where this layer appears to thin, but data and control are poor for all three locations. Because the locations are farther from the trench than sites 1

and 2, more complex geologic structures exist between each site and the earthquake region. Site 3 is similar to site 1 in acoustic stratigraphy, sediment thickness, weather, and current conditions. Likely problems at site 3 are acoustic noise from currents and ships, unpredictable basement, and large seismic energy input for earthquakes from the Japan Trench. Sites 4 and 5 are more centrally located opposite the Kuril-Kamchatka Trench, but each have only about 200 m of sediment and are very poorly surveyed. Acoustic noise due to shipping and currents are less likely to be a problem, and weather conditions are slightly more severe than at site 3.

VI. Recommendations

In summary, the areas selected on the basis of environmental parameters are plotted on Figure 2. Sites 1 and 2 were chosen primarily because they have the best available local geological environments. Relative to other Northwest Pacific locations, site 1 has mild weather conditions and high acoustic noise, and is located south of the geographic center of the Kuril-Kamchatka seismic zone. On the other hand, site 2 has moderate weather conditions, moderate acoustic noise, and is centered geographically opposite the seismic zone. Sites 1 and 2 are located within the seismic "shadow zone" positioned by Hart et al. (1980). Three sites outside the shadow zone have been designated but in the opinion of the authors the sites are inferior to sites 1 and 2.

VII. References

Agapova, G. V. and G. B. Udintsev (1973). Zony Drobleniya Rel'yefu Dno V Severo Zapadnoy Kotlovine Tikhogo Okeana (Fracture Zone in Areas of Bottom Relief in the Northwestern Pacific Ocean Basin). Geomorfologiya, (GMFLAG), n. 2, p. 35-40.

Aver'yanova, V. N. (1965). Some Patterns of Seismic Dislocations in the

Far East, J.P.R.S. technical translation 65-31297, 28 p.

Aver'yanova, V. N. (1975). Glubinnaya Seismotektonika Ostrovnykh Dug Severo-Zapad Tikhogo Okeana (Deep-Seated Seismotectonics of Island Arcs, the Northwestern Pacific Ocean). Izd. Nauka, Moscow, SUN., p. 219.

Buffington, Edwin C. (1973). The Aleutian-Kamchatka Trench Conversion, An Investigation of Lithospheric Plate Interaction in Light of Modern Geotectonic Theory. Doctoral Dissertation, University of Southern California 233 pp.

Burk, C. A. and H. S. Gnibidenko (1977). The Structure and Age of the Acoustic Basement in the Okhotsk Sea. IN: Island Arcs, Deep Sea Trenches and Back Arc Basins, M. Talwani and W. Pitman III, eds., AGU, p. 451-461.

Chase, T., H. Menard and J. Mammerickx, (1970). Topography of the North Pacific. Technical Report TR-17, Inst. of Mar. Resources, Scripps Inst. of Oceanography, La Jolla, Calif.

Clague, D. A. and R. I. Jarrard (1973). Tertiary Pacific Plate Motion Reduced from Hawaiian-Emperor Chain. Geol. Soc. Am. Bull. 84:1135-1154.

Connolly, J. R. and M. Ewing (1970). Ice Rafted Detritus in Northwest Pacific Deep-Sea Sediments. From Hays ed., Geol. Soc. Am., Memoir 126, p. 219-232.

Cormier, V. F. (1975). Tectonics Near the Junction of the Aleutian and Kuril-Kamchatka Arcs and a Mechanism for Middle Tertiary Magmatism in the Kamchatka Basin. Geological Society of America Bulletin, Vol. 86, p. 443-453.

Creager, J. S., D. W. Scholl et al. (1973). Initial Reports of the Deep Sea Drilling Project. Vol. 19, Washington, D. C. (U.S. Govt. Printing Office).

Den, N. J., H. Holta, S. Asano, T. Yoshii, N. Sakajiri, and Y. Ichinose (1971). Seismic Refraction and Reflection Measurements Around Hokkaido, Part I, Crustal Structure of the Continental Slope Off Tokachi. J. Phys. Earth 19, 329-345.

Ewing, J., M. Ewing, T. Aitken, W. Ludwig (1968). North Pacific Sediment Layers Measured by Seismic Profiling. IN: The Crust and Upper Mantle of the Pacific Area, AGU Mono. 12, p. 147-186.

Fedotov, S. A. (1968). On Deep Structure, Properties of the Upper Mantle, and Volcanism of the Kuril-Kamchatka Island Arc According to Seismic Data. IN: The Crust and Upper Mantle of the Pacific Area Internat. Upper Mantle Proj. Sci. Rept. 15. Am. Geophys. Union Geophys. Mon. 12 (NAS-NRC Pub. 1687), p. 131-139.

Fedotov, S. A. (1965). Upper Mantle Properties of the Southern Part of the Kuril Island Arc According to Detailed Seismological Investigation Data. Tectonophysics, v. 2, n. 2-3, p. 219-225.

Frazer, J. F., D. L. Hawkins, and G. Arrhenius, T. E. Chase, H. W. Menard and J. Mammerickx (1972). Surface Sediments and Topography of the North Pacific. Inst. Marine Resources, Scripps Inst. Oceanog., TR 27, 28.

Fukao, Y. (1977). Upper Mantle P Structure on the Ocean Side of the Japan-Kurile Arc. R. Astron. Soc., Geophys. J. (GBR) (GEOJAN), v. 50, n. 3, p. 621-642.

Gorshkov, S. G., (1974). Atlas of the Oceans. Pacific Ocean Ministry of the Defense, USSR. 302 pp. English Introductions and Index (1976), Pergamon Press, 87 pp.

Griffin, J. J., H. Windom, and E. D. Goldberg (1968). The Distribution of Clay Minerals in the World Ocean. Deep Sea Research, vol. 15, p. 433-459.

Hart, R. S. and S. K. Kaufman (1980). Seismic Propagation in the Kuriles/Kamchatka Region. Sierra Geophysics, Inc., Technical Report S.G.I.-R-80-022, Arcadia, Calif., 77 p.

Hilde, T. W. C., N. Isezaki, and J. M. Wageman (1976). Mesozoic Seafloor Spreading in the North Pacific. IN: Geophys. Monogr. 19, Am. Geophys. Union, p. 205-226.

Hilde, T. W. C., S. Uyeda and L. Kroenke (1977). Evolution of the Western Pacific and its Margin. Tectonophysics, vol. 38, p. 145-165.

Horn, D. E., B. M. Horn and M. N. Delach (1970). Sedimentary Provinces of the North Pacific. IN: Geological Investigations of the North Pacific, Hays, ed., Geol. Soc. America Memoir 126, p. 1-20.

Houtz, R. (1976). Seismic Properties of Layer 2A in the Pacific. J. Geophys. Res., 81, p. 6321-6331.

Houtz, R. E., and W. J. Ludwig (1979). Distribution of Reverberant Subbottom Layers in the Southwest Pacific Basin. J. Geophys. Res., vol. 84, n. B7, p. 3497-3504.

Houtz, R. and J. Ewing (1976). Upper Crustal Structure as a Function of Plate Age. J. Geophys. Res., 81, p. 2490-2498.

Houtz, R., J. Ewing, and P. Buhl (1970). Seismic Data from Sonobuoy Stations in the Northern and Equatorial Pacific. J. Geophys. Res., 75, p. 5093-5111.

Kasahara, J. and R. R. Harvey (1976). Ocean Bottom Seismometer Study of the Kuril Trench Area. Hawaii Univ., Inst. Geophys., Rep. (USA) (HIGRAC), n. HIG-76-9, 24 pp.

Keller, G. H. (1969). Engineering Properties of Some Sea-floor Deposits. Journal of the Soil Mechanics and Foundations Division, SM6, p. 1379-1392.

Keller, G. H. and R. H. Bennett (1970). Variations in the Mass Physical Properties of Selected Submarine Sediments. Marine Geology 9, p. 215-223.

Kort, V. G. (1970). Sedimentation in the Pacific Ocean, Book I. Academy of Sciences of the USSR, Moscow, 427 pp.

Kosminskaya, I. P. and S. M. Zverev (1968). Deep Seismic Sounding in the Transition Zones from Continents to Oceans. IN: The Crust and Upper Mantle of the Pacific Area-Internat. Upper Mantle Proj. Sci. Rept. 15. Am. Geophys. Union Geophys. Mon. 12 (NAS-NRC PUB. 1687), p. 122-130.

Kosminskaya, I. P., S. M. Zverev, P. S. Veitsman and Yu. V. Tulina (1964). General Features of the Structure of the Earth's Crust in a Transition Zone, IN: Structure of the Earth's Crust in the Region of Transition from the Asiatic Continent to the Pacific Ocean. Edited by Ye. I. Galperin and I. P. Kosminskaya, p. 274-293. Izd. Nauka Moscow, 308 pp.

Lancelot, Y., and R. L. Larson (1975). Sedimentary and Tectonic Evolution of the Northwestern Pacific. Initial Reports of D.S.D.P. vol 32, p. 925-935.

Lancelot Y. (1978). Relation entre Evolution Sedimentaire et Tectonique de la Plaque Pacifique depuis le Crétacé Inférieur (Relations between Sedimentary Evolution and Tectonics of the Pacific Plate During the Lower Cretaceous. Soc. Geol. Mem. No. 134, 39 pp.

Langseth, M. C. and R. P. Von Herzen (1970). Heat Flow Through the Floor of the World Oceans. From The Sea, vol. 4 part I, p. 299-352.

Larson, R. L. and W. C. Pittman III. (1972). World-wide Correlation of Mesozoic Magnetic Anomalies and Its Implications. Geol. Soc. America Bull. vol. 83, p. 3645-3662.

Larson, R. L. and R. Moberly et al. (1975). Initial Reports of the Deep

Sea Drilling Project, vol. 32,
Washington, D. C. (U.S. Govt. Printing
Office) 980 pp.

Lee, H. J. (1973). Measurements and
Estimates of Engineering and Other
Physical Properties, Leg 19. IN: J.
S. Creager, D. W. Scholl et al. (1973).
Initial Reports of the Deep Sea
Drilling Project, vol. 19, Washington,
D.C. (U.S. Govt. Printing Office) p.
701-720.

Loomis, P., J. Bowman, C. Ross, E.
Kelly (1973). A Summary of Sediment
Size, Sound Velocities, X-Radiography,
and Mass Physical Properties of Nine
Cores from the North Pacific. U.S.
Naval Oceanographic Office, Washington,
D. C.

Ludwig, W. J., J. I. Ewing, M. Ewing,
S. Marauchi, N. Den, S. Asano, H.
Hoffa, H. Hayakawa, T. Asanuma, K.
Ichikawa and I. Noguzhi (1966).
Sediments and Structure of the Japan
Trench. *J. Geophys. Res.*, 71, p.
2121-2137.

Ludwig, W. J. J. Nafe and C. Drake
(1970). Seismic Refraction. IN: *The
Sea*, Maxwell, ed., v. 4, Part I, p.
53-84.

McAdoo, D. C., J. G. Cladwell and D. L.
Turcotte (1978). On the Elastic-
Perfectly Plastic Bending of the
Lithosphere under Generalized Loading
with Application to the Kuril Trench.
Geophys. J., v. 54, n. 1, p. 11-26.

Mammerickx, J. A. (1980). Deep Sea
Channel in the Northwest Pacific Basin.
Marine Geology 34, p. 207-218.

Markinin, E. K. (1968). Volcanism as
an Agent of Formation of the Earth's
Crust. IN: *The Crust and Upper Mantle
of the Pacific Area*. Amer. Geophys.
Union Monograph 12, p. 413-422.

Moore, D. G. (1962). Bearing Strength
and Other Physical Properties of Some
Shallow and Deep-Sea Sediments from the
North Pacific. *Geol. Soc. America Bull.*
vol. 73, p. 1163-1166.

Naval Oceanographic Office (1978).
Field Data Report: Pac-Oceano Survops
Summer 1977, Phase I. TN-3440-5-78,
26 p.

Naval Oceanographic Office (1969).
Bathymetric Atlas of the Northwestern
Pacific Ocean. N.O. Pub. 1301.

Naval Oceanographic Office (1971).
Bathymetric Atlas of the North Central
Pacific Ocean. N.O. Pub. 1302.

Ninkovich, D. and J. H. Robertson
(1975). Volcanogenic Effects on the
Rates of Deposition of Sediments in the
Northwest Pacific Ocean. *Earth and
Planetary Science Letters*, vol. 27, p.
127-136.

Reid, J. L. (1973). Northwest Pacific
Ocean Waters in Winter. *Johns Hopkins
Oceanographic Studies* no. 5, 93 pp.

Reid, J. L. and R. S. Arthur (1975).
Interpretation of Maps of Geopotential
Anomaly for the Deep Pacific Ocean.
J. Mar. Res., Supplement, p. 37-52.

Richards, A. F. (1961). Investigations
of Deep Sea Sediment Cores. U.S. Navy
Hydrographic Office Technical Report
63, 61 pp.

Scholl, D. W., J. R. Hein, M. Marlow,
and E. C. Buffington (1977). Meiji
Sediment Tongue: North Pacific Evidence
for Limited Movement Between the
Pacific and North American Plates.
Geological Society of America Bulletin,
vol. 88, p. 1567-1576.

Senior, C. W. (1976). Oceanographic
Observations of the Subarctic
Subtropical Transition Zone in the
Western North Pacific. Naval Ocean-
ographic Office TN-344-6-76, 34 pp.

Sergeyev, K. F. (1976a). *Tektonika
Kuril'skoy Ostrovnoy Sistemy* (Tectonics
of the Kuril Island System). Izd.
Nauka, Moscow, SUN., p. 239.

Shor, G. G., H. W. Menard and R. W.
Raitt (1970). Structure of the Pacific
Basin, from *The Sea* vol. 4, Part II, p.
3-27.

Solov'yeva, O. N. and A. G. Gainanov (1963). Geological Structure in the Zone of Transition from the Asiatic Continent to the Pacific Ocean in the Region of the Kuril-Kamchatka Island Arc, Soviet Geology 3, p. 113-123.

Sychev, P. M., H. Aoki, ed. and A. Iizuka, ed. (1976). Deep Fractures and Crust Formation in the North-West Pacific. IN: Volcanoes and Tectonosphere. Tokai Univ. Press, Tokyo, Japan, p. 341-357.

Sykes, Lynn R., Jack Oliver and Brian Isacks (1970). Earthquakes and Tectonics. IN: The Sea, vol. 4, Part I, A. E. Maxwell, ed., p. 353-420.

Tarakanov, R. Z. and N. V. Leviy (1968). A Model for the Upper Mantle with Several Channels of Low Velocity and Strength. IN: The Crust and Upper Mantle of the Pacific Area, Knopoff et al., ed., Amer. Geophys. Union Monograph 12, p. 43-50.

Tuyezov, I. K. (1970). Seismicheskiye Razrezy Zemnoy Kory Severo-Zapadnogo Chasti Tikhookeanskogo Pordivizhnogo Poyasa (Seismic Sections of the Earth's Crust in the Northwestern Part of the Pacific Ocean Mobile Belt). Akad. Nauk SSSR, n. 3, p. 100-104.

Tuyezov, I. K., P. M. Sichev, R. Z. Tarakanov and M. L. Krasny (1968). Structure of the Folded Areas and Recent Geosynclines of the Okhotsk Area. IN: The Crust and Upper Mantle of the Pacific Area, Knopoff et al. eds., Amer. Geophys. Union Monograph 12, p. 473-480.

Ukawa, M. (1979). The Landward Thinning of the Low-Velocity Layer Across the Kurile-Japan Trench: Earth Planet. Sci. Lett., v. 43, n. 3, p. 434-440.

U.S. Navy (1977). Surface Currents. Naval Oceanographic Special Pub. 1402, NP4, NPS, NP7.

Uyeda, S. (1967). Results of Geomagnetic Survey during the Cruise of R/V ARGO in Western Pacific 1966 and the Compilation of Magnetic Charts of the Same Area. Bulletin of the Earthquake Research Institute, vol. 45, p. 799-814.

Veith, K. F. (1974). Relationship of Island Arc Seismicity to Plate Tectonics. Doctoral Dissertation, Southern Methodist University, Dallas, Texas, 67 pp.

Watts, A. B. (1976). Gravity Field of the Northwest Pacific Ocean Basin and Its Margin. Geol. Soc. Am., MC 10.

Watts, A. B. (1977). Gravity Field of the Northwest Pacific Ocean Basin and Its Margin Kuril Island Arc-Trench System. Geol. Soc. Am., MC-27.

Weisman, P. S. (1966). On the Deep Structure in the Kuril-Kamchatka Region. IN: Continental Margins and Island Arcs-Internat. Upper Mantle Comm. Symposium, Ottawa, 1965. Canada Geol. Survey Paper 66-15, p. 244-251.

Zverev, S. M., B. S. Vol'govskiy, ed. and A. G. Rodnikov, ed. (1977). Seismicheskiye Svoystva Zemnoy Kory i Verkhney Mantii Severo-Zapadnogo Chasti Tikhogo Okeana (Seismic Properties of the Earth's Crust and Upper Mantle of the Northwestern Pacific Ocean). Izd. Nauka, Moscow, SUN., p. 28-34.

Bibliography I: Environment of the Northwest Pacific Ocean

Argo (1966). Lists of Cores and Dredge Hauls, Zetes Expedition. University of California, Scripps Institution of Oceanography.

Aver'yanova, V. N. (1965). Some Patterns of Seismic Dislocations in the Far East. News of the Academy of Seismic USSR, Geological Series, No. 5, p. 93-114,

Aver'yanov, V. S., and B. I. Mil'nikov (1975). The Evolution of the Earth's Magnetic Field in Kamchatka from Paleomagnetic Data. No. 6, p. 86-91.

Baud (1961). List of Sediment Cores, Legs II, IV and V, Japanyon Expedition. Scripps Institution of Oceanography.

Belyayev, I. V. (1970). Osnovnyye Geologicheskiye Rezul'taty Regional'nykh Geofizicheskikh Rabot (Main Geological Results of Regional Geophysical Surveys). Geologiya SSSR, Geologicheskoye Opisaniye, Kniga 2, USSR, Minist. Geol., Moscow, p. 236-246.

Bezrukov, P. L. (1955). Bottom Deposits of the Kurilo-Kamchatka Depression. Works of the Institute of Oceanology, Vol. XXI, p. 97-129.

Bezrukov, P. I. (1970). Sedimentation in the Pacific Ocean. Parts I and II, Akad. Nauk SSSR, 419 and 428 pp.

Bottom Sediment Listings, Cruise 29 of the Vityaz 1958-1959 WDC-A Cruise 137.1B5, Akademiya Nauk, SSSR, Institut Okeanologii.

Bottom Sediment Listings. Beringovo Morskaya Ekspeditsiya Nov-Dec 1958, WDC-A Cruise 137.11E-1 (7hemchug), Akademiya Nauk, SSSR, Institut Okeanologii.

Braitseva, O. A., and Melekestsev (1970). Principal Stages of Development of the Relief of Kamchatka. Geomorphology, no. 3, p. 197-202.

Buffington, Edwin C. (1973). The Aleutian-Kamchatka Trench Conversion; an Investigation of Lithospheric Plate Interaction in Light of Modern Geotectonic Theory. Doctoral Dissertation, U. Southern California, 233 p.

Chase, T., H. Menard, and J. Mannerickx (1971). Topography of the North Pacific. Tech. Rep. TR-17, Inst. of Mar. Resour., Scripps Inst. of Oceanogr., La Jolla, California.

Coleman, P. J. (1973). The Western Pacific, Island Arcs, Marginal Seas, Geochemistry. Crane, Russak & Co., N.Y., 675 pp.

Cormier, V. F. (1975). Tectonics Near the Junction of the Aleutian and Kuril-Kamchatka Arcs and a Mechanism for Middle Tertiary Magmatism in the Kamchatka Basin. Geological Society of America Bulletin, Vol. 86, p. 443-453.

Cormier, V. F. (1972). Tectonics of Northeast Kamchatka and the Commander Island (abs.). Eos (Am. Geophys. Union, Trans.), (EOSTAJ), v. 53, n. 11, p. 1043.

Creager, J. S., D. W. Scholl, R. E. Boyce, R. J. Echols, T. J. Fullam, J. A. Grow, I. Koizumi, H. J. Lee, H. Y. Ling, R. J. Stewart, P. R. Supko and T. R. Worsley (1973). Site 192 from Deep Sea Drill. Proj. Initial R.p. (IDSDA6), v. 19, Kodiak, Alaska to Yokohama, Japan; July-Sept. 1971, p. 463-553.

Davydov, M. N. and Dunichev (1968). Neogene Deposits of the Southern Greater Kuril Islands. Geologiya i

Geofizika, vol. 12, p. 112-116, In Russian.

Dobretsov, N. L. (1975). Metamorphic Belts of the Northwestern Circum-Pacific Region. Geological Society of America, Special Paper 151, p. 133-144.

Drozdov, V. N. and A. S. Sarkisyan (1975). Calculation of Currents for the Northwestern Pacific. Atmospheric and Oceanic Physics, vol. 11, no. 4, p. 394-403.

Eremenko (1973). Geologic Structure and Oil and Gas Prospects of USSR. AAPG Bulletin, vol. 57, p. 241-243.

Erickson, B. H., F. P. Naugler and D. K. Rea (1971). Evidence of Crustal Plate Movements in the Western North Pacific (abs.). IN: Ocean Floor Spreading, Int. Union Geod. Geophys., 15th Gen. Assem. (24ZNAK), Moscow, p. 38.

Ewing, J., M. Ewing, T. Aitken and W. Ludwig (1968). North Pacific Sediment Layers Measured by Seismic Profiling. IN: The Crust and Upper Mantle of the Pacific Area, AGU Mono. 12, p. 147-186.

Ewing, M., S. Tsunematsu, J. Ewing, and L. H. Burckle (1966). Lower Cretaceous Sediments from the Northwest Pacific. Science (AAAS), v. 152, n. 3723, p. 751-755.

Frazer, J. Z., et al. (1972). Surface Sediments and Topography of the North Pacific. IMR TR 27, 28, Maps.

Freitag, H. P. (1979). Structure and Path of the Kuroshio Over the Izu Ridge. University of Washington.

Fullam, T. J. (1973). Some Aspects of Late Cenozoic Sedimentation in the Bering Sea and North Pacific Ocean. Initial Reports D.S.D.P. 19, p. 887-896.

Fujita, Yukinori, Hoshino, Michihei, ed.; and Hitoshi Aoki, ed. (1972). Crustal Movements Around Island-Arcs in Northwest Pacific since Late Cretaceous. Tokai Univ. Press, Tokyo, Japan, p. 1-30.

Fujita, Y. and Hoshino (1970). Crustal Movements Around Island-Arcs in the Northwest Pacific since Cretaceous. from Island Arcs and Ocean, Tokai Univ., p. 27-30.

Garkalenko, I. A. and S. A. Ushakov (1978). Zemnaya Kora Kurilskogo Regiona (The Crust of the Kuril Region). Sov. Geol., n. 11, p. 46-59.

Gaynanov, A. G., Ye. I. Isayev and G. B. Uditsev (1968). Magnitnye Anomalii i Morfologiya Dna Ostrovnykh Dug Severo-Zapadnoy Chasti Tikhogo Okeana (Magnetic Anomalies and Bottom Morphology of Island Arcs in the Northwest Pacific Ocean). Okeanol. (Akad. Nauk SSSR), v. 8, n. 6, p. 1017-1024.

Gaynanov, A. G., I. P. Kosminskaya and P. A. Stroyev (1968). Geofizicheskiye Issledovaniya Glubinnogo Stroyeniya Beringom Morya. Akad. Nauk SSSR Izv. Fizika Zemli, n. 8, p. 3-11.

Gaynanov, A. G. and L. P. Smirnov (1962). Stroyeniye Zemnoy Kory v Oblasti Perekhoda Ot Aziatskogo Kontinentalnogo Tikhomu Okeanu. Sov. Geolo., n. 3, p. 108-118.

Gnibidenko, G. S. (1970). On the Basement of the Northwest Sector of the Pacific Belt. Tectonophysics, (TCTOAM), v. 9, n. 6, p. 513-523.

Gnibidenko, G. S. (1976). Rift System of the Sea of Okhotsk. Acad. Sci. USSR, Dokl., Earth Sci. Sect. (USA) (DKESA9), v. 229, n. 1-6, p. 36-38.

Gnibidenko, H. S. (1973). Crustal Structure and Evolution in the Northwestern part of the Pacific Belt. IN: The Western Pacific, ed. Coleman, p. 435-449.

Gnibidenko, G. S. ed., Yu. A. Kosygin, ed. and K. F. Sergeev (1976). Stroyeniye Zemnoy Kory i Verkhneye Mantii v Zone Perekhoda Ot Aziatskogo Kontinenta K Tikhomu Okeanu (Structure

of the Earth's Crust and Upper Mantle in the Transition Zone from the Asiatic Continent to the Pacific Ocean). Izd. Nauka, Novosibirsk, SUN., 368pp.,

Gnibidenko, G. S., M. L. Krasnyy and N. P. Luk'yanov (1975). Novyye Dannyye O Strukture Osadochnogo Chekhla Podnyatiya Shatskogo i Severo-Zapadnoy Plity Tikhogo Okeana (New Data on the Sedimentary Cover Structure of the Shatsky Rise and the Northwestern Plate of the Pacific Ocean). Akad. Nauk SSSR, Dokl. SUN, (DANKAS), v. 221, n. 1, p. 209-212.

Gorshkov (1974). World Ocean Atlas, Pacific Ocean. Vol. 1, Ministry of Defense, USSR Navy, 302 pp, Russian.

Grabkov, V. K. (1973). O Sootnoshenii Strukturny Rel'yefa Sveremennyy Kuril' Skoy Geosinklinal'noy Oblasti (Inter-relationship of the Structure and Relief of the Present-Day Kuril Geosynclinal Province). Akad. Nauk SSSR, Geomorfol. Kom., Plenum, Mater., (33ZXAK), n. 10, p. 159-160.

Grabkov, V. K. and Yu A. Pavlov (1973). Neotectonic Movements and Isostatic State of the Crust in the Kurile Island Arc Region. Acad. Sci. USSR, Dokl., Earth Sci. Sect. (USA) (DKESA9), v. 203, n. 1-6, p. 55-57.

Greene, H. G., G. B. Dalrymple, and D. A. Clague (1978). Evidence for Northward Movement of the Emperor Seamounts, Geology, vol. 6, p. 70-74.

Hamilton, E. L., D. G. Moore, E. C. Buffington and P. L. Sherrer (1974). Sediment Velocities from Sonobuoys: Bay of Bengal, Bering Sea, Japan Sea, and North Pacific. Journal of Geophysical Research, vol. 79, no. 17, p. 2653-2668.

Hanks, T. C. (1970). The Kuril Trench-Hokkaido Rise System: Large Shallow Earthquakes and Simple Models of Deformation (abs.). Eos (Am. Geophys. Union, Trans.), v. 51, n. 11, p. 823.

Hanks, T. C. (1971). The Kuril Trench-Hokkaido Rise System: Large Shallow Earthquakes and Simple Models of Deformation. R. Astron. Soc., Geophys. J., (GEOJAN), v. 23, n. 2, p. 173-189.

Hays, J. D. (1970). Geological Investigations of the North Pacific, GSA Memoir 126, 323 pp.

Hein, J. R., D. W. Scholl and C. E. Guthmacher (1976). Diagenesis of Neogene Diatomaceous Sediment from the Far Northwest Pacific and Southern Bering Sea (abs.). Geol. Soc. Am., Abstr. Programs (USA) (GAAPBC), v. 8, n. 3, Cordilleran Section, 72nd Annual Meeting, p. 379-380.

Hilde, T. W. C., N. Isezaki, and J. M. Wageman (1976). Mesozoic Seafloor Spreading in the North Pacific. IN: Geophys. Monogr. 19, Am. Geophys. Union, p. 205-226.

Hilde, T. W. C., S. Uyeda and L. Kroenke (1977). Evolution of the Western Pacific and its Margin. Tectonophysics, vol. 38, p. 145-165.

Hill, H. D. S., W. Johnson, J. Knop and V. Williams (1967). A Summary of Sediment Size and Composition Analyses of a Core and Grabs Off Kamchatka. U.S. Oceanographic Office, Washington, D. C.

Honza, E. (1978a). Basic Framework of the Island Arc System in the NW Pacific Margin (abs.). Sci. Counc. Japan., Tokyo, Japan.

Honza, E. (1978b). Geological History of the Kuril Basin and the Tertiary Trough; Preliminary Concluding Remarks. (GH77-3 Cruise) Jap., Geol. Surv. Cruise Rep., n. 11, p. 60-69.

Honza, E., ed., K. Tamaki and K. Nishimura (1978). Sonobuoy Refraction Measurement. (GH77-3 Cruise) Jap., Geol. Surv., Cruise Rep., n. 11, p. 46-49.

Horn, D. R., Horn and Delach (1970). Sedimentary Provinces of the North Pacific. GSA Memoir 126, p. 1-20.

Houtz, R. (1976). Seismic properties of layer 2A in the Pacific. *J. Geophys. Res.*, 81, p. 6321-6331.

Houtz, R. E. and W. J. Ludwig (1979). Distribution of Reverberant Sub-bottom Layers in the Southwest Pacific Basin. *JGR*, vol. 84, no. B7, p. 3497-3504.

Houtz, R., and J. Ewing (1976). Upper Crustal Structure as a Function of Plate Age. *J. Geophys. Res.*, 81, p. 2490-2498.

Houtz, R., J. Ewing, and P. Buhl (1970). Seismic Data from Sonobuoy Stations in the Northern and Equatorial Pacific. *J. Geophys. Res.*, 75, p. 5093-5111.

Hulsemann, J., J. C. Bowman, J. E. McLane, B. Strong and W. J. Vestal (1971). A Summary of Sediment Size and Composition (exclusive of Organic Matter) of Cores from the Sea of Okhotsk, U.S. Naval Oceanographic Office, Washington, D. C.

Hulsemann, J., J. C. Bowman, R. M. Jeso, J. E. McLane and W. J. Vestal (1971). A Summary of Sediment Size and Composition (exclusive of Organic Matter) of Cores from the Northwest Pacific Ocean (Area 19). U.S. Naval Oceanographic Office, San Diego, California.

Jackson, E. D., E. A. Silver, and G. B. Dalrymple (1972). Hawaiian-Emperor Chain and its Relation to Cenozoic Circumpacific Tectonics. *Geological Society of America Bulletin*, vol. 83, p. 601-618.

Johnson, O. A. (1974). Deep Pacific Circulation Intensification During the Early Cenozoic. *Marine Geology*, 17: p. 71-78.

Kaneoka, Ichiro (1972). Evidence of Subsidence of Seamounts in the North-Western Pacific. *Marine Geophysical Research*, vol. 1, Issue 4, p. 412-417.

Knopoff, L., Drake and Hart (1968). The Crust and Upper Mantle of the Pacific Area. *AGU Monograph* 12, 522 pp.

Kosygin, V. U. and L. A. Pavlov (1975). Edge Effect as a Factor in Interpretation of Gravity Anomalies in the Transition Zone from Asian Mainland to Pacific Ocean. *Akademii Nauk SSSR Doklady*, vol. 221, no. 4, p. 917-920, in Russian.

Kosygin, V. Yu, and L. A. Pavlov (1975). Geology and Gravity of the Kuril Region. *Akademii Nauk SSSR Doklady*, vol. 220, no. 3, p. 661-675, in Russian.

Karsnyy, M. I. and K. Kochergin (1975). The Nature of the Regional Magnetic Anomalies in the Northwestern Pacific. *Geologiya Goefizika*, vol. 3, p. 84-94, in Russian.

Krasnyy, M. L. and Ye. U. Kochergin (1977). Magnetic Anomalies in the NW Pacific. IN: *Geofizicheskiye Issledovaniya Zony Perekhodaya*, p. 117-126, in Russian.

Kropotkin, P. N. and Shakhavarstova (1965). Geological Structure of the Circum-Pacific Mobile Belt. *Transactions* vol. 134 of *Akad. of Sciences, USSR, Geological Inst.* 366 pp., in Russian.

Lancelot, Y. and R. L. Larson (1975). Sedimentary and Tectonic Evolution of the Northwestern Pacific. Initial Rpts. of D.S.D.P. vol. 32, p. 925-935.

Lancelot, Y. (1978). Relations Entre Evolution Sedimentaire et Tectonique de La Plaque Pacifique Depuis le Cretace Inferieur (Relations Between Sedimentary Evolution and Tectonics of the Pacific Plate During the Lower Cretaceous). *Soc. Geol. Fr., Mem.*, No. 134, 39 pp. (incl. English sum.).

Larson, R. L. and C. G. Chase (1972). Late Mesozoic Evolution of the Western Pacific Ocean. *Geological Society of American Bulletin*, vol. 83, p. 3627-3644.

Legler, V. A. and O. G. Sprokhtin, ed. (1976). Deformatsiya Pogruzhayushchey Litosfernoy Plity i Prodol'nyye Sdvigi Kuril-Kamchatskoy Ostrovnoy Dugi (Deformation of the Subsiding Lithospheric Plate and Longitudinal Shifts of the Kuril-Kamchatka Island Arc). Akad. Nauk SSSR, Inst. Okeanologii, im. P. P. Shirpova, Moscow, SUN, p. 103-147.

Lisitsyn, A. P. (1959). Bottom Sediments of the Bering Sea, Trudy Inst. Okean., vol. 29, p. 65-183.

Lisitsyn, A. P., I. E. Mikhaltsev N. N. Sysoev and G. B. Uditsev (1956). New Data on the Thickness and Bedding of the Porous Deposits of the North-western Pacific Ocean. The Oceanographic Institute of the Academy of Sciences of the USSR, No. 2.

Lisitsyn, A. P. (1955). Some Data on the Distribution of Suspended Particles in the Waters of the Kurile-Kamchatka Trench. Trudy Instituta Okeanologii, vol. XII, p. 62-96.

Lisitzin, A. P. (1966). Processes of Recent Sedimentation in the Bering Sea. Acad. of Sciences of the USSR Inst. of Oceanology, 575 pp, in Russian.

Lisitzin, N. A. and Dvopetzkaye (1972). Lithologic Profile of the Northwest Pacific Ocean. Litologiya Polezniye Iskopaemiye, p. 3-25, in Russian.

Liu, Hsi-Ping (1980). The Structure of the Kuril Trench-Hokkaido Rise System Computed by a Plastic Time-Dependent Plastic Plate Model Incorporating Rock Deformation Data. JGR, v. 85.

Ljama, A. (1960). The Bottom Sediments of the Japan and Kuril Trenches Collected by the Ryofu Maru During JEDS Contribution #8. Oceanographical Magazine, vol. 11, issue 2, p. 225-231.

Loomis, P., J. Bowman, C. Ross, and E. Kelly (1973). A Summary of Sediment Size, Sound Velocities, X-Radiography, and Mass Physical Properties of Nine Cores from the North Pacific. U.S.

Naval Oceanographic Office, Washington, D. C.

Loomis, P. B. and J. C. Bowman (1968). A Summary of Sediment Size, X-Radiography, Sound Velocities, and Mass Physical Properties of 16 cores from the North Pacific. West Coast Lab Facility, U.S. Naval Oceanographic Office, Washington, D. C.

Lynn, R. J. and J. C. Reid (1968). Characteristics and Circulation of Deep and Abyssal Waters. Deep-Sea Research, 76(33), 8089-8097.

Lyubimova, Ye. A., V. N. Nikitina and G. A. Tomara (1976). Teplovyye Polya Vnutrennikh i Okrainnykh Morey SSSR; Sostoyaniye Nablyudeniy i Teoriya Interpretatsii Dyunernykh Neodnorodnostey (Heat Field of the Inland and Marginal Seas of the USSR; State of Observations and the Theory of Interpretation of Two-Dimensional Inhomogeneities). Izd. Nauka, Moscow, SUN, p. 222.

McAdoo, D. C., J. G. Cladwell and D. L. Turcotte (1978). On the Elastic-Perfectly Plastic Bending of the Lithosphere Under Generalized Loading with Application to the Kuril Trench. Geophys. J., v. 54, n. 1, p. 11-26.

Mantyla, A. W. (1975). On the Potential Temperature in the Abyssal Pacific Ocean. J. Mar. Res. 33:341-354.

Markev, M. S. and M. Yu. Khotin (1973). Structures and Geological History of the Kuril-Kamchatka Island Arc. Univ. West. Austr. Press, Nedlands, p. 239-246.

Marr, J. C. (1970). The Kuroshio. A Symposium of the Japan Current. East-West Center Press, Honolulu, 611 pp.

Marshall, M. (1978). The Magnetic Properties of some DSDP Basalts from the North Pacific and Inferences for Pacific Plate Tectonics. J. Geophys. Res. (USA), (JGREA2), v. 83, n. B1, p. 289-308.

Marshall, Monte C. (1975). Summary of Physical Properties, Leg 32. Deep Sea Drill. Proj., Initial Rep. (IDSDA6), v. 32, p. 961-962.

Masuzawa, J. (1962). The Deep Water in the Western Boundary of the North Pacific. *J. Oceanogr. Soc. Japan*, 20th Ann. vol., p. 279-285.

Melville (1971). List of Cores and Dredge Hauls Antipode Expedition. Scripps Institute of Oceanography.

Minayev, Yu. N. and A. A. Suvorov (1974). Structure of Sediment Cover in the Kuril-Japanese Trench Based on Seismic Data. *Geol. Geofiz.* vol. 2, p. 113-117, in Russian.

Mogi, Kiyoo (1973). Relationship Between Shallow and Deep Seismicity in the Western Pacific Region. *Tectonophysics*, vol. 17, p. 1-22.

Moriyasu, S. (1972). Deep Waters in the Western North Pacific. IN: *Kuroshio Its Physical Aspects*, Stommel, H. and Yoshida eds. Univ. Tokyo Press, p. 387-407.

Murdmaa, I. O. and Bezrukov (1970). Sedimentation in the Kuril-Kamchatka Trench. *Akademia Nauk SSSR, Institute Okeanolgii Trudy*, vol. 86.

Naval Oceanographic Office (1978). Field Data Report: Pac-Oceano Surveys Summer 1977, Phase I. TN-3440-5-78, 26 pp.

Naval Oceanographic Office (1969). Bathymetric Atlas of the Northwestern Pacific Ocean. N.O. Pub. no. 1301.

Naval Oceanographic Office (1971). Bathymetric Atlas of the North Central Pacific Ocean. N.O. Pub. no. 1302.

Ninkovich, D. and J. H. Robertson (1975). Volcanogenic Effects on the Rates of Deposition of Sediments in the Northwest Pacific Ocean, *Earth and Planetary Science Letters*, vol. 27, p. 127-136.

Oser, R. K. (1972). *Textural Analysis of Fine-Grained Sediments: Pelagic Sediments of the Northwest Pacific*. Oregon State University (Thesis).

Panfilova, S. G. (1965). Characteristics of the Distribution of Water Temperature and Salinity in the North Pacific Ocean. *Okeanolgicheskiye Issledovaniya*, no. 13, p. 47-54.

Peive, A. V. and Markov (1973). 'Basaltic' Layer of the Crust in the West Pacific, from the Western Pacific. IN: *The Western Pacific*, Coleman ed., p. 349-354.

Radzikovskaya, M. A. (1965). Basic Features of Water Structure in the North Pacific Ocean. *Okeanolgicheskiye Issledovaniya*, no. 13, p. 41-46.

Regan, R. D., J. C. Cain, and W. M. Davis (1975). A Global Magnetic Anomaly Map. *Journal of Geophysical Research*, vol. 80, no. 5, p. 794-802.

Reed, R. K. (1969). Deep Water Properties and Flow in the Central North Pacific. *J. Mar. Res.*, 27:24-31.

Reid, J. L. (1973). Northwest Pacific Ocean Waters in Winter. *Johns Hopkins Oceanographic Studies* no. 5, 93 pp.

Reid, J. L. (1965). Intermediate Waters of the Pacific Ocean. *Johns Hopkins Oceanographic Studies* no. 2, 85 pp.

Reid, J. L. and R. S. Arthur (1975). Interpretation of Maps of Geopotential Anomaly for the Deep Pacific Ocean. *Journal of Marine Research*, supplement, p. 37-52.

Romankevich, E. A. (1962). Organic Substance in the Surface Layer of Bottom Sediments in the Western Region of the Pacific Ocean. *Oceanological Researchers*, Akademia Nauk SSSR, vol. 5, p. 67-111.

Romankevich, E. A. (1966). Stratigraphy and Absolute Age of Deep-Sea Sediments in the Western Pacific.

Results of Researchers on IGY Projects,
p. 5-165.

Romankevich, Ye. A. (1969). Composition of the Organic Matter of Sediments from the Kuril-Kamchatka Trench. *Oceanology*, vol. 9, no. 5, p. 644-653.

Rotman, V. K. (1976). Geochemical Data on Structural Relationships Between the Pacific Ocean Floor and the Circum-Pacific Geosynclinal Belt in the Southern Part of the Kurile Arc. *Akad. Sci. USSR, Earth Science Section*, vol. 228, Iss. 1-6, p. 29-32.

Rozinov, M. I. and D. I. Kolesnikov (1977). Relationship of Most Recent Volcanism with Tectonics in the East Kamchatka and Kurile Zone. *Geotectonics (USA)* (GEOTBK), v. 10, no. 5, p. 371-377.

Scholl, D. W. (1974). Sedimentary Sequences in the North Pacific Trenches. IN: *Geology of Continental Margins*, Burke, C. A. and Drake, eds., N.Y., Springer, Verlag, p. 493-504.

Scholl, D. W. and J. S. Creager (1975). Geological Synthesis of Leg 19 (DSDP) Results; Far North Pacific Aleutian Ridge and Bering Sea. *Initial Reports D.S.D.P.*, v. 19, p. 897-913.

Scholl, D. W., J. R. Hein, M. Marlow and E. C. Buffington (1977). Meiji Sediment Tongue: North Pacific Evidence for Limited Movement Between the Pacific and North American Plates. *Geological Society of America Bulletin*, vol. 88, p. 1567-1576.

Senior, C. W. (1976). Oceanographic Observations of the Subarctic, Sub-tropical Transition Zone in the Western North Pacific. *Naval Oceanographic Office TN-344-6-76*, 34 pp.

Sergeyev, K. F. (1976). Tectonics of the Kuril Island System. *Nauka*, Moscow, USSR, 239 pp.

Serova, M. Ya., G. P. Borzunova and M. N. Shapiro (1977). The Paleogene in the Southern Part of Karagin Island

(Eastern Kamchatka). *Int. Geol. Rev. (USA) (IGREAP)*, v. 19, n. 3, p. 349-357.

Shapiro, M. N. (1976a). Northeastern Continuation of the East Kamchatka Synclinorium. *Geotectonics (USA) (GEOTBK)*, v. 10, n. 1, p. 76-78.

Shapiro, M. N. (1976b). *Tektonicheskoye Razvitiye Vostochnogo Obramleniya Kamchatki (Tectonic Evolution of the Eastern Part of the Kamchatka Peninsula)*. Izd. Nauka, Moscow, SUN, p. 122.

Shapiro, M. N. and V. A. Seliverstov (1976). Morphology and Age of Folded Structures in Eastern Kamchatka, at the Latitude of the Kronotskiy Peninsula. *Geotectonics (GEOTBK)*, v. 9, n. 4, p. 240-244.

Sheymann, Yu. M. (1968). Tectonics of the Upper Parts of the Mantle Under Geosynclines and Island Arcs, IN: *The Crust and Upper Mantle of the Pacific Area Internat.* Upper Mantle Proj. Sci. Rept. 15, Am. Geophys. Union Geophys. Mon. 12, p. 466-472.

Skorikova, M. F. (1977). Physical Properties of Rocks in the Zone of Transition from the Asian Continent to the Pacific Ocean. *Int. Geol. Rev. (USA) (IGREAP)*, v. 19, n. 11, p. 1321-1325.

Snegovskoy, S. S. (1970). Reflection Studies Near Southern Kurile Islands During 1968. *Akad. Sci. USSR Doklady Earth Science Section*, vol. 195, p. 9-11.

Snegovskoy, S. S. and Yu. L. Neverov (1970). Structure of Sediments in the Sea Basins Adjacent to Iturup Island. *Trudy-Akad. Nauk SSSR*, vol. 24, p. 95-101, in Russian.

Snegovskoy, S. S. and S. M. Aleksandrov (1971). *O Tektonike Zapadnogo Borta Kuril'skoy Kotloviny (Tectonics of the West Flank of the Kuril Deep)*. *Geotektonika*, (GTKTA2), n. 5, p. 105-110.

Snegovskoy, S. S. and S. M. Aleksandrov (1971). Tectonics of the West Flank of the Kuril Deep. *Geotectonics (GEOTBK)*, v. 5, p. 324-326.

Solomon H. and K. Ahlnas (1977). Eddies in the Kamchatka Current. *Deep-Sea Research*, vol. 25, p. 403-410.

Solomon, L. P., A. E. Barnes and C. R. Lunsford (1977). Ocean Route Envelopes. Planning Systems, Inc., McLean, Virginia.

Solov'yeva, I. A. (1976). Deep Structure of the Pacific Crust. *Geotectonics (USA) (GEOTBK)*, v. 10, n. 3, p. 157-168.

Solov'yeva, N. A. (1968). Role of Volcanism in the Genesis of Rocks of the Lesser Kurile Suite. *Acad. Sci. USSR, Dokl., Earth Sci. Sect.*, v. 179, p. 64-66.

Stauder, W. and L. Maulchin (1976). Fault Motion in the Larger Earthquakes of the Kurile-Kamchatka Arc and of the Kurile-Hokkaido Corner. *J. Geophys. Res. (JGREA2)*, v. 81, n. 2, p. 297-308.

Stommel, H. and K. Yoshida (1972). Kuroshio, Physical Aspects of the Japan Current. U. Wash. Press, 517 pp.

Sugenaga (1976). Isostasy and Flexure of the Lithosphere under the Hawaiian Islands and Emperor Seamounts. *EOS*, v. 57, Iss. 4, p. 325.

Sugimara, Yukio and Miyake Yasuo (1968). Studies of a Deep Sea Core V-20-130, pt. 7 Western North Pacific, Natural Science and Museums (Tokyo) Bulletin, v. 11, Iss. 3, p. 327-332.

Suprunenko, O. I. (1973). Relationship Between the Structures of Eastern Kamchatka and the Pacific Ocean Floor. *Akad. Sci., USSR, Dokl. Earth Sci. Sect.*, v. 206, p. 46-48.

Sychev, P. M. (1976). Volcanoes and Tectonosphere. Tokai Univ. Press, p. 341-357.

Sychev, P. M. and Snegovskoy (1976). Abyssal Depressions of the Okhotsk, Japan, and Bering Seas. *Pacific Geology*, v. 11, p. 57-80.

Sychev, P. M. (1971). Geologic Nature of Gravity Anomalies of the Bering Sea. IN: *Island Arcs and Marginal Seas*, p. 257-260.

Sychev, P. M., H. Aoki, ed. and A. Iizuka, ed. (1976). Deep Fractures and Crust Formation in the North-West Pacific. IN: *Volcanoes and Tectonosphere*. Tokai Univ. Press, Tokyo, Japan, p. 341-357.

Sychev, P. M. and R. Z. Tarakanov (1976). Some Inferences on the Upper Mantle Structure and Deep Processes Occurring in the Northwest Pacific. *Can. J. Earth Sci. (CJESAP)*, v. 13, n. 12, p. 1725-1729.

Taft, B. A. (1978). Structure of Kuroshio South of Japan. *J. Marine Res.*, v. 36, n. 1, p. 77-117.

Taft, B. A., A. R. Robinson and Schmitz (1973). Current Path and Bottom Velocity of the Kuroshio. *J. of Physical Oceanography*, v. 3, p. 247-256.

Tarr, A. C. and F. J. Mauk (1976). Focal Mechanism Map of the Northwestern Pacific Ocean (abs.). *EOS, (Am. Geophys. Union Trans.) (USA) (EOSTAJ)*, v. 57, n. 10, p. 760.

Tsunogai, S., Matsumoto, Kido, Nozaki and Hatteri (1972). Two Discontinuities in the Deep Water of the Western North Pacific Ocean. *Deep-Sea Research* v. 20, p. 527-536.

Tuyezov, I. K. (1970a). Seismicheskiye Razrezy Zemnoy Kory Severo-Zapadnog Chasti Tikhookeanskogo Pordiviznogo Poyasa (Seismic Sections of the Earth's Crust in the Northwestern Part of the Pacific Ocean Mobile Belt). *Akad. Nauk SSSR*, n. 3, p. 100-104.

Tuyezov, I. K. (1970b). Seismicheskiye Razrezy Zemnoy Kory Severo-Zapadnog Chasti Tikhookeanskogo Povizhnogo

Poyasa (Seismic Profiles of the Crust in the Northwestern Part of the Pacific Ocean Belt. Geol. Goefiz. Akad. Nauk SSSR, Sib. Otd., (GGASAS), n. 3, p. 100-104.

Tuyezov, I. K., M. L. Krasnyy, S. A. Solov'yev and E. V. Kochergin (1970). The Earth-Kurile Magnetic Anomaly. Phys. Solid Earth, (IPSEBQ), n. 1, p. 60-62.

Tuyezov, I. K. (1975a). Litosfera Aziatsko-Tikhookeanskoy Zony Perekhoda (Lithosphere of the Transition Zone Between Asia and the Pacific Ocean). Izd. Nauka, Sib. Otd., Novosibirsk, SUN, p. 230.

Tuyezov, I. K. (1975b). Models of the Subsurface Structure of Some Areas in the Northwest Sector of the Asia-Pacific Transition Zone with a Continental Crustal Structure. Acad. Sci. USSR, Dokl., Earth Sci. Sect., (USA) (DKESA9), v. 220, n. 1-6, p. 103-106.

Tuyezov, I. K., M. L. Krasnyy, B. I. Vasil'yev and A. A. Kulikov (1975c). Geologicheskoye Stroyeniye Yuzhnogo Zvena Kuril'skoy Ostrovnoy Dugi (Structure of the Southern Part of the Kuril Island Arc). Geol. Geofiz., Akad. Nauk SSSR, Sib. Otd., (SUN), (GGASAS), n. 12, p. 63-71.

Tuyezov, I. K. (1975d). Inhomogeneities in the Upper Mantle of the Asiatic Margin of the Pacific. Acad. Sci. USSR, Dokl., Earth Sci. Sect. (USA) (DKESA9), v. 219, n. 1-6, p. 26-28.

Tuyezov, I. K. (1976a). Modeli Glubinnogo Stroyeniya Osnovnykh Tipov Struktur Severo-Zapadnogo Sektora Zony Perekhoda ot Aziatskogo Kontinenta K Tikhomu Okeanu (Models for the Deep-Seated Structure of the Main Structural Types in the Northwestern Sector of the Transitional Zone Between the Asian Continent and the Pacific Ocean). Geol. Geofiz., Akad. Nauk SSSR, Sib. Otd., (SUN), (GGASAS), n. 1, p. 86-90.

Tuyezov, I. K., H. Aoki, ed. and S. Iizuka, ed. (1976b). On the Geologic Nature of the Okhotsk and Japan Sea Abyssal Depressions. Tokai Univ. Press, Tokyo, Japan, p. 333-340.

Uda, M., and K. Hasunuma (1969). The Eastward Subtropical Countercurrent in the Western North Pacific Ocean. Journal of Oceanographical Society of Japan, v. 25, n. 4, p. 201-210.

Udintsev, G. V. (1954). New Data on the Belief of the Kurile-Kamchatka Depression, Dokl. Akad. Nauk SSSR, v. 94, p. 315-318.

Udintsev, G. B. (1959). The Bottom Relief of the Bering Sea, Akad. Nauk SSSR, v. 29, p. 17-64.

Udintsev, G. B. and Beresnev (1976). Geological/Geophysical Interpretations from Vityaz Cruise in the Northwest Pacific and Sea of Okhotsk. IN: Geologo-Geofizicheskie Issledovaniya Zony Perekhoda ot Aziatskovo Kontinenta K Tikhomu, p. 19-29, in Russian.

Uyeda, S. (1975). Northwest Pacific Trench Margins. IN: Geology of Continental Margins, Burk, C.A. and Drake eds., p. 473-491.

Uyeda, S. (1967). Results of Geomagnetic Survey during the Cruise of R/V ARGO in Western Pacific 1966 and the Compilation of Magnetic Charts of the Same Area. Bulletin of the Earthquake Research Institute, v. 45, p. 799-814.

U.S. Navy (1977). Surface Currents. Naval Oceanographic Office Special Pub. 1402, NP 4, NP 5, NP 7.

Vasillyev, B. I. (1975). Geologic Structure of the Pacific Shelf of the Lesser Kurile Ridge. Akad. Science USSR, Doklady Earth Science Section, v. 219, p. 105-107.

Vlasov, G. M. (1976). Island Arcs and the New Global Tectonics. Geotectonics, v. 10, n. 1, p. 3-10.

Watts, A. B., M. Talwani, and J. R. Cochran (1976). Gravity Field of the Northwest Pacific Ocean Basin and Its Margin. AGU Monograph #19, p. 17-34.

Watts, A. B. (1976). Gravity Field of the Northwest Pacific Ocean Basin and Its Margin. Geological Society of America, MC 10.

Watts, A. B. (1977). Gravity Field of the Northwest Pacific Ocean Basin and Its Margin. Kuril Island Arc-Trench System, Geological Society of America, MC 27.

Veselov, O. V., N. A. Volkova, G. D. Yeremin, N. A. kozlov and V. V. Soinov (1974). Izmereniye Teployogo Potoka v Zone Perkhoda ot Aziatskogo Materika k Tikhomu Okeanu (Measurement of the Heat Flow in the Transition Zone Between the Asian Continent and the Pacific Ocean). Akad. Nauk SSSR, Dokl. (DANKAS), v. 217, n. 4, p. 897-900.

Von Huene, R., N. Nasu, M. Arthur, J. P. Cadet, B. Carson, R. Reynolds, B. L. Shaffer, S. Sato, and G. Bell (1978). On Leg 57, Japan Trench Transected. Geotimes (USA) (GEOTAJ), v. 23, n. 4, p. 16-20.

Watts, A. B. and M. Talwani (1975). Gravity Effect of Downgoing Lithospheric Slabs Beneath Island Arcs. Geol. Soc. Am., Bull., (BUGMAF), v. 86, n. 1, p. 1-4.

Weisman, P. S. (1966). On the Deep Structure in the Kuril-Kamchatka Region. IN: Continental Margins and Island Arcs Internat. Upper Mantle Comm. Symposium, Ottawa, 1965, Canada Geol. Survey Paper 66-15, p. 244-251.

Yasui, M., S. Uyeda, T. Watanabe, Asano, Shuzo, ed. and G. B. Udintsev, ed. (1971). Heat Flow in the Western Margin of the North Pacific and Its Geophysical Implications. IN: Island Arc and Marginal Sea; Proceedings of the First Japan-USSR Symposium on Solid Earth Sciences, Tokai Univ. Press., Japan, p. 289-296.

Zverev, S. M., B. S. Vol'govskiy, ed. and A. G. Rodnikov, ed. (1977). Seismicheskiye Svoystva Zemnoy Kory i Verkney Mantili Severo-Zapadnoy Chasti Tikhogo Okeana (Seismic Properties of the Earth's Crust and Upper Mantle of the Northwestern Pacific Ocean). Izd. Nauka, Moscow, SUN., P. 28-34.

Bibliography II: Seismology and Geophysics of the Kuril-Kamchatka Trench Area

Abe, K. (1975). Reliable Estimation of the Seismic Moment of Large Earthquakes. *J. Phys. Earth (Tokyo)* (UPN) (UPHEAF), v. 23, n. 4, p. 381-390.

Abe, Katsuyuki, Sato, Yasuo and Jose, Frez (1970). Free Oscillations of the Earth Excited by the Kurile Islands Earthquakes 1963. *Tokyo Univ., Earthquakes Res. Inst., Bull.*, (TDJKAZ), v. 48, Part 2, p. 87-114.

Agapova, G. V. and G. B. Ustinov (1973). Zony Drobleniya Rel'yefa Dna V Severo Zapadnoy Kotlovine Tikhogo Okeana (Fracture Zone in Areas of Bottom Relief in the Northwestern Pacific Ocean Basin). *Geomorfologiya*, (GMFLAG), n. 2, p. 35-40.

Alekseyev, B. V., E. G. Zhiltsov, A. A. Suvorov, and A. A. Kulikov (1972). Novyye Dannyye O Glubinnom Stroyenii Zemnoy Kory V Rayone Yuzhnykh Kuril' Skikh Ostrovov (New Data on the Deep Structure of the Earth's Crust in the Southern Kuril Island Area). *Geol. Geofiz. Akad Nauk SSSR, Sib. Otd.*, (GGSASA), n. 4, p. 107-114.

Andriyeva, T. A. (1972). Tipovyye Geofizicheskiye Kharakteristiki Osnovnykh Otritsatel'nykh Struktur Kamchatki (Typical Geophysical Characteristics of Main Negative Structures in Kamchatka). IN: *Tektonika I Neftegazonosnost' Vostoka SSSR.*, Vses. Neft. Nauchno-Issled. Geologorazved. Inst., Tr. (INGIAG), n. 309, p. 96-104.

Andreyev, A. A. (1973). K Voprosu Ob Izostazii Okhotskogo Regiona (Isostasy of the Okhotsk Region). *Geol. Geofiz. Akad. Nauk SSSR. Sib. Otd.* (GGASAS), n. 8, p. 108-112.

Aprelkov, S. Ye. (1977). K Voprosu O Meso-Kaynozoyskom Razvitiu Kurilo-

Kamchatskoy Ostrovnoy Dugi (The Meso-Cenozoic Evolution of the Kuril-Kamchatka Island Arc). *Akad. Nauk SSSR, Sib. Otd., Sakhalin. Kompleksn. Nauchno-Issled. Inst. Tr.*, n. 41, Part 1, p. 82-89

Aver'yanov, V. S. and B. I. Mill'nikov (1976). The Evolution of the Earth's Magnetic Field in Kamchatka from Paleomagnetic Data. *Phys. Solid Earth (IPSEBQ)*, v. 11, n. 6, p. 395-398.

Aver'yanova, V. N., R. N. Burymskaya and Yu. V. Riznichenko, ed. (1976). Defitsit Aftershokov Soprovozhdayushchikh Forshokov Katastroficheskikh Zemletryaseniy (The Deficit of Aftershocks Following the Foreshocks of Catastrophic Earthquakes). *Izd. Nauka, Moscow, SUN.*, p. 132-149.

Aver'yanova, V. N. (1975). Glubinnaya Seismotektonika Ostrovnykh Dug Severo-Zapad Tikhogo Okeana (Deep-Seated Seismotectonics of Island Arcs, the Northwestern Pacific Ocean). *Izd. Nauka, Moscow, SUN.*, p. 219.

Aver'yanova, V. N. (1973). Seismic Foci in the Far East. *Isr. Program Sci. Transl.*, Jerusalem, p. 270.

Aver'yanova, V. N., A. A. Borisov, ed. and Yu. K. Shchukin, ed. (1975). Svyaz' Parametrov Seismichnosti I Glubinnogo Stroyemyy-Kurilo-Kamchatskoy Zony (Relationship Between Seismicity and Deep Structure Parameters of the Kuril-Kamchatka Zone). *Izd. Nauka, Moscow, SUN.*, p. 84-104.

Averyanova, V. N., Shuzo, Asuno ed. and G. B. Ustinov, ed. (1971). Seismological Description of the Upper Mantle Processes Within the Northwest Pacific Belt. IN: *Island Arc and Marginal Sea, Proceedings of the First Japan-USSR*

Symposium on Solid Earth Sciences.
Tokai Univ. Press., Japan p. 225-238.

Bailey, K. A., A. K. Cooper, M. A. Marlow and D. W. Scholl (1976). Preliminary Residual Magnetic Map of the Eastern Bering Shelf and Parts of Western Alaska. U.S. Geol. Surv. Misc. Field Stud. Map (USA) (XMFSD), n. MF-716.

Belov, S. V., N. I. Migunov and G. A. Sobolev (1974). Magnetic Effects Accompanying Strong Earthquakes on Kamchatka. Geomagn. Aeron. (GMARAX), v. 14, n. 2, p. 321-323.

Belyayev, I. V. (1970). Osnovnyye Geologicheskiye Rezul'taty Regional'nykh Geofizicheskikh Rabot (Main Geological Results of Regional Geophysical Surveys). Geologiya SSSR, Geologicheskoye Opisanie, Kniga 2, USSR, Minist. Geol., Moscow, p. 236-246.

Belyayevskiy, N. A., I. S. Vol'vovskiy and V. Z. Ryaboy (1971). Seismicheskaya Rassloennyost' Zemnoy Kory i Verkhney Chasti Mantii (Seismic Layering of the Earth's Crust and the Upper Mantle). Priroda Seismicheskikh Granits V Zemnoy Kore, Akad. Nauk SSSR, Nauchn. Sovet Kompleksn. Issled. Zemnoy Kory Verkn. Mantiy, Moscow, p. 6-31.

Bodunov, Ye. I. (1976). Seismogeologicheskaya Kharakteristika i Uchet Izmeneniya Skorostey Pri Provedenii Rabot MOV V Rayonakh Vostochnoy Sibiri (Seismic Characteristics and Velocity Variation Determined by the Reflected Wave Technique, East Siberia). Geol. Geofiz. Akad. Nauk SSSR, Sib. Otd. (SUN) (GGASAS), n. 10 (202), p. 113-121.

Boldyrev, S. A. and Yu. V. Riznichenko, ed. (1976). Gorizontall'nyye Neodnorodnosti i Seismicheskaya Anizotropiya Verkhney Mantii U Yugo-Vostochnogo Poberezhiya Kamchatki. IN: Issledovaniya Po Fizike Zemletryaseniy (Horizontal Heterogeneities and Seismic Anisotropy of the Upper Mantle Beneath the Southeastern Coast of Kamchatka). Izd. Nauka, Moscow, SUN., p. 201-217.

Boldyrev, S. A. (1974). Distribution of Elastic Wave Velocities at the Juncture of the Kuril-Kamchatka and Aleutian Island Arc. Acad. Sci. USSR, Dokl., Earth Sci. Sect. (USA) (DKESA9), v. 215, n. 1-6, p. 1-3.

Boldyrev, S. A. and S. A. Fedotov, ed. (1974). Spektry Blizkikh Kuril'skikh Zemletryaseniy i ikh Izmeneniye Vo Vremeni IN: Seismichnost' i Seismicheskiy Prognoz, Svoystva Verkhney Mantii i ikh Svyazi S Vulkanizmom Na Kamchatke (Spectra of Close Kuril Earthquakes and Their Changes in Time). Izd. Nauka, Sib. Otd., Novosibirsk, SUN., p. 119-133.

Bolt, B. A. (1977). Ocean Bottom Seismometry; A New Dimension to Seismology. Bull. Geofis. Teor. Appl. v. 20, n. 75-76, p. 107-115.

Bulin, N. K. (1977). Glubinnoye Stroyeniye Kamchatki i Kuril'skikh Ostrovov Po Seismicheskim Dannym (Deep-Seated Structure of Kamchatka and the Kuril Islands Based on Seismic Data). Sov. Geol. (SUN) (SVGLA2), n. 5, p. 140-148.

Burymskaya, R. N. (1976). The June Earthquakes of 1973 in the Region of the Lesser Kurile Ridge. Phys. Solid Earth (USA) (IPSEBQ), v. 12, n. 5, p. 294-299.

Chang, F. S. and L. Knopoff (1977). Improved Regionalization of the Eurasian Continent Using Rayleigh Waves (abs.). Geol. Soc. Am., Abstr. Programs (USA) (GAAPBC), v. 9, n. 4, p. 398-399.

Cockerham, R. (1976). Upper Cretaceous Pacific DSDP Basalt Magnetic Paleolatitudes and their Implications for Pacific Plate Motion and Secular Variation (abs.). EOS (Am. Geophys. Union, Trans.) (USA) (EOSTAJ), v. 57, n. 12, p. 932.

Cooper, A. K., K. A. Bailey, J. I. Howell, M. S. Marlow, and D. W. Scholl (1976). Preliminary Residual Magnetic Map of the Bering Sea Basin and the

Kamchatka Peninsula. U.S. Geol. Surv., Misc. Field Stud. Map (USA) (XMFSD), n. MF-715.

Cooper, A. K., J. R. Childs, M. S. Marlow and D. W. Scholl (1977). Multi-channel Seismic Reflection Data in the Bering Sea Basin (abs.). Geol. Soc. Am., Abstr. Programs (USA) (GAAPBC), v. 9, n. 7, p. 934.

Cormier, Vernon F. (1972). Tectonics of Northeast Kamchatka and the Commander Island (abs.). EOS (Am. Geophys. Union, Trans.) (EOSTA), v. 53, n. 11, p. 1043.

Creager, J. S., D. W. Scholl, R. E. Boyce, R. J. Echols, T. J. Fullam, J. A. Grow, I. Koizumi, H. J. Lee, J. Y. Ling, R. J. Stewart, P. R. Supko and T. R. Worsley (1973). Site 192. Deep Sea Drill. Proj. Initial Rep. (IDSDA6), v. 19, Kodiak, Alaska to Yokohama, Japan; July-Sept. 1971, p. 463-553.

Creager, J. S., D. W. Scholl, R. E. Boyce, R. J. Echols, T. J. Fullam, J. A. Grow, I. Koizumi, H. J. Lee, H. Y. Ling, R. J. Stewart, P. R. Supko and T. R. Worsley (1973). Site 193. Deep Sea Drill. Proj. Initial Rep. (IDSDA6). v. 19, Kodiak, Alaska to Yokohama, Japan; July-Sept. 1971, p. 555-566.

Davydova, N. I., S. M. Zverev, G. G. Mikhota, and Yu. V. Tulina (1971). Characteristics of Waves from the Mohorovicia Discontinuity Based on Explosion Seismology Data (abs.). Geosci. Bull., Ser. A (GSCBB4), v. 2, n. 11, p. 6.

Devyyatilova, A. D., Yu. S. Zhelubovskiy, V. K. Roman, and B. A. Sal'nikov (1972). Okhotskiy Basseyn Sedimentatsii (The Okhotsk Sedimentary Basin). IN: Geologiya Severo-Vostochnoy Azii. Tom 2. Stratigrafiya I Paleogeografiya; Neogenovaya Sistema, p. 408-413.

Dziewonski, A. and M. Landisman (1979). Great Circle Rayleigh and Love Wave Dispersion from 100 to 900 Seconds. R. Astron. Soc., Geophys. J., (GEOJAN), v. 19, n. 1, p. 37-91.

Erickson, B. H., F. P. Naugler, and D. K. Rea (1971). Evidence of Crustal Plate Movements in the Western North Pacific (abs.). IN: Ocean Floor Spreading, Int. Union Geod. Geophys., 15th Gen. Assem. (24ZNAK), Moscow, p. 38.

Ewing, Maurice, Tsunematsu Saito, John Ewing and L. H. Burckle 1966). Lower Cretaceous Sediments from the Northwest Pacific. Science (AAAS), v. 152, n. 3723, p. 751-755.

Fedotov, S. A. (1965). Upper Mantle Properties of the Southern Part of the Kuril Island Arc According to Detailed Seismological Investigation Data. Tectonophysics, v. 2, n. 2-3, p. 219-225.

Fedotov, S. A., P. I. Tokarev, M. F. Bobkov, and I. P. Kuzin (1967). Zemletryaseniya Kamchatki I Domandorskikh Ostrosov Po Dannym Detal'nykh Seismologicheskikh Nablyudeniy (Earthquakes in Kamchatka and the Komandorski Islands According to Data from Detailed Seismic Observations). Akad. Nauk SSSR, Moscow, p. 166-184.

Fedotov, S. A. (1968). On Deep Structure, Properties of the Upper Mantle, and Volcanism of the Kuril-Kamchatka Island Arc According to Seismic Data. IN: The Crust and Upper Mantle of the Pacific Area Internat. Upper Mantle Proj. Sci. Rept. 15. Am. Geophys. Union Geophys. Mon. 12 (NAS-NRC Pub. 1687), p. 131-139.

Fedotov, S. A. (1969). Seismicity of the Focal Region of the Catastrophic Iturup Earthquake of November 6, 1958 and Seismic Forecasting. Phys. Solid Earth, n. 1, p. 1-6.

Fedotov, S. A. and S. A. Boldyrev (1969). O Zavisimosti Poglosheniya Ob'Yemnykh Voln Ot Chastoty V Kore I Verkhney Mantii Kuril'Skoy Ostrovnoy Dugi (On the Dependence of Body Wave Absorption of Frequency in the Crust and Upper Mantle of the Kuril Island Arc). Akad. Nauk SSSR Izv. Fizika Zemli, n. 9, p. 17-33.

Fedotov, S. A., N. A. Dolbilkina, V. N. Morozov, V. I. Myachkin, V. B. Preobrazensky, and G. A. Sobolev (1970). Investigation on Earthquake Prediction in Kamchatka. IN: Earthquake Mechanics. Tectonophysics, v. 9, n. 2-3, p. 249-258.

Fedotov, S. A., A. M. Bagdasarova, I. P. Kuzin, and R. Z. Tarakanov (1971a). Earthquakes and the Deep Structure of the South Kurile Island Arc. Isr. Program Sci. Transl., p. 249.

Fedotov, S. A., A. A. Gusev, S. A. Boldyrev, G. A. Sobolev, V. I. Morozov, V. I. Myachkin, V. B. Preobrazhenskiy, and N. A. Dolbilkina (1971b). Progress V Issledovaniyakh Po Prognozu Zemlet-ryaseniy Na Kamchatke abs. (Progress on the Earthquakes Prediction in Kamchatka). Int. Union Geod. Geophys., 15th Gen. Assem., (24ZNAK), Moscow, p. 12-13.

Fedotov, S. A. and L. S. Shumilina (1971c). Sysmicheskaya Sotryasayemost' Kamchatki (Seismic Vibrations of Kamchatka). Fix. Zemli, (IAFZAK), n. 9, p. 3-15.

Fedotov, S. A. and L. S. Shumilina (1971d). Seismic Shakeability of Kamchatka. Phys. Solid Earth, (IPSEBZ), n. 9, p. 607-615.

Fedotov, S. A. and P. I. Tokarev (1971e). Zemletryaseniya, Svoystva Verkhney Mantii Kamchatki I Ikh Svyazi S Vulkanizmom/Po Dannym Na 1970 Rod (abs.). Int. Union Geod. Geophys., 15th Gen. Assem. (24ZNAK), Moscow, p. 7-8.

Fedotov, S. A., A. A. Gusev and S. A. Boldyrev (1972a). Progress of Earthquake Prediction in Kamchatka. Tectonophysics, (TCTOAM), v. 14, n. 3-4, p. 279-286.

Fedotov, S. A. (1972b). Energeticheskaya Klassifikatsiya Kurilo-Kachatskikh Semietryaseniy I Problema Magnitud (Classification, Based on Energy, of Kuril-Kamchatka Earthquakes, and the Problem of Magnitude). Izd. Nauka, p. 116.

Fedotov, S. A. (1973). Deep Structure Under the Volcanic Belt of Kamchatka. Univ. West. Austr. Press. Nedlands, p. 247-254.

Fedotov, S. A., ed. and A. M. Bagdasarova (1974a). Seysmichnost' Kamchatki I Komandorskikh Ostrovov V 1897-1961 Gg. Po Dannym Instrumental'nykh Nablyudeniy (Seismicity of Kamchatka and Komandorski Islands in 1897-1961 According to Instrument Measurements). Izd. Nauka, Sib. Otd., Novosibirsk, SUN., p. 7-34.

Fedotov, S. A., ed. (1974b). Seysmichnost' I Seysmicheskiy Prognoz, Svoystva Verkhney Mantii I Ikh Svyazi S Vulkanizmom Na Kamchatke (Seismicity and Seismic Prediction, Properties of the Upper Mantle and Their Relation with Volcanism on Kamchatka. Izd. Nauka, Sib. Otd., Novosibirsk, SUN., p. 220.

Fedotov, S. A., ed. (1974c). Realiatsiya Dolgosrochnogo Seysmicheskogo Prognoza Dlya Tikhookeanskoy Fokal'noy Zony U Baregoy Kurilo-Kamchatskoy Dugi Na 1965-1970 Gg. I Utochnenny Prognoz Na 1971-1975 Gg. (Substantiation of a Long-Range Seismic Prediction for the Pacific Ocean Focal Zone Near the Coast of the Kuril-Kamchatka Arc for the Years 1965-1970 and Refinement of the Forecast for the Years 1971-1975). Izd. Nauka, Sib. Otd., Novosibirsk, SUN., p. 101-109.

Fedotov, S. A., ed. and O. V. Potapova (1974d). Predvaritel'naya Karta Tel Na Glubinakh 30-100 km V Verkhney Mantii Pod-Kamchatkoy, Ekraniruyushchikh P I S Volny (Preliminary Map of Bodies Occurring in the Upper Mantle at the Depth 30-100 km and Reflecting P and S Waves). Izd. Nauka, Sib. Otd., Novosibirsk, SUN., p. 176-179.

Fedotov, S. A. and P. I. Tokarev (1974e). Earthquakes, Characteristics of the Upper Mantle Under Kamchatka, and Their Connection with Volcanism (According to Data Collected up to 1971). Bull. Volcanol., (BUVOAS). v. 37 (1973), n. 2, p. 245-257.

Fedotov, S. A., ed., P. I. Tokarev, A. A. Godzikovskaya, and V. M. Zobin (1974f). Detal'nyye Dannyye O Seismichnosti Kamchatki I Komandorskikh Ostrovov (Detailed Data on the Seismicity of Kamchatka and Komandorski Islands). Izd. Nauka, Sib. Otd., Novosibirsk, SUN, p. 35-46.

Fedotov, S. A., ed., P. P. Firstov and V. A. Shirokov (1974g). Vliyaniye Korney Kamchatskikh Vulkanov Na Rasprostraneniye Seismicheskikh Voin Blizkikh Zemietryaseniy (Influence of Roots of Kamchatka Volcanoes on the Distribution of Seismic Waves Generated by Close Earthquakes). Izd. Nauka, Sib. Otd., Novosibirsk, SUN. p. 179-188.

Fornari, D. J. and G. G. Shor, Jr. (1976). Crustal Structure of the Kamchatka Basin, Western Bering Sea. EOS (Am. Geophys. Union, Trans.) (USA) (EOSTAJ), v. 57, n. 4, p. 264.

Fujita, Yukinori, Michihei Hoshino, ed. and Hitoshi Aoki, ed. (1972). Crustal Movements Around Island-Arcs in Northwest Pacific Since Late Cretaceous. Tokai Univ. Press, Tokyo, Japan, p. 1-30.

Fukao, Y. (1977). Upper Mantle P Structure on the Ocean Side of the Japan-Kurile Arc. R. Astron. Soc., Geophys. J. (GBR) (GEOJAN), v. 50, n. 3, p. 621-642.

Fukao, Y., M. H. Manghnani, ed. and S. I. Akimoto, ed. (1977). Upper Mantle P Structure and the 650 km Discontinuity. Acad. Press, Inc., New York, N.Y., USA., p. 151-161.

Furuta, T. (1976). Petrographic and Magnetic Properties of Tephra in a Deep-Sea Core From the Northwest Pacific. Mar. Geol. (MAGEA6), v. 20, n. 3, p. 229-137.

Furuzawa T. (1976). Group Velocities of Surface Waves From Near Earthquakes Around Japan. J. Phys. Earth (Tokyo) (JPN) (JPHEAF), v. 24, n. 2, p. 131-147.

Gadomska, Bozenna and Roman Teisseyre (1970). Distribution of the Seismic Energy Released in the Kuril-Kamchatka Region and Hypothesis Concerning the Dislocation Flow. Pol. Akad. Nauk Zakl. Geofiz., Mater. Pr., (PGMPB9), n. 34, p. 45-63.

Galkin, I. N. and A. V. Nikolayev (1968). Cpyt Issledovaniya Mutnosti Zemnoy Kory I Verkha Mantii Po Amplitudam Prelomleniykh Vолн. Fiz. Zemli, n. 8, p. 36-47.

Garkalenko, I. A. and S. A. Ushakov (1968). Zemnaya Kora Kuril'skogo Regiona (The Crust of the Kuril Region). Sov. Geol., n. 11, p. 46-59.

Gaynanov, A. G., Ye. I. Isayev, and G. B. U dintsev (1968). Magnitnyye Anomalii I Morfologiya Dna Ostrovnykh Dug Severo-Zapadnoy Chasti Tikhogo Okeana (Magnetic Anomalies and Bottom Morphology of Island Arcs in the Northwest Pacific Ocean). Okeanol Akad. Nauk SSSR, v. 8, n. 6, p. 1017-1024.

Gaynanov, A. G., Ye. N. Isayev, and G. B. U dintsev (1968b). Magnitnyee Anomalii I Morfologiya Dna Ostrovnykh Dug Severo-Zapadnoy Chasti Tikhogo Okeana (Magnetic Anomalies and Bottom Topography of the Island Arcs of the Northwestern Part of the Pacific Ocean with English Summ). Okeanologiya, v. 8, n. 6, p. 1017-1024.

Gaynanov, A. G., I. P. Kosminskaya, and P. A. Stroyev (1968c). Geofizicheskiye Issledovaniya Glubinnogo Stroyeniya Beringom Morya. Akad. Nauk SSSR Izv. Fizika Zemli, n. 8. p. 3-11.

Gaynanov, A. G. and L. P. Smirnov (1962). Stroyeniye Zemnoy Kory V Oblasti Perekhoda Ot Aziatskogo Kontinenta K Tikhomu Okeanu. Sov. Geol., n. 3, p. 108-118.

Gnibidenko, G. S. (1970). On the Basement of the Northwest Sector of the Pacific Belt. Tectonophysics, (TCTOAM), v. 9, n. 6, p. 513-523.

Gnibidenko, G. S. (1967a). Rift System of the Sea of Okhotsk. Acad. Sci. USSR, Dokl., Earth Sci. Sect. (USA) (DKESA9), v. 229, n. 1-6, p. 36-38.

Gnibidenko, G. S., ed., Yu. A. Kosygin, ed. and K. F. Sergeev (1976b). Stroyeniye Zemnoy Kory i Verkhney Mantii V Zone Perekhoda Ot Aziatskogo Kontinenta K Tikhomu Okeanu (Structure of the Earth's Crust and Upper Mantle in the Transition Zone From the Asiatic Continent to the Pacific Ocean). Izd. Nauka, Novosibirsk, SUN., p. 368.

Gnibidenko, G. S., M. L. Krasnyy, and N. P. Luk'yanov (1975). Novyye Datiyye O Strukture Osadochnogo Chekhla Pednyatiya Shatskogo i Severo-Zapadnoy Plity Tikhogo Okeana (New Data on the Sedimentary Cover Structure of the Shatsky Rise and the Northwestern Plate of the Pacific Ocean). Akad. Nauk SSSR, Dokl. SUN, (DANKAS), v. 221, n. 1, p. 209-212.

Gnibidenko, G. S. and A. Ya. Il'yev (1978). Composition, Age and Seismic Wave Velocity in the Acoustic Basement in the Middle of the Sea of Okhotsk. Acad. Sci. USSR, Dokl., Earth Sci. Sect. (USA) (DKESA9), v. 229, n. 1-6, p. 64-67.

Gorel'chik, V. I. and S. A. Fedotov, ed. (1974). Seismichnost' Yuzhnoy Kamchatki (Seismicity of Southern Kamchatka). Izd. Nauka, Sib. Otd., Novosibirsk, SUN, p. 52-62.

Grabkov, V. K. (1973a). O Sootnoshenii Strukturny Rel'yefa Svermenney Kuril' Skoy Geosinklinal'noy Oblasti (Inter-relationship of the Structure and Relief of the Present-Day Kuril Geosynclinal Province). Akad. Nauk SSSR, Geomorfol. Kom., Plenum, Mater., (33ZXAK), n. 10, p. 159-160.

Grabkov, V. K. and Yu. A. Pavlov (1973b). Neotectonic Movements and Isostatic State of the Crust in the Kurile Island Arc Region. Acad. Sci. USSR, Dokl., Earth Sci. Sect. (USA) (DKESA9), v. 203, n. 1-6, p. 55-57.

Gusev, A. A. and Yu V. Riznichenko, ed. (1974). Seysmostatisticheskiye Prediktory Zemletrayaseniy (Statistical Prediction of Earthquakes). Izd. Shtintsa, Kishinev, SUN, p. 43-50.

Hanks, Thomas C. (1970). The Kuril Trench-Hokkaido Rise System: Large Shallow Earthquakes and Simple Models of Deformation (abs.). EOS (Am. Geophys. Union, Trans.), v. 51, n. 11, p. 823.

Hanks, Thomas C. (1971). The Kuril Trench-Hokkaido Rise System: Large Shallow Earthquakes and Simple Models of Deformation. R. Astron. Soc., Geophys. J., (GEOJAN), v. 23, n. 2, p. 173-189.

Hasegawa, A., N. Umino, and A. Takagi (1978). Double-Planned Structure of the Deep Seismic Zone in the Northeastern Japan Arc. Tectonophysics (III) (TCTOAM), v. 47, n. 1-2, p. 43-58.

Hein, J. R., D. W. Scholl, and C. E. Guthmacher (1976). Diagenesis of Neogene Diatomaceous Sediment From the Far Northwest Pacific and Southern Bering Sea (abs.). Geol. Soc. Am., Abstr. Programs (USA) (GAAPMC), v. 8, n. 3, Cordilleran Section, 72nd Annual Meeting, p. 379-380.

Honza, E. (1978a). Basic Framework of the Island Arc System in the Northwest Pacific Margin (abs.). Sci. Counc. Japan, Tokyo, Japan.

Honza, E. (1978b). Geological History of the Kuril Basin and the Taryt Trough; Preliminary Concluding Remarks. (GH77-3 Cruise) Jap., Geol. Surv., Cruise Rep., n. 11, p. 60-69.

Honza, E., ed., K. Tamaki, and K. Nishimura (1978c). Sonobuoy Refraction Measurement. (GH77-3 Cruise) Jap., Geol. Surv., Cruise Rep., n. 11, p. 46-49.

Isayev, Ye. N. and V. I. Tikhonov (1967). O sootnoshenii Tektoniki I

Magnitnogo Polya Kurilo-Kamchatskoy Dugi (Relationship Between Tectonics and the Magnetic Field of the Kuril-Kamchatka Arc). Aka. Nauk SSSR, Dokl., v. 175, n. 1, p. 161-164.

Ivashchenko, A. I. and S. L. Solov'yev (1969). Moschnost' Zemnoy Kory V Kurilo-Okhotskom Regione Po Dispersii Voln Lyava I Releya (Thickness of the Earth's Crust in the Kuril-Okhotsk Region on the Basis of Love and Rayleigh Wave Dispersion). Geol. Geofiz. (Akad. Nauk SSSR, Sib. Otd.), n. 9, p. 94-102.

Iwabuchi, Y. (1971). Submarine Geology of Trenches in the Northwest Pacific. Oceanogr. Soc. Jap., J., (NKGKB4), v. 27, n. 3, p. 128-135.

Johnson, Rockne H. (1966). Routine Location of T-Phase Sources in the Pacific. Seismol. Soc. Amer., Bull., v. 56, n. 1, p. 109-118.

Johnson, Rockne H., Roger A. Norris, Frederick K. Duennebier, and John Northrob (1971). T-Phase Data on Kamchatka/Kurils Earthquakes; A Reply. Seismol. Soc. Am., Bull., (BSSAAP), v. 61, n. 3, p. 791-795.

Kakuta, Toshiki (1968). The Structure of the Upper Mantle in the Vicinity of the Low Velocity Layer. Zisin (Seismol. Soc. Jap., J.), v. 21, n. 3, p. 202-221.

Kanamori, Hiroo (1970). Synthesis of Long-Period Surface Waves and Its Application to Earthquake Source Studies - Kurile Islands Earthquake of October 13, 1963. J. Geophys. Res., v. 75, n. 25, p. 5011-5027.

Kanamori, Hiroo (1976). Re-Examination of the Earth's Free Oscillations Excited by the Kamchatka Earthquake of November 4, 1952. Phys. Earth Planet, Inter. (III) (PEPIAM), v. 11, n. 3, p. 216-226.

Kasahara, J. and R. R. Harvey (1976). Ocean Bottom Seismometer Study of the Kuril Trench Area. Hawaii Univ., Inst.

Geophys., Rep. (USA) (HIGRAC), n. HIG-76-9, p. 24.

Kasahara, J. and R. R. Harvey (1977). Seismological Evidence for the High-Velocity Zone in the Kuril Trench Area From Ocean Bottom Seismometer Observations. J. Geophys. Res. (USA) (JGREA2), v. B2, n. 26, p. 3805-3814.

Kasahara, D. and R. R. Kharui (1977). Gidrofizicheskiye Issledovaniya Okeana (Ocean Bottom Seismograph Study of the Kuril Trench Area). Lappo, S., ed. Aka. Nauk SSSR, Nauchno-Issled Inst. Tr., n. 54, p. 17-34.

Kerimov, I. G. (1969). K Voprosu Ob Opredelenii Stroyeniya Zemnoy Korp Pod Stantsiyey Po Polaryarizatsii Seismicheskikh Voln (Determination of the Earth's Crustal Structure by Means of Polarized Seismic Waves). Aka. Nauk Azerb. SSSR, Dokl., (DAZRA7), v. 25, n. 6, p. 56-62.

Kochergin, Ye. V., M. L. Krasnyy, O. A. Solov'yev, and I. K. Tuyezov (1972). Svyazi transformirovannogo V Verkhneye Poluprostranstvovo Anomali'nogo Magnitnogog Polya S Tektonicheskim Stroyeniyem Okhotsko-Kuril'skogo Regiona (The Relationship Between the Transformed-Into-Upper-Half-Space, Anomalous Magnetic Field and the Tectonic Structure of the Okhotsk-Kurils Region). Akad. Nauk SSSR, (RIGPAE), n. 8, p. 105-113.

Kosminskaya, I. P. and S. M. Zverev (1968). Deep Seismic Sounding in the Transition Zones From Continents to Oceans. IN: The Crust and Upper Mantle of the Pacific Area-International Upper Mantle Proj. Sci. Rep. 15. Am. Geophys. Union Geophys. Mon. 12 (NAS-NRC PUB. 1687), p. 122-130.

Kosminskaya, I. P., S. M. Zverev, and G. B. Udinstsev (1973). Soviet Seismic Studies of the Earth's Crust in the Pacific Ocean During the International Upper Mantle Project, A Summary. Dev. Geotectonics (DEVGAG), v. 8, p. 147-151.

Kosygin, V. Yu and Yu A. Pavlov (1975a). Rol' Krayevogo Effekta V Istolkovalii Gravitatsionnykh Anomalii V Zone Perekhoda Ot Aziatskogo Kontinenta K Tikhonu Okeanu (Role of the Edge Effect in Interpretation of Gravity Anomalies in the Transition Zone Between Asia and Pacific Ocean). Akad. Nauk SSSR, Dokl. (SUN) (DANKAS), v. 221, n. 4, p. 917-920.

Kosygin, V. Yu and Yu A. Pavlov (1975b). Edge Effect as a Factor in Interpretation of Gravity Anomalies in the Transition Zone From the Asian Mainland to the Pacific Ocean. Acad. Sci. USSR, Dokl., Earth Sci. Sect. (USA) (DKESA9), v. 221, n. 1-6, p. 101-103.

Krasnyy, M. L., S. L. Solov'yev, I. K. Tuyezov, and Yu. S. Shumilov (1976). Comprehensive Geophysical, Geological, and Hydrophysical Investigations in the Sea of Okhotsk (Sixth Cruise of the R/V PEGAS). Oceanology (USA) (ONLGAE), v. 15, n. 4, p. 517-519.

Kurochkina, R. I. (1977). The Effect of the Focal Mechanism on the Dispersion of (A/T) Max Values of a P-Wave and on Magnitudes Estimated From Longitudinal Waves. Phys. Solid Earth (Engl. Ed.) (USA) (IPSEBQ), v. 13, n. 4, p. 287-289.

Kuzin, I. P. (1972). Elastic Wave Velocities in the Kamchatka Focal Zone. Phys. Solid Earth (Engl. Ed.), (IPSEBQ), n. 12, p. 793-802.

Kuzin, I. P. (1973). P and S Wave Velocities in the Upper Mantle of Kamchatka. Phys. Solid Earth (Engl. Ed.), (IPSEBA), n. 1, p. 69-75.

Kuzin, I. P. (1974). Fokal'naya Zona I Stroyeniye Verkhney Mantil V Rayone Vostochnoy Kamchatki (The Focal Zone and Upper Mantle Structure in the Eastern Kamchatka Region). Izd. Nauka, Moscow, SUN, p. 131.

Legler, V. A. and O. G. Sorokhtin, ed. (1976). Deformatsiya Pogruzhayushchey Litosfernoy Plity I Prodol'

nyye Sdvigi Kuril-Kamchatskoy Ostrovnay Dugi (Deformation of the Subsiding Lithospheric Plate and Longitudinal Shifts of the Kuril-Kamchatka Island Arc). Adak. Nauk SSSR, Inst. Okeanology. im. P. P. Shirpova, Moscow, SUN, p. 103-147.

Leonov, N. N., L. S. Oskorbin, N. A. Shchetnikov, Ch. N. Go, A. N. Boychuck, and L. N. Poplavskaya (1972). Sil'nyye Zemletryaseniya I Tsunami V Rayone Maloy Kuril'Skoy Gryady, 1961-1966 gg (Strong Earthquakes and Tsunamis in the Lesser Kuril Arc Region, 1961-1969). Akad. Nauk SSSR, Sib. Otd., Nauchno-Issled. Inst., Tr., (TSKSAX), n. 29, p. 284-298.

Lin, Jua-Wen (1974). A Study of Upper Mantle Structure in the Pacific Northwest Using P Waves From Teleseisms (abs.). Doctoral Dissertation, Washington, 107 pp.

Listitsyna, N. A. and C. A. Dvoretskaya (1972). Litologicheskiy Profil'Cherez Severo-Zapadnyu Kotlovinu Tikhogo Okeana (Lithologic Profile of the Northwest Pacific Basin). Litol. Poley. Iskop., (LPIKAQ), n. 4, p. 3-25.

Liu, Hsi-Ping (1980). The Structure of the Kuril Trench-Hokkaido Rise System Computed by a Plastic Time-Dependent Plastic Plate Model Incorporating Rock Deformation Data. JGR, v. 85.

Lopatina, N. P. and V. Z. Ryaboy (1974). Velocity and Density Inhomogeneities in the Upper Mantle of the USSR. Acad. Sci. USSR, Dokl., Earth Sci. Sect. (DKESA9), v. 207, n. 1-6, p. 9-12.

Luchitskiy, I. V., ed. and N. A. Florentsov, ed. (1974). Kamchatka, Kuril'skiye I Komandorskiye Ostrova (Kamchatka, Kuril and Komandorski Islands). Izd. Nauka, Moscow, SUN, p. 438.

Lurismanashvili, O. V. (1973). O zakonomernom izmenenii vremeni vozniknoveniya zemletryaseniy v nekotorykh seismoaktivnykh regionakh

(Regular Changes of Time of Earthquake Occurrences in Some Seismic Regions). Akad. Nauk Gruz. SSSR, Soobshch., (SAKNAH), v. 70, n. 1, p. 69-72.

Kybinova, Ye. A., An. N. Gorshkov, V. I. Vlasenko, A. V. Yefimov and A. L. Aleksandrov (1974). Heat Flux Measurements Near the Kurile Island Chain, in Kamchatka, and the Kurile Lake. Acad. Sci. USSR, Dokl., Earth Sci. Sect. (DKESA9), v. 207, n. 1-6, p. 24-28.

Lyubimova, Ye. A., V. N. Nikitina, and G. A. Tomara (1976). Teplovyye Polya Vnutrennikh i Okrainnykh Morey SSSR; Sostoyaniye Nablyudeniy i Teoriya Interpretatsii Dyunernykh Neodnorodnostey (Heat Field of the Inland and Marginal Seas of the USSR; State of Observations and the Theory of Interpretation of Two-Dimensional Inhomogeneities). Izd. Nauka, Moscow, SUN, p. 222.

Markev, M. S. and M. Yu. Khotin, (1973). Structures and Geological History of the Kuril-Kamchatka Island Arc. Univ. West. Austr. Press, Nedlands, p. 239-246.

Marshall, M. (1978). The Magnetic Properties of Some DSDP Basalts From the North Pacific and Inferences for Pacific Plate Tectonics. J. Geophys. Res. (USA), (JGREA2), v. 83, n. B1, p. 289-308.

Marshall, Monte C. (1975). Summary of Physical Properties, Leg 32. Deep Sea Drill. Proj., Initial Rep. (IDSDA6), v. 32, p. 961-962.

Matveyeva, N. N., V. Z. Ryaboy, V. V. Belousov, ed. and A. V. Vikhert, ed. (1975). Izuchenije Stroyeniya Verkhney Chasti Mantii Po Dannym Glubinnykh Seismicheskikh Zondirovaniy (Interpretation of the Upper Mantle Structure From Deep Seismic Sounding Data). Izd. Mosk. Univ., Moscow, SUN, p. 94-109

McAdoo, D. C., J. C. Cladwell and D. L. Turcotte (1978). On the Elastic-Perfectly Plastic Bending of the

Lithosphere Under Generalized Loading With Application to the Kuril Trench. Geophys. J., v. 54, n. 1, p. 11-26.

Melekestsev, I. V., I. A. Yegorova, Ye. B. Lupikina, E. N. Erlikh, I. V. Luchitskiy, ed. and N. A. Florentsov, ed. (1974). Vnutrenniy Khrebet Kuril'skoy Dugi (Interior Ridge of the Kuril Arc). Izd. Nauka, Moscow, SUN, p. 265-337.

Mesko, A. (1971). Velocities of P and S Waves at Depths Between 50 and 600 km. Acta Geod. Geophys. Montan., (AGGMB9), v. 6, n. 1-2, p. 117-125.

Mesko, A. (1972). Velocities of P and S Waves at Depths Between 50 and 600 km (abs.). Geosci. Bull., Ser. A, (GSCBB4), v. 3, n. 4, p. 10.

Mogl, Kiyoo (1973). Relationship Between Shallow and Deep Seismicity in the Western Pacific Region. Tectonophysics, (TCTOAM), v. 17, n. 1-2, p. 1-22.

Monakhov, V. I., V. A. Nesterov, Yu. S. Rozhkov, and G. N. Khristoforov (1976). Conditions for the Formation of Storm Microseisms on Shikotan Island During the Period of February 8-11, 1974. Phys. Solid Earth (Engl. Ed.) (USA) (IPSEBQ), v. 12, n. 5, p. 345-347.

Moskyina, A. G., O. A. Korchagina and G. L. Kosarev (1977). Study of the P-Wave of the Ust'-Kamchatka Earthquake of December 15, 1971. Phys. Solid Earth (Engl. Ed.) (USA) (IPSEBQ), v. 13, n. 4, p. 251-260.

Mualchin, L. (1974). The Descending Slab Beneath the Kuril-Kamchatka Arc and its Influence on Ray Paths of Body Waves (abs.). Doctoral, St. Louis, v. 36, n. 6, p. 222.

Myachkin, V. I., N. A. Dolbilkina, G. S. Kushnir, O. A. Maksimov, A. M. Palenov, V. B. Preobrazhenskiy and S. A. Fedotov, ed. (1974). Seismicheskoye "Prosvechivaniye" Ochagovykh Zon Zemletryaseniy Na Kamchatke (Seismic "X-Ray" of Focal Zones of Earthquakes

on Kamchatka). Izd. Nauka, Sib. Otd., Novosibirsk, SUN, p. 151-160.

Myachkin, V. I., G. A. Sbolej, N. A. Dolbilkina, V. N. Morozow, and V. B. Preobrazensky (1972). The Study of Variations in Geophysical Fields Near Focal Zones of Kamchatka. Tectonophysics, (TCTOAM), v. 14, p. 3-4, p. 287-293.

Mirilo, Hiroshi and K. O. Emery (1966). Continental Shelf Sediments Off Northeastern Asia. J. Sediment. Petrology, v. 36, n. 1, p. 152-161.

Pulmanabhamurthy, B., R. B. Pathak, and Rao S. Trivikrama (1969). A Study of the Aftershock Sequence of the Kurile Islands Earthquake of October 13, 1963. Indian Geophys. Union J., v. 6, n. 2, p. 137-144.

Pavlov, Yu. A. and A. Yu. Yumov (1970). Thickness of the Crust of Kamchatka. Acad. Sci. USSR, Dokl., Earth Sci. Sect., (DKESA9), v. 191, p. 38-40.

Porter, L. D. (1974a). Seismic Masking of an Underground Nuclear Explosion, (abs.). EOS (Am. Geophys. Union Trans.) (EOSTA), v. 56, n. 12, p. 1148.

Porter, Lawrence D. (1974b). The Kurile Island Earthquake Sequence of August 1969 (abs.). Geol. Soc. Am., (GAAPBC), v. 6, n. 3, p. 307.

Potapova, O. V. and S. A. Fedotov, ed. (1974). Issledovaniye Parametra Theta = LogE S /E P Dlya Kamchatskikh Zemletryaseniy (Calculation of the Parameter Theta = LogE S/E p for Kuril Earthquakes). Izd. Nauka, Sib. Otd., Novosibirsk, SUN, p. 133-140.

Pushcharovskiy, Uu. M., Ye. N. Melankholina, Yu. N. Raznitsin and O. A. Schmidt (1978). Comparative Tectonics of the Bering Sea, Sea of Okhotsk, and Sea of Japan. Geotectonics (USA) (GEOTBK), v. 11, n. 5, p. 373-381.

Ringdal, F. (1977). P-Wave Amplitudes and Sources of Scattering in M B-Observations. J. Geophys. (DEU) (JGEOD4), v. 43, n. 4, p. 611-622.

Rodnikov, A. G., ed. and B. S. Vol'govskiy, ed. (1976). Osobennosti Tektonicheskogo Stroyeniya Fundamenta Ostrovnykh Dug (Peculiarities in the Tectonic Structure of the Island Arc Basement). Sovetskoye radio, Moscow, SUN, p. 54-59.

Romankevich, Ye. A. and V. E. Artem'yev (1969). Composition of the Organic Matter of Sediments From the Kuril-Kamchatka Trench. Oceanology, (ONLGAE), v. 9, n. 5, p. 644-653.

Rozinov, M. I. and D. I. Kolesnikov (1977). Relationship of Most Recent Volcanism with Tectonics in the East Kamchatka and Kurile Zone. Geotectonics (USA) (GEOTBK), v. 10, n. 5, p. 371-377.

Russ, V. V. and D. A. Kirikov (1976). Structural-Formation Analysis of Northwestern Part of Pacific Mobile Belt, USSR. Am. Assoc. Pet. Geol., Mem. (USA) (MAPGAN), n. 25, p. 59-61.

Santo, Tetsuo (1970). Regional Study on the Characteristic Seismicity of the World: Part VII, Activity of Aftershocks in Kurile Islands Region. Int. Inst. Seismol. Earthquake Eng. Bull., (IISBB2), v. 7, p. 119-131.

Sasatani, T. (1976). Source Process of a Large Deep-Focus Earthquake of 1970 in the Sea of Okhotsk. J. Phys. Earth (Tokyo) (JPN) (JPHEAF), v. 24, n. 1, p. 27-42.

Savostin, L. A., A. F. Beresnev and G. B. Udnitsev (1974). New Data on the Sea-Floor Heat Flux in the Sea of Okhotsk. Acad. Sci. USSR, Dokl., Earth Sci. Sect. (USA) (DKESA9), v. 215, n. 1-6, p. 6-8.

Sazhina, N. B. (1962). Moshchnost' Zemnoy Kory I Svyaz, Yeye S Rel'yefom I Anomaliyami Sily Tyazhesti. Sov. Geol., n. 8, p. 151-157.

Schule, J. W. and L. Knopoff (1977). Shear-Wave Polarization Anisotropy in the Pacific Basin. *R. Astron. Soc., Geophys. J. (GBR) (GEOJAN)*, v. 49, n. 1, p. 145-165.

Scholl, D. W., J. R. Hein, M. S. Marlow and E. C. Buffington (1976). Meiji Sediment Tongue, a Thick Sequence off Neogene Deposits in the Northwest Pacific; Evidence for Limited Movement Between the Pacific and American Plates, (abs.). *U.S. Geol., Menlo Pac.-Artic Branch Marine Geol. Menlo Park, Ca (USA)*.

Slater, John G. (1972). Heat Flow and Elevation of the Marginal Basins of the Western Pacific. *J. Geophys. Res.*, (JGREA2), v. 77, n. 29, p. 5705-5719.

Sergeyev, K. F. (1970). *O Tektonicheskoy Prinadlezhnosti i Geologicheskoy Istorii Kuril'skoy Ostrovnoy Dugi (Tectonics and Geologic History of the Kuril Island Arc)*. Akad. Nauk SSSR, Sib. Otd., Sakhalin. Kompleksn. Nauchno-Issled. Inst., Tr., (TSKSAX), n. 25, p. 102-116.

Sergeyev, K. F. (1976a). *Tektonika Kuril'skoy Ostrovnoy Sistemy (Tectonics of the Kuril Island System)*. Izd. Nauka, Moscow, SUN, p. 239.

Sergeyev, K. F., B. S. Vol'vovskiy, ed. and A. G. Rodnikov, ed. (1976b). *Nekotoryye Aspekty Tektoniki Duril'skoy Ostrovnoy Dugi (Some Tectonic Aspects of the Kuril Island Arc)*. Sovetskoye Radio, Moscow, SUN, p. 60-65.

Serova, M. Ya., G. P. Borzunova and M. N. Shapiro (1977). The Paleogene in the Southern Part of Karagin Island (Eastern Kamchatka). *Int. Geol. Rev. (USA) (IGREAP)*, v. 19, n. 3, p. 349-357.

Shapiro, M. N. (1976a). Northeastern Continuation of the East Kamchatka Synclinorium. *Geotectonics (USA) (GEOTBK)*, v. 10, n. 1, p. 76-78.

Shapiro, M. N. (1976b). *Tektonicheskoye Razvitiye Vostochnogo Obramleniya Kamchatki (Tectonic Evolution of the Eastern Part of the Kamchatka Peninsula)*. Izd. Nauka, Moscow, SUN, p. 122.

Shapiro, M. N. and V. A. Seliverstov (1976c). Morphology and Age of Folded Structures in Eastern Kamchatka, at the Latitude of the Kronotskiy Peninsula. *Geotectonics (GEOTBK)*, v. 9, n. 4, p. 240-244.

Sheynmann, Yu. M. (1968). Tectonics of the Upper Parts of the Mantle Under Geosynclines and Island Arcs. IN: *The Crust and Upper Mantle of the Pacific Area-Internat. Upper Mantle Proj. Sci. Rept. 15. Am. Geophys. Union Geophys. Mon. 12*, p. 466-472.

Shilin, N. L. (1970). *Otsenka Temperatury i Davleniya, Sushchestvovavshikh Pri Formirovaniyu Dvukhfazovykh Gipabisal'Nykh Tel (Evaluation of the P-T Conditions of Formation of Two-Phase Hypabyssal Rock Bodies, Central Kamchatka)*. Akad. Nauk SSSR, Sib. Otd., Inst. Vulkanol., Moscow, p. 53-67.

Shimamura, H. and T. Asada (1975). T Waves From Deep Earthquakes Generated Exactly at the Bottom of Deep-Sea Trenches. *Earth Planet. Sci. Lett. (EPSLA2)*, v. 27, n. 2, p. 137-142.

Shimamura, H. and T. Asada (1976). Apparent Velocity Measurements on an Oceanic Lithosphere. *Phys. Earth Planet. Inter. (III) (PEPIAM)*, v. 13, n. 1, p. 15-22.

Shimamura, H., T. Asada and M. Kumazawa (1977). High Shear Velocity Layer in the Upper Mantle of the Western Pacific. *Nature (GBR) (NATUAS)*, v. 269, n. 5630, p. 680-682.

Shimarayev, V. N. and V. E. Volk (1972). *Privlecheniye Aeromagnitnykh Dannyykh Dlya Izucheniya Stroyeniya Zemnoy Kory Okhotsko-Tikhookeanskoy Perekhodnoy Zony Na Uchastke Kurilo-Kamchatskoy Ostrovnoy Dugi (Use of Airborne Magnetic Survey Data in the Study of the Earth's Crust Structure in*

the Okhotsk-Pacific Transition Zone in the Area of the Kuril-Kamchatka Island Arc). *Geofiz Metody Razv. Arkt.* (GMRABY), n. 7, p. 61-67.

Sheteynberg, G. S. (1966). Composition of the Crust of Southern Kamchatka and the Tectonic Position of Quaternary Volcanoes. *Acad. Sci. USSR, Dokl., Earth Sci. Sect.*, v. 166, n. 1-6, p. 44-47.

Simbireva, I. G., S. A. Fedetov, and V. D. Feofilkov (1976). *Neodnorodnosti Polya Napryazheniy Kurilo-Kamchatskoy Dugi Po Seismologicheskim Dannym* (Inhomogeneities in the Strain Field of the Kuril-Kamchatka Arc Based on Seismological Data). *Geol. Geofiz. Akad. Nauk SSSR, Sib. Otd.* (SUN) (GGASAS), n. 1, p. 70-85.

Skorikova, M. F. (1977). Physical Properties of Rocks in the Zone of Transition from the Asian Continent to the Pacific Ocean. *Int. Geol. Rev. (USA)* (IGREAP), v. 19, n. 11, p. 1321-1325.

Slavina, L. B. and S. A. Fedetov, ed. (1974). *Skorosti Prodil'nykh Voln V Verkhney Mantii Pod Kamchatkoy* (Velocities of Longitudinal Waves in the Upper Mantle Beneath Kamchatka). Izd. Nauka, Sib. Otd., Novosibirsk, SUN, p. 188-200.

Slavina, L. B. and Yu. V. Riznichenko, ed. (1976). *Metodika I Rezul'taty Izucheniya V p /V s V Fokal'noy Zone Kamchatki* (Methods and Results of the Studies of V p /V s in the Focal Zone of Kamchatka). Izd. Nauka, Moscow, SUN, p. 217-236.

Sleep, Norman H. (1973). Teleseismic P-Wave Transmission Through Slabs. *Seismol. Soc. Am., Bull.*, (BSSA), v. 63, n. 4, p. 1349-1373.

Snegovskoy, S. S. and S. M. Aleksandrov (1971). *O Tektonike Zapadnogo Borta Kuril'skoy Kotloviny* (Tectonics of the West Flank of the Kuril Deep). *Geotektonika*, (GKTA2), n. 5, p. 105-110.

Snegovskoy, S. S. and S. M. Aleksandrov (1971). *Tectonics of the West Flank of the Kuril Deep. Geotectonics (GEOTBK)*, n. 5, p. 324-326.

Sobolev, G. A. and L. B. Slavina (1977). The Spatial and Temporal Changes in V p /V s. *Pure Appl. Geophys. (CHE)* (PAGYAV), v. 115, n. 4, p. 1047-1060.

Sokolova, L. S. and A. Adam, ed. (1976). *Temperatures, Heat Flow and Heat Generation in South and West Siberia and Kamchatka*. Akad. Kiado, Budapest, HUN., p. 463-472.

Sokolova, L. S., U. I. Moiseyenko and A. D. Duchkov (1972). *Teplovoy Potok Na Nekotorykh Ploshchadyakh Yugo-Vostochnoy Kamchatki* (Heat Flow in Some Regions of Southeastern Kamchatka). *Geol. Geofiz. Akad. Nauk SSSR, Sib. Otd.*, (GGASAS), n. 6, p. 102-105.

Solov'yeva, O. N. (1972). *Opredeleniye Magnitu Dy Kurilo-Kamchatskikh Zemletraseniy Po Zapisyam Mekhanicheskikh Seismografov Ispol'zuyemykh V Sluzhbe Preduprezhdeniya O Tsunami* (Determination of the Magnitude of the Kuril-Kamchatka Earthquakes from the Mechanical Seismograph Records Used in Tsunami Forecasting). IN: *Volny Tsunami, Akad. Nauk SSSR, Sib. Otd., Sakhalin. Kompleksn. Nauchno-Issled. Inst., Tr.*, (TSKSAX), n. 29, p. 250-261.

Solov'yev, S. L. and O. N. Solov'yeva (1968). Determination of Magnitude for Kurile-Kamchatka Earthquakes. *Ceskoslovenska Akad. Ved Studia Geophys. Et Geod.*, v. 12, n. 2, p. 179-191.

Solov'yeva, I. A. (1976). Deep Structure of the Pacific Crust. *Geotectonics (USA)* (GEOTBK), v. 10, n. 3, p. 157-168.

Solov'yeva, N. A. (1968). Role of Volcanism in the Genesis of Rocks of the Lesser Kurile Suite. *Acad. Sci. USSR, Dokl., Earth Sci. Sect.*, v. 179, p. 64-66.

Soloviev, S. L., I. K. Touezov and B. I. Vasiliev (1977). The Structure and Origin of the Okhotsk and Japan Sea Abyssal Depressions According to New Geophysical and Geological Data. *Tectonophysics* (111) (TCTOAM), v. 37, n. 1-3, p. 153-166.

Stauder, William and G. A. Bollinger (1966). The S-Wave Project for Focal Mechanism Studies, Earthquakes of 1963. *Seismol. Soc. America Bull.*, v. 56, n. 6, p. 1363-1371.

Stauder, William and Mualchi Lillian (1971). Larger Earthquakes of the Kurile Islands, 1962-1968 (abs.). *EOS (Am. Geophys. Union, Trans.)*, (EOSTAJ), v. 52, n. 4, p. 276.

Stauder, W. and L. Mualchin (1976). Fault Motion in the Larger Earthquakes of the Kurile-Kamchatka Arc and of the Kurile-Hokkaido Corner. *J. Geophys. Res.* (JGREA2), v. 81, n. 2, p. 297-308.

Strel'tsov, M. I. (1977). K Voprosu O Printsipakh Vydeleniya Strukturnykh Yarusov (Principles of the Formation of Structural Layers in the Kuril Islands are Model). *Aka. Nauk SSSR, Sib. Otd., Sakhalin. Kompleksn. Nauchno-Issled. Inst., Tr.*, n. 41, Part 1, p. 66-74.

Stroyev, P. A. and V. V. Fedynskiy, ed. (1975). *Gravimetrichekiye Issledovaniya V Tikhom Okeane V 51-M Reyes NIS "Vityaz"* (1972) (Gravity Surveys of the Pacific Ocean During the 51st Cruise of the R/V VITYAZ' (1972)). Izd. Mosk. Univ., Moscow, SUN., p. 115-120.

Sutton, George H. and Daniel A. Walker (1972). Oceanic Mantle Phases Recorded on Seismographs in the Northwestern Pacific at Distances Between 7° and 40°. *Seismol. Soc. Am., Bull.*, (BSSAAP), v. 62, n. 2, p. 631-655.

Sychev, P. M., H. Aoki, ed. and A. Iizuka, ed. (1976). Deep Fractures and Crust Formation in the North-West Pacific. IN: *Volcanoes and Tectonosphere*. Tokai Univ. Press, Tokyo, Japan, p. 341-357.

Sychev, P. M. and R. Z. Tarakanov (1976). Some Inferences on the Upper Mantle Structure and Deep Processes Occurring in the Northwest Pacific. *Can. J. Earth Sci. (CJESAP)*, v. 13, n. 12, p. 1725-1729.

Takano, Kei (1973). On Some Characteristics of Source Spectra of Hokkaido-Kuril Earthquakes Observed at Tsukuba Station. *J. Phys. Earth (Tokyo)*, (JPHEAF), v. 21, n. 2, p. 141-153.

Talwani, M. and W. Pitman III, eds. (1977). *Island Arcs, Deep Sea Trenches and Back Arc Basins*, America Geophysical Union, 470 pp.

Talwani, M. and A. B. Watts (1975). Gravity Field of the Northwest Pacific Ocean Basin and Its Margin; Hawaii and Vicinity. *Geol. Soc. Am., Boulder, Colo., USA*. p. 6.

Tarakanov, R. Z., Asano, ed. and G. B. U dintsev, ed. (1971). Peculiarities of the Upper Mantle Structure of the Kuril-Japanese Region. IN: *Island Arc and Marginal Sea; Proceedings of the First Japan-USSR Symposium on Solid Earth sciences*. Tokai Univ. Press., Japan, p. 215-223.

Tarakanov, R. Z. (1955). The Velocity Section of the Upper Mantle in the Transition Zone from Asia to the Pacific Ocean. *Tectonophysics*, v. 2, n. 2-3, p. 227-237.

Tarakanov, R. Z. and Kim Chun Un (1969). *Statisticheskoye Issledovaniye Anomaly Vo Vremenakh Probega Prodol' nukh Voin* (Statistical Studies of Anomalies in the Travel Times of P Waves). *Akad. Nauk SSSR, Sib. Otd., Sakhalin. Kompleksn. Nauchno-Issled. Inst., Tr.*, (TSKSAX), n. 20, p. 153-164.

Tarakanov, R. Z. and Kim Chun Un (1970). Low Velocity of Longitudinal Seismic Waves in the Weakly Seismic Part of the Kurile-Kamchatka Focal Zone. *Acad. Sci. USSR, Dokl., Earth Sci. Sect.*, (DKESA9), v. 186, n. 1-6, p. 56-58.

Tarakanov, R. Z., Kim Chun Un, R. I. Sukhomlinova, B. S. Vol'vovskiy, ed. Gipotsentrov Kurilo-Kamchatskogo I Yaponskogo Regionov I Ikh Svyaz' S Osobennostyami Geofizicheskikh Poley (Regularities of the Spatial Distribution of Hypocenters in the Kuril-Kamchatka-Japan Region and Their Connection with the Peculiarities of the Geophysical Fields). Izd. Nauka, Moscow, SUN., p. 67-77.

Tarr, A. C. and F. J. Mauk (1976). Focal Mechanism Map of the Northwestern Pacific Ocean (abs.). EOS (Am. Geophys. Union Trans.) (USA) (EOSTAJ), v. 57, n. 10, p. 760.

Theyer, F., C. Mato and P. Lineberger (1977). Sediment Core Descriptions; R/V Kana Keoki, 1973 North Central Pacific Cruise, 1974 Southeastern Pacific Cruise, and a 1974 Mid-Atlantic Ridge IPOD Site-Survey. Hawaii, Univ., Inst. Geophys., Rep. (USA) (HIGRAC), n. 77-79, Data Report 33, p. 13.

Tokarev, P. I. (1964). Roy Zemletryaseniya Vulkana Sheveluch V Maye 1964 G. (The Earthquake Swarm at Sheveluch Volcano in May 1964). Akad. Nauk SSSR Sibirskoye Otdeleniye, Vulkanol. Sta. Byull., n. 38, p. 41-44.

Tokarev, P. I. (1969). On a Focal Layer, Seismicity and Volcanism of the Kuril-Kamchatka Zone. Symposium of Volcanoes and Their Roots, Oxford 1969, p. 205.

Tokarev, P. I. and V. N. Zobin (1972). Characteristics of Propagation of Seismic Waves Generated by Near Earthquakes Originating in the Crust and Upper Mantle in the Region of the Klyuchevskoy Groups of Volcanoes in Kamchatka (abs.). Geosci. Bull., Ser. A, (GSCBB4), v. 3, n. 6-9, p. 83.

Tokarev, P. I. and S. A. Fedotov, ed. (1974). Seismicheskaya Aktivnost' Fokal'nogo Sloya Kamchatki i Yeye Svyaz' S Vulkanizmom (Seismic Activity of the Focal Layer of Kamchatka and its Relation to Volcanism). Izd. Nauka, Sib. Otd., Novosibirsk, SUN., p. 166-176.

Tokarev, P. I., H. Aoki, ed. and S. Iizuka, ed. (1976). Seismic Activity of the Kamchatka Focal Layer and its Relationship to Volcanism. Tokai Univ. Press. Tokyo, Japan, p. 217-223.

Tulina, Yu V., S. M. Zverev and G. A. Krasil'shchikova (1975). The Earth's Crust and Upper Mantle in the Focal Zone Near Eastern Kamchatka. IN: Seismic Properties of the Mohorovicic Discontinuity, N. I. Davydova, ed., p. 76-90.

Tulina, Yu V. (1969). Detal'nyye Seismicheskiye Issledovaniya Zemnoy Kory Yuzhnykh Kuril'Skikh Ostrovov (Detailed Seismic Investigations of the Earth's Crust of the Southern Kurile Islands). Moscow, Akad. Nauk SSSR, p. 90-96.

Tulina, Yu V., S. M. Zverev, G. G. Mikhota and Ye N. Zaytseva (1972). Osobennosti Voln ot Poverkhnosti Mokhorovichicha na Okeana i v Perekhodnoy Zone (Characteristic Waves from the Mohorovicic Discontinuity Under the Ocean and in the Transitional Zone). Akad. Nauk SSSR, Inst. Fiz. Zemli, Moscow, p. 50-56.

Tuyezov, I. K. (1970a). Seismicheskiye Razrezy Zemnoy Kory Severo-Zapadnoy Chasti Tikhookeanskogo Pordivizhnogo Poyasa (Seismic Sections of the Earth's Crust in the Northwestern Part of the Pacific Ocean Mobile Belt). Akad. Nauk SSSR, n. 3, p. 100-104.

Tuyezov, I. K. (1970b). Seismicheskiye Razrezy Zemnoy Kory Severo-Zapadnoy Chasti Tikhookeanskogo Podvizhnogo Poyasa (Seismic Profiles of the Crust in the Northwestern Part of the Pacific Ocean Belt). Geol. Geofiz. Akad. Nauk SSSR, Sib. Otd., (GGASAS), n. 3, p. 100-104.

Tuyezov, I. K., M. L. Krasnyy, O. S. Solov'yev and E. V. Kochergin (1970c). The East-Kurile Magnetic Anomaly. Phys. Solid Earth, (IPSEBQ) n. 1, p. 60-62.

Tuyezov, I. K. (1975a). Litosfera Aziatsko-Tikhoceanskoy Zony Perekhoda (Lithosphere of the Transition Zone Between Asia and the Pacific Ocean). Izd. Nauka, Sib. Otd., Novosibirsk, SUN, p. 230.

Tuyezov, I. K. (1975b). Models of the Subsurface Structure of Some Areas in the Northwest Sector of the Asia-Pacific Transition Zone with a Continental Crustal Structure. Acad. Sci. USSR, Dokl., Earth Sci. Sect., (USA) (DKESA9), v. 220, n. 1-6, p. 103-106.

Tuyezov, I. K., M. L. Krasnyy, B. I. Vasil'yev and A. A. Kulikov (1975c). Geologicheskoye Stroyeniye Yuzhnogo Zvena Kuril'skoy Ostrovnoy Dugi (Structure of the Southern Part of the Kuril Island Arc). Geol. Geofiz. Akad. Nauk SSSR, Sib. Otd. (SUN) (GGASAS), n. 12, p. 63-71.

Tuyezov, I. K. (1975d). Inhomogeneities in the Upper Mantle of the Asiatic Margin of the Pacific. Acad. Sci. USSR, Dokl., Earth Sci. Sect. (USA) (DKESA9), v. 219, n. 1-5, p. 26-28.

Tuyezov, I. K. (1976a). Modeli Glubinogo Stroyeniya Osnovnykh Tipov Struktur Sever-Zapadnogo Sektora Zony Perekhoda ot Aziatskogo Kontinenta k Tikhomu Okeanu (Models for the Deep-Seated Structure of the Main Structural Types in the Northwestern Sector of the Transitional Zone Between the Asian Continent and the Pacific Ocean). Geol. Geofiz. Akad. Nauk SSSR, Sib. Otd. (SUN) (GGASAS), n. 1, p. 86-90.

Tuyezov, I. K., H. Aoki, ed. and S. Iizuka, ed. (1976b). On the Geologic Nature of the Okhotsk and Japan Sea Abyssal Depressions. Tokai Univ. Press, Tokyo, Japan, p. 333-340.

Udias, Agustin and William Stauder (1964). Application of Numerical Method for S-Wave Focal Mechanism Determinations to Earthquakes of Kamchatka-Kurile Islands Region. Seismol. Soc. America Bull., v. 54, n. 6, pt. A, p. 2049-2065.

Ukawa, M. (1979). The Landward Thinning of the Low-Velocity Layer Across the Kurile-Japan Trench; Earth Planet. Sci. Lett., v. 43, n. 3, p. 434-440.

Utnasin, V. K., S. T. Balesta, E. N. Erlikh, G. I. Anosov, L. L. German and A. Ye. Shantser (1975). Glubinoye Stroyeniye Strukturnykh Zon Kamchatki (The Deep Structure of the Kamchatka Structural Zone). Sov. Geol. (SUN) (SVGLA2), n. 2, p. 67-80.

Utnasin, V. K., A. I. Abdurakhmanov, G. I. Anosov, Yu. A. Budyansky, V. I. Fedorchenko, Ye. K. Markhinin, S. T. Balesta, H. Aoki, ed. and S. Iizuka, ed. (1976a). Types of Magma Foci of Island Arc Volcanoes and Their Study by the Method of Deep Seismic Sounding in Kamchatka. Tokai Univ. Press, Tokyo, Japan, p. 123-137.

Utnasin, V. K., S. T. Balesta, E. N. Erlikh, G. I. Anosov, L. L. German and A. Ye. Shantser (1976b). Deep-Seated Construction of the Structural Zones of Kamchatka. Int. Geol. Rev. (USA) (IGREAP), v. 18, n. 1, p. 1-12.

Uyeda, S. and V. Vacquier (1967). Results of Geomagnetic Survey During the Cruise of R/V ARGO in the Western Pacific 1966 and the Compilation of Magnetic Charts of the Same Area (with Japanese Abs.). Tokyo Univ. Earthquake Research Inst. Bull., v. 45, pt. 3, p. 799-814.

Vashchilov, Yu. Ya. and A. G. Gayanov (1972). Plotnostnyye Neodnorodnosti Zemnoy Kory i Verkhney Mantii (Density Irregularities of the Crust and Upper Mantle). Akad. Nauk SSSR. (RIGPAE), n. 8, p. 44-52.

Vasil'yev, B. I. (1974). O Geologicheskem stroyenii Tikhookeanskogo Shel'fa Maloy Kuril'skoy Gryady (Geology of the Pacific Shelf of the Lesser Kuril Ridge). Akad. Nauk SSSR, Dokl. (DANKAS), v. 219, n. 6, p. 1437-1440.

Vasill'yev, B. I. (1975). Geologic Structure of the Pacific Shelf of the Lesser Kurile Ridge. *Acad. Sci. USSR, Dokl., Earth Sci. Sect. (USA) (DKESA9)*, v. 219, n. 1-6, p. 105-107.

Veith, Karl F. (1972). Accurate Hypocenters and Reliability Estimates (abs.). *EOS (Am. Geophys. Union Trans.)*, (EOSTAJ), v. 53, n. 11, p. 1051.

Veith, Karl Fredrick (1974). The Relationship of Island Arc Seismicity to Plate Tectonics (Parts I and II) (abs.). Doctoral, Southern Methodist University, Dallas, Texas.

Veith, K. F. (1975). Refined Hypocenters and Accurate Reliability Estimates. *Seismol. Soc. Am., Bull. (BSSAAP)*, v. 65, n. 5, p. 1199-1222.

Verba, M. L., G. I. Gaponenko, S. S. Ivanov, A. N. Orlov, V. I. Timofeyev, and Yu. F. Chernyakov (1971). Glubinnoye Stroyeniye i Perspektivy Neftegazonosnosti Sever-Zapadnoy Chasti Beringova Morya (Deep Structure and Oil and Gas Possibilities in the Northwestern Part of the Bering Sea). *Geofiz. Metody Razv. Arkt.*, (GMRABY), n. 6, p. 70-74.

Vereshchagin, V. N., O. P. Dundo and G. P. Terekhova (1972). Kamchatsko-Koryakskiy Basseyn Sedimentatsii (The Kamchatka-Koryak Sedimentary Basin). IN: *Geologiya Sever-Vostochnoy Azii*, tom 2, Stratigrafiya i Paleogeografiya; Melovaya Sistema V. N. Vereshchagin et al., eds., p. 343-347.

Veltsman, P. S. (1966). On the Deep Structure in the Kuril-Kamchatka Region with Discussion. *Can., Geol. Surv. Paper 66-15*, p. 244-251.

Vesanen, E., H. V. Tuominen, U. Luosto and M. L. Maki (1973). The Spatial Distribution of Earthquakes in the Kurile-Okhotsk Region. *Int. Inst. Seismol. Earthquake Engl., Bull. (IISBB2)*, v. 10, p. 91-95.

Veselov, O. V., N. A. Volkova, G. D. Sremen, N. A. Kozlov and V. V. Soinov (1974). *Izmereniye Teplovogo Potoka v Zone Perkhoda ot Aziatskogo Materika k Tikhomu Okeanu* (Measurement of the Heat Flow in the Transition Zone Between the Asian Continent and the Pacific Ocean). *Akad. Nauk SSSR, Dokl. (DANKAS)*, v. 217, n. 4, p. 897-900.

Von Huene, R., N. Nasu, M. Arthur, J. P. Cadet, B. Carson, R. Reynolds, B. L. Shaffer, S. Sato and G. Bell (1978). On Leg 57; Japan Trench Transected. *Geotimes (USA) (GEOTAJ)*, v. 23, n. 4, p. 16-20.

Walker, D. A. (1966). The Observation and Analysis of Body Waves Recorded in the Northwestern Pacific (abs.). In *Pacific Sci. Cong.*, 11th, Tokyo 1966, Proc., v. 3, Tokyo, Sci. Council Japan, Div. Mtg. Solid Earth Physics I, p. 28.

Walker, D. A. (1965). A Study of the Northwestern Pacific Upper Mantle. *Seismol. Soc. America Bull.*, v. 55, n. 5, p. 925-939.

Watts, A. B. and A. R. Leeds (1977). Gravimetric Geoid in the Northwest Pacific Ocean. *R. Astron. Soc., Geophys. J. (GBR) (GEOJAN)*, v. 50, n. 2, p. 249-277.

Watts, A. B., M. Talwani and J. R. Cochran (1976). Gravity Field of the Northwest Pacific Ocean Basin and Its Margin. *Am. Geophys. Union. Geophys. Monogr. (USA) (GPMGAD)*, n. 19, p. 17-34.

Watts, A. B. (1975a). Gravity Field of the Northwest Pacific Ocean Basin and Its Margin: Aleutian Island Arc-Trench System. *Geol. Soc. Am., Map Chart Ser.*, n. MC-10, 5 pp.

Watts, A. B. and M. Talwani (1975b). Gravity Effect of Downgoing Lithospheric Slabs Beneath Island Arcs. *Geol. Soc. Am., Bull.*, (BUGMAF), v. 86, n. 1, p. 1-4.

Weisman, P. S. (1966). On the Deep Structure in the Kuril-Kamchatka

Region. IN: Continental Margins and Island Arcs-Internat. Upper Mantle Comm., Symposium, Ottawa, 1965. Canada Geol. Survey Paper 66-15, p. 244-251.

Yasui, M., S. Uyeda, T. Watanabe, Asano. Shuzo, ed. and G. B. Udintsev, ed. (1971). Heat Flow in the Western Margin of the North Pacific and its Geophysical Implications. IN: Island Arc and Marginal Sea; Proceedings of the First Japan-USSR Symposium on Solid Earth Sciences. Tokai Univ. Press., Japan, p. 289-296.

Zhadin, V. V. (1975). Absorption of Seismic Waves and the Nature of Earthquakes in the Kamchatka Zone of the Pacific Mobile Belt. Acad. Sci. USSR, Dokl., Earth Sci. Sect. (DKESA9), v. 218, n. 1-6, p. 15-16.

Zhadin, V. V. (1976). Measurements of the Q Factor of the Upper Mantle in the Active Kamchatka Zone. Phys. Solid Earth (USA) (IPSEBQ), v. 12, n. 2, p. 91-95.

Zobin, V. M. and I. G. Simbireva (1977). Focal Mechanism of Earthquakes in the Kamchatka-Commander Region and Heterogeneities of the Active Seismic Zone. Pure Appl. Geophys. (CHE) (PAGYAV'), v. 115, n. 1-2, Stress in the Earth, p. 283-299.

Zverev, S. M., B. S. Vol'vovskiy, ed. and A. G. Rodnikov, ed. (1977). Seismicheskiye Svoystva Zemnoy Kory i Verkhney Mantii Severo-Zapadnoy Chasti Tikhogo Okeana (Seismic Properties of the Earth's Crust and Upper Mantle of the Northwestern Pacific Ocean). Izd. Nauka, Moscow, SUN., p. 28-34.

Figure 1. Location Map of the North Pacific showing study areas, great circle routes between major ports, and centered locations of summer and winter atmospheric pressure cells.

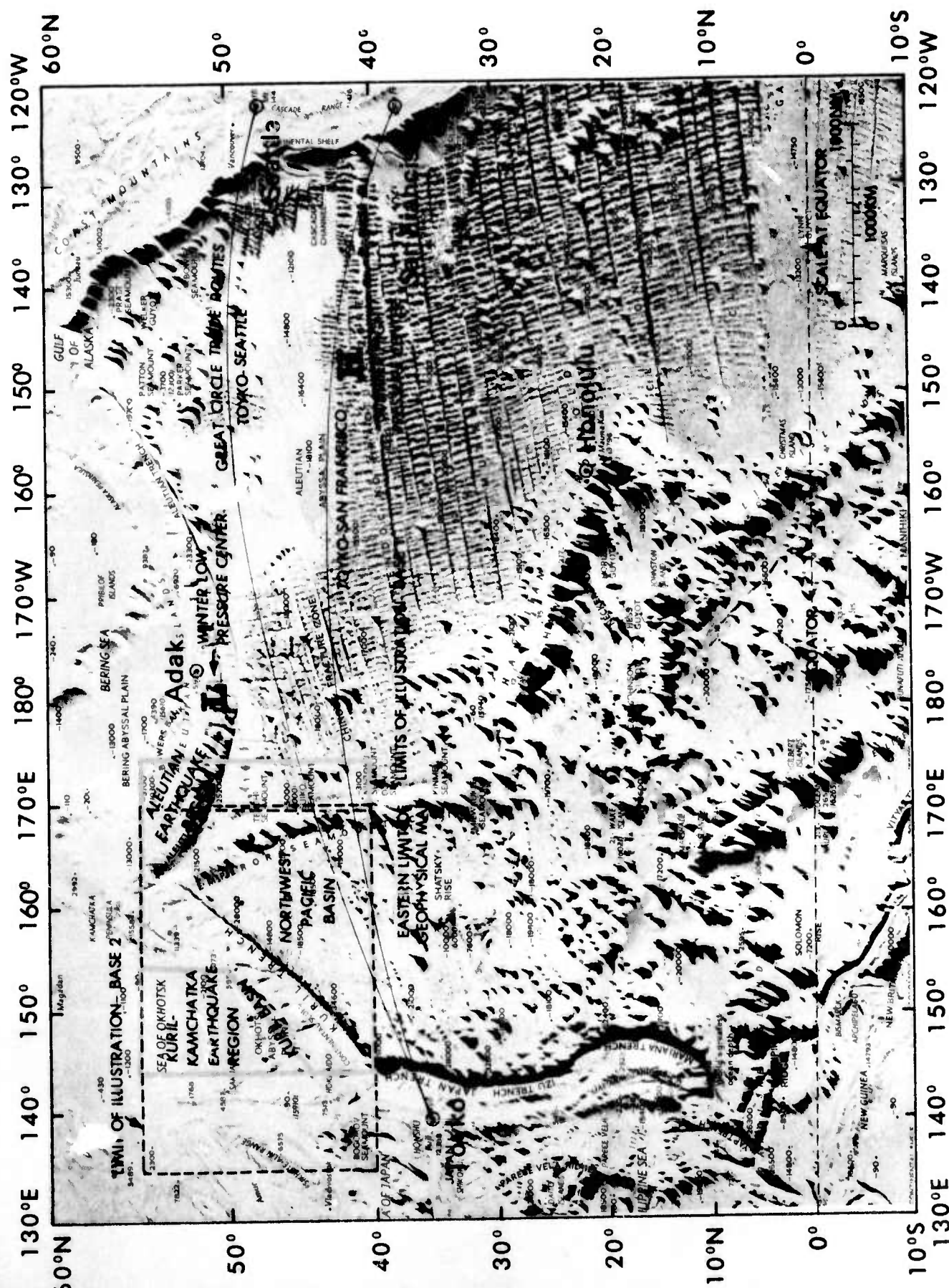


Figure 2. Northwest Pacific base map 1 for locating major features with respect to other mapped parameters.

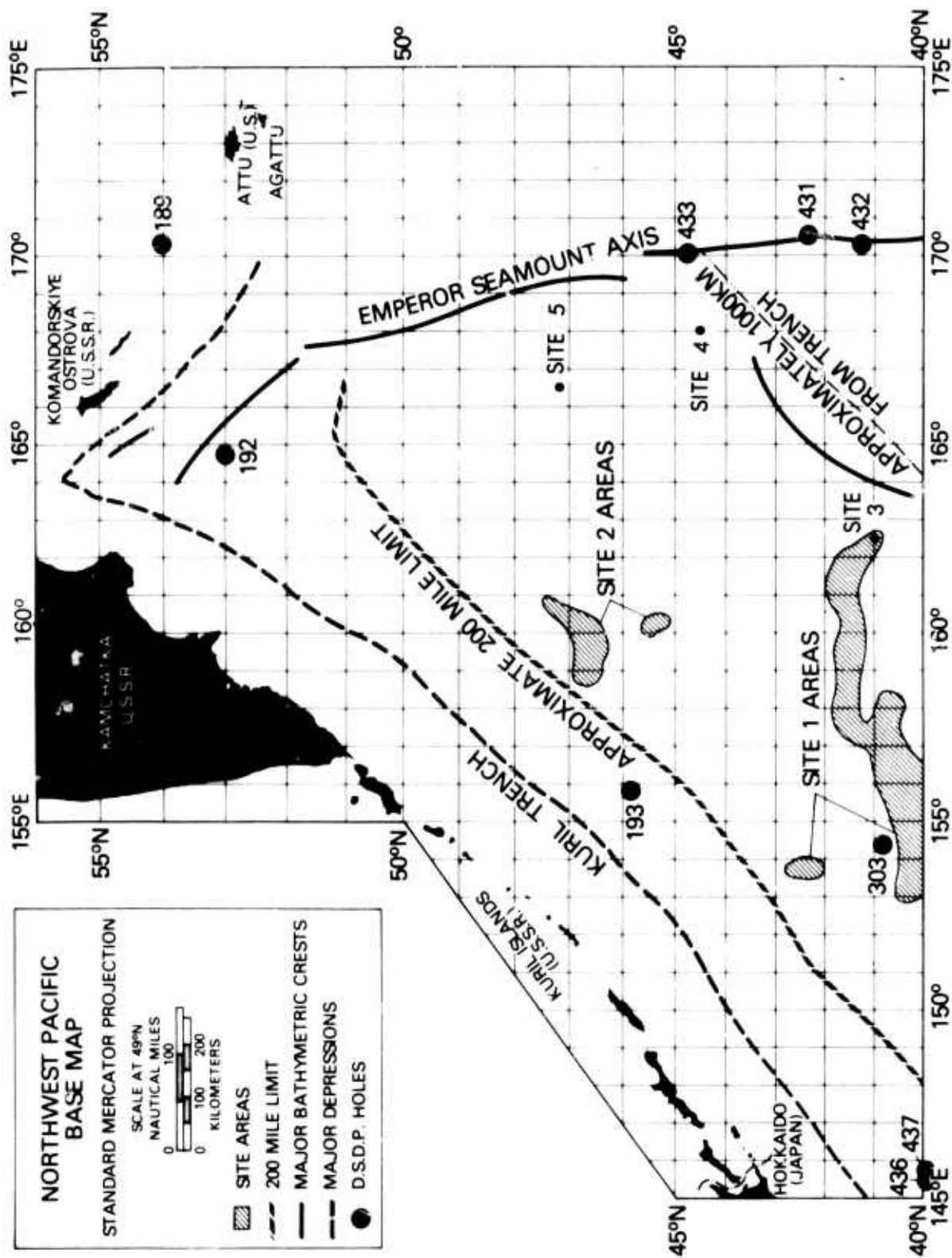


Figure 3. Merchant shipping by instantaneous number based on number of merchant ships in a 10 square at any point in time (from unpublished Planning Systems Inc., data).

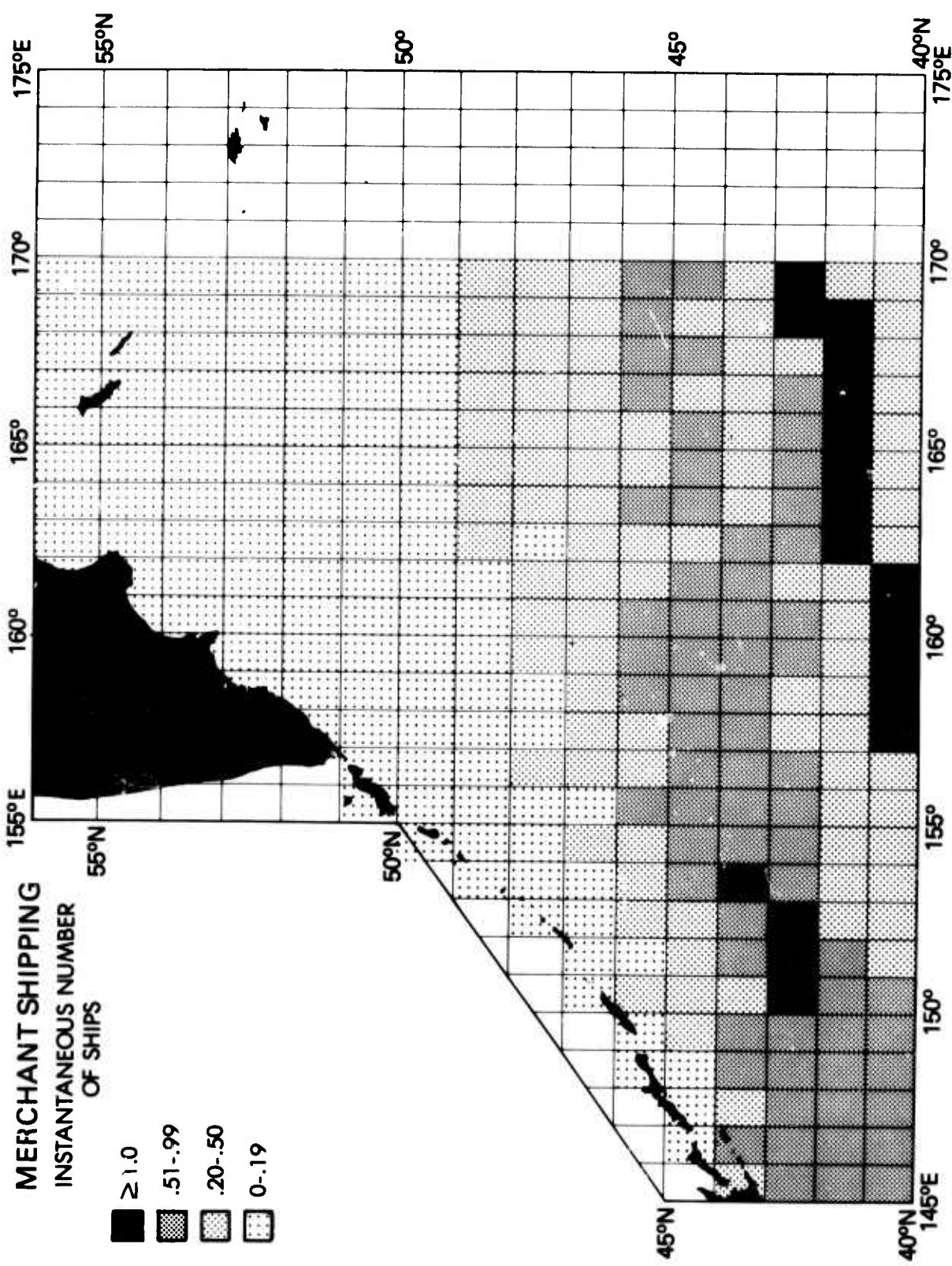


Figure 4. Fishing ships by instantaneous number based on number of fishing ships in a 1° square at any point in time (from unpublished Planning Systems, Inc., data).

FISHING SHIPS
INSTANTANEOUS NUMBER
OF SHIPS

- > .5
- .2-.5
- 0-.19

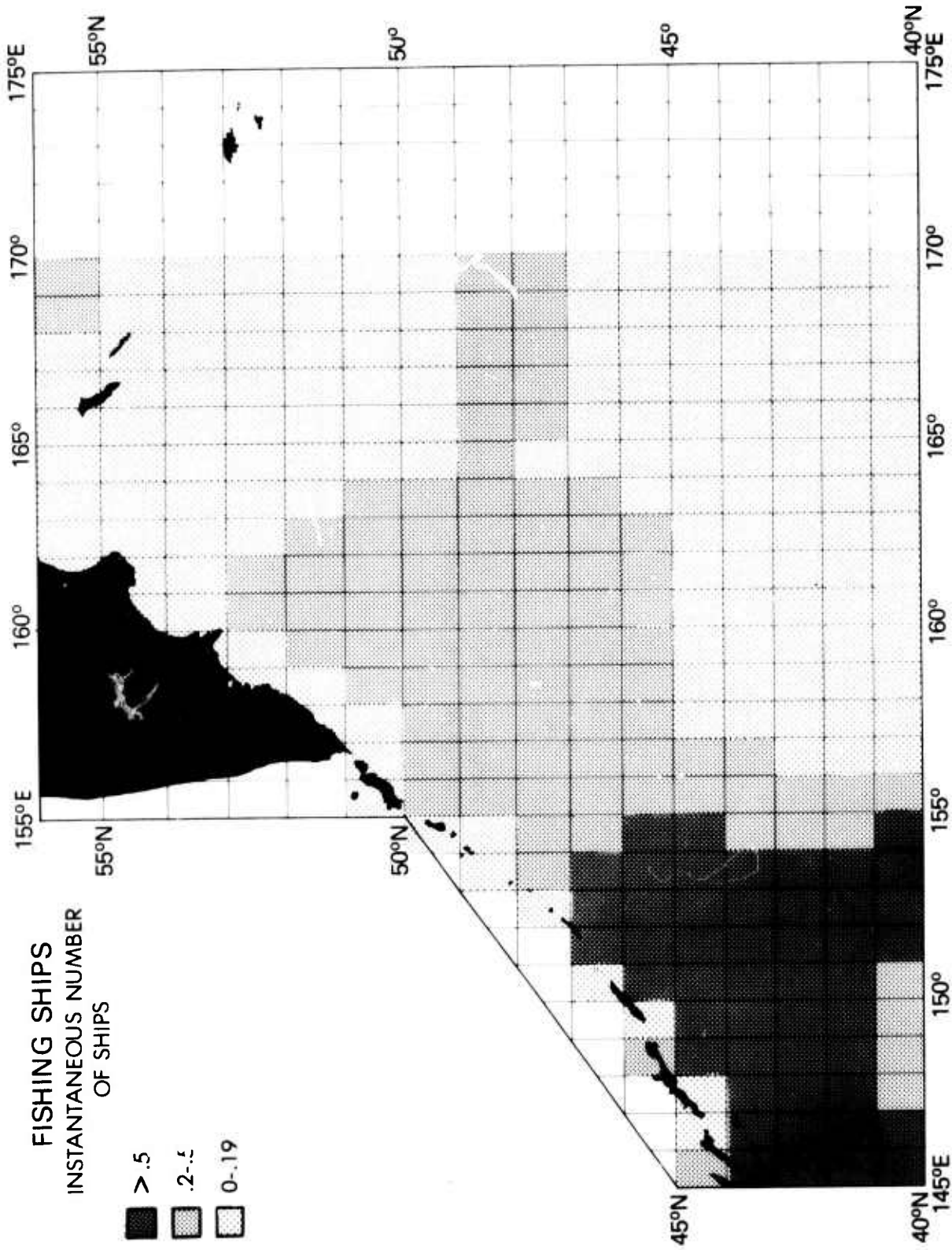


Figure 5. Winter surface current distribution. Arrows denote direction only; shaded areas denote location of major currents (adapted from Gorskoy, 1974).

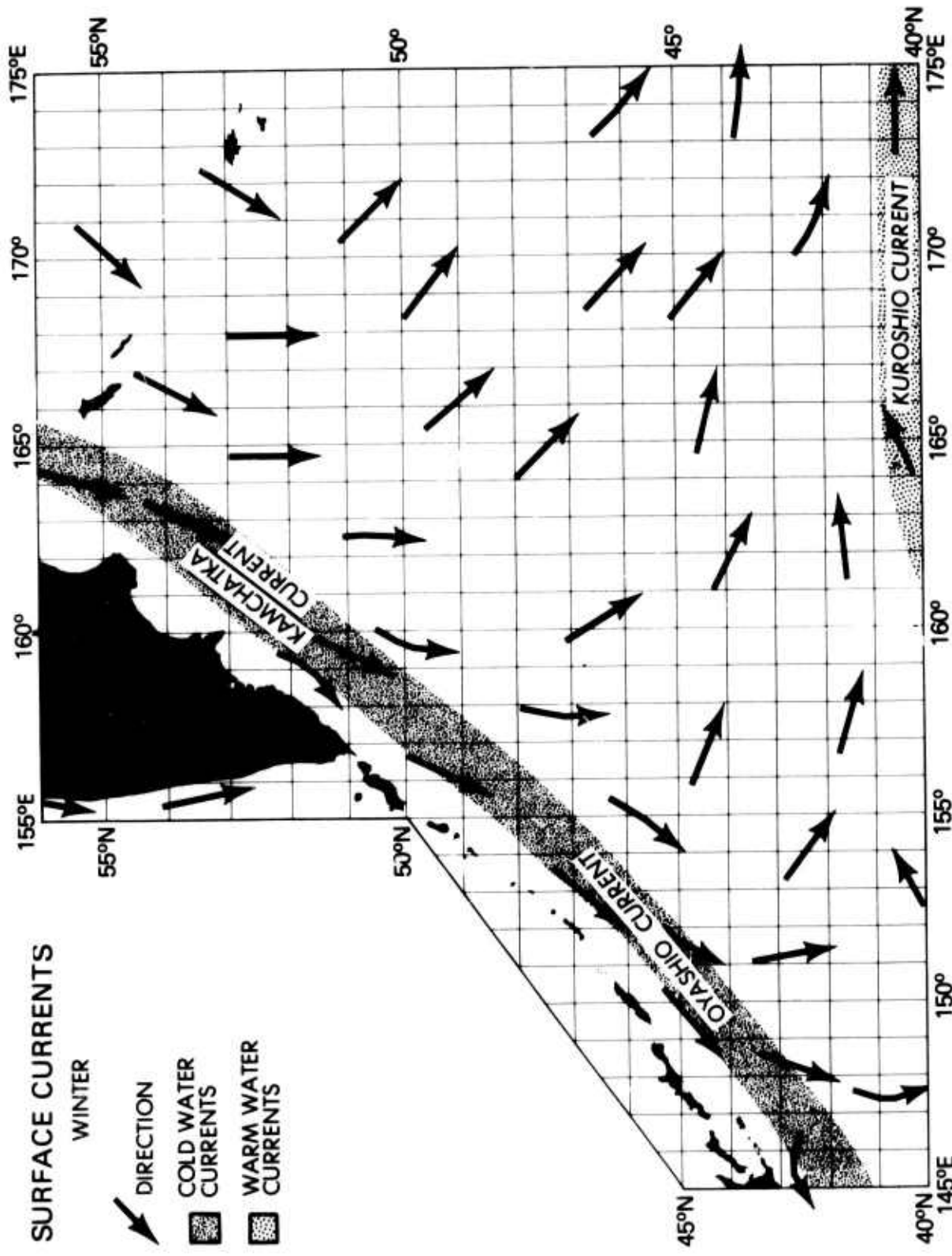


Figure 6. Summer surface current distribution. Arrows denote direction only; shaded areas denote location of major currents (adapted from Gorskoy, 1974).

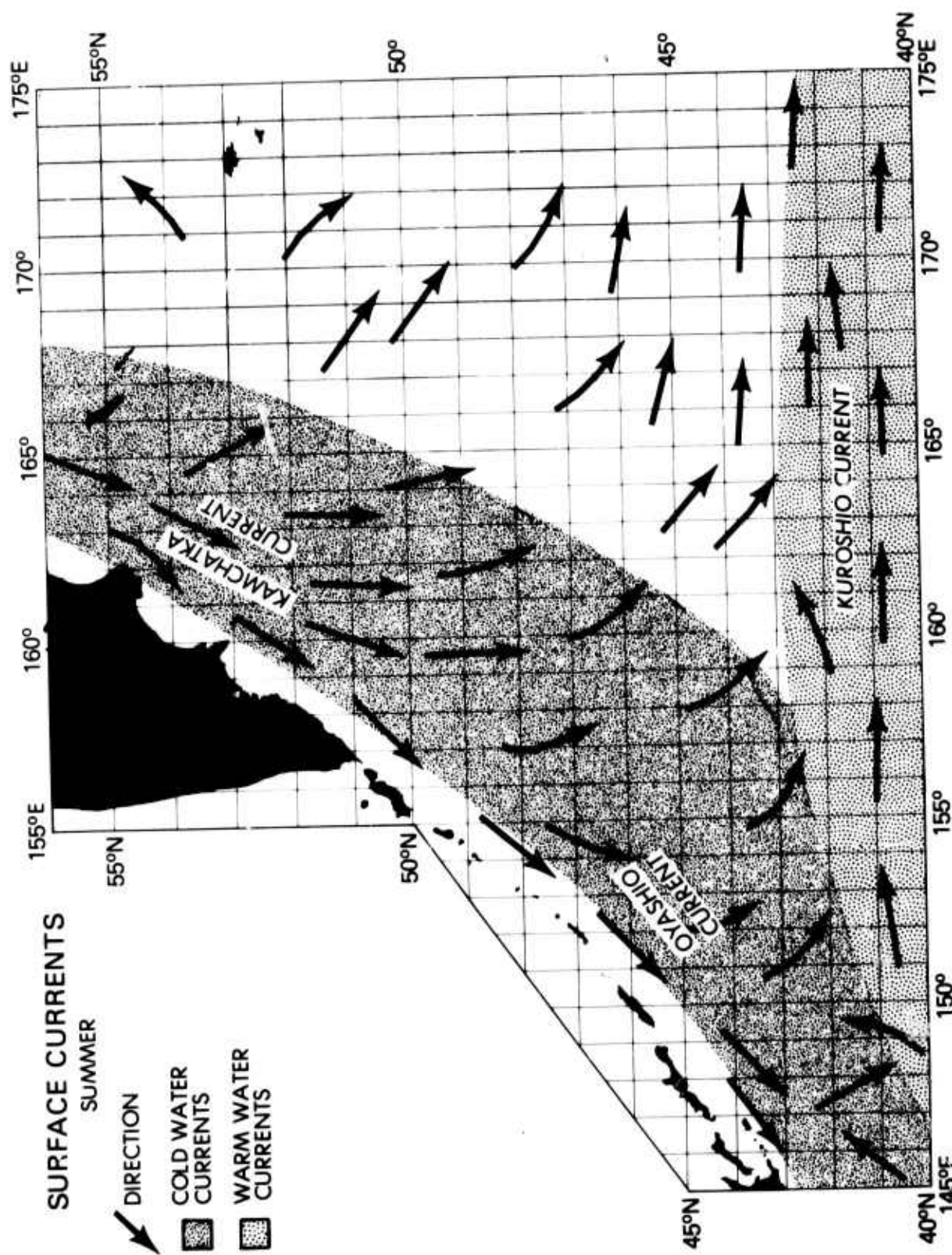


Figure 7. Composite traffic by adjusted instantaneous number based on twice the instantaneous fishing number plus the merchant ship number for one degree squares (from unpublished Planning Systems, Inc., data).

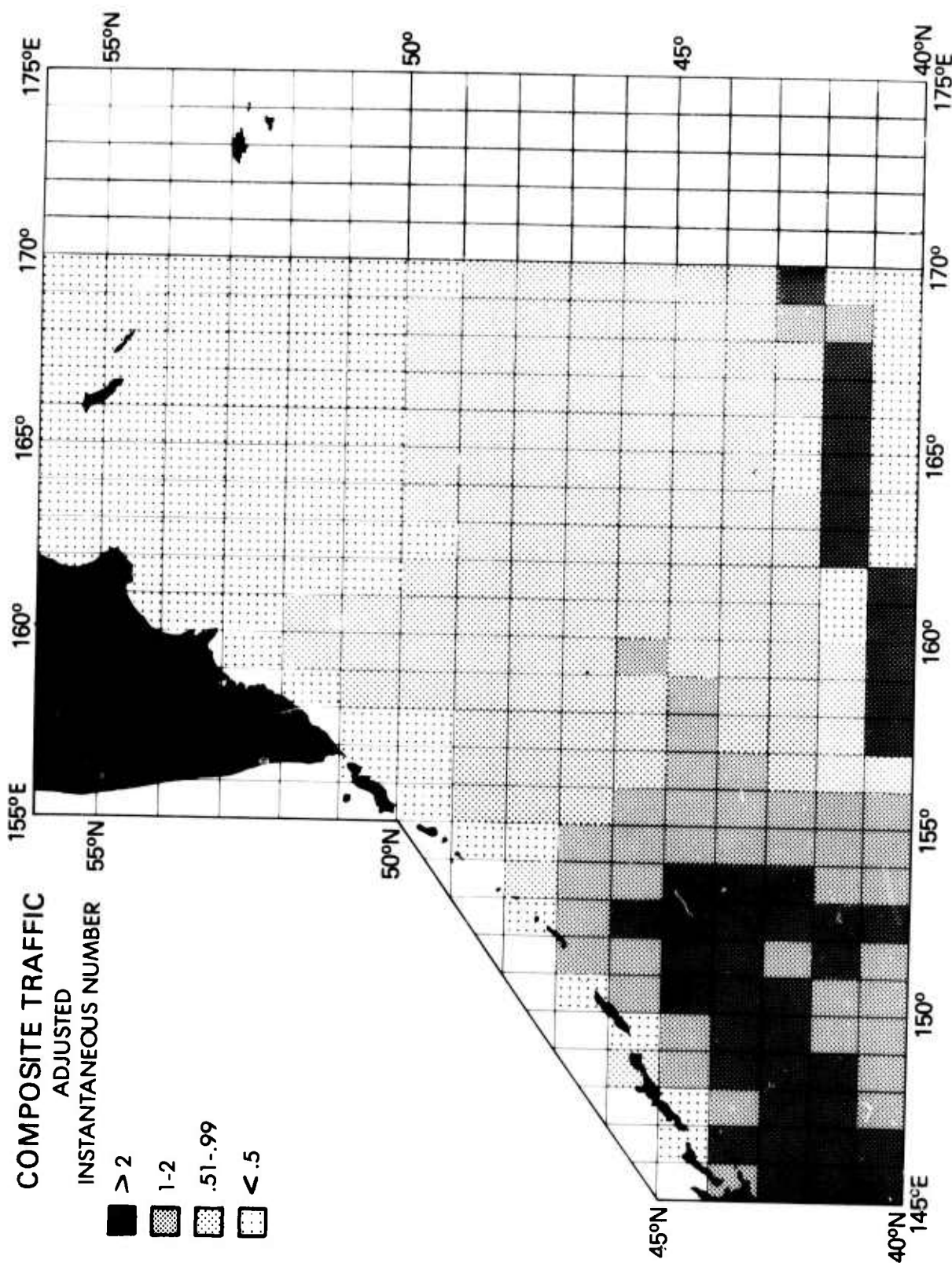


Figure 8. Highest concentration of low pressure areas as noted by month abbreviations centered to show the maximum percent of time each month will have low pressure coverage (adapted from Gorskoy, 1974).

LOW PRESSURE AREAS
HIGHEST CONCENTRATION
PERCENT OF TIME FOR SPECIFIC
MONTHS REPRESENTED BY
CENTRED MONTH ABBREVIATION

F 30-35%

S 25-30%

JY 20-25%

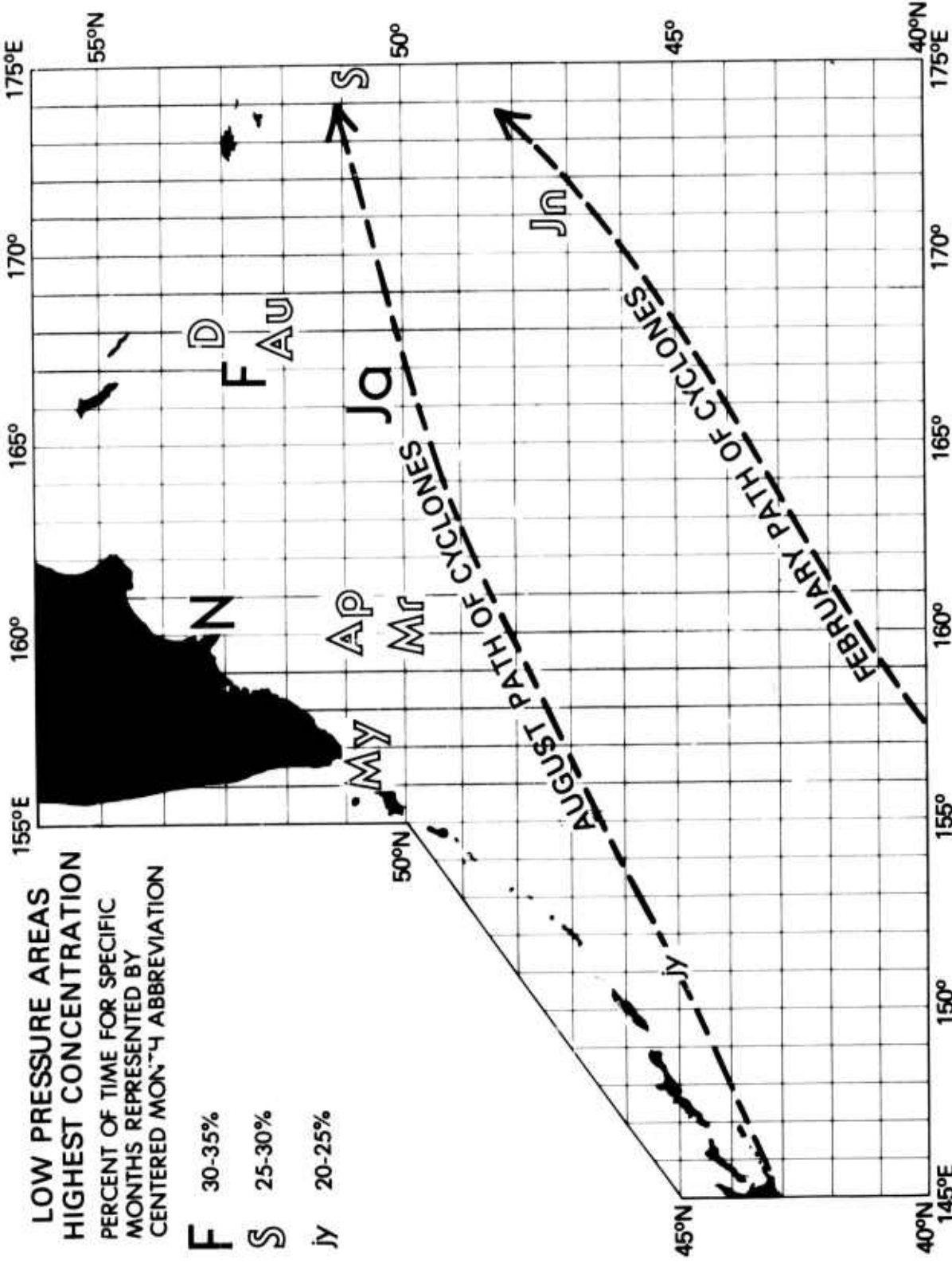


Figure 9. Percent of time areas will have strong winds and the months (represented by centered month abbreviations) when strong winds occur. Mean wind directions are given for August and February (adapted from Gorskoy, 1974).

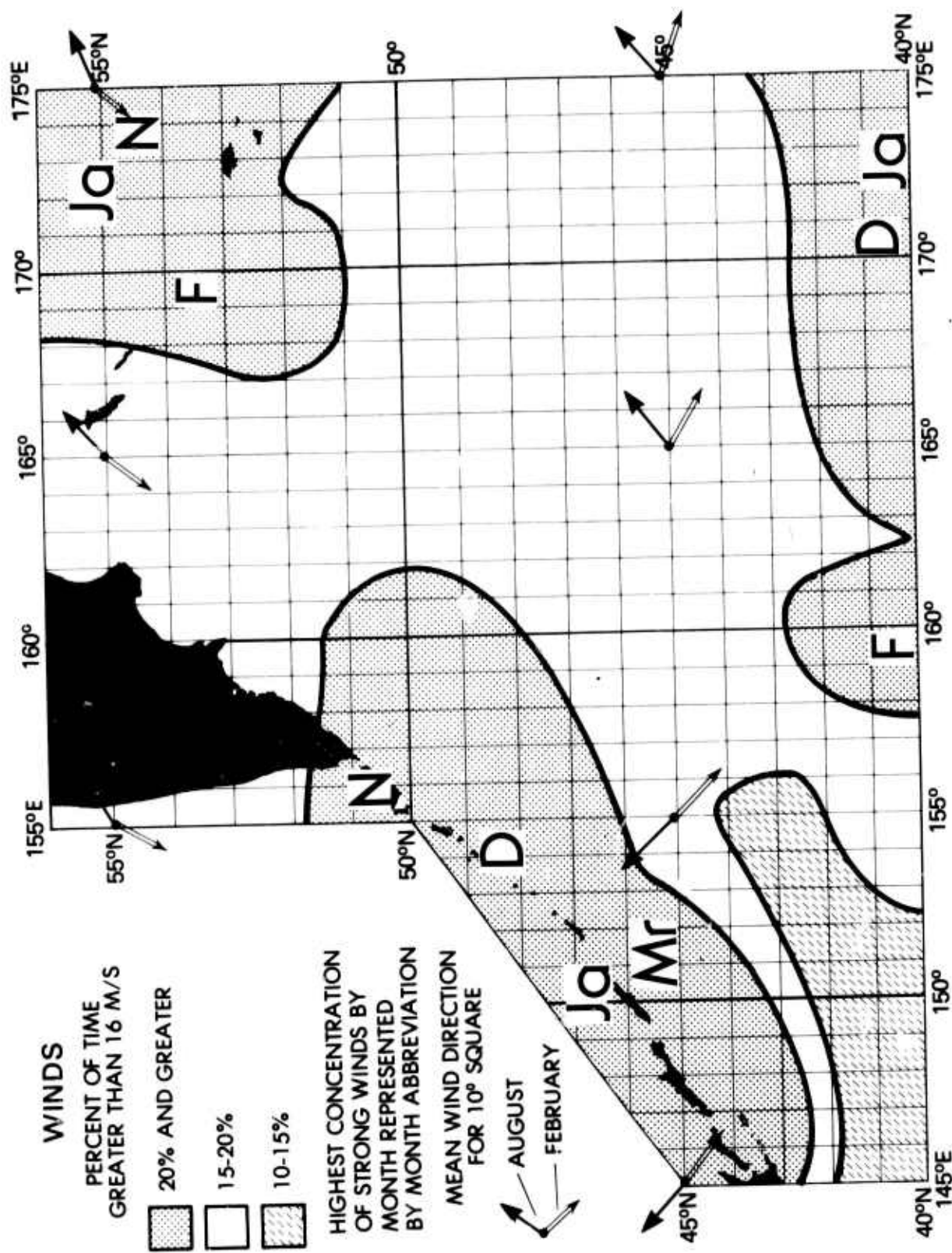


Figure 10. Number of months when minimum sea-surface air temperatures are below 0°C. Expected minimum freezing temperatures for the coldest Northwest Pacific locations are listed by month:

October	0°C	January	-10°C
November	-8°C	February	-14°C
December	-10°C	March	-8°C

April -6°C
May -2°C

(adapted from Gorshkov, 1974)

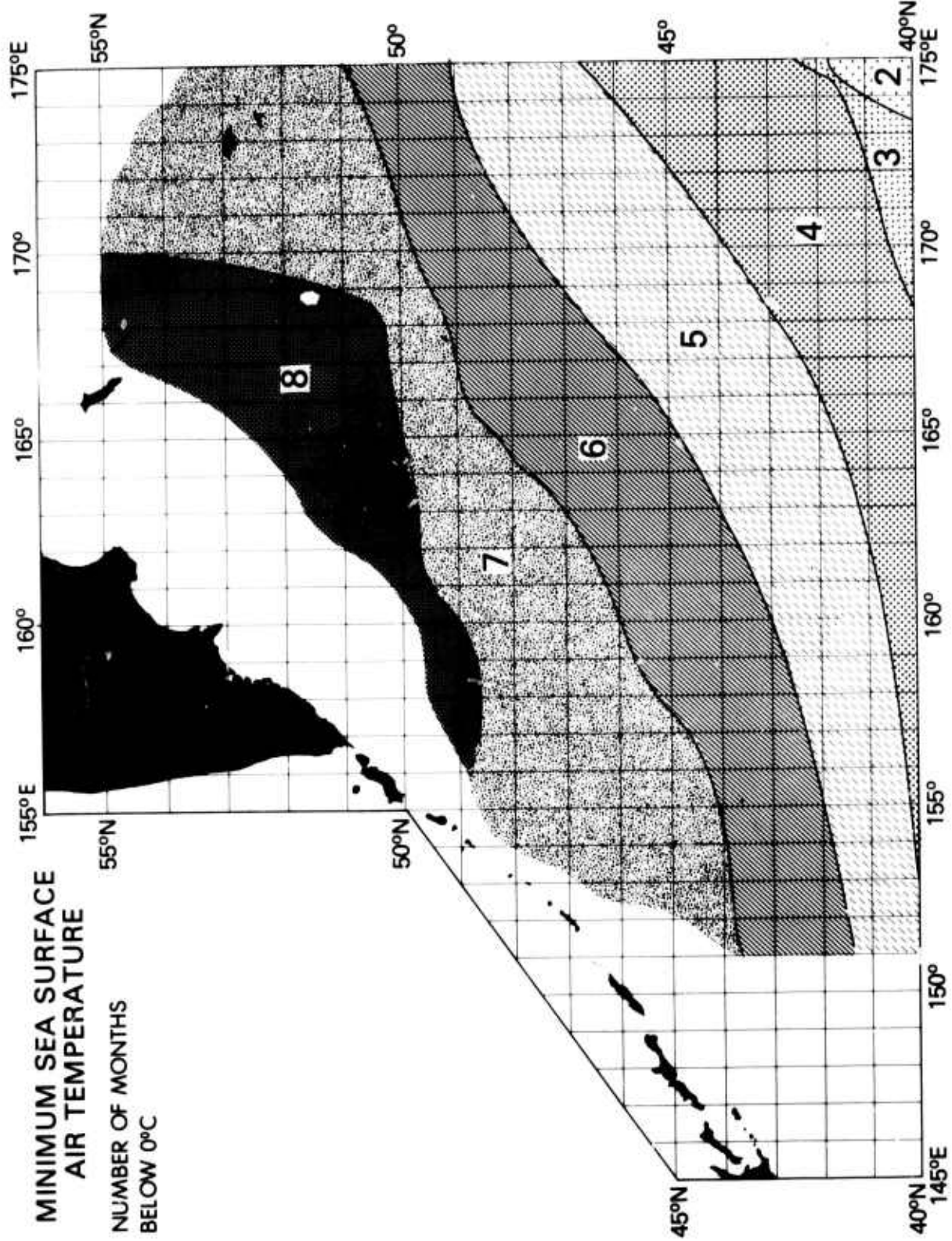


Figure 11. Number of months when minimum sea surface air temperatures are below -8°C (adapted from Gorsikov, 1974).

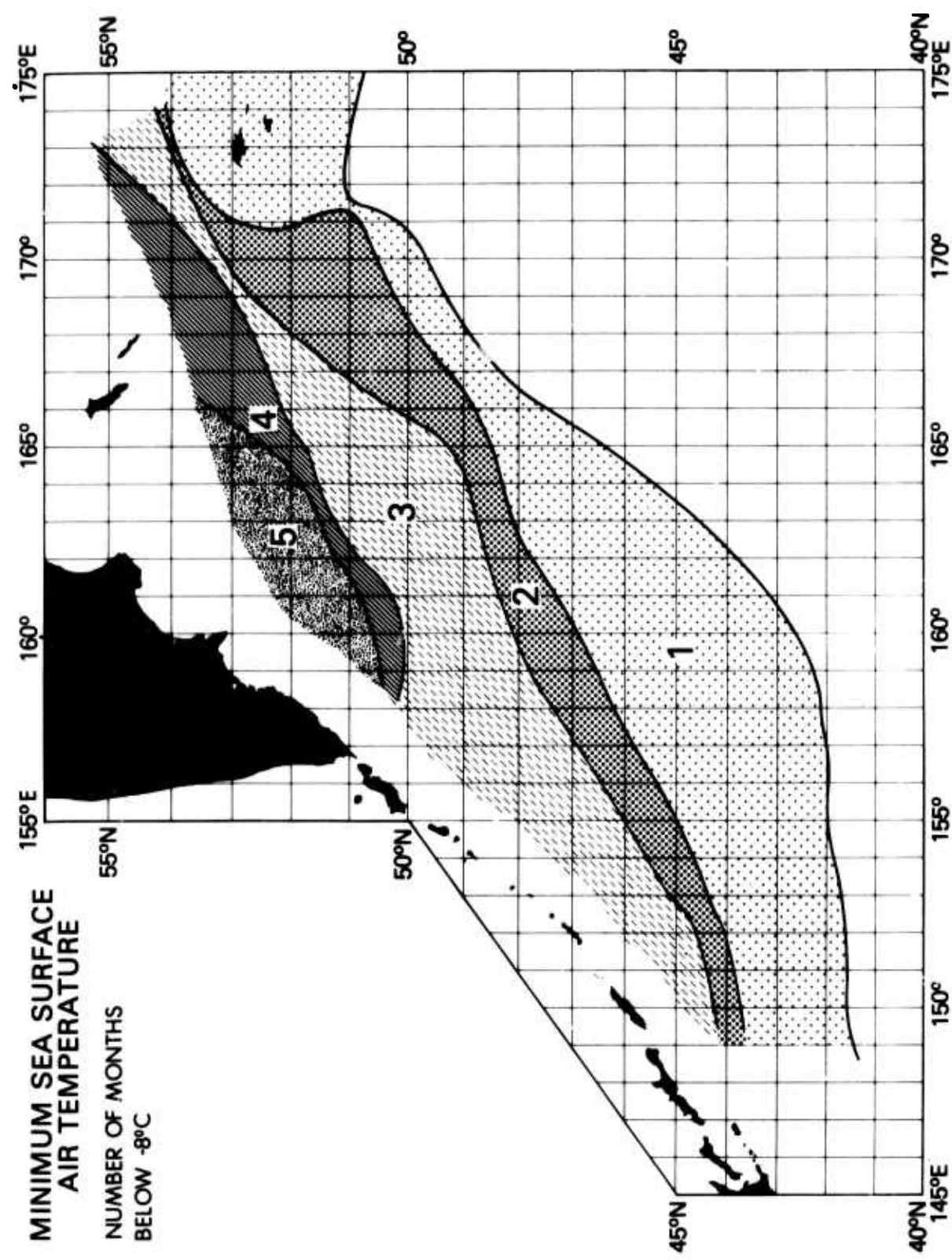


Figure 12. Contours represent the highest 1% of waves contoured for the months having the highest waves. Centered month abbreviations show highest concentration of high waves for the month indicated (adapted from Gorskoy, 1974).

MAXIMUM WAVE HEIGHTS BY MONTH

LOCATION REPRESENTED BY
CENTERED MONTH ABBREVIATIONS

F GREATER THAN
17.5 METERS

N GREATER THAN
15.0 METERS

L LESS THAN 15.0
METERS NOT
SHOWN

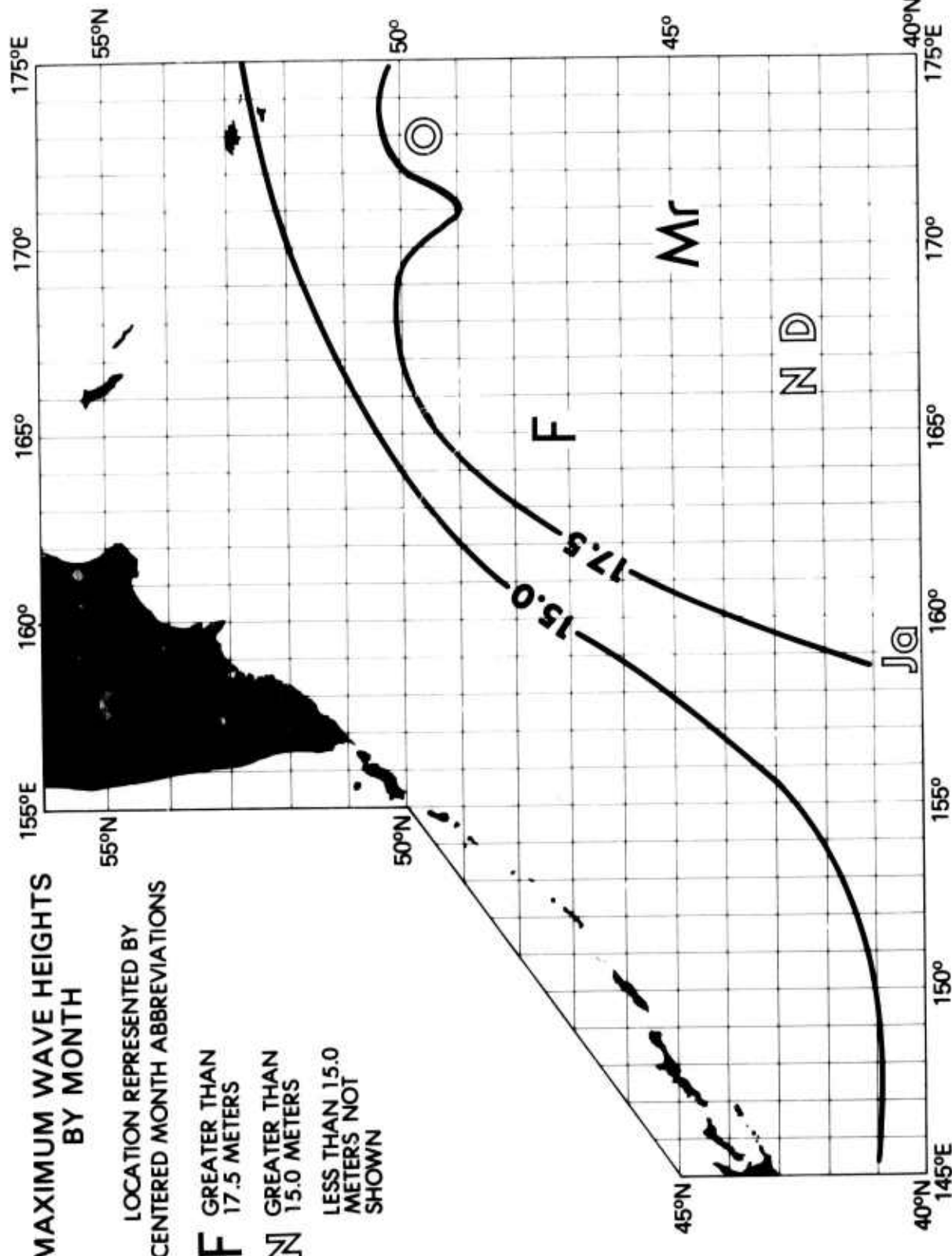


Figure 13. Surface water temperature for February (black) and the annual variation in temperature for the year (shaded) (adapted from Gorskoy, 1974).

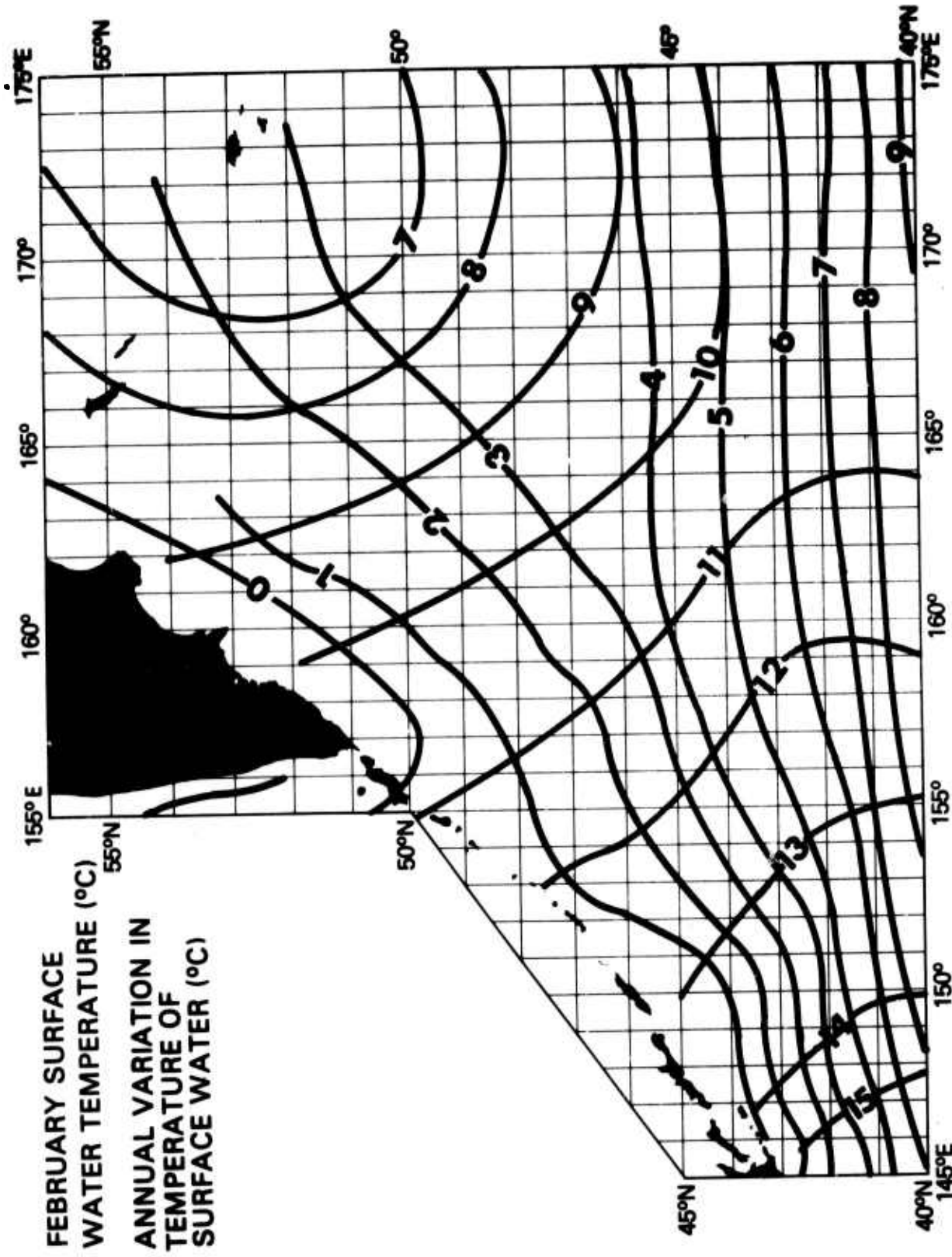


Figure 14. Depth and value of the February temperature maximum (adapted from Reid, 1973).

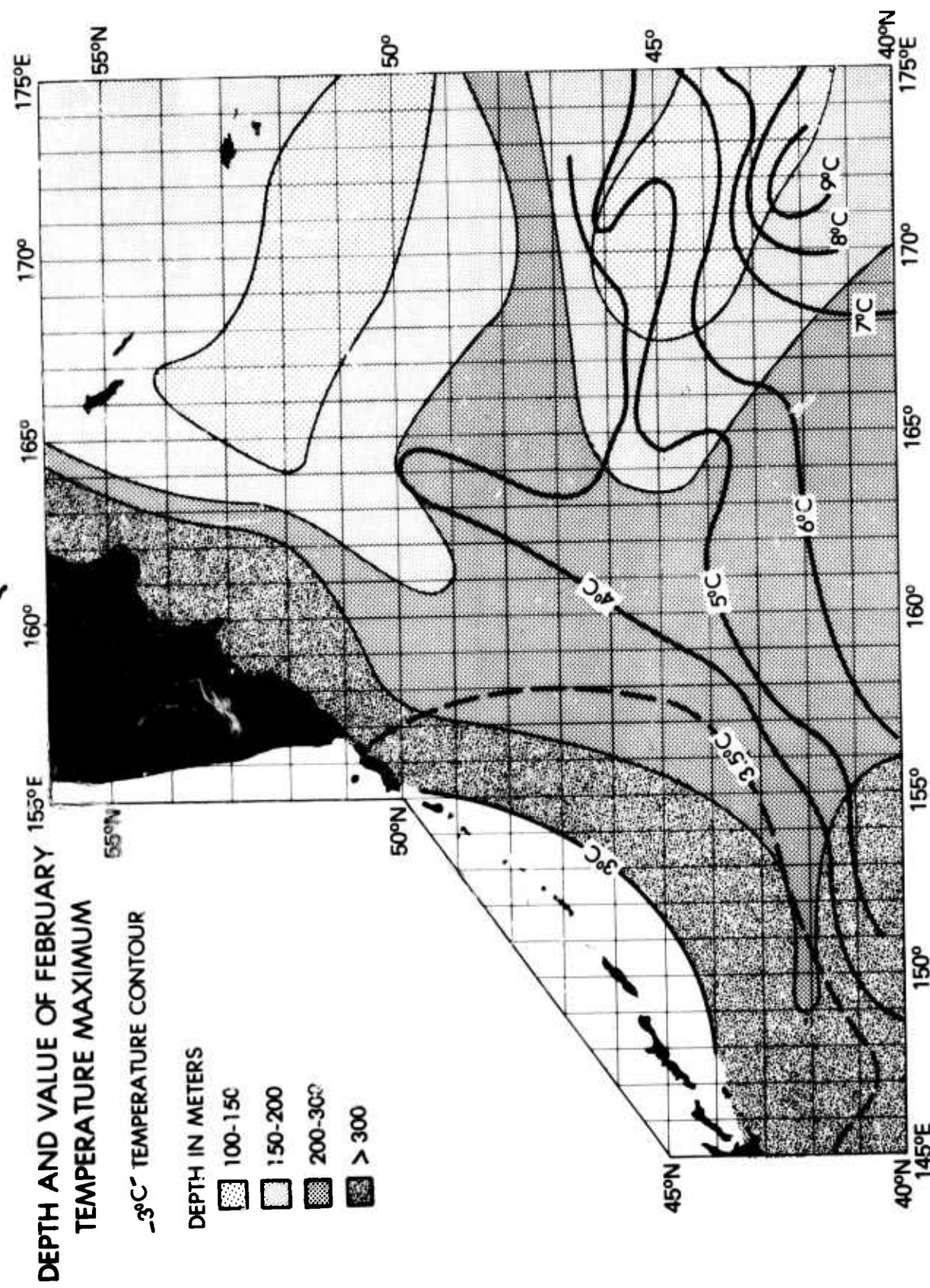


Figure 15. Surface current speed distribution. Speeds for 1° squares are the average speed for the month with the highest speed. Speeds are based on ship drift (adapted from NAVOCEANO Sp. Pub. 1402, NP 4, 5, 7).

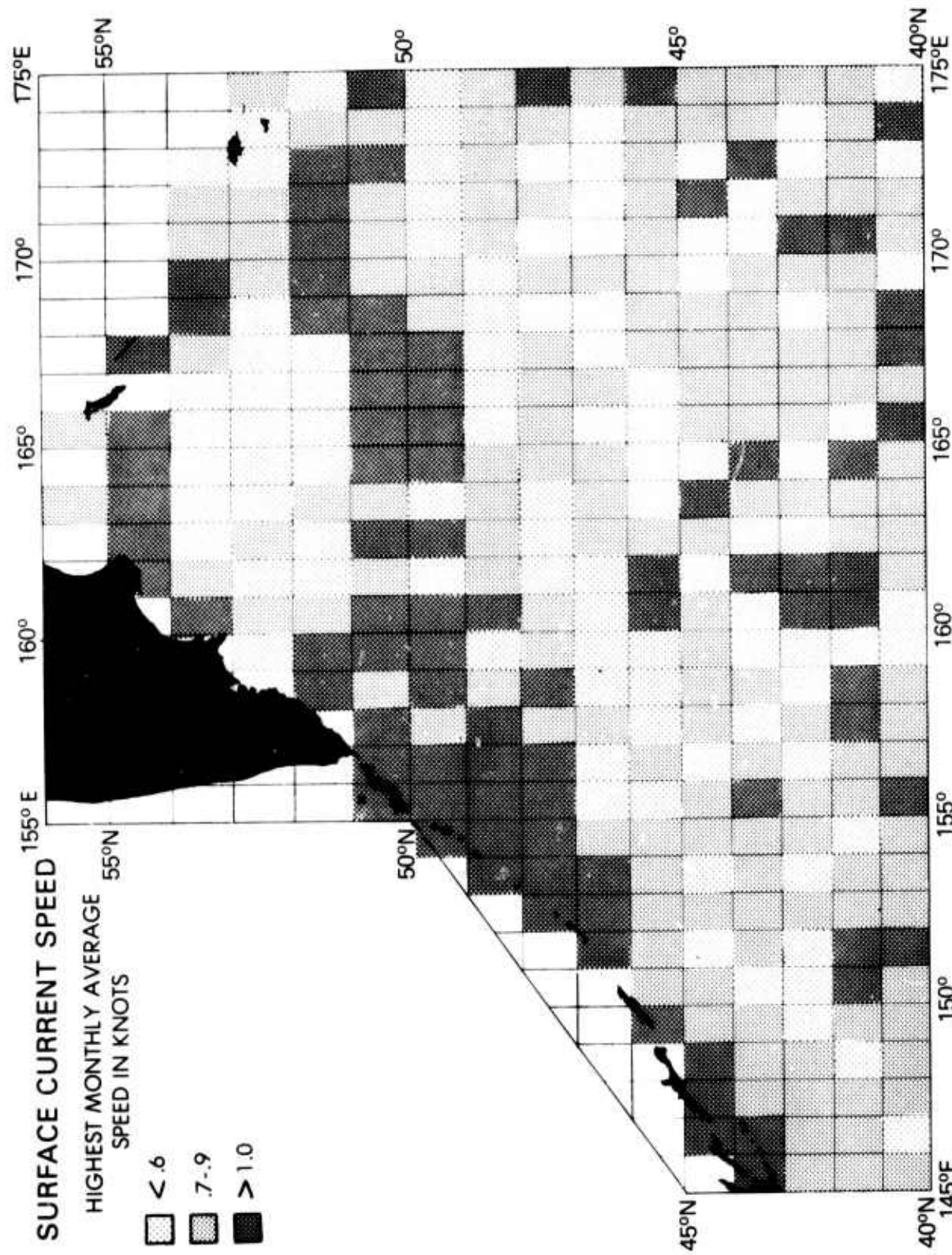


Figure 16. Surface current speed histogram. Values are average surface current speeds for the maximum month based upon ship drift for areas of one square degree (see distribution of same data on Fig. 15) (adapted from NAVOCANO Sp. Pub. 1402, NP 4, 5, 7).

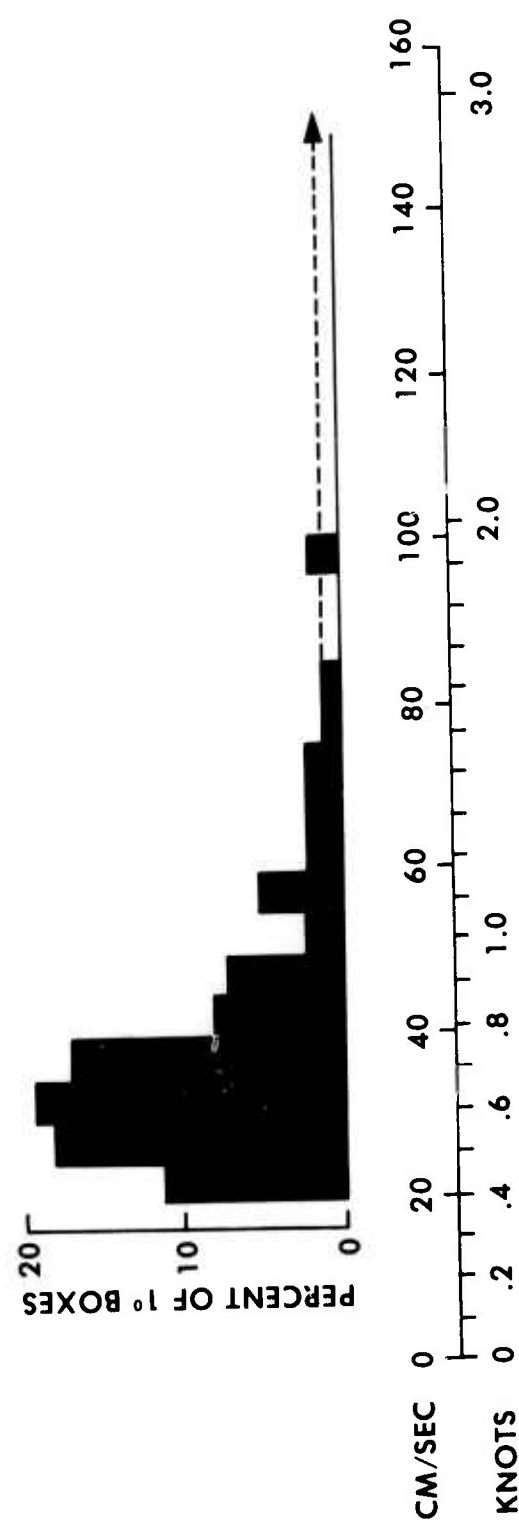


Figure 17. Current speed model showing speed vs. depth. Maximum expected speeds for the Northwest Pacific are presented by the heavy dashed line to the right. Measured speeds for the top 500 m are from unpublished Naval Oceanographic Office files; black bars for 1000 to 4000 m are calculated from geopotential maps (Reid, 1975); and the 20 cm/sec speed for the bottom is derived from observation of LDGO bottom photographs.

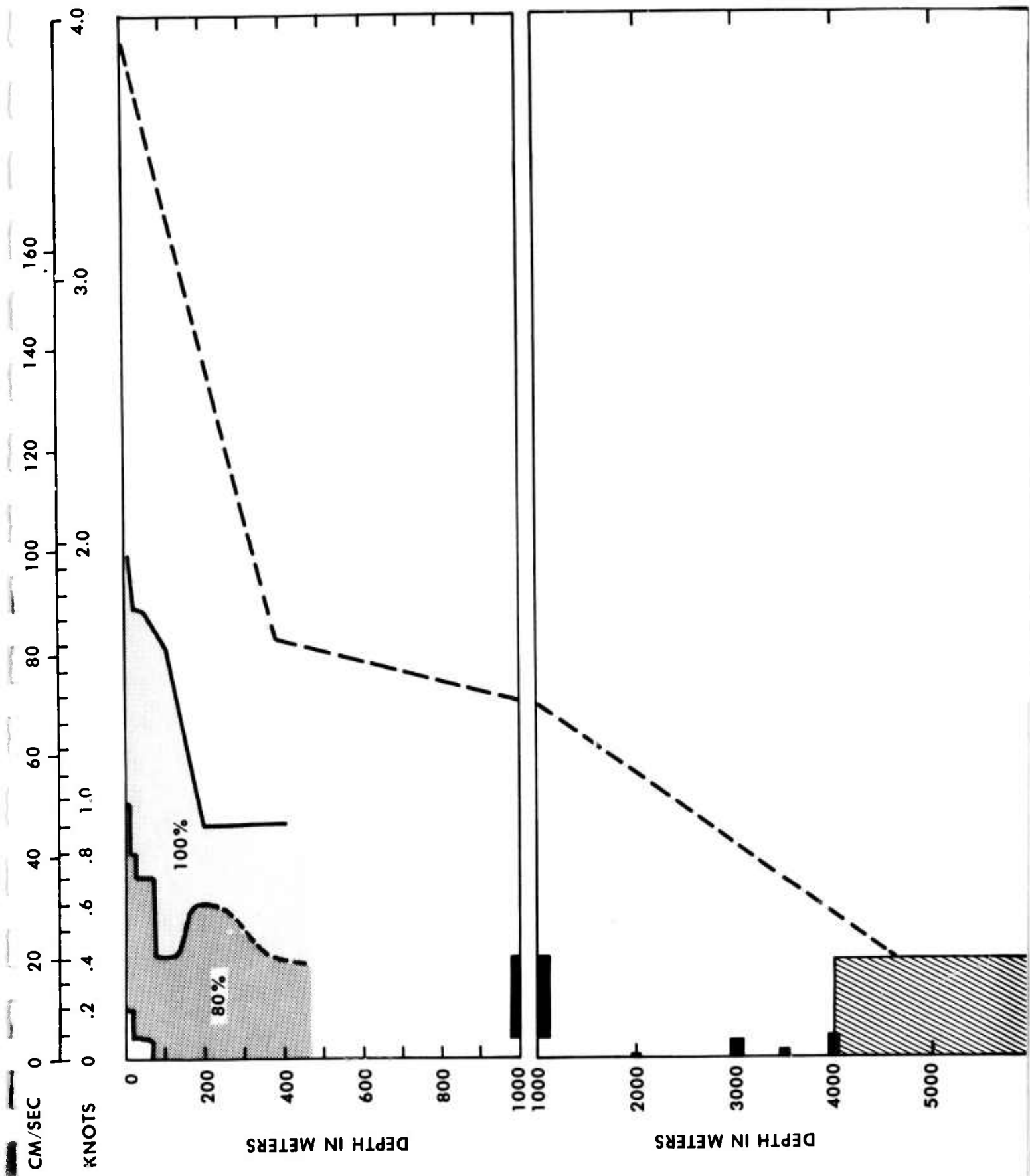


Figure 18. Index for sound speed profiles. April readings denoted by 0 and July by +. Profiles are presented in Figure 19 (adapted from Senior, 1976, and NAVOCEANO, 1978).

SOUND VELOCITY
PROFILE INDEX MAP

X — JULY
O — APRIL

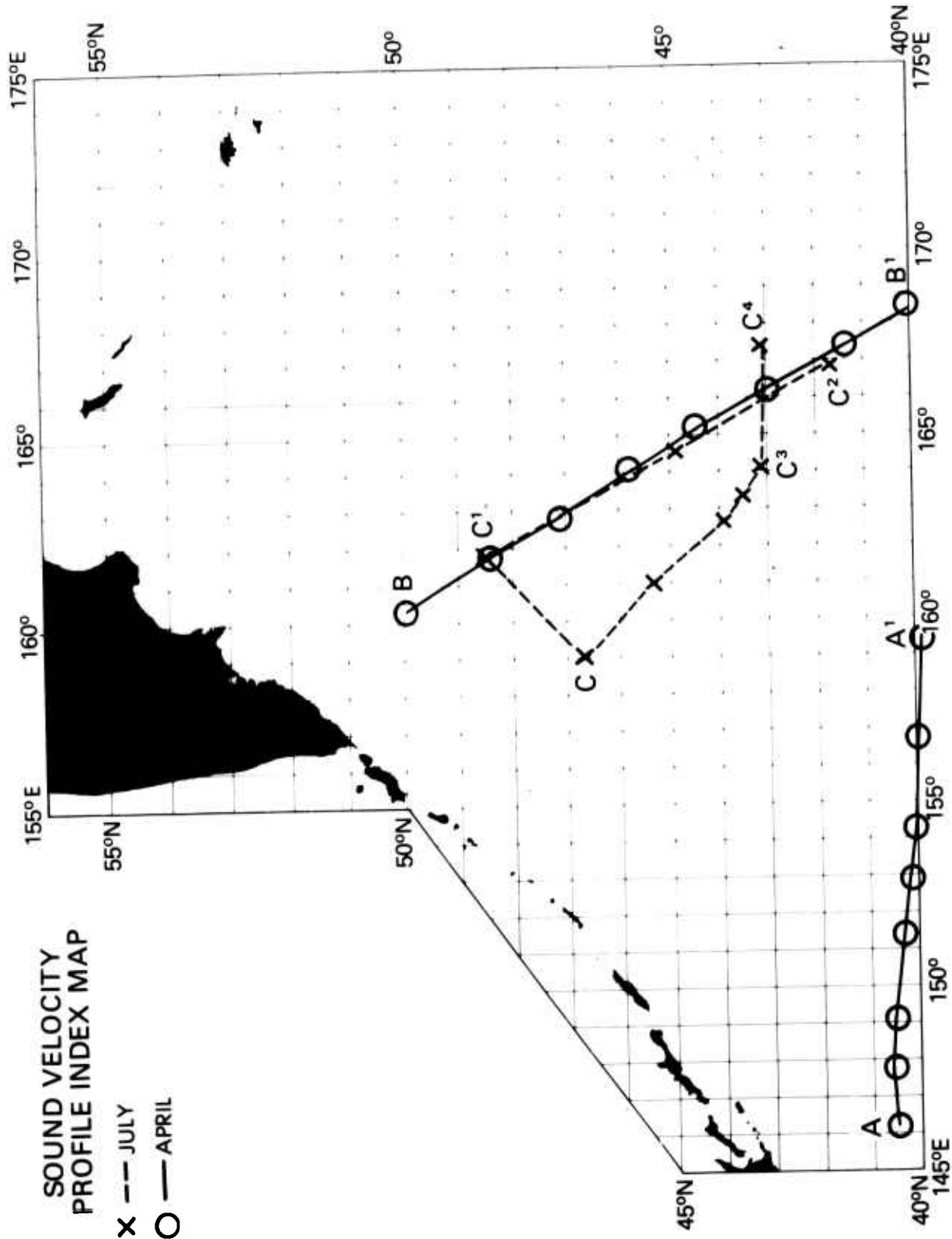


Figure 19. Sound speed profiles. Stations for sound speed measurements of the upper 1600 m of the water column are denoted for April by O and July by x (adapted from Senior, 1976, and NAVOCEANO, 1978).

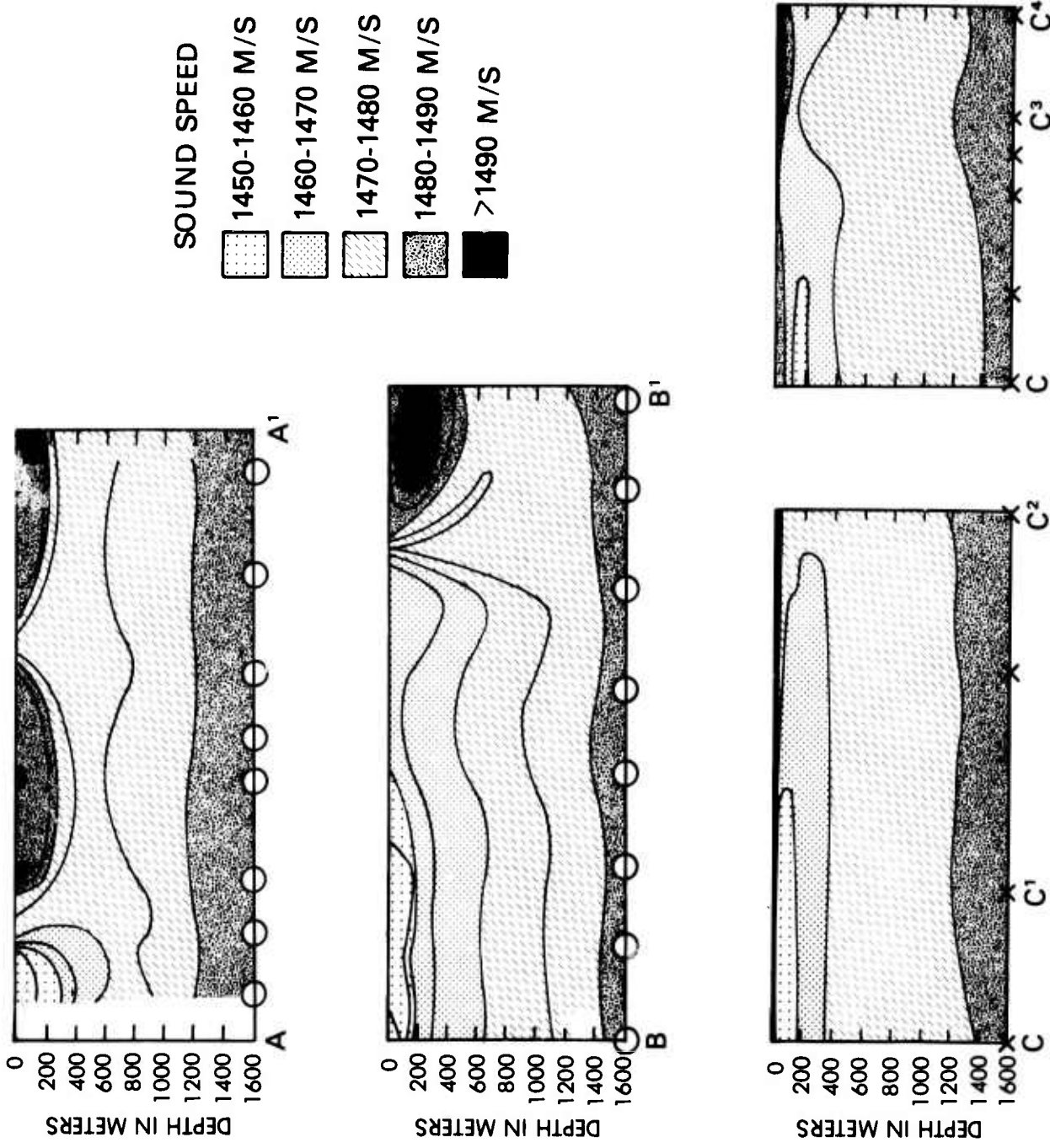


Figure 20. February sound channel depth (adapted from Gorskoy, 1974).

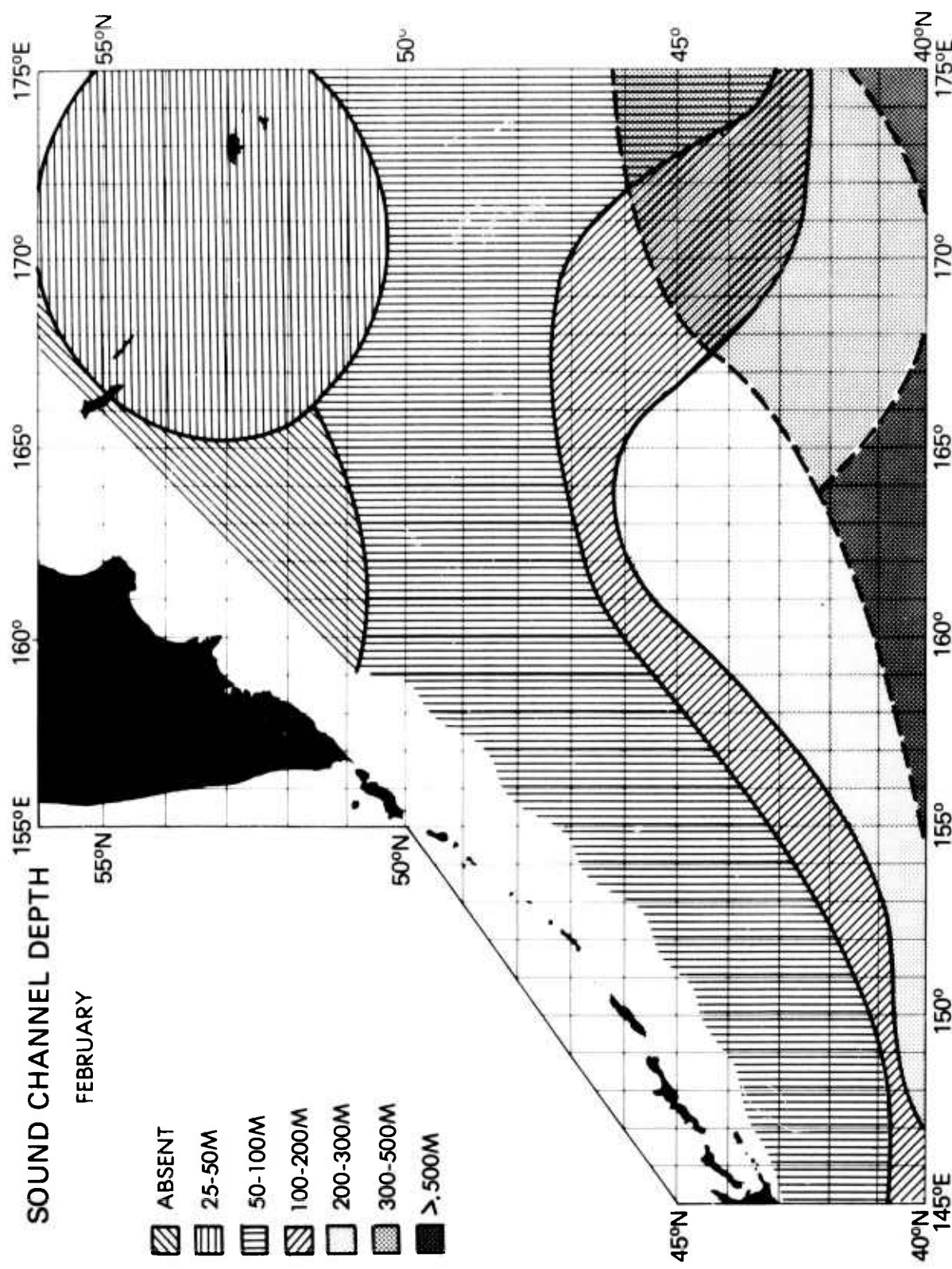


Figure 21. August sound channel depth (adapted from Gorshkov, 1974).

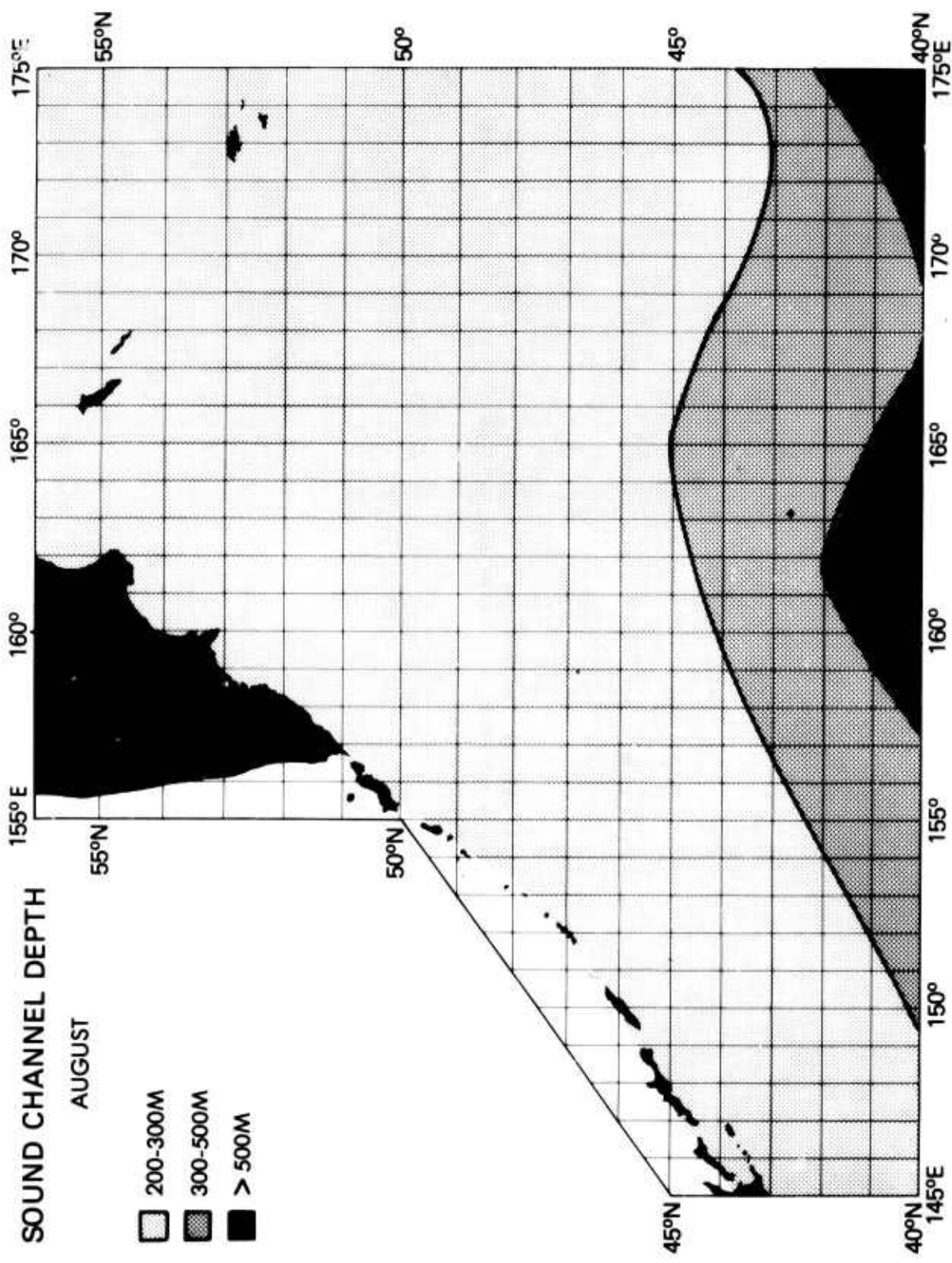


Figure 22. Physiography and province map of the Northwest Pacific. Physiography map has an exaggerated vertical scale of 10:1; provinces are labeled by Roman numerals (compiled and drawn by J. A. Green).

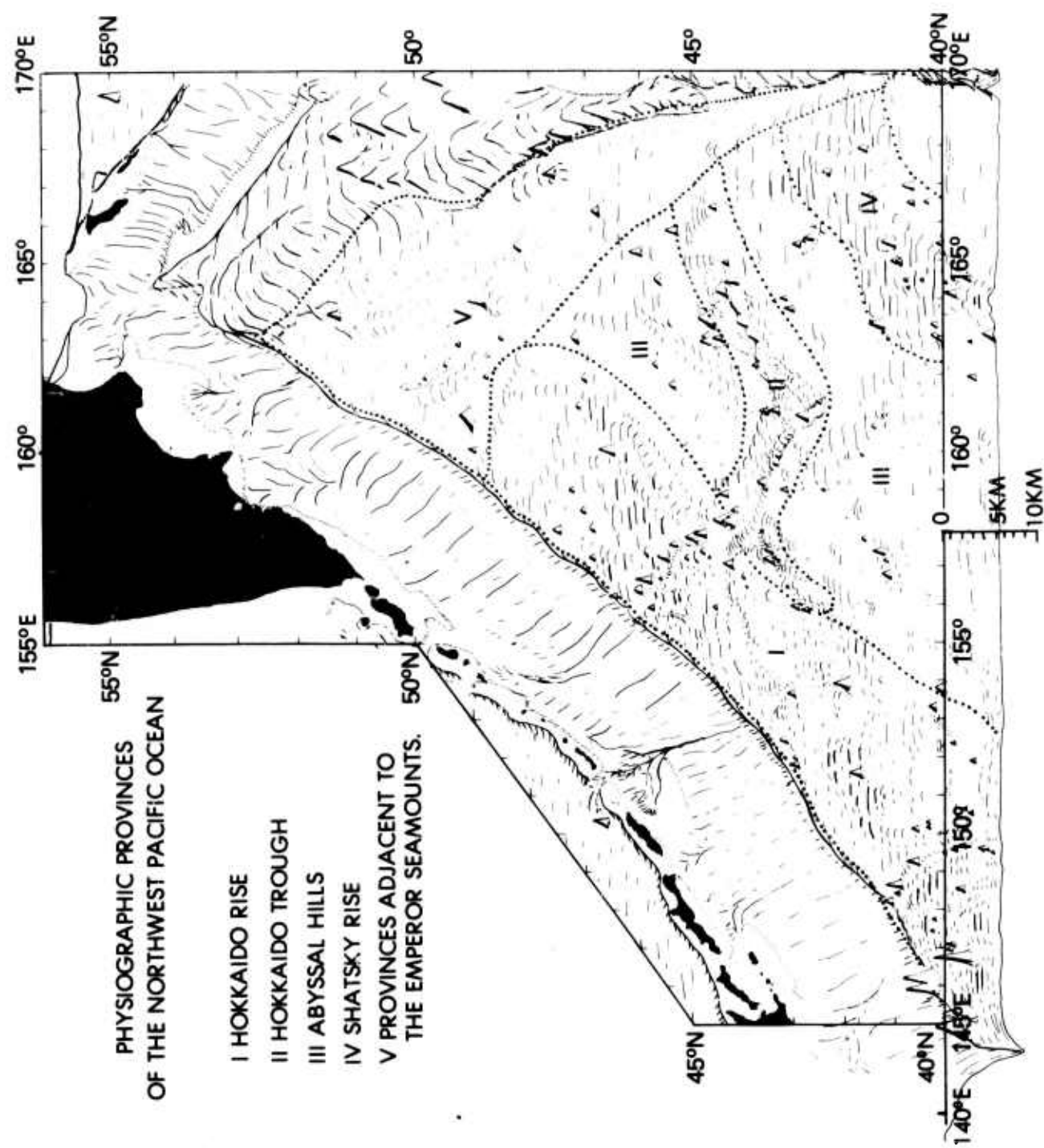


Figure 23. Index to continuous seismic reflection profiles depicted in Figures 24-26.

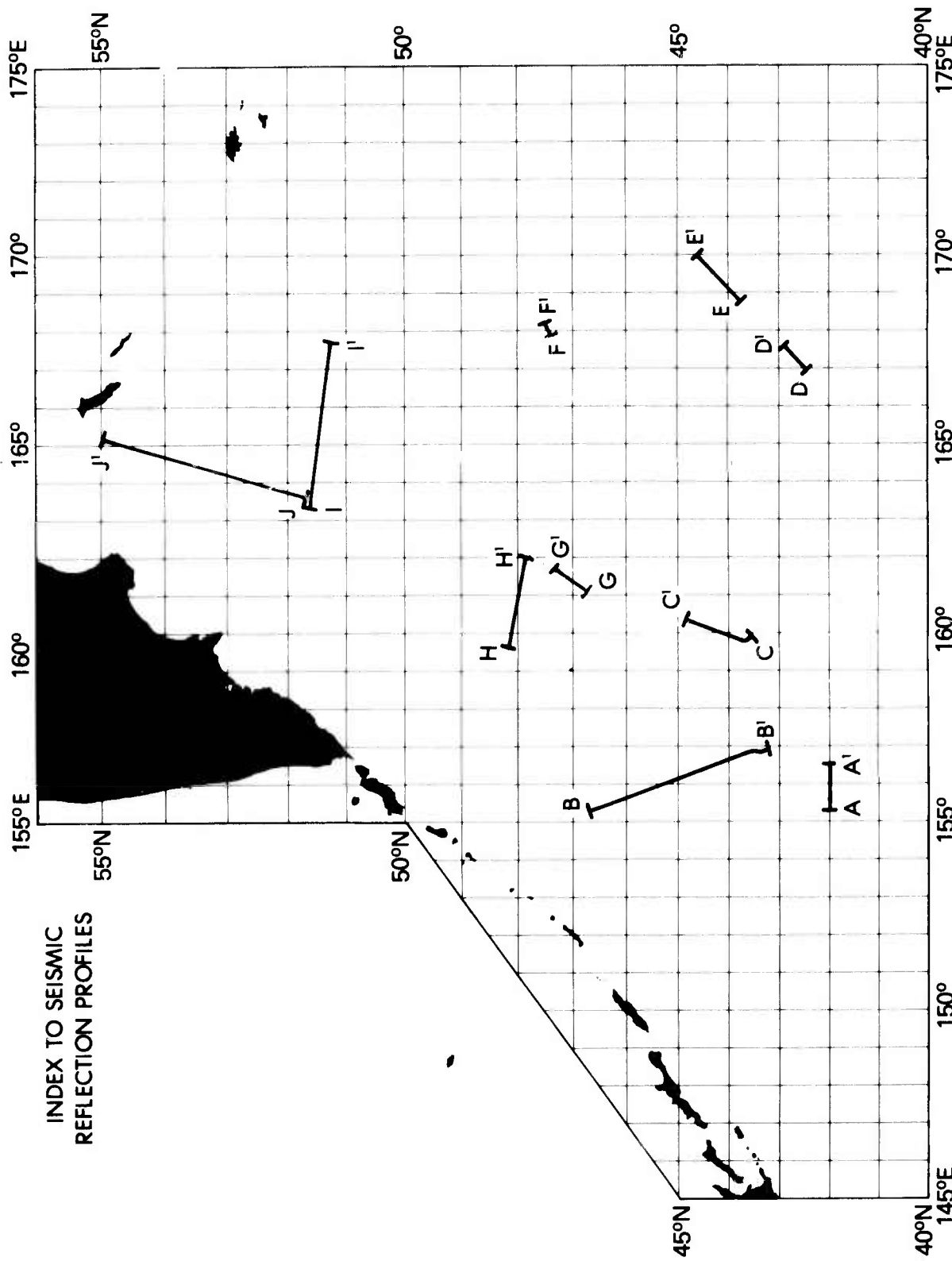


Figure 24. Continuous seismic reflection profiles. AA' (R/V ROBERT CONRAD 12, 1968), low bottom and acoustic basement roughness of the southern Abyssal Hill area. BB' (R/V ROBERT CONRAD 14, 1971) rough bottom and basement on the central Hokkaido Rise. CC' (R/V VEMA 21, 1965), the Hokkaido Trough. Vertical exaggeration is about 12:1 for AA' and 25:1 for BB' and CC'.

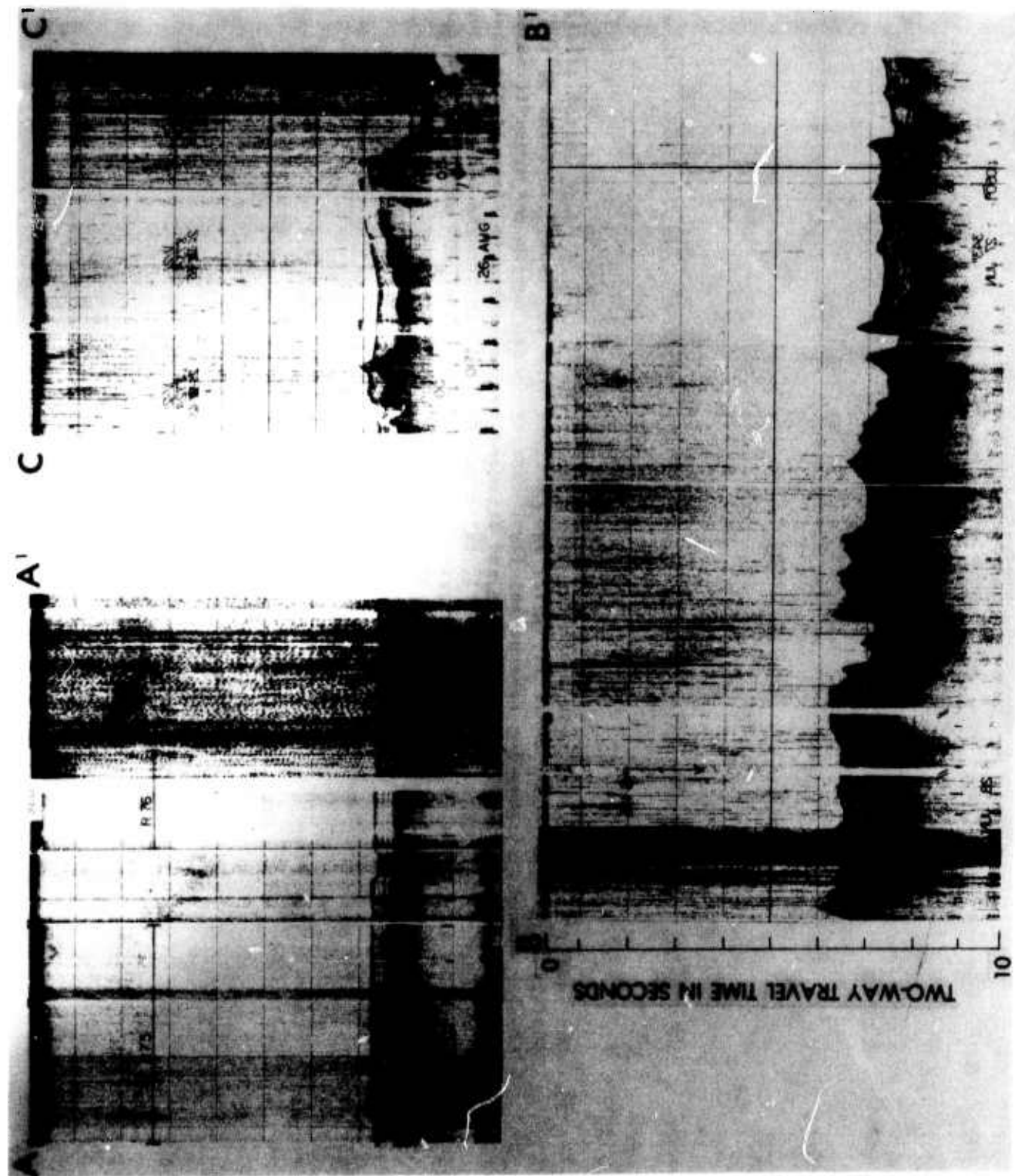


Figure 25. Continuous seismic reflection profiles. DD' (USNS BARTLETT, 1972) rough bottom of the Shatsky Rise. EE' (USNS BARTLETT, 1972) and FF' (R/V VEMA 20, 1965), adjacent to the Emperor Seamounts, show the reverberant layer beneath smooth bottom and acoustic basement. GG' (R/V VEMA 21, 1965), smooth bottom and basement on the northeast flank of the Hokkaido Rise. HH' (R/V ROBERT CONRAD 14, 1971), intermediate rough bottom and basement of the northern Hokkaido Rise. Vertical exaggeration is about 12:1 for DD' and EE', 25:1 for FF', GG' HH'. Profile positions on Figure 23.

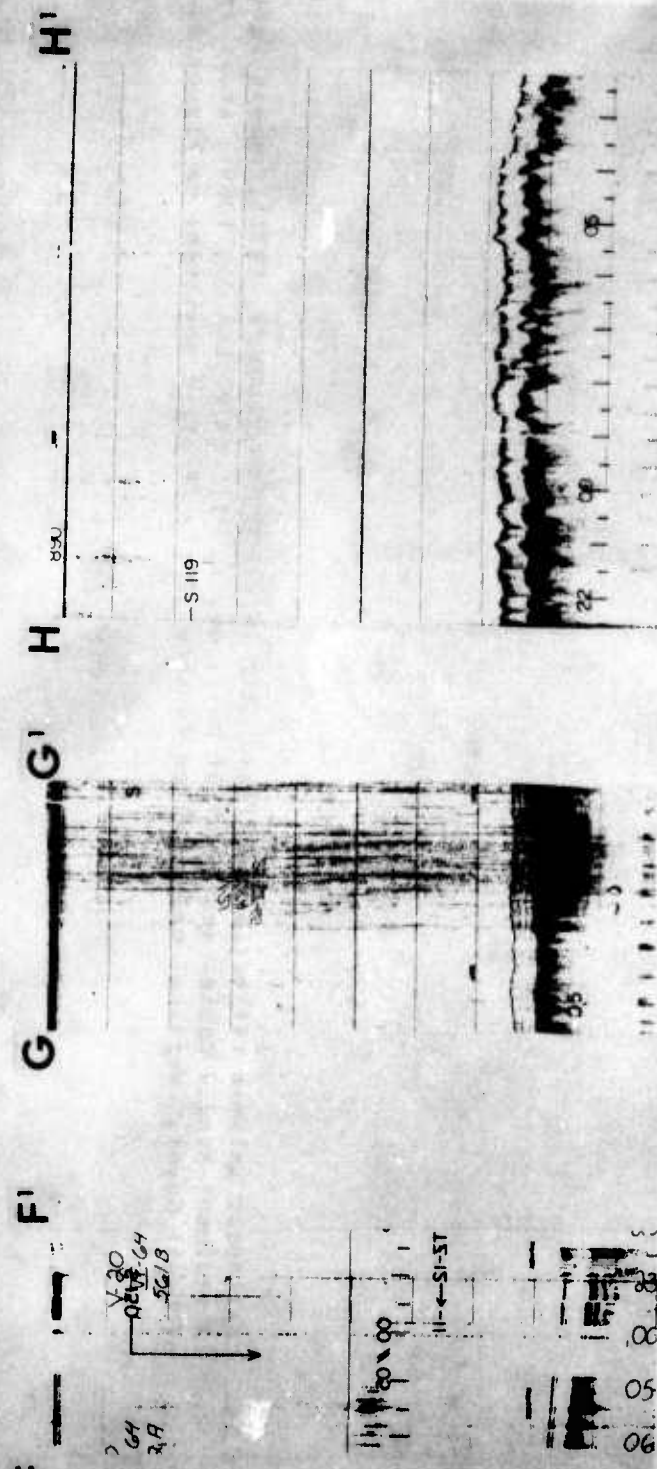
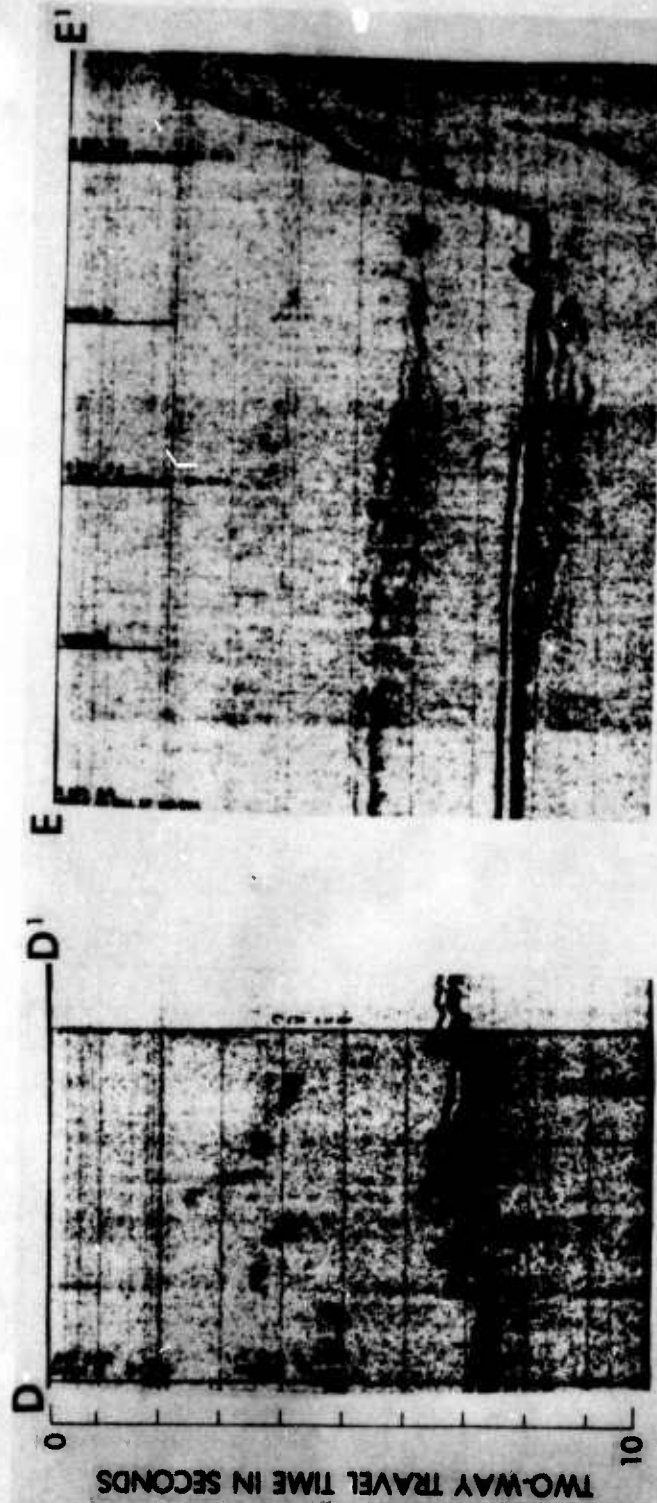


Figure 26. Continuous seismic reflection profiles. 11' (R/V ROBERT CONRAD 14, 1971), smooth bottom in sediment-ponded basins southwest of Meiji Guyot. 11' (R/V VEMA 21, 1965), cross section of Meiji Guyot. Vertical exaggeration is about 25:1. Profile positions on Figure 23.

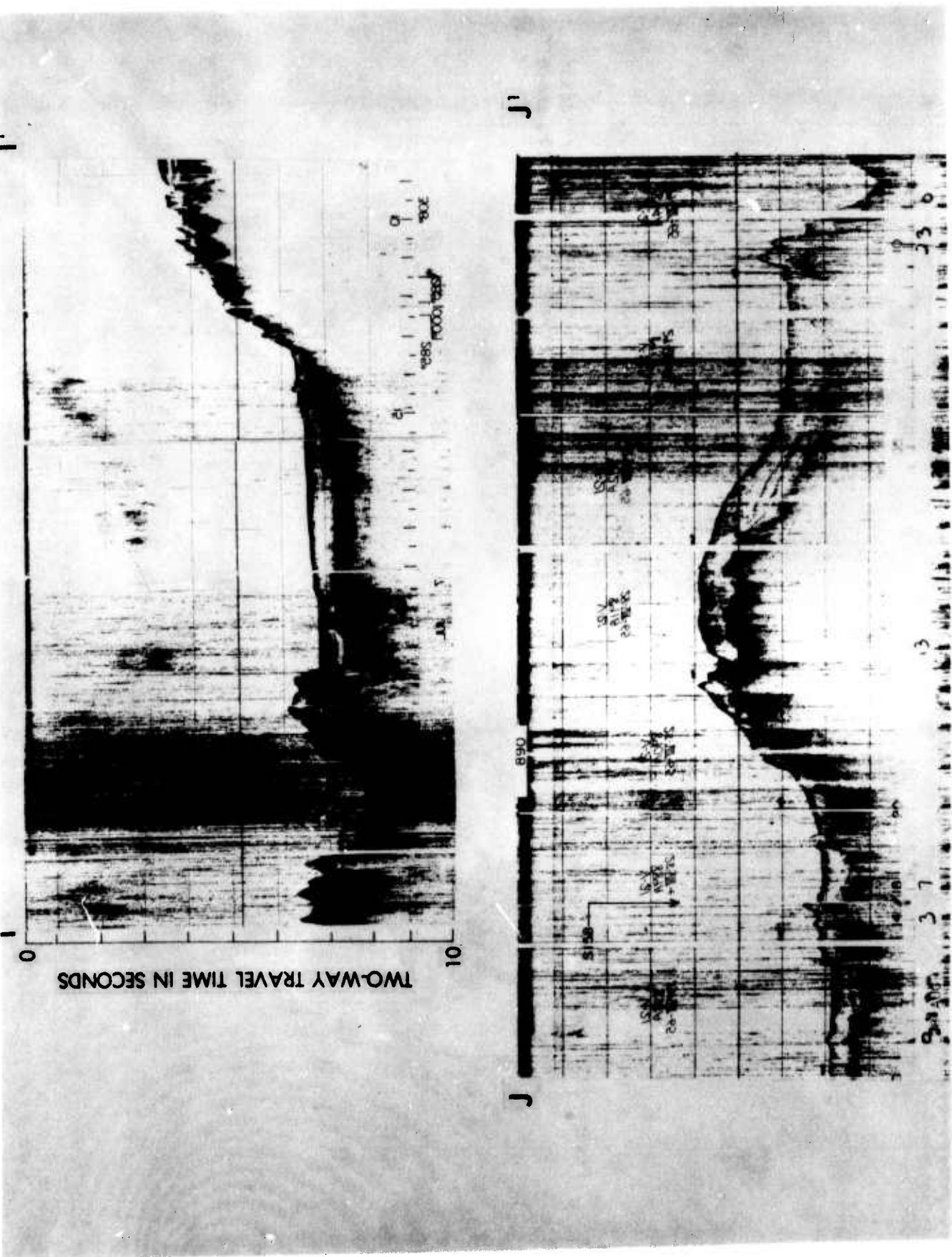


Figure 27. Surface sediment type. Major lithologies are presented in combination. Contours denote mean grain size of sediments (sediment type map adapted from Frazer et al., 1972, grain size data from Horn et al., 1970).

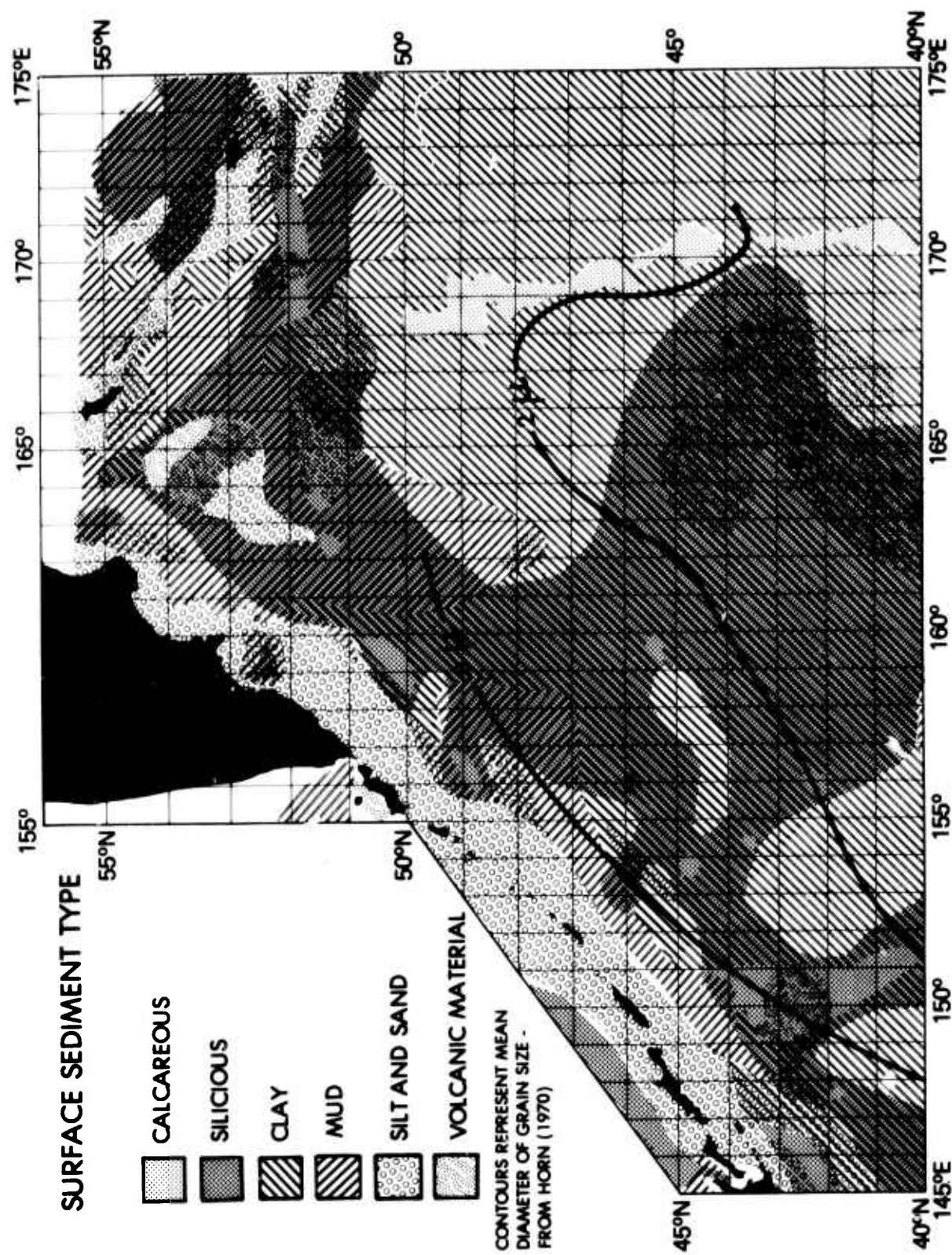


Figure 28. Surface sediment type. Lithologic components of the surface sediments of Figure 27 are presented separately (adapted from Frazer et al., 1972).

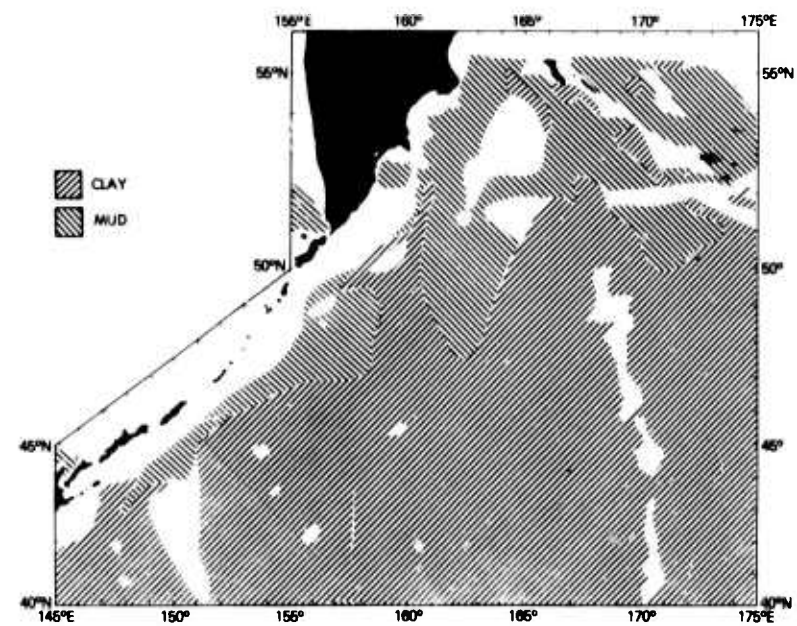
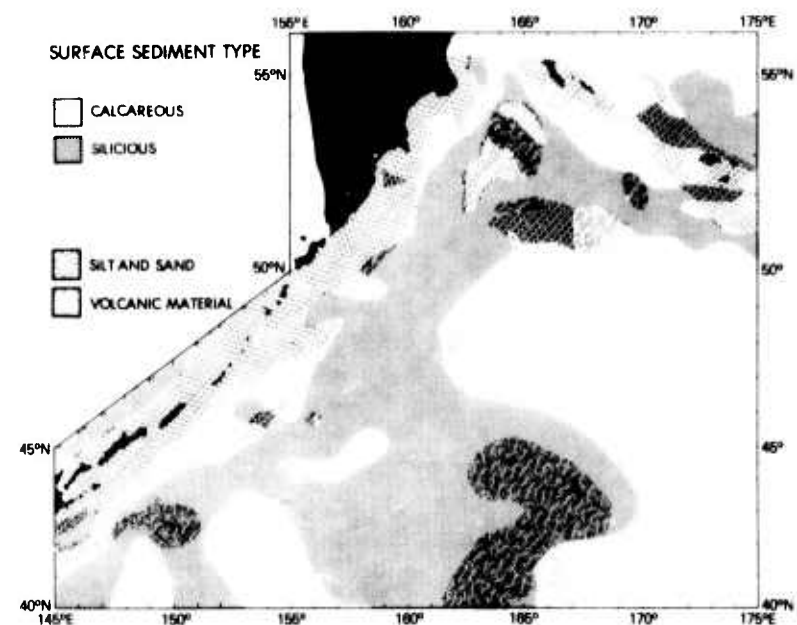


Figure 29. Core index shows locations of cores that have significant analytical compiled data. Cores used in Horn et al. (1970) grain size map denoted by *H (see Fig. 27).

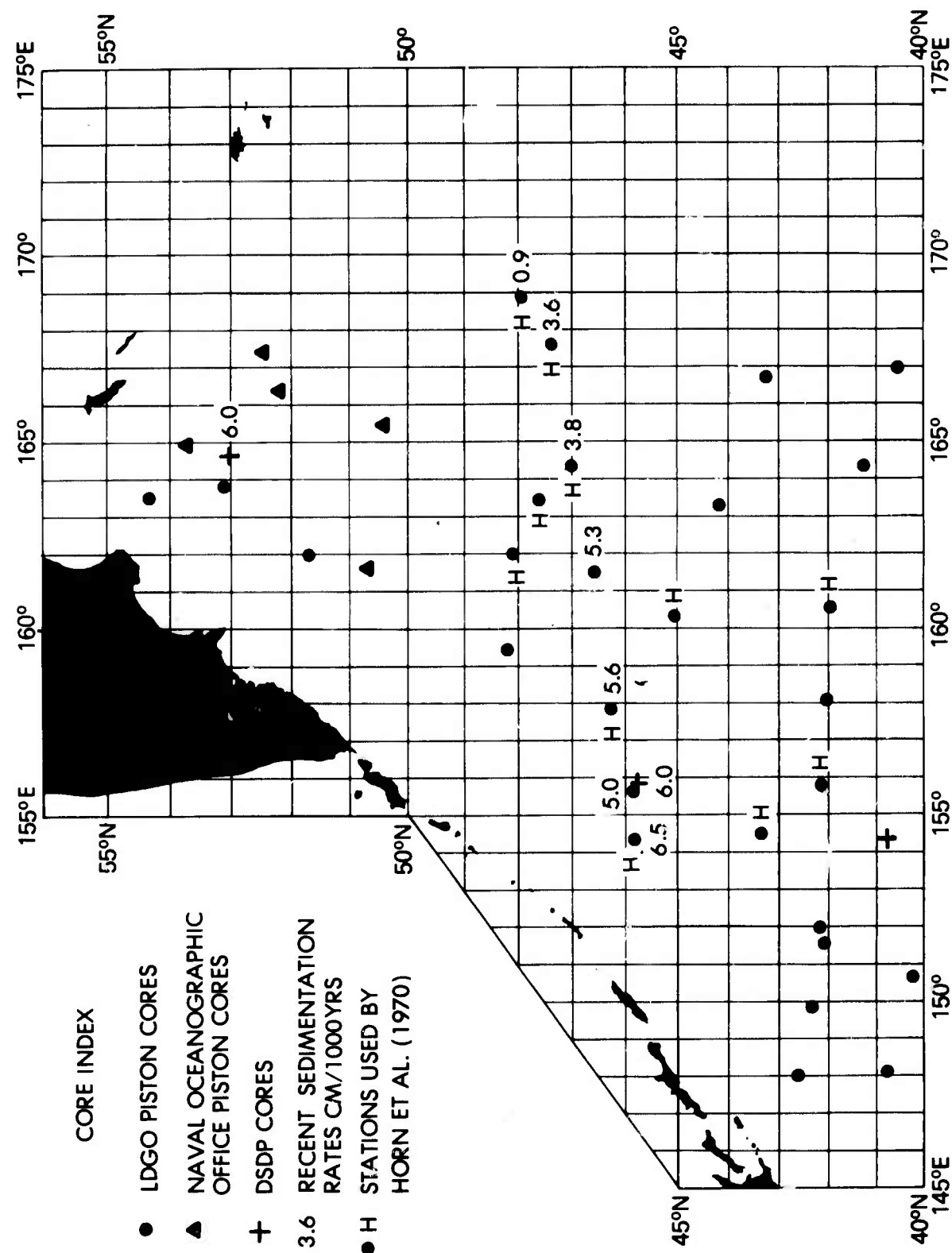
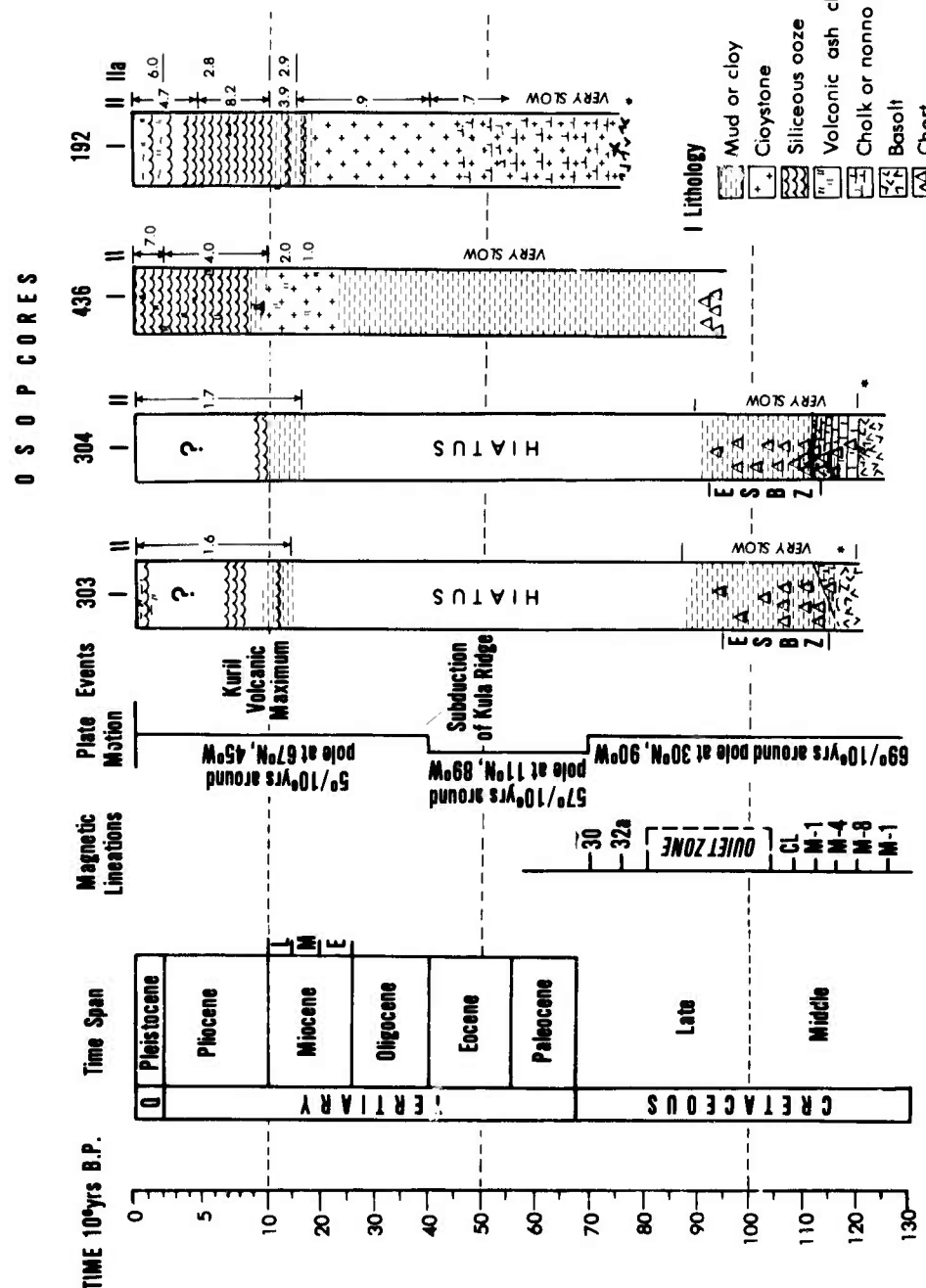


Figure 30. Time columns representing occurrence, and duration of geologic events. The magnetic lineations column is adapted from Larson et al. (1972), Plate motions from Lancelot et al. (1975), Kuril volcanic maximum from Ninkovich (1975), subduction of Kula Ridge from Hilde (1977). DSDP sediment data are from Larson et al. (1975) for sites 303 and 304, from the initial core descriptions of leg 56 for site 436, and from Creager et al. (1973) and Scholl et al. (1977) for site 192. Lithologies are illustrated in column I and deposition rates in column II.



- || Sedimentation rate $\text{cm}/10^3\text{yrs}$
- ||a Non-biogenic sedimentation rate . $\text{cm}/10^3\text{yrs}$
- * Denotes formation of crust

Figure 31. Sediment cores by depth of penetration. Lithologies in column 1 and deposition rates in column 11. Lines representing the upper, middle/lower Miocene and transparent layer/acoustic basement boundaries are designated. Data from Larson et al. (1975), Creager et al. (1973), Scholl et al. (1977), core descriptions from LDGO and DSDP leg 56.

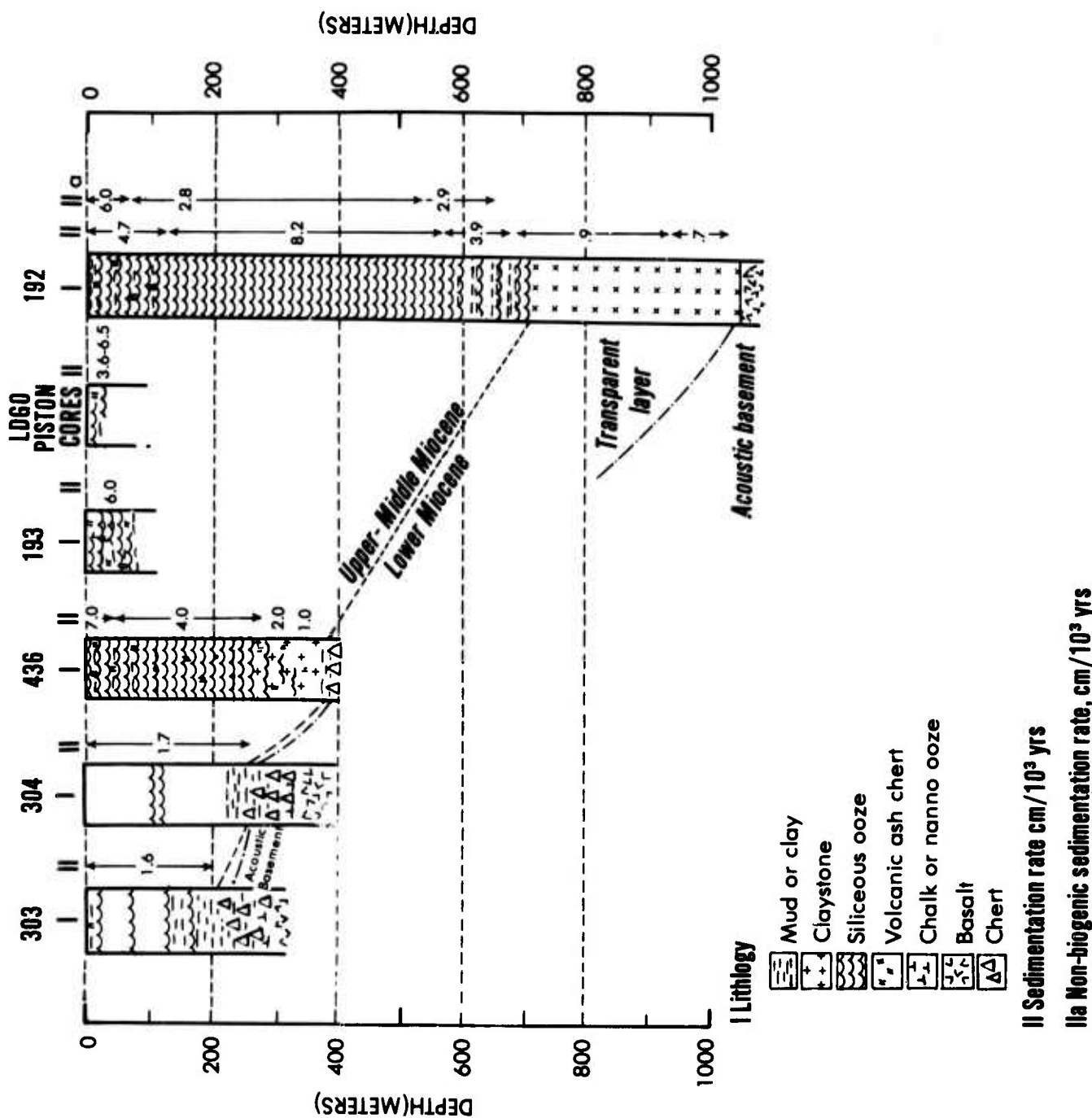


Figure 32. Summary of DSDP site 303 (from Snow et al., in press).

SITE DATA

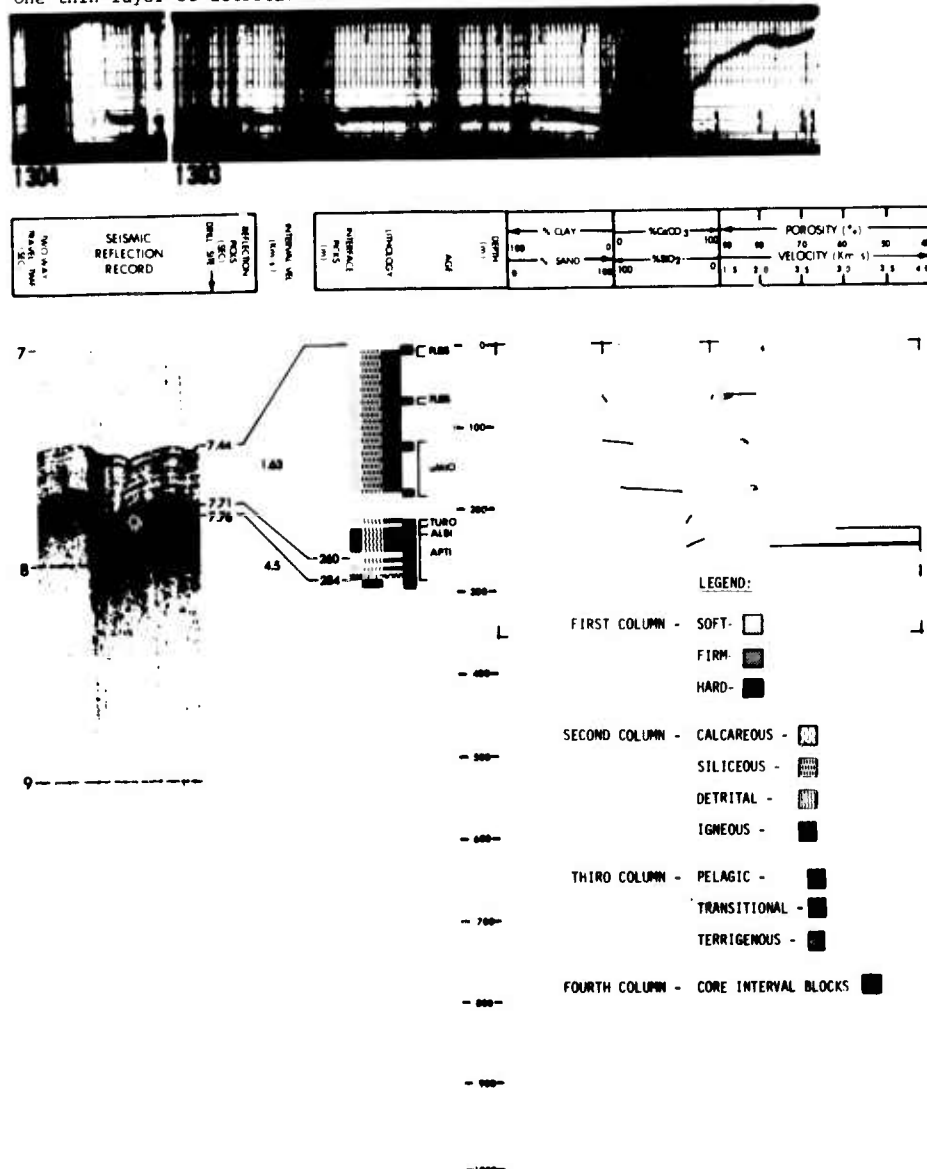
CORE DATA

Position:
Latitude 40°48.5' N
Longitude 154°27.1' E
Date: 08/18/73
Time: 1318Z
Water depth: 5609 meters
Location: Japanese Magnetic
Lineations

Penetration: 303 303A
 Drilled-- 175 211 meters
 Cored---- 54 82 meters
 Total---- 229 293 meters
Recovery:
 Basement- 0 2 cores
 0 0 1 meters
 Total---- 6 10 cores
 26 6 meters

Most of the section consists of sediments deposited below the carbonate compensation depth except for the lowermost layers recovered immediately above basement. The relatively high rates of sedimentation observed in the upper part probably result from a combination of high productivity related to the Kuroshio-Oyashio current system as well as contributions from volcanogenic components. A major unsampled hiatus is probably present at the base of the Tertiary and top of the Cretaceous, and the upper Mesozoic section appears to be very thin. This interval was probably deposited in areas of rather low productivity north of the equatorial zone. The carbonate-rich layers recovered at the base of the section appear too thin to account for accumulation of "ridge flank" and "equatorial" types of sedimentation. This suggests that the crust at this site was not generated under the equatorial zone of high productivity. It is probable that the crust was generated south of the equator and that the equatorial crossing is recorded by large amounts of siliceous deposits after the area had subsided beneath the carbonate compensation depth (CCD).

One thin layer of calcareous, nannofossil rich sediment occurs in Aptian time. One thin layer of detrital sediment occurs in Turonian time.



16
+
m
303

四百九十二

Figure 33. Summary of DSDP site 304 (from Snow et al., in press).

SITE DATA

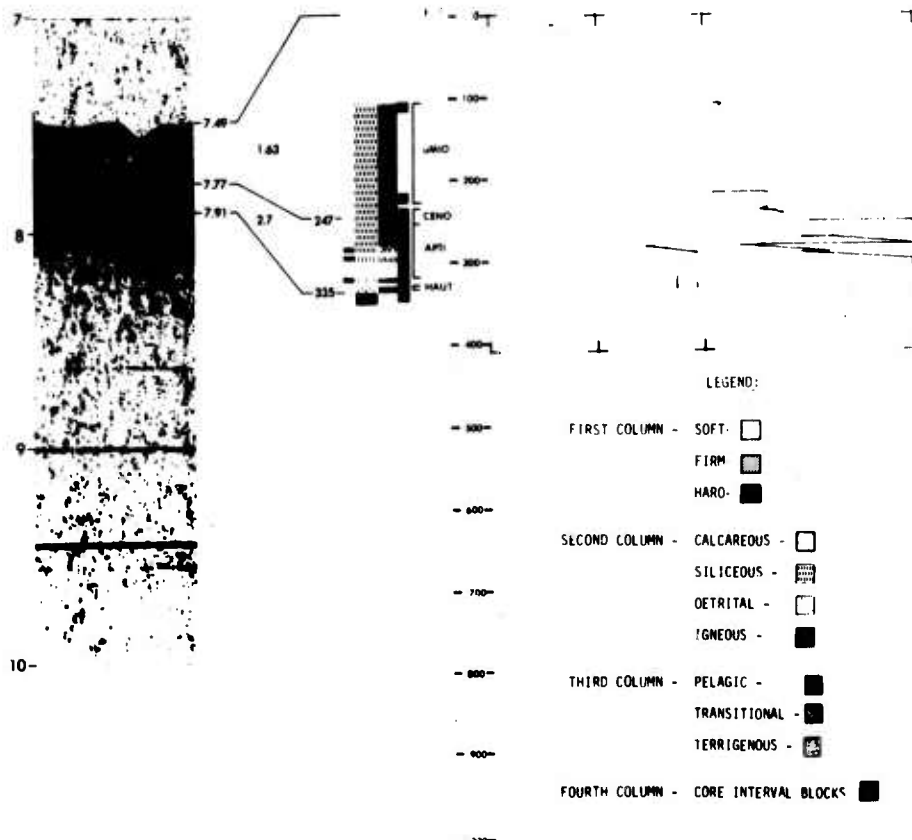
Position:
 Latitude 39°20.3' N
 Longitude 155°04.2' E
 Date: 08/24/73
 Time: 0756Z
 Water depth: 5630 meters
 Location: Japanese Magnetic
 Lineations

CORE DATA

Penetration:
 Drilled-- 216 meters
 Cored---- 131 meters
 Total---- 347 meters
 Recovery:
 Basement- 3 cores
 12 meters
 Total---- 17 cores
 30 meters

The lithologies sampled at Site 304 are essentially identical to the section sampled at Site 303. The bottommost sediments recovered, the nanno ooze unit (Cores 12-14), represent sediments accumulated just above the carbonate compensation depth (CCD). The thickness of the Cretaceous section is not as large as would be expected from a high productivity zone such as the equator. These sediments were most likely deposited toward the outer edge of the equatorial high productivity area, yet above the CCD. An unrecovered unconformity (also inferred from Site 303) probably exists between the Upper Cretaceous and the Miocene as suggested by the sedimentation rates. The time represented by the hiatus was the time that sedimentation shifted from above to below the CCD. The clays and partially crystallized cherts of Unit 2 represent a dissolution facies deposited on the outer margin of a high productivity zone below the CCD. The radiolarian-diatom ooze of Unit 1 is simply the uncristallized equivalent of Unit 2. The moderate average accumulation rates for these two units (16 m/m.y.) suggest they are not abyssal clay facies, which typically have rates an order of magnitude less than this.

One thin layer of detrital sediment occurs in Aptian time. Calcareous sediment; nannofossil rich. Siliceous; chert fragment rich, at bottom of the cored interval.



SITE 304

LEG 32

Figure 34. Summary of DSDP site 192 (from Snow et al., in press).

SITE DATA

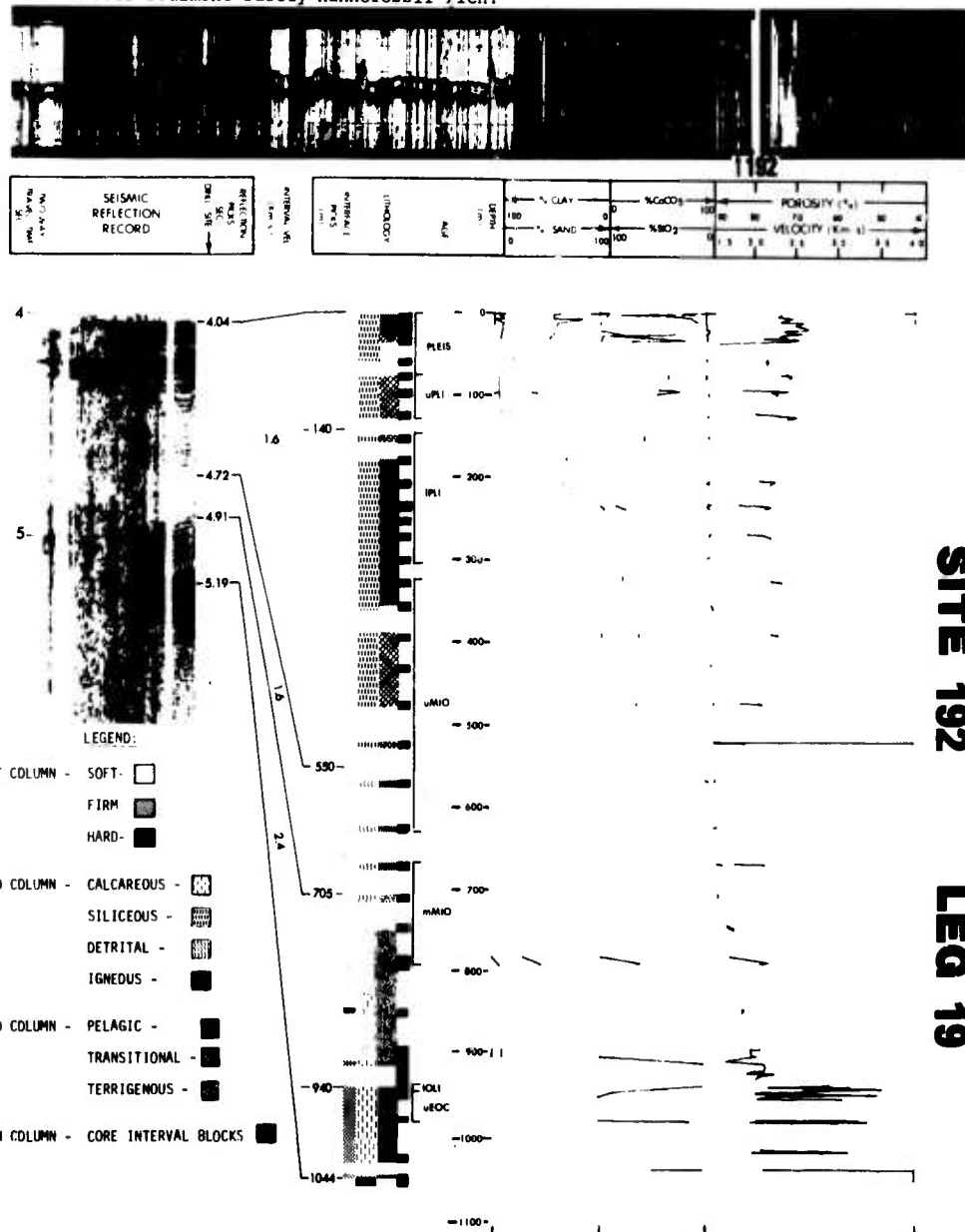
Position:
 Latitude 53°00.6' N
 Longitude 164°42.8' E
 Date: 09/04/71
 Time: 0400Z
 Water depth: 3014 meters
 Location: Meiji Guyot

CORE DATA

Penetration: 192 192A
 Drilled-- 634 1010 meters
 Cored---- 308 47 meters
 Total---- 942 1057 meters
 Recovery:
 Basement- 0 2 cores
 0 13 meters
 Total---- 35 6 cores
 152 38 meters

An unconformity separates middle Eocene and Cretaceous (middle Maestrichtian) beds. At 1044 meters the sedimentary sequence apparently depositorially overlies a complex of alkali basalt and trachybasalt flows. It is notable that abundant ice-rafted (?) debris and volcanic ash occur down to middle Pliocene deposits, although a few ash layers occur in lower Pliocene beds. Presumably this means that formation of glaciers in Kamchatka and a late Cenozoic episode of intense volcanism in the Kamchatka-Kuril region began about 3 m.y. ago. The richly diatomaceous beds, 550 meters thick, overlying the seamount attest to high fertility of the overlying surface waters back to early late Miocene time. Prior to this, and through the Oligocene, the seamount was buried beneath a nearly equally thick pile of pelagic clay. Microfauna and flora suggest that the sediment-water interface has remained near the carbonate compensation depth throughout deposition of the entire sediment section. The thick, lower Miocene to lower upper Miocene pelagic clay requires that parts of Meiji Guyot was near a sediment source at this time. The only possible source areas are Kamchatka to the west and the Aleutian Ridge to the north, which were both tectonically and volcanically active in the mid-Tertiary.

Interbedded detrital sediment and siliceous, diatom rich, sediment. Earlier calcareous sediment rarely nannofossil rich.



SITE 192

LEG 19

Figure 35. Summary of DSDP site 193 (from Snow et al., in press).

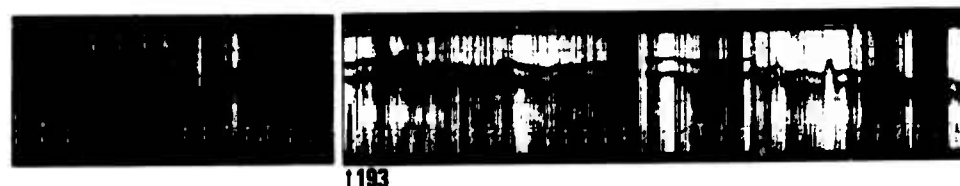
SITE DATA

Position:
 Latitude 45° 48.2' N
 Longitude 155° 52.3' E
 Date: 09/06/71
 Time: 2153Z
 Water depth: 4811 meters
 Location: Hokkaido Rise

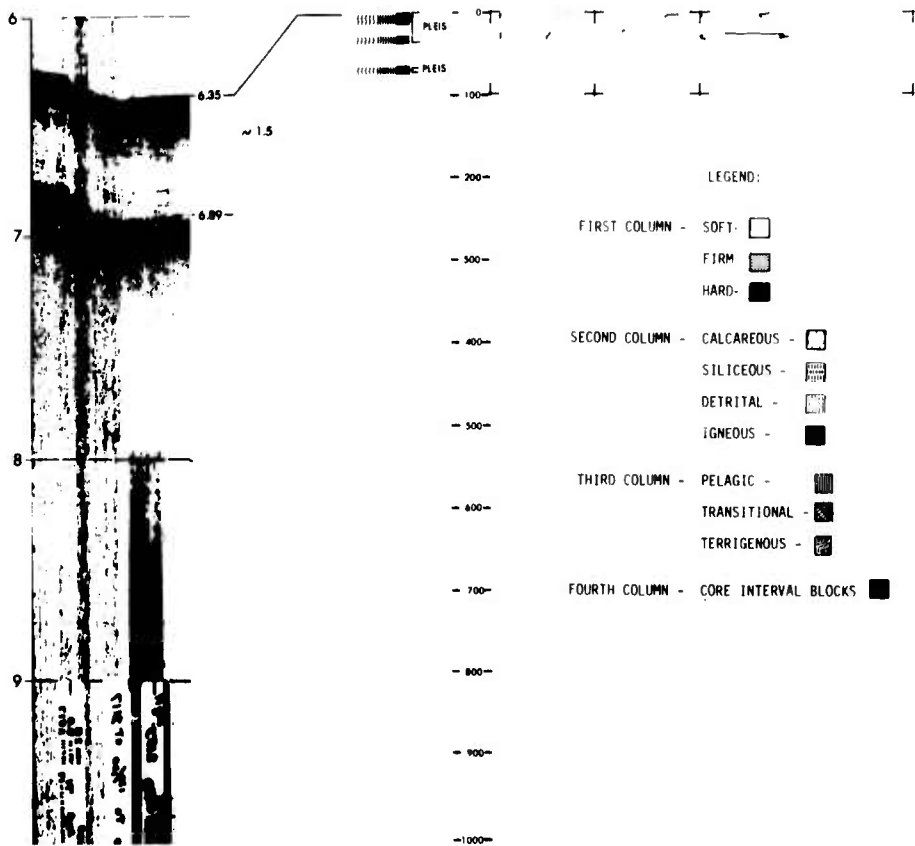
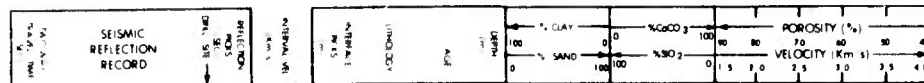
CORE DATA

Penetration:
 Drilled-- 42 meters
 Cored---- 29 meters
 Total---- 71 meters
 Recovery:
 Basement- 0 cores
 0 meters
 Total---- 4 cores
 12 meters

The entire section is high in volcanic glass and terrigenous silt content, probably pyroclastic and terrigenous debris supplied by the Japanese and Kuril islands. Although we have only spotty recovery, discrete ash units may be more numerous in the upper part of the section. Hays and Ninkovich (1970) state that Northwest Pacific ashes, from Kamchatka and the Kuril Islands, are light in color and composed of colorless shards, while the Aleutians supply both dark and light-colored ashes to the Northeast Pacific. The ashes at Site 193 are dark in color as they appear in the core, but the shards themselves are colorless. The color of the ash as seen in the core is due to contained opaques plus the fact that the shards are being altered to clay. Cores 1 and 2 are richer in diatoms than are Cores 3 and 4. The overall low rate of Pleistocene sedimentation at Site 193 indicates this may be due more to a fluctuation in diatom productivity than to a change in rate of supply of terrigenous components.

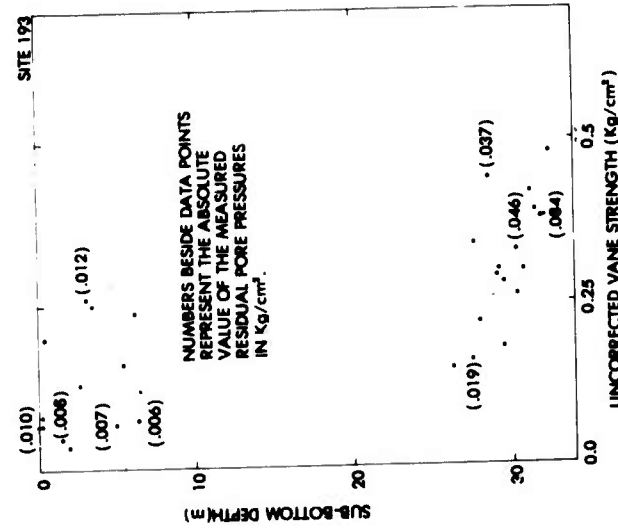
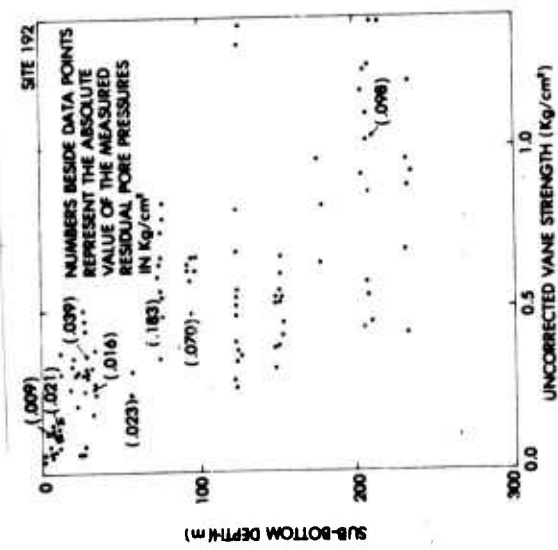


1193



SITE 193
LEG 19

Figure 36. Measured shear velocities vs. depth for DSDP cores 192 and 193. The shear velocities are corrected for pore pressure to derive assumed in situ shear velocities (from Lee, 1975).



a.

b.

Figure 37. Residual magnetics data from three sources: (1) positive and negative aeromagnetics data of Solov'yeva (1963) in the north; (2) contoured anomalies of Uyeda et al. (1967) for the south; and (3) seafloor spreading anomaly isochrons of Hilde (1975).

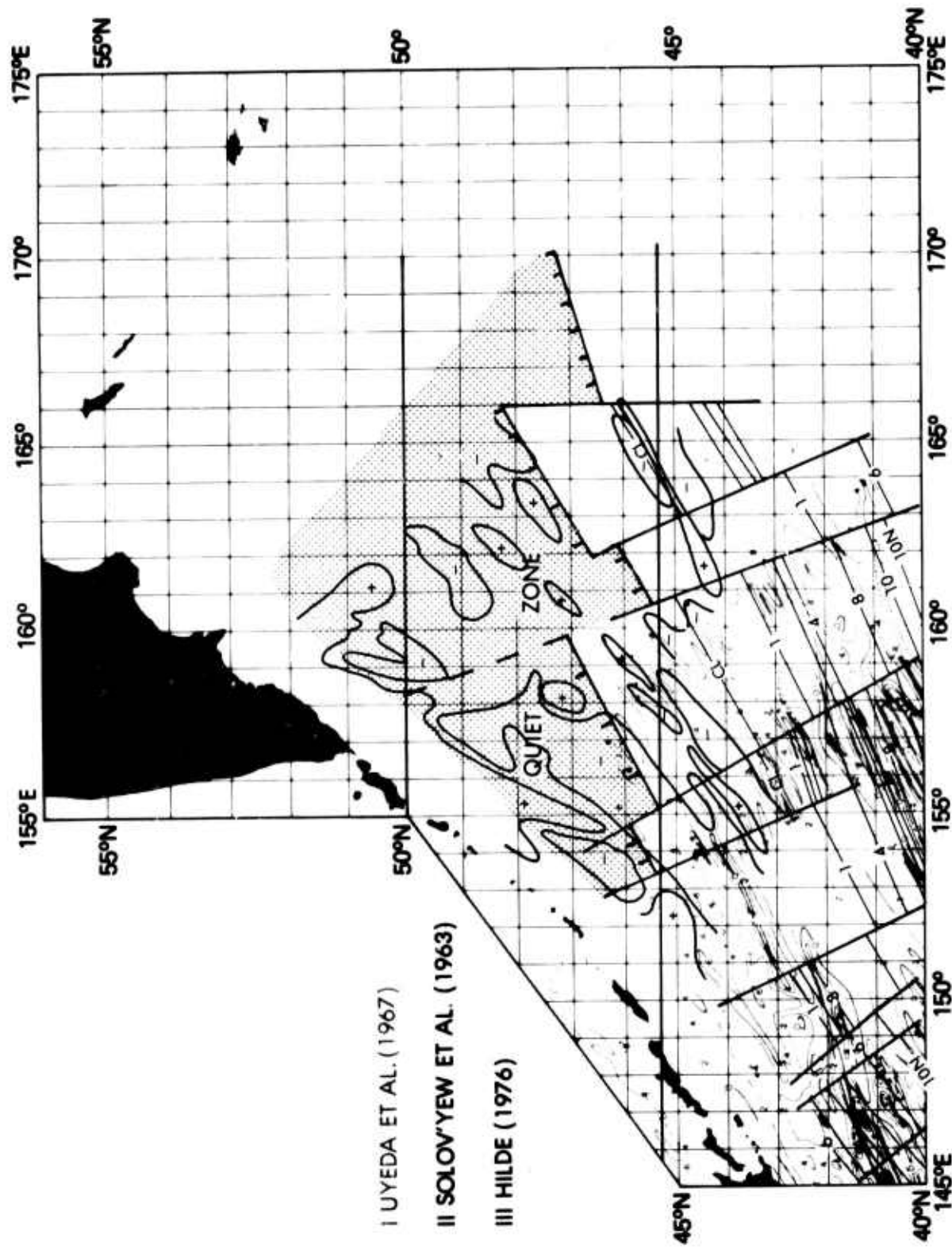


Figure 38. Formation and migration of the Northwest Pacific. (a) back-traced path of the Northwest Pacific DSDP sites 303, 304, and 192. This figure traces the movement of Northwest Pacific crust, which is outlined at its present location farthest to the northwest. Other outlines represent the positions of the same crust with increasing age to the southeast. Triangles indicate positions where basalt retrieved from DSDP cores was formed; dotted lines represent the fossil Kula Ridge crest; dashed lines represent unformed crust. The southeastern outlines of crust represent partial formation of Northwest Pacific crust. (b) cross sections of Northwest Pacific crust showing the latitude position with respect to time.

FORMATION AND MIGRATION OF THE NORTHWEST PACIFIC

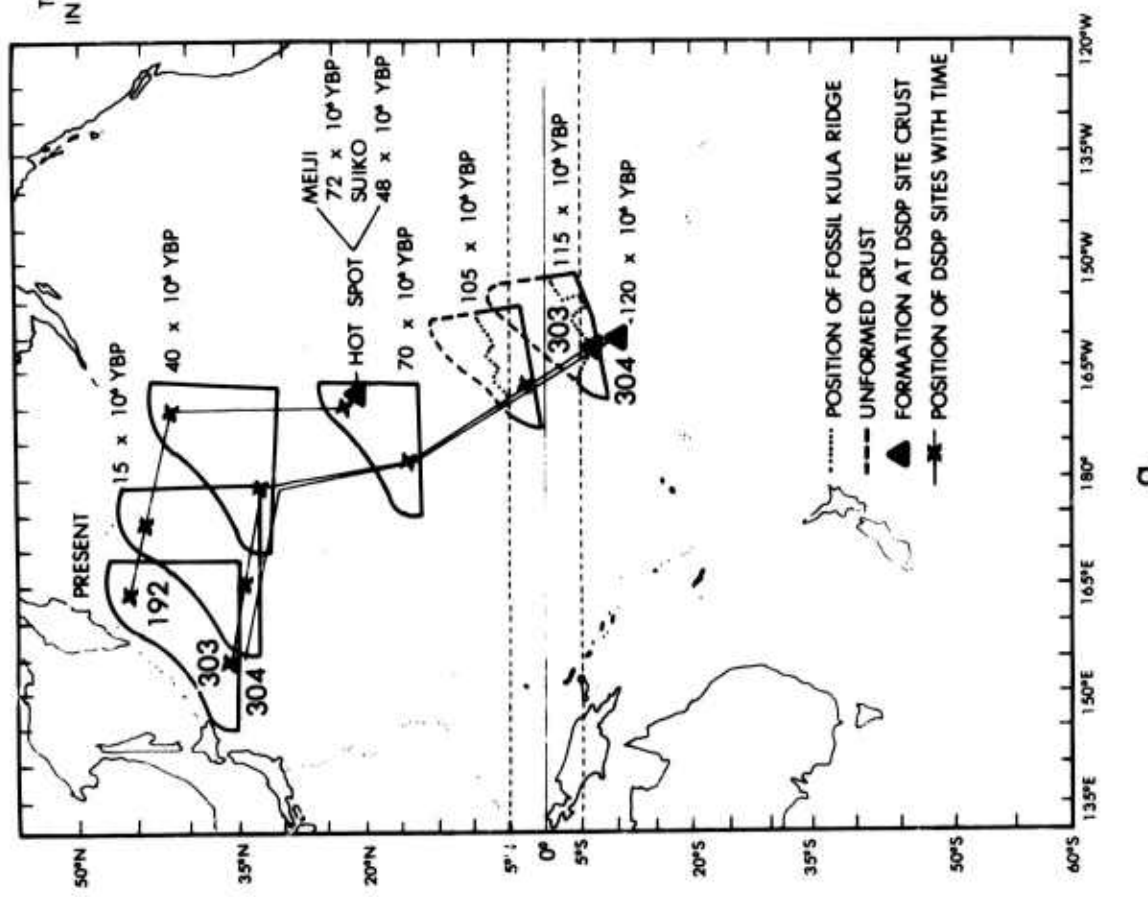


Figure 39. Earthquake epicenters of 0-40 km depth range for earthquakes occurring 1965-1975 (data from NEIS, Boulder, Colorado).

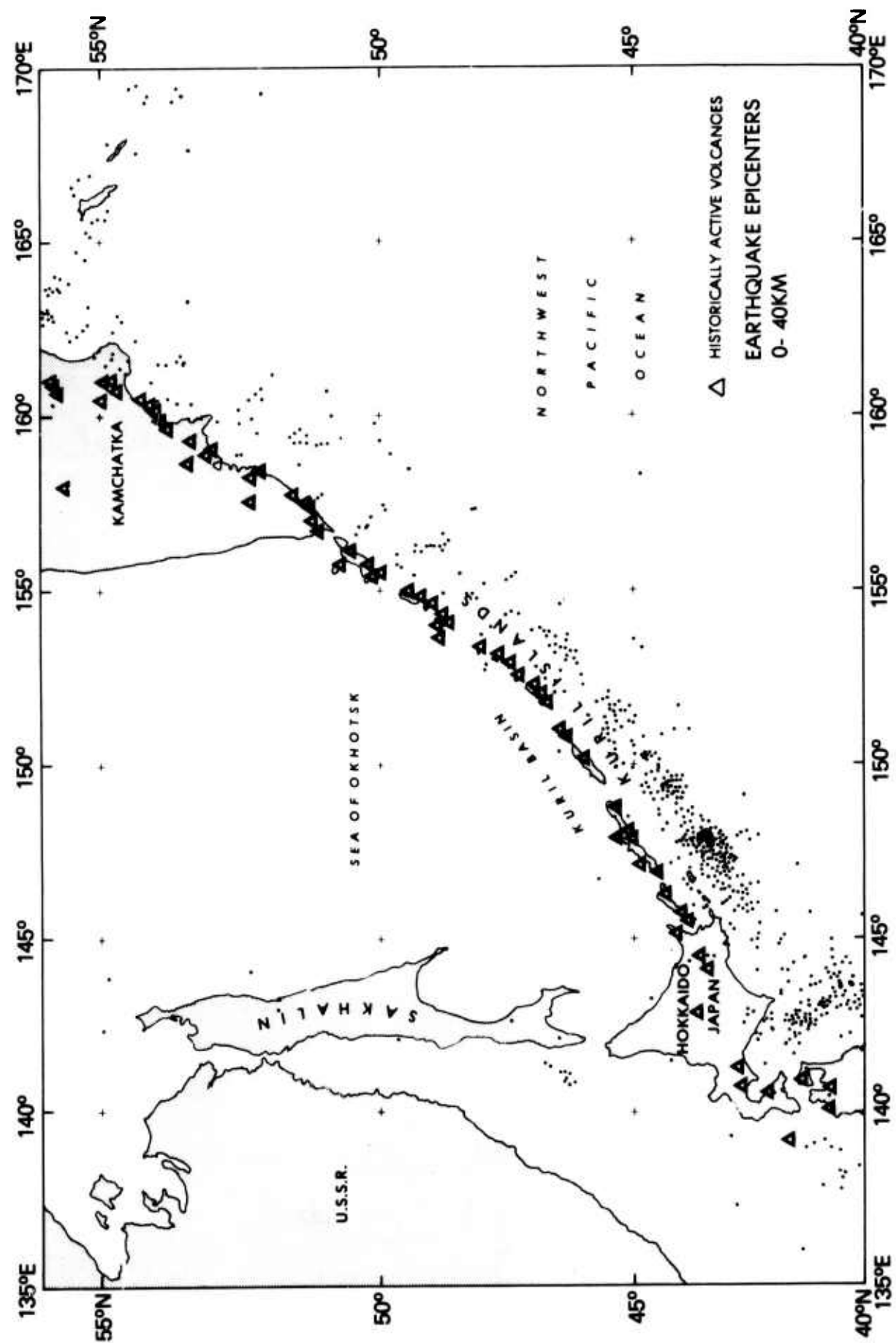


Figure 40. Earthquake epicenters of 40-70 km depth range for earthquakes occurring 1965-1975 (data from NEIS, Boulder, Colorado).

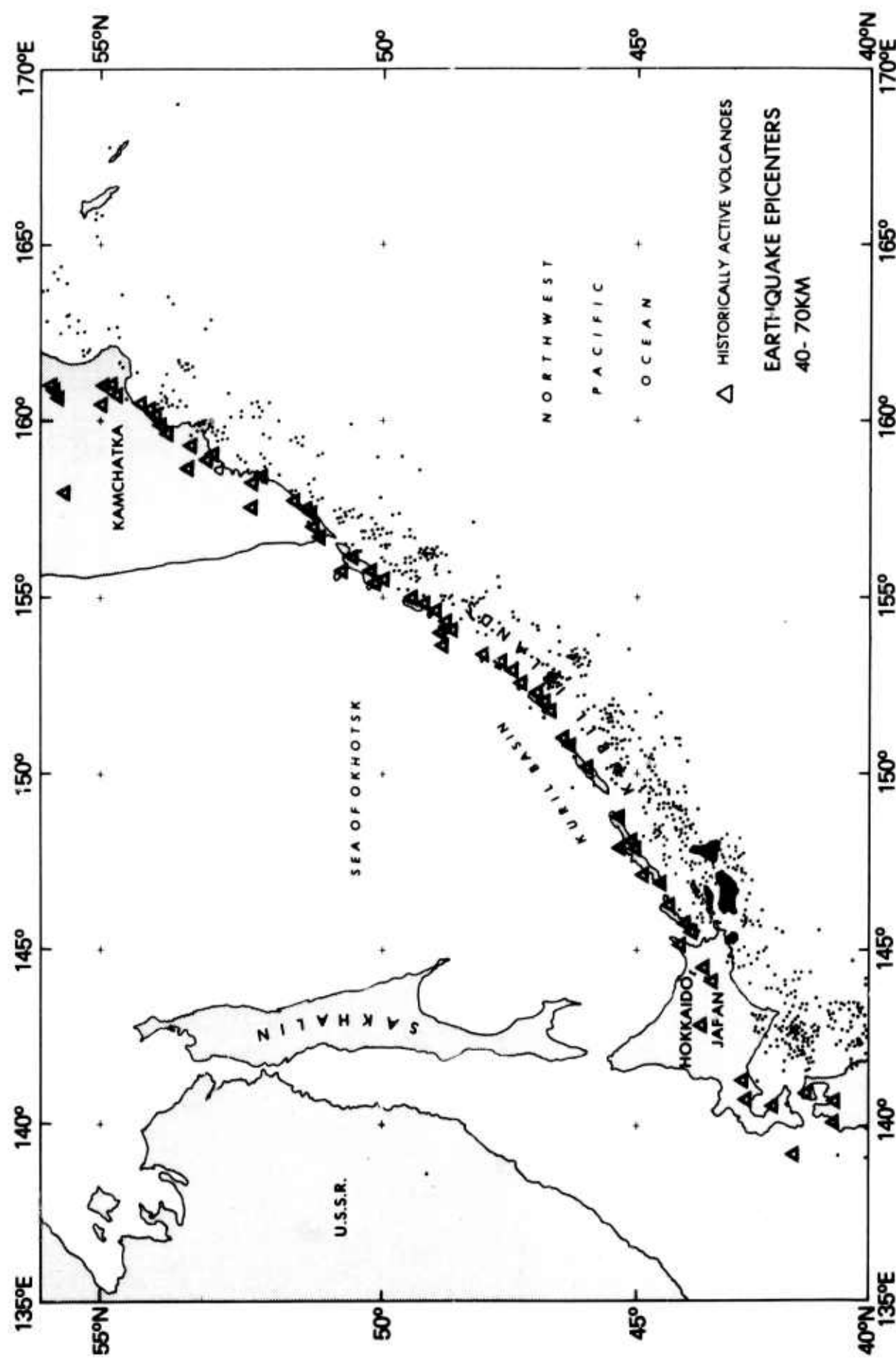


Figure 41. Earthquake epicenters of 70-120 km depth range for earthquakes occurring 1965-1975 (data from NEIS, Boulder, Colorado).

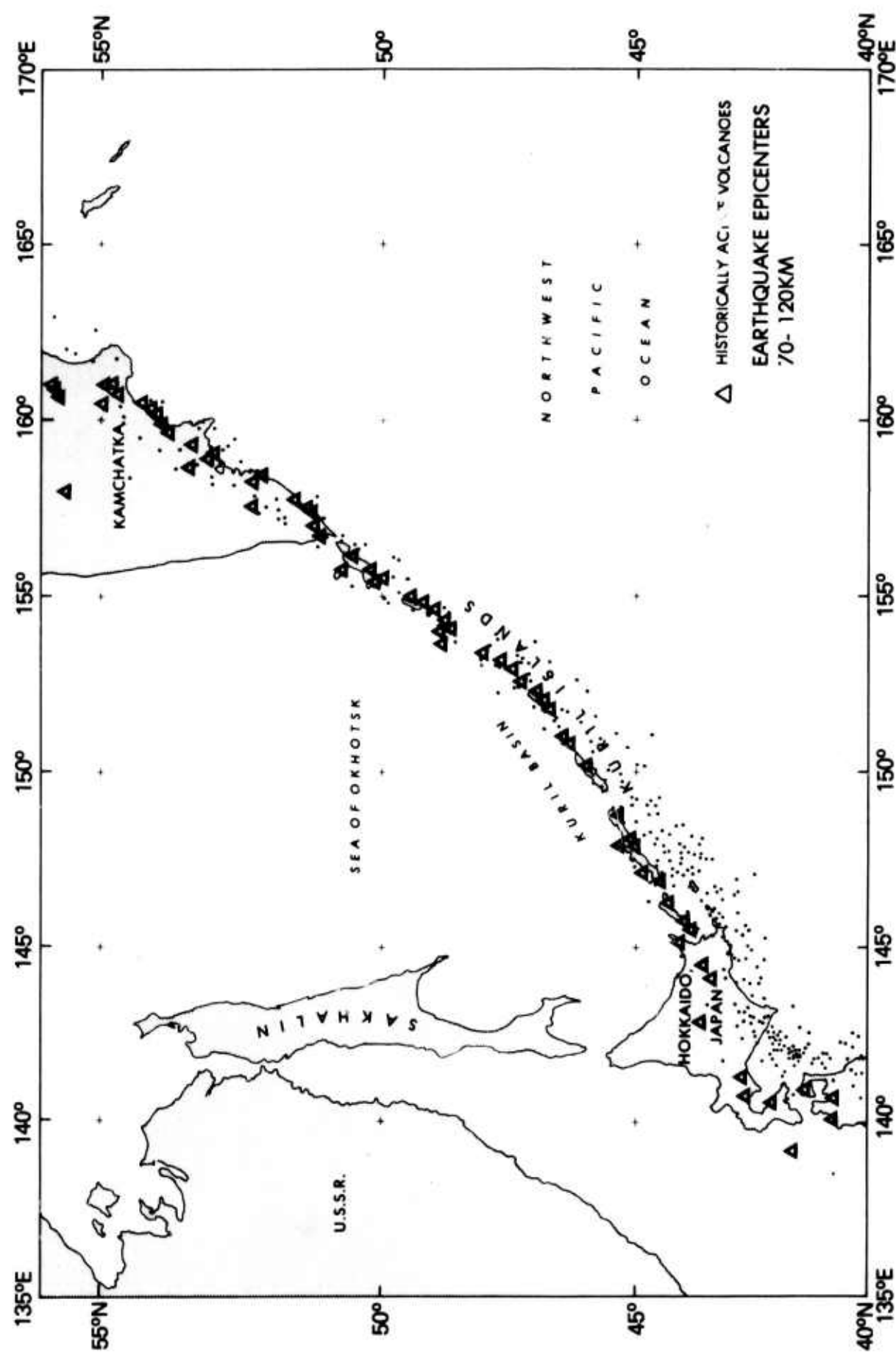


Figure 42. Earthquake epicenters of 120-200 km depth range for earthquakes occurring 1965-1975 (data from NEIS, Boulder, Colorado).

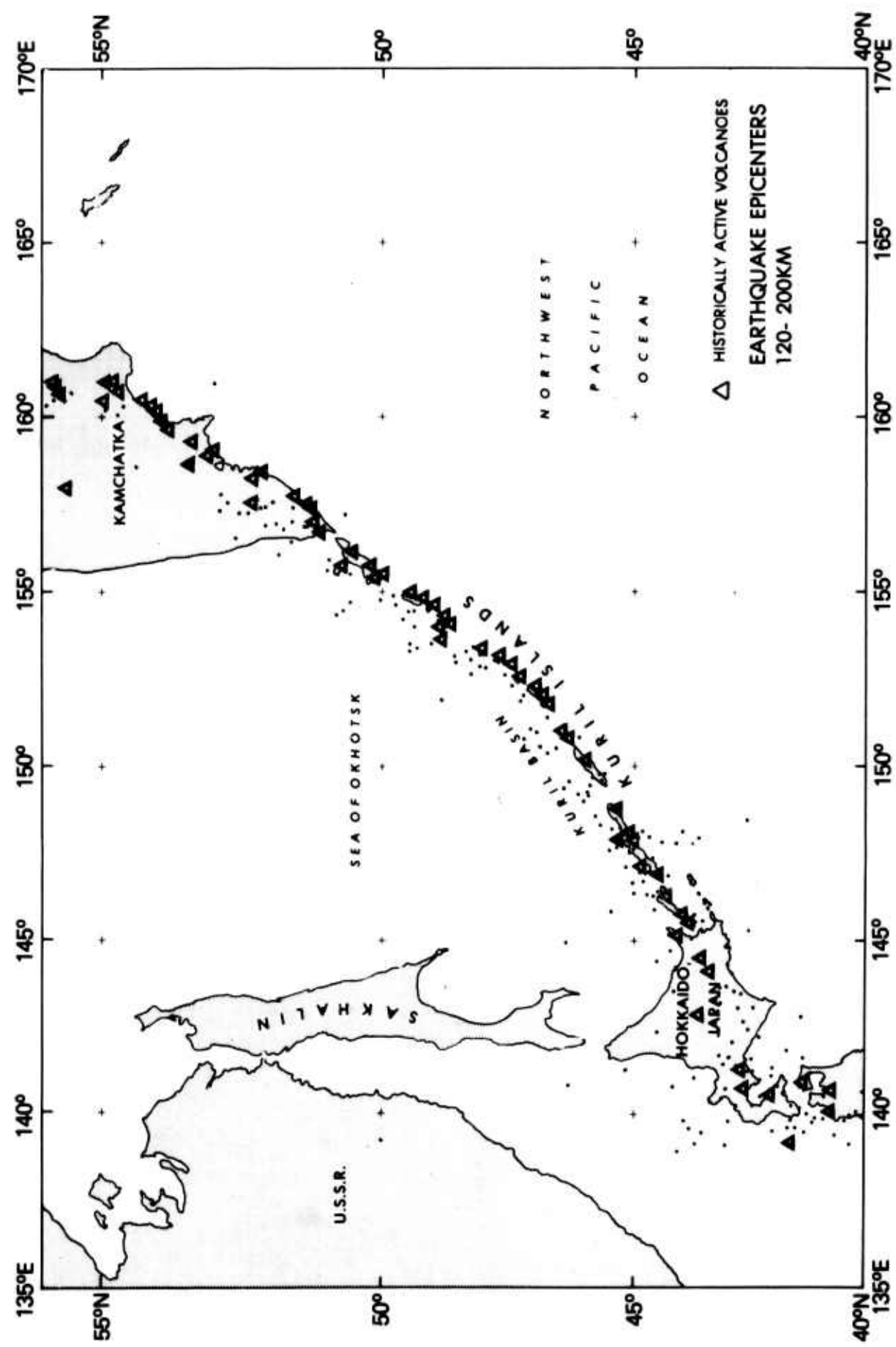


Figure 43. Earthquake epicenters of 200-300 km depth range for earthquakes occurring 1965-1975 (data from NEIS, Boulder, Colorado).

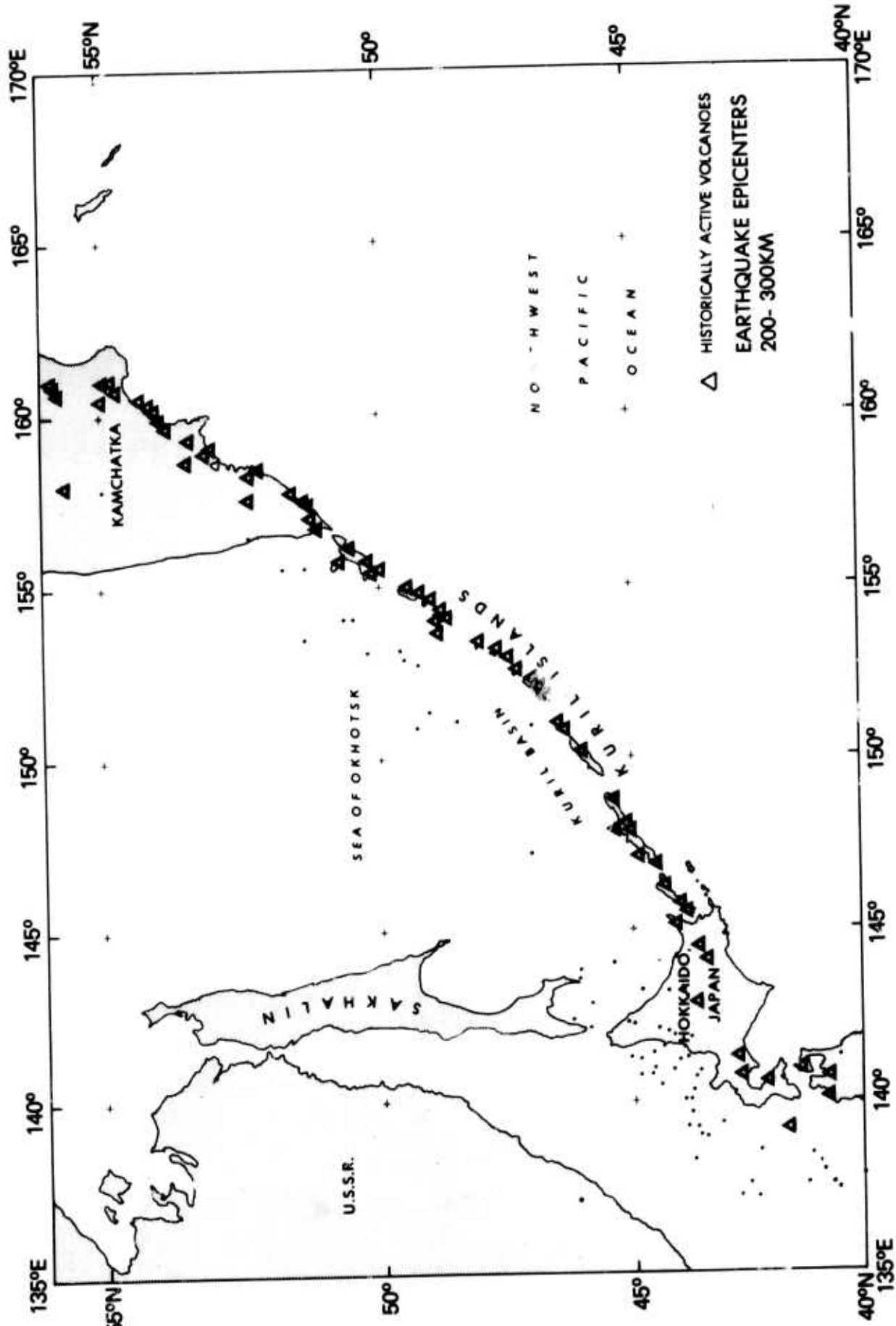


Figure 44. Earthquake epicenters of 300-400 km depth range for earthquakes occurring 1965-1975 (data from NEIS, Boulder, Colorado).

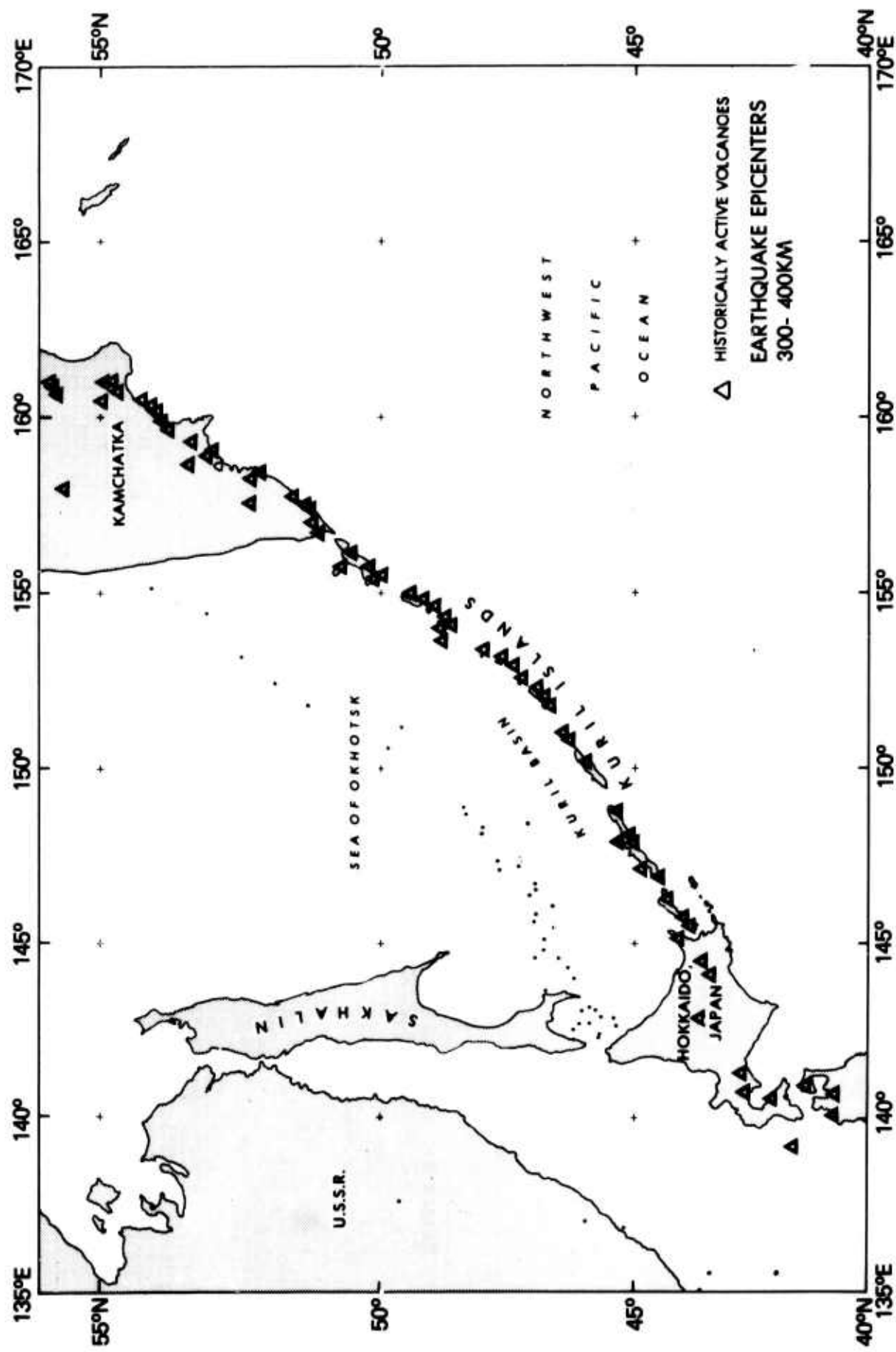


Figure 45. Earthquakes epicenters greater than 400 km depth range for earthquakes occurring 1965-1975
(data from NEIS, Boulder, Colorado).

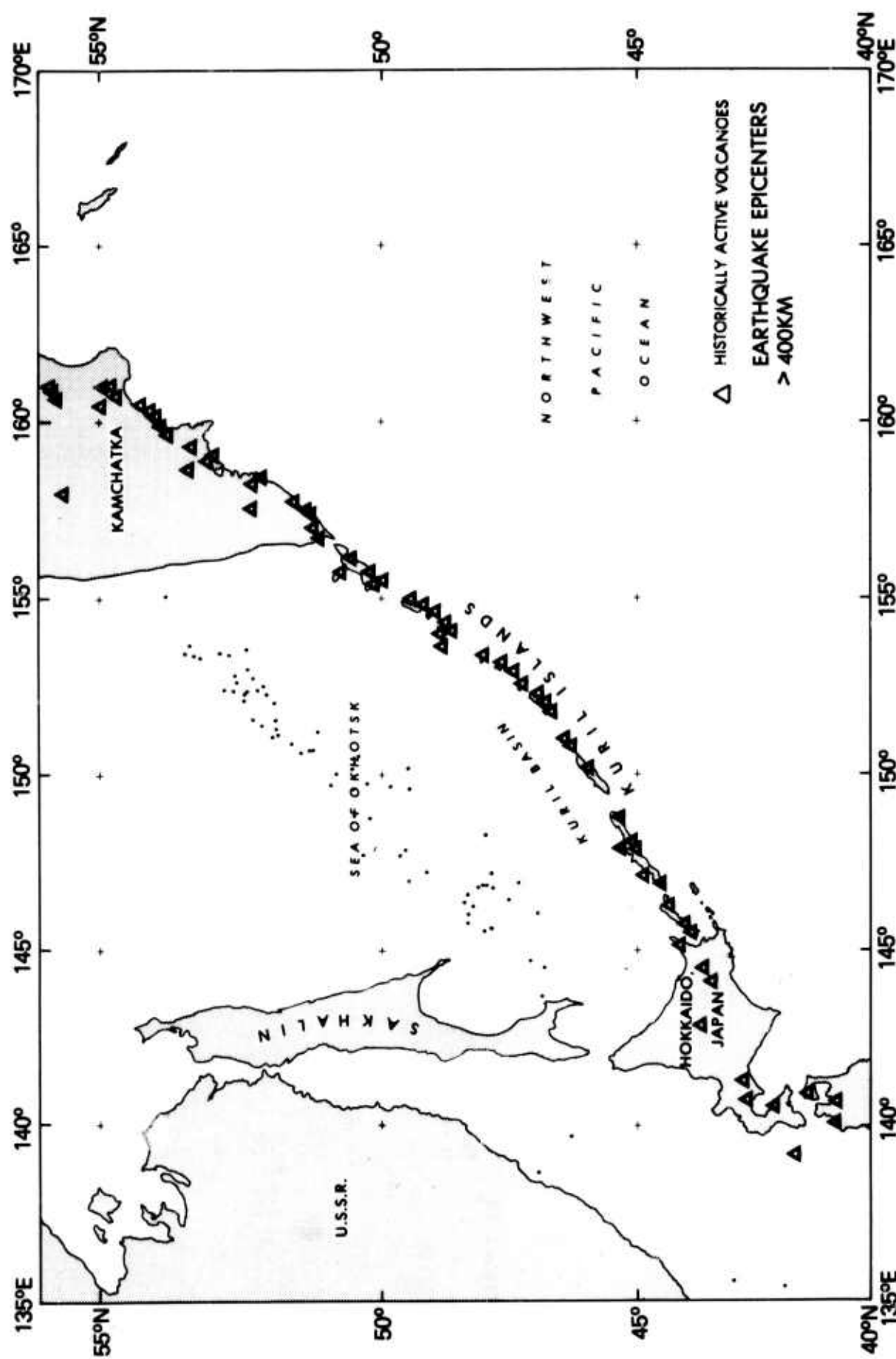


Figure 46. Index map for (1) crustal columns on Figure 40, (2) crustal cross sections on Figure 49, (3) position of Hawaii Institute of Geophysics. OBS and two earthquakes detected by the OBS (Kasahara, 1976).

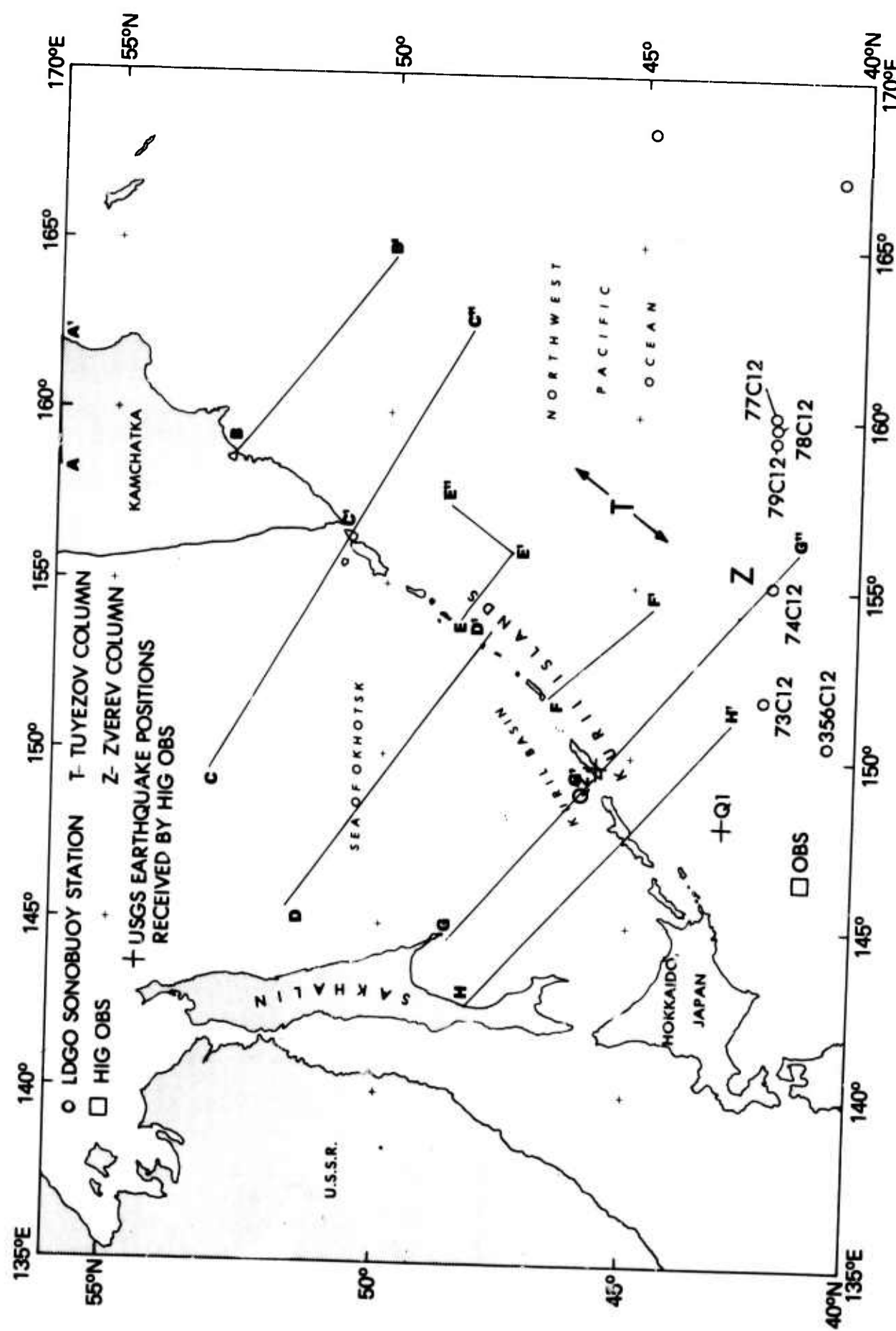


Figure 47. Northwest Pacific oceanic crust sections. The first five columns are from Houtz (1976); the D column is from Den et al. (1969) and Ludwig et al. (1966); the T column from Tuyezov (1970) and the Z column from Zverev (1977). Layer velocities in km/sec are noted by small vertical type; layer divisions of Houtz (1976) are represented by large slanted type.

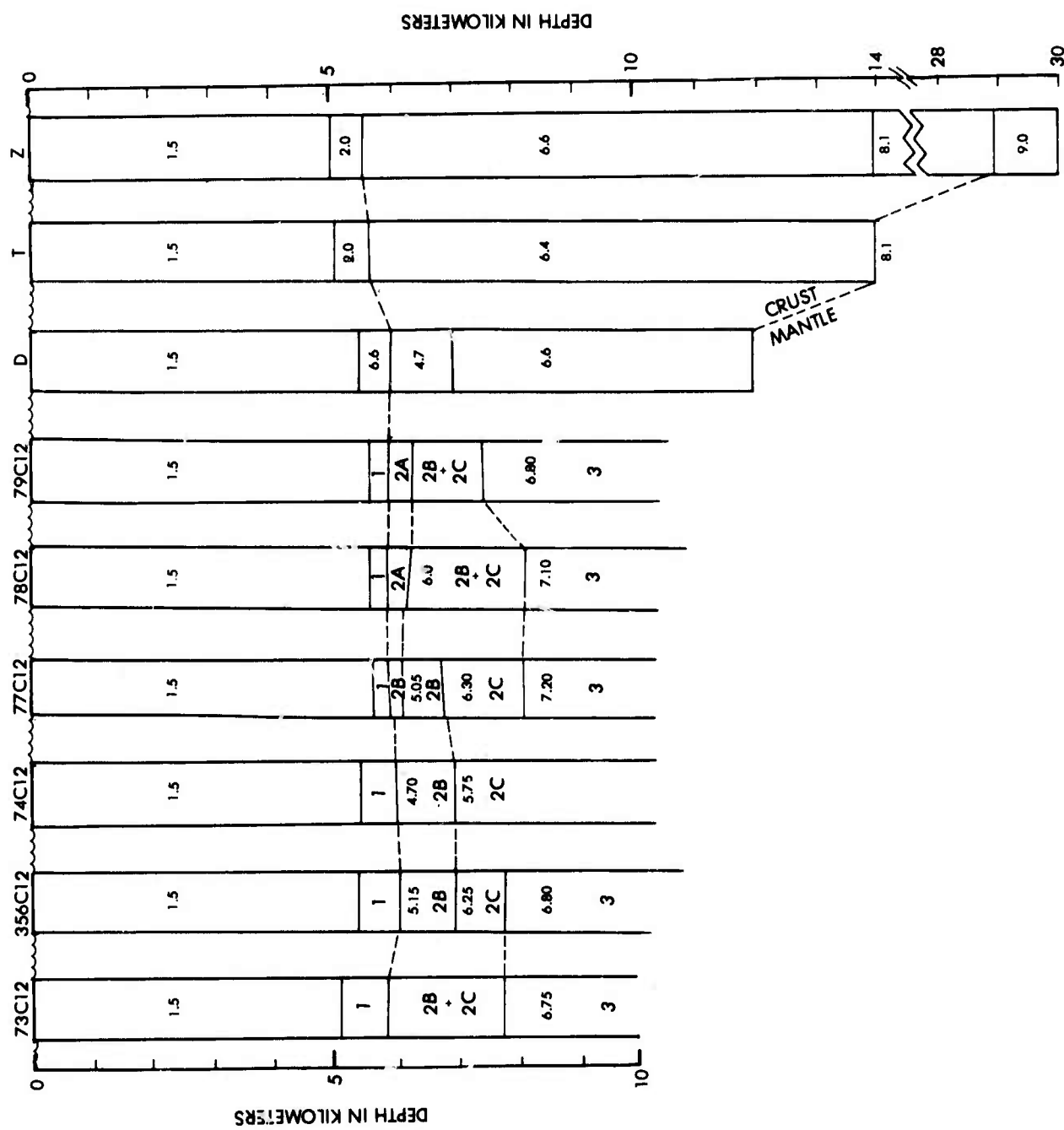
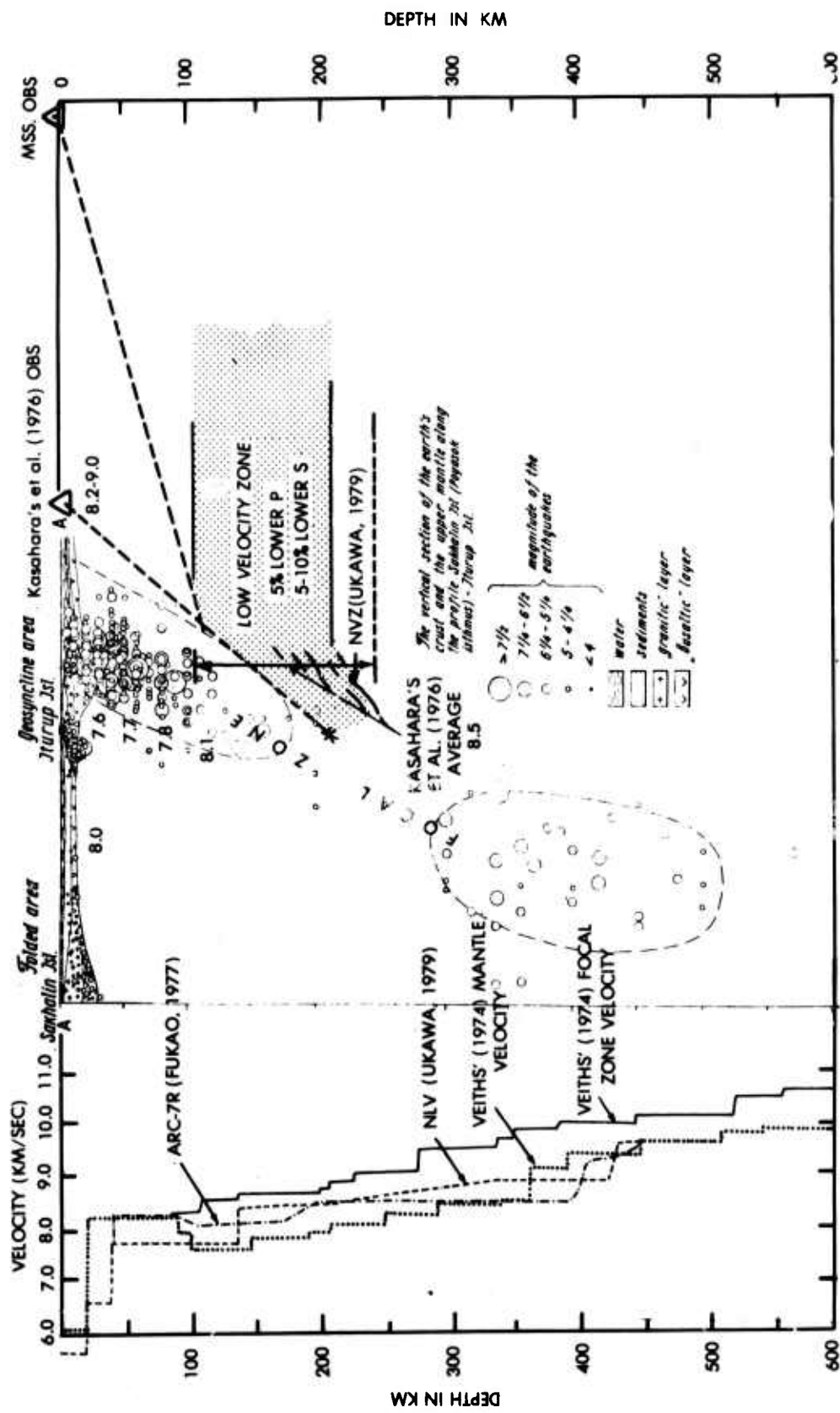


Figure 48. a. Seismic velocity models for the Kuril Earthquake region.
b. Cross section of the Southern Kuril's showing 1911-1963 earthquake distribution with depth (Tuyezov, 1968). Seismic velocities (km/sec) to the left of the focal zone are from Fedotov (1965). The low velocity zone (shaded) has 1-5% lower V_p and 5-10% lower V_s than crust immediately above it, but the zone does not parallel the downgoing slab (Ukawa, 1979). The average low velocity zone of Kasahara et al. (1976) is 8.5 km/sec. Straight line paths from the plotted Kasahara OBS and a potential MSS OBS site (400 km from the trench) indicate the maximum depth of potential focal zone earthquakes for which the OBS will not have to pass through the low velocity layer.



६

2

Figure 49. Crustal cross sections of the Kuril-Kamchatka earthquake region. Positions of sections are plotted on Figure 46. Cross sections are aligned to the Kuril-Kamchatka Trench and are positioned roughly according to their actual relative position on a map. Crustal depth units are kilometers. Geographic names are added where appropriate. Actual velocity measurements are plotted in positions where measured. Data are from Weizman (1965), Zverev (1977) and Sychev (1977), and are based upon Soviet deep seismic sounding work.

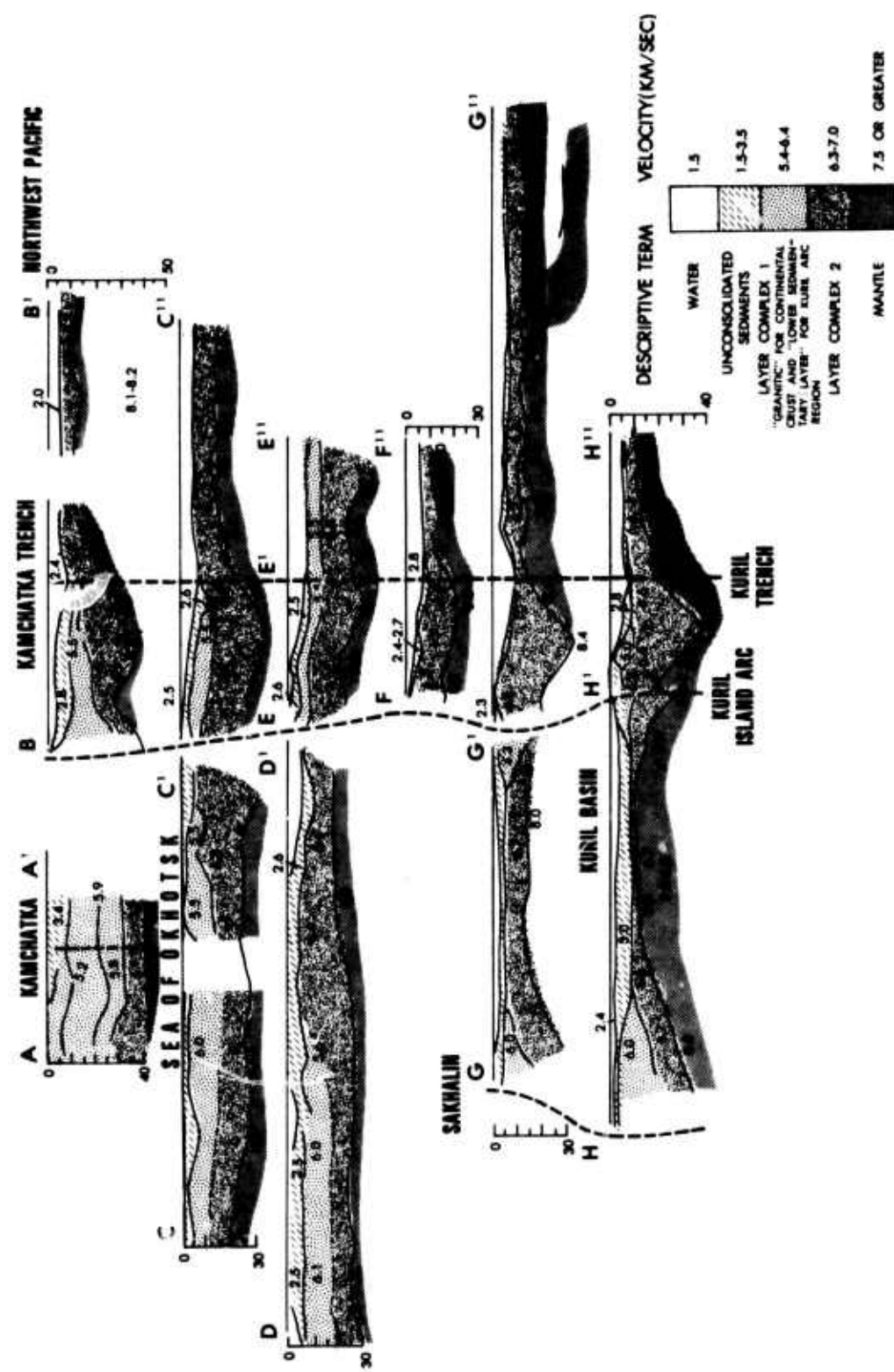


Figure 50. Depth to the Moho and velocities used to define the Moho (adapted from Sergeyev, 1977, and Burk et al., 1977).

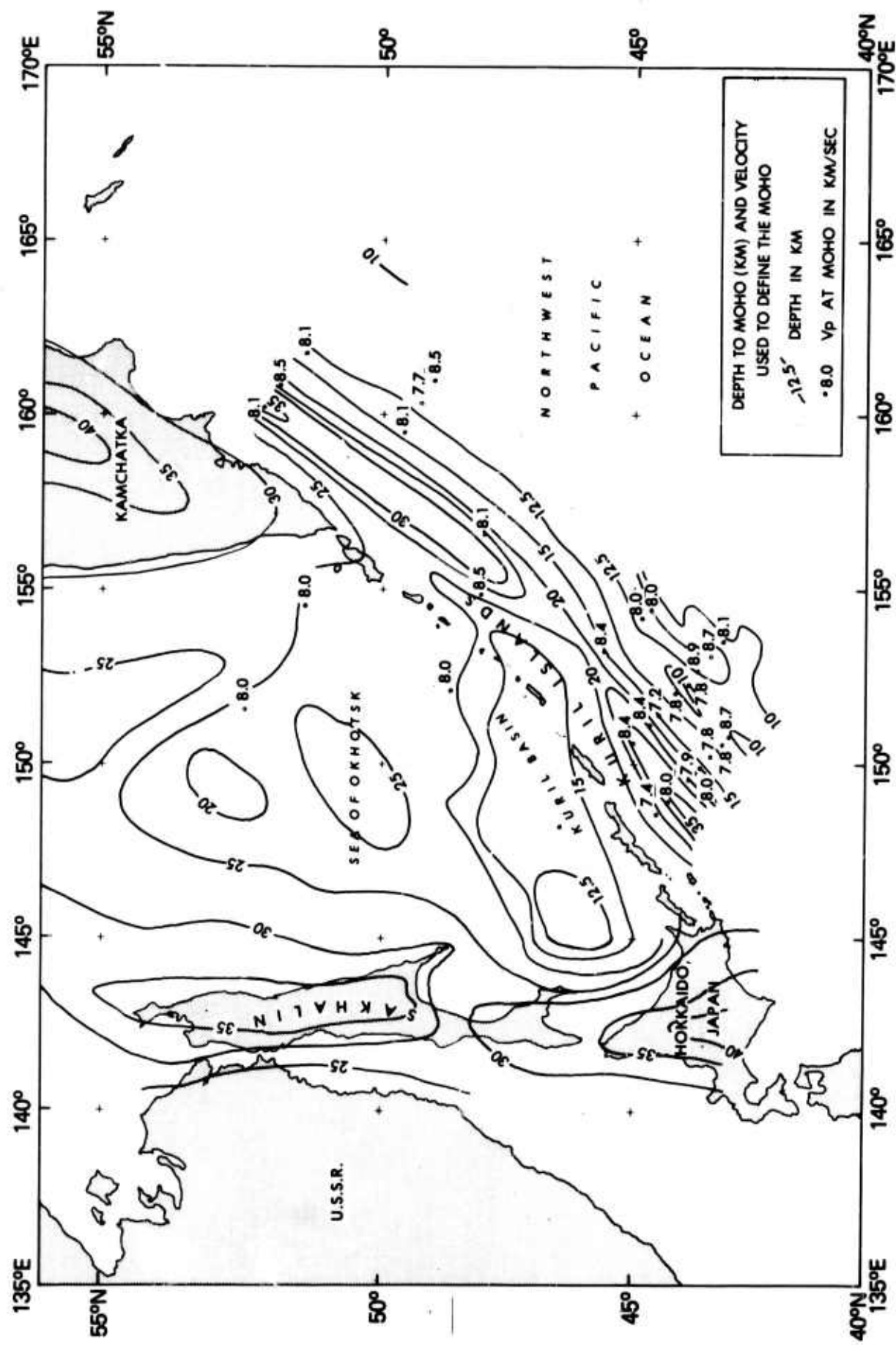


Figure 51. Depth to layer complex2. Layer complex2 is a Soviet term for the "oceanic" crustal layer with characteristic velocities of 6.3-7.0 km/sec (see Fig. 49) (adapted from Sergeyev, 1977).

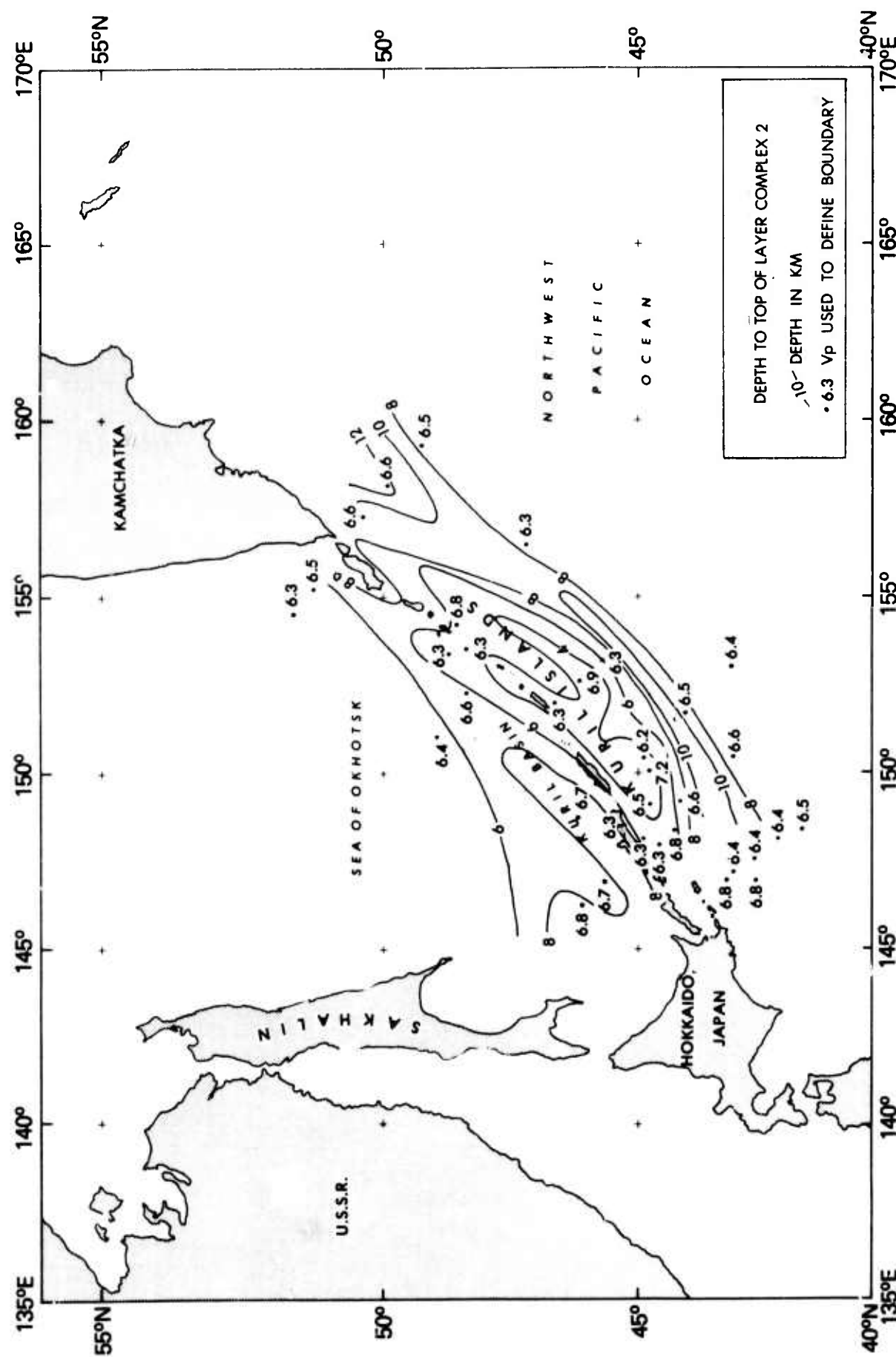


Figure 52. Thickness of the upper sedimentary layer. This layer is believed to consist of unconsolidated sediments (see Fig. 49) (adapted from Sergeyev, 1977).

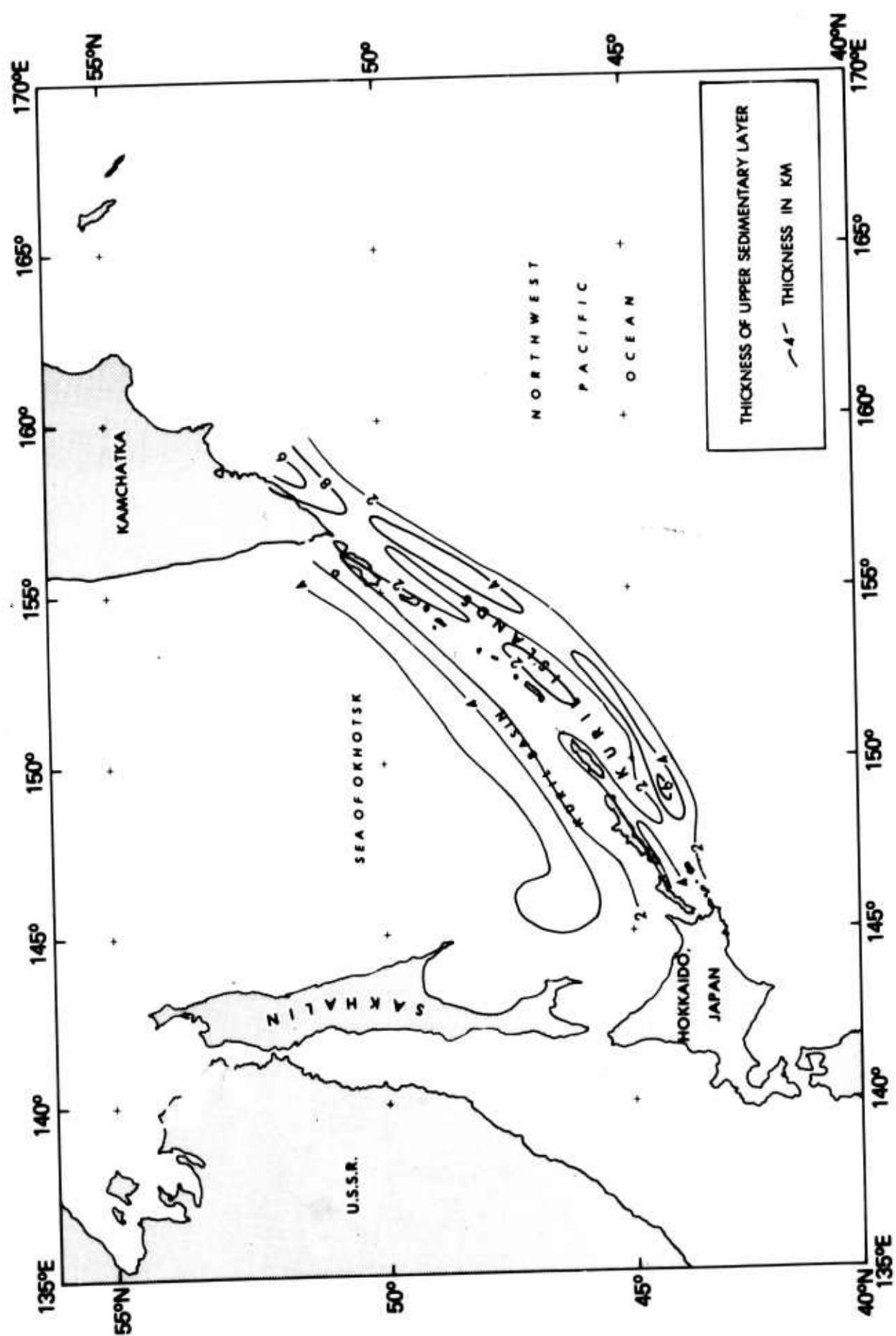


Figure 53. Thickness of the lower sedimentary layer. This layer lies under the Kuril Islands and is believed to be consolidated sediments (Tuyezov, 1968). The layer has velocities equivalent to the "granitic layer", which is not mapped on this figure (adapted from Sergeyev, 1977).

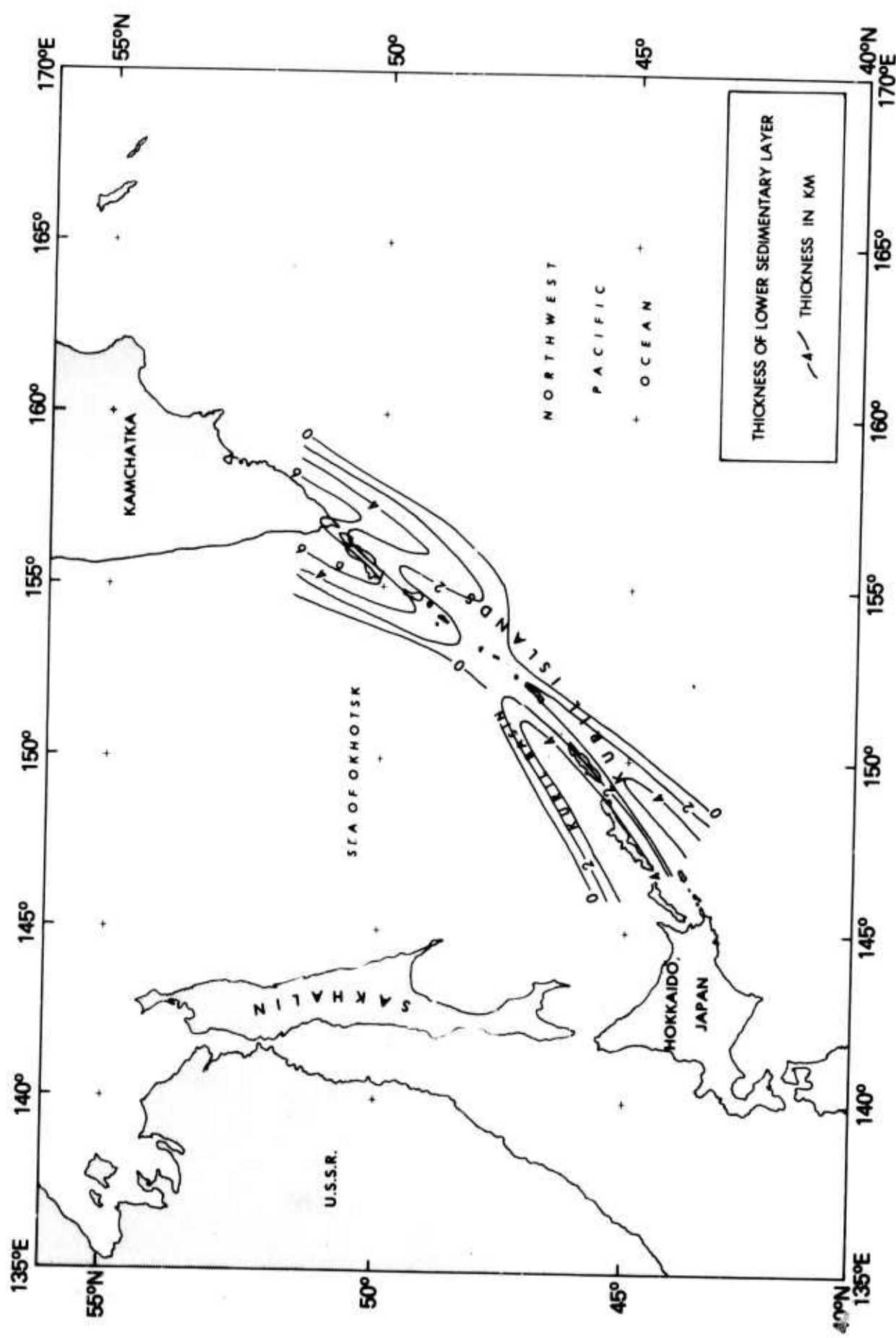


Figure 54. Free-air gravity (adapted from Watts, 1977).

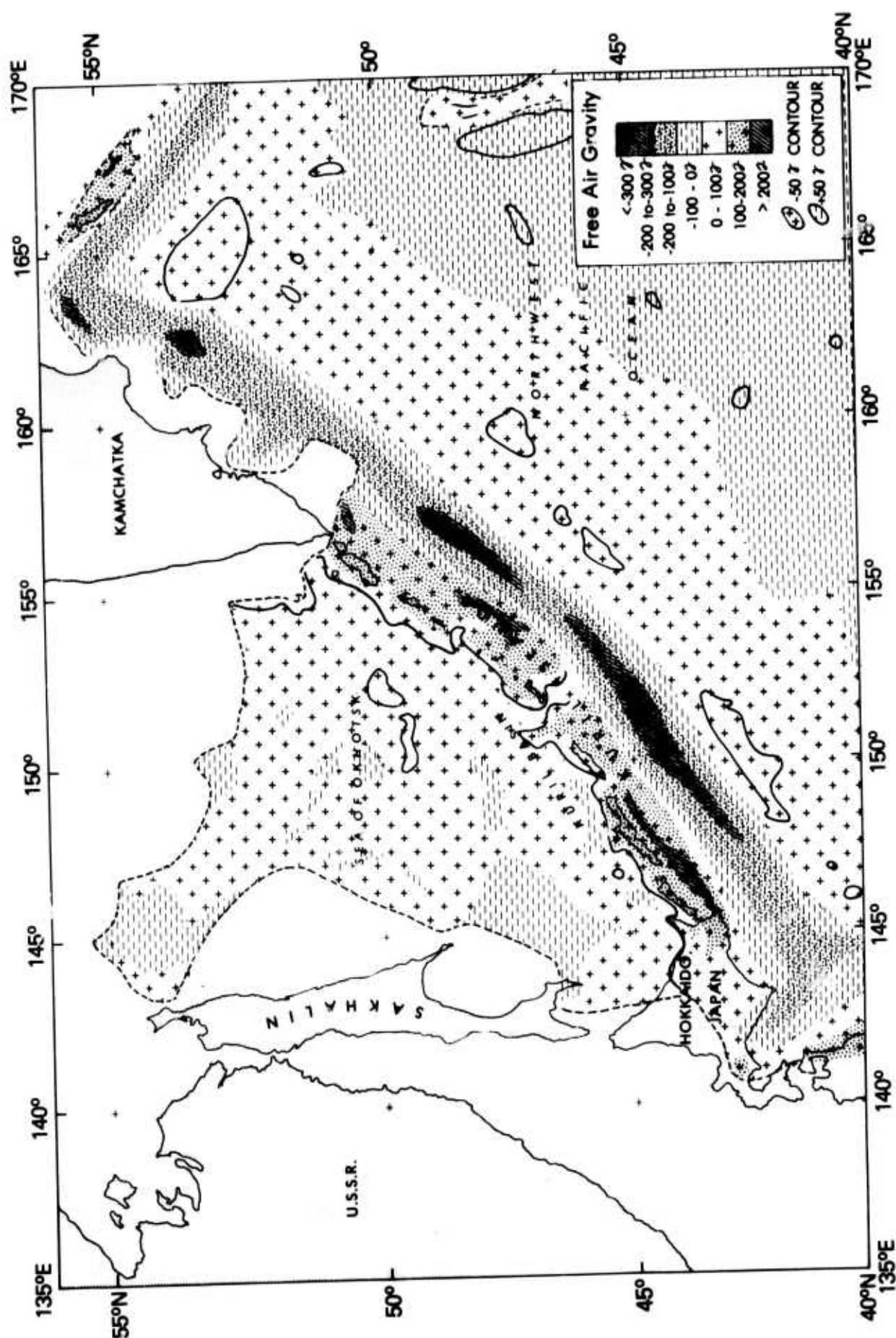


Figure 55. Heat flow in heat flow units is presented as contoured data (Uyeda et al., 1967) and as 5° averages (Langseth et al., 1970) with 5° average thermal conductivity (K) (Langseth et al., 1970) also included.

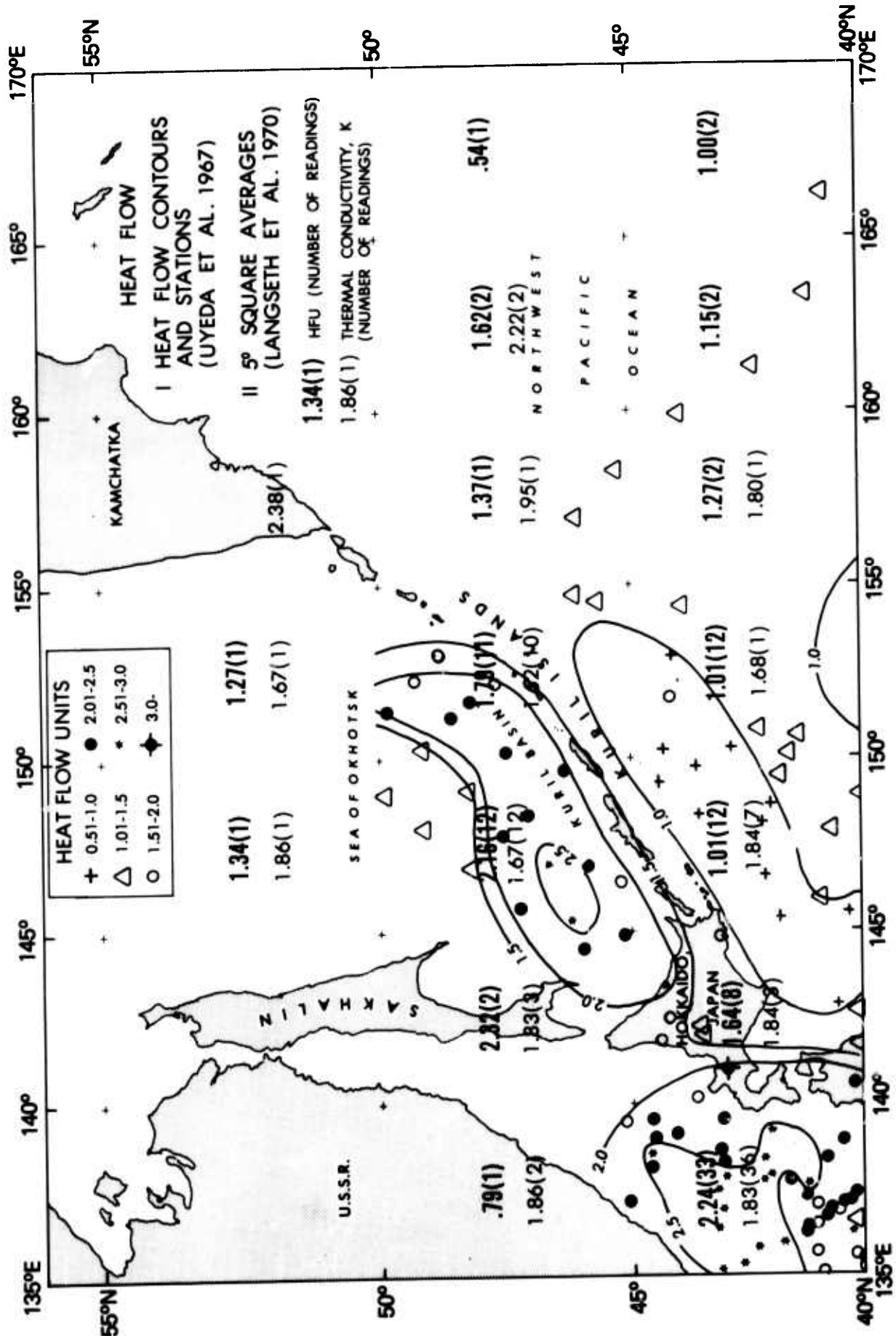


Table I. Surface sediment types

Map Patterns	Sediment Name	Description
Clay and Calcareous	Calcareous clay	10-30% biogenic carbonate, size <4 μ m
Mud and Calcareous	Calcareous mud	10-30% biogenic carbonate, fine mostly grained terrigenous with some silt and sand
Clay and Siliceous	Siliceous clay	10-30% biogenic silica, size <4 μ m
Mud and Siliceous	Siliceous mud	10-30% biogenic silica, fine mostly grained terrigenous with some silt and sand
Siliceous and Silt/Sand	Siliceous silt and sand	10-30% biogenic silica, size 4 μ m to 2 mm

Table II. Grain size of surface sediments by geologic province

	<u>Sand</u>	<u>Aleurite</u>	<u>Pelite</u>	<u>Subcolloidal</u>
Emperor Seamounts	10-50%	10-50%	10-50%	<10%
Meiji Guyot	10-20%	30-50%	30-50%	<10%
Kuril Trench	<10%	10-30%	70-90%	10-20%
Southeast Abyssal Hills	10%	10-30%	70-90%	<10-20%
Hokkaido Rise	0-20%	30-50%	50-70%	<10%
Shatsky Rise	<10%	30-50%	50-70%	<10%

PRECEDING PAGE BLANK-NOT FILMED

Table III. Northwest Pacific DSDP core data

DSDP Core	Location	Province	Depth	Approximate Unconsolidated Sediment Thickness		Penetration	Deepest Layer Penetration
				1057 m	71 m		
192	53° 00.6N 164° 42.8E	Meiji Guyot	3014 m	700 m	1057 m	Basalt at 1045 m	
193	45° 48.4N 155° 56.3E	Central Hokkaido Rise	4811 m	480 m	71 m	Unconsolidated sediments	
303	40° 48.5N 154° 27.1E	South Abyssal Hills	5609 m	250 m	293 m	Basalt at 285 m	
304	39° 20.3N 155° 04.2E	South Abyssal Hills	5640 m	250 m	347 m	Basalt at 340 m	
431	42° 25.4N 170° 32.7E	Seamount	1715 m	—	17 m	Unconsolidated sediments	
432	41° 20.0N 170° 22.7E	Nintiku	1320 m	—	74 m	Basalt	
433	44° 46.6N 170° 01.3E	Suiyo	1874 m	—	551 m	Basalt	
436	39° 56.0N 145° 33.5E	South Hokkaido Rise	5240 m	380 m	398 m	Chert	

Table IV. Physical properties of Northwest Pacific Ocean sediments, terrigenous, and red clays

	γ (g/cm ³)	W (%)	e	n (%)	c (g/cm ²)	St	Gs	LL	PL	PI	LI (%)
Pacific											
Maximum	2.03	423	10.43	91	556	57	3.83	231	86	105	356
Minimum	1.15	24	0.80	45	1	1	2.32	25	24	16	86
Average	1.45	175	3.29	77	49	4	2.71	100	41	68	152
Terrigenous material											
Maximum	1.93	259	6.43	87	722	57	3.26	143	53	95	324
Minimum	1.21	28	0.79	44	1	1	2.27	25	15	11	84
Average	1.46	112	2.51	73	64	4	2.67	85	29	36	153
"Red clay"											
Maximum	2.03	423	10.43	91	230	25	3.83	231	86*	83*	166*
Minimum	1.15	23	0.69	41	2	1	2.41	106	-	-	-
Average	1.44	159	3.30	74	45	9	2.54	167	-	-	-

(after Keller et al., 1970)

γ Bulk Density
 W Water % dry weight
 e Void ratio
 n Porosity
 c Cohesion
 St Sensitivity
 Gs Grain specific gravity
 LL Liquid limit
 PL Plastic limit
 PI Plasticity
 LI Liquidity limit

Table V. Physical properties of sediments from the North Pacific and calculated bearing capacities

Sample	Lat. N. Long. W.	Water depth m Fm.	Sample burial depth below surface cm	Sediment type	Sediment size			Per cent sand	Per cent silt	Wet density gm/cm ³	Wet density lb/ft ³	Porosity	Void ratio	θ des.	Direct shear		Sensitivity	Bearing capacity psi	Geomorphic areas			
					Md (mm)	Per cent clay	Per cent silt								C gm/cm ²	C psi						
CK-5	43°-16'	163°-40'	5399	2952	0	5	Silty clay	.0022	2	32.5	65.5	1.14	71.2	54.9	1.22	**	7.23	0.103	7.20	0.819		
CK-5	43°-16'	163°-40'	5399	2952	8.5	8.5	Clayey silt	.0042	2.6	50.1	47.3	1.30	81.2	79.3	3.83	47	19.90	0.283	**	**	Deep sea	
CK-7	47°-10'	165°-45'	51175	2830	0	5	Silty clay	.0048	12.2	41.8	46	1.36	84.9	75.9	3.15	*	**	11.18	0.159	3.80	**	
CK-7	47°-10'	165°-45'	51175	2830	65	69	Silty clay	.0039	5	46	49	1.30	81.0	75.7	3.12	*	**	53.08	0.759	11.00	**	
CK-7	47°-10'	165°-45'	51175	2830	162	171	Clayey silt	.0090	7.8	61.1	31.1	1.36	84.9	74.3	2.89	52	17.46	0.354	**	**		
CK-7	45°-03.5'	144°-39.5'	4722	2822	125	Silty clay	.0014	0	25	75	1.42	88.7	74.3	19.1	0	0.272	**	3.1	2.170	**	**	
CK-7	45°-01.4'	144°-28.5'	4690	2864	100	Silty clay	.0018	2	26	72	1.34	83.7	76.7	3.39	33	30.6	0.435	**	**	**	**	
CK-2	37°-30'	158°-30'	5670	3100	200	Silty clay	.0015	3	17	**	**	1.26	78.7	84.0	5.25	**	**	101.90	1.450	2.94	**	
CK-3	39°-50.2'	158°-36'	5692	3112	0	Silty clay	.0026	3	34	64	1.41	88.0	76.9	3.33	**	**	**	8.16	0.116	5.15	0.922	
CK-3	39°-56.2'	158°-38'	5692	3112	113	118	Silty clay	.0030	3.5	39.5	57	1.36	84.9	74.4	2.91	**	**	**	63.42	0.902	8.41	**
CK-4	42°-30'	162°-08'	5399	2952	0	5	Clayey silt	.0078	1	16.5	82.5	1.35	84.3	77.6	3.46	**	**	**	5.91	0.084	3.50	0.678
CK-4	42°-30'	162°-08'	5399	2952	154	163	Silty clay	.0030	4	40	56	1.39	86.8	71.9	2.56	34	36.90	0.526	**	**	**	

(after Moore, 1962)

Table VI. Grain size of DSDP sediments

DSDP Core	Core, Section Interval (cm)	Depth (m)	Sand (%)	Silt (%)	Clay (%)	Classification
192	1-1(47.0)	0.5	10.5	52.1	37.4	Clay
	1-1(134.0)	1.3	5.0	50.5	44.4	Clay
	2-4(63.0)	6.1	10.3	46.3	43.4	Clay
	2-4(87.0)	6.4	1.0	87.4	11.6	Sand
	3-2(47.0)	12.0	10.1	49.1	40.8	Clay
	4-2(34.0)	20.8	7.7	50.7	41.6	Clay
	5-2(102.0)	30.5	6.0	46.4	47.6	Clayey silt
	6-2(37.0)	56.9	2.9	32.1	65.0	Clayey silt
	8-3(110.0)	96.1	3.0	33.1	63.8	Clayey silt
	8-4(87.0)	97.4	0.8	40.4	58.7	Clayey silt
	9-3(56.0)	124.6	1.4	34.1	64.4	Clayey silt
	10-2(36.0)	149.9	1.8	31.1	67.1	Clayey silt
	11-2(34.0)	177.8	4.0	31.4	64.6	Clayey silt
	12-2(93.0)	206.4	4.9	38.5	56.6	Clayey silt
	13-2(118.0)	234.7	6.5	36.9	56.6	Clayey silt
	21-2(86.0)	477.4	3.4	38.5	58.1	Clayey silt
	23-2(60.0)	571.1	0.9	38.1	61.0	Clayey silt
	27-4(63.0)	751.1	0.2	35.2	64.6	Clayey silt
	28-1(58.0)	784.6	0	28.9	71.1	Clayey silt
	29-1(128.0)	794.3	7.3	39.3	53.4	Clayey silt
	30-2(140.0)	851.9	0.3	37.7	62.0	Clayey silt
	31-2(38.0)	897.9	0.2	9.4	90.5	Silt
	32-2(31.0)	906.8	0	9.3	90.7	Silt
193	2-1(48.0)	2.5	10.1	55.5	34.4	Clay
	3-1(80.0)	25.8	10.1	47.1	42.8	Clay
	3-5(87.0)	31.9	9.6	44.3	46.1	Clayey silt
303		65.2	2.6	47.2	55.1	
		124.85	5.1	48.6	45.9	
		176.83	1.0	10.7	80.3	

Table VII. Density and porosity of DSDP cores

Hole	Core	Section	Interval	Shore Lab. Density (g/cc)	GRAPE Density (g/cc)	Shore Lab. Water Content (% dry wt.)	Syringe Water Content (% dry wt.)
192	1	1	68-76	1.41		115.57	119.2
	2	2	137-140	1.46	1.44		
	2	4	104-105	1.50	1.43		
	3	1	82-85	1.48	1.41	91.12	84.3
	3	2	65-67	1.56	1.56		
	3	3	53-55	1.57	1.60		
	3	4	115-118	1.49	-		
	4	1	52-55	1.48	1.54	92.90	88.0
	4	2	46-48	1.57	1.61		
	4	3	85-88	1.48	1.46		
	4	4	51-54	1.55	1.58		
	4	5	23-26	1.56	1.54		
	4	6	20-22	1.54	1.50	77.14	81.0
	5	1	89-91	1.45	1.51		
	5	2	32-34	1.55	1.55		
	5	3	16-18	1.47	1.41		
	5	4	99-102	1.51	1.53	83.95	89.9
	5	5	7-10	1.51	1.50		
	6	2	143-145	1.39	-	109.04	112.1
	7	1	134-137	1.49	1.51		
	7	2	88-91	1.57	1.59	71.08	75.0
	7	3	87-89	1.55	1.55		
	7	4	104-106	1.49	1.50		
	8	5	35-38	1.51	1.49		
	8	6	88-90	1.52	1.46	81.63	77.1
	9	3	85-87	1.48	1.45		
	9	4	49-52	1.47	1.47		
	9	5	9-11	1.55	1.54	74.90	71.4
	9	6	120-123	1.53	1.55		
	10	3	13-16			104.67	104.9
	12	1	77-79	1.39	1.41		
	12	2	41-43	1.39	1.43		
	12	3	57-59	1.39	1.41	109.03	105.7
	12	4	44-46	1.37	1.38		
	13	2	66-68	1.30	1.26		
	13	3	44-46	1.37	1.38		
	13	5	119-121	1.36	1.36		
	15	4	29-31	1.41	1.40		
	15	4	93-95	1.41	1.41	106.55	101.2
	17	3	139-141	1.41	1.45		
	19	2	60-63	1.41	1.44	105.53	96.9
	21	2	131-133	1.39	1.39		
	21	1	125	1.36	1.28		
	25	2	70	1.44	1.39		
192A	5	1	40	2.16	1.80		
	5	1	130	2.82	2.31		
	5	2	40	2.61	2.33		
	5	3	135	2.72	2.13		
	5	4	40	2.63	2.11		
	5	5	35	2.61	2.31		
193	1	1	114-116	1.43	1.42		
	1	1	136-138	1.40	1.40	115.46	97.4
	1	2	96-98	1.49	1.42	88.85	93.5
	2	1	107-108	1.39	1.39	119.28	107.0
	2	3	107-109	1.49	1.51	87.49	91.2
	3	1	131-134	1.49	1.42		
	3	2	95-97	1.45	1.50		
	3	2	105-108	1.50	1.56	86.36	83.4
	3	3	48-51	1.38	1.42		
	3	3	96-98	1.49	1.57		
	3	4	70-73	1.50	1.52	85.33	90.2
	3	4	124-126	1.44	1.49		
	3	5	71-74	1.43	1.44	105.68	86.2
	3	5	125-128	1.54	1.51		
303			65	1.3	2.81		85*
	Depth (m)		180	1.5	3.12		80*
			110	1.2	2.58		85*
304			220	1.5	3.52		80*

*Porosity

UNCLASSIFIED

SECURITY CLASSIFICATION OF THIS PAGE (When Data Entered)

REPORT DOCUMENTATION PAGE		READ INSTRUCTIONS BEFORE COMPLETING FORM
1. REPORT NUMBER NORDA Report 31	2. GOVT ACCESSION NO. AD-A099 820	3. RECIPIENT'S CATALOG NUMBER
4. TITLE (and Subtitle) Environmental Report of the Northwest Pacific for the Marine Seismic System (MSS)		5. TYPE OF REPORT & PERIOD COVERED
		6. PERFORMING ORG. REPORT NUMBER
7. AUTHOR(s) James A. Green Peter Fleischer	8. CONTRACT OR GRANT NUMBER(s)	
9. PERFORMING ORGANIZATION NAME AND ADDRESS Naval Ocean Research & Development Activity Ocean Science & Technology Division, Code 360 NSTL Station, Mississippi 39529		10. PROGRAM ELEMENT, PROJECT, TASK AREA & WORK UNIT NUMBERS
11. CONTROLLING OFFICE NAME AND ADDRESS		12. REPORT DATE December 1980
		13. NUMBER OF PAGES 181
14. MONITORING AGENCY NAME & ADDRESS (if different from Controlling Office)		15. SECURITY CLASS. (of this report) UNCLASSIFIED
		16. DECLASSIFICATION/DOWNGRADING SCHEDULE
17. DISTRIBUTION STATEMENT (of the abstract entered in Block 20, if different from Report)		
Unlimited		
18. SUPPLEMENTARY NOTES		
19. KEY WORDS (Continue on reverse side if necessary and identify by block number) Environmental data Kuril-Kamchatka earthquake zone Northwest Pacific seafloor Acoustic basement MSS site areas		
20. ABSTRACT (Continue on reverse side if necessary and identify by block number) This report presents data compilations to aid in planning and site selection for the Marine Seismic System (MSS). Data are compiled for two geographic areas: the Northwest Pacific (40-56°N, 145-170°E) and the Kuril-Kamchatka earthquake region. Included for the Northwest Pacific are cultural, meteorological, oceanographic, geological, geophysical and seismological data to define the environment in which the potential MSS will operate. Kuril-Kamchatka earthquake zone data consist of seismic velocity structure of the crust and upper mantle and earthquake hypocenters.		

BATHYMETRY OF THE NORTHWEST PACIFIC OCEAN

Compiled by

James A. Green
Naval Ocean Research and Development Activity
NSTL Station, MS.
1980

55°

CONTOURS

- 1000— 1000 meter intervals
- 200— Even 200 meter intervals
- 500— Odd hundred meter intervals

Depths are uncorrected and are based upon a sound speed of 1500 meters/second two-way travel time.

|||| Approximate 200 mile limit from foreign territory

● 303 D.S.D.P. Drill Sites

DATA SOURCES

Defense Mapping Agency, Washington, D.C.
Japanese Hydrographic Office, Tokyo, Japan
Lamont-Doherty Observatory, Palisades, NY
Naval Oceanographic Office, Bay St. Louis, MS
National Oceanic and Atmospheric Administration, Rockville, MD

National Geophysical and Solar Terrestrial Data Center, Boulder, CO

Oregon State University, School of Oceanography, Corvallis, OR

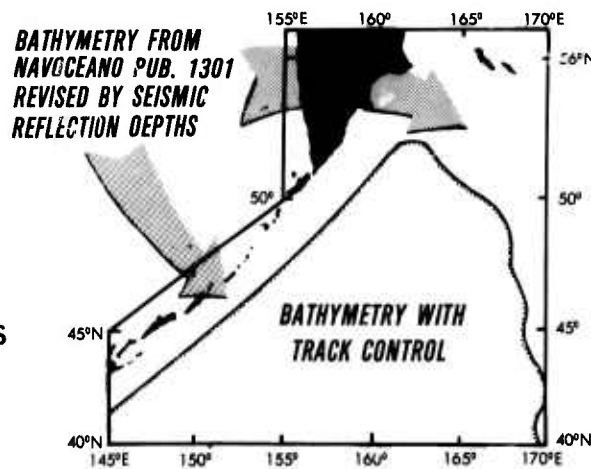
Scripps Institute of Oceanography, La Jolla, CA

Shirshov Institute of Oceanology, Academy of Science, Moscow, USSR

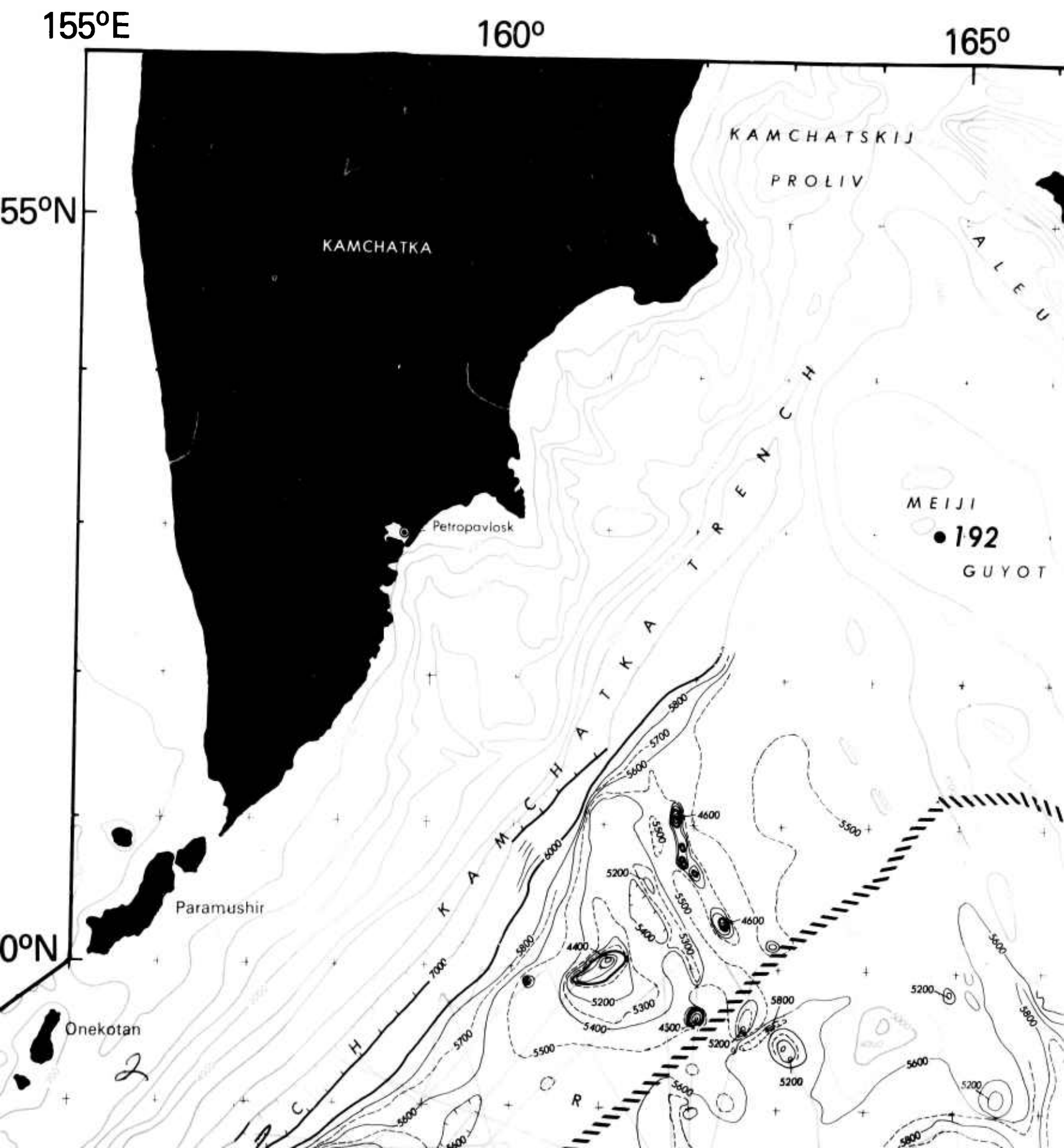
United States Geological Survey, Menlo Park, CA

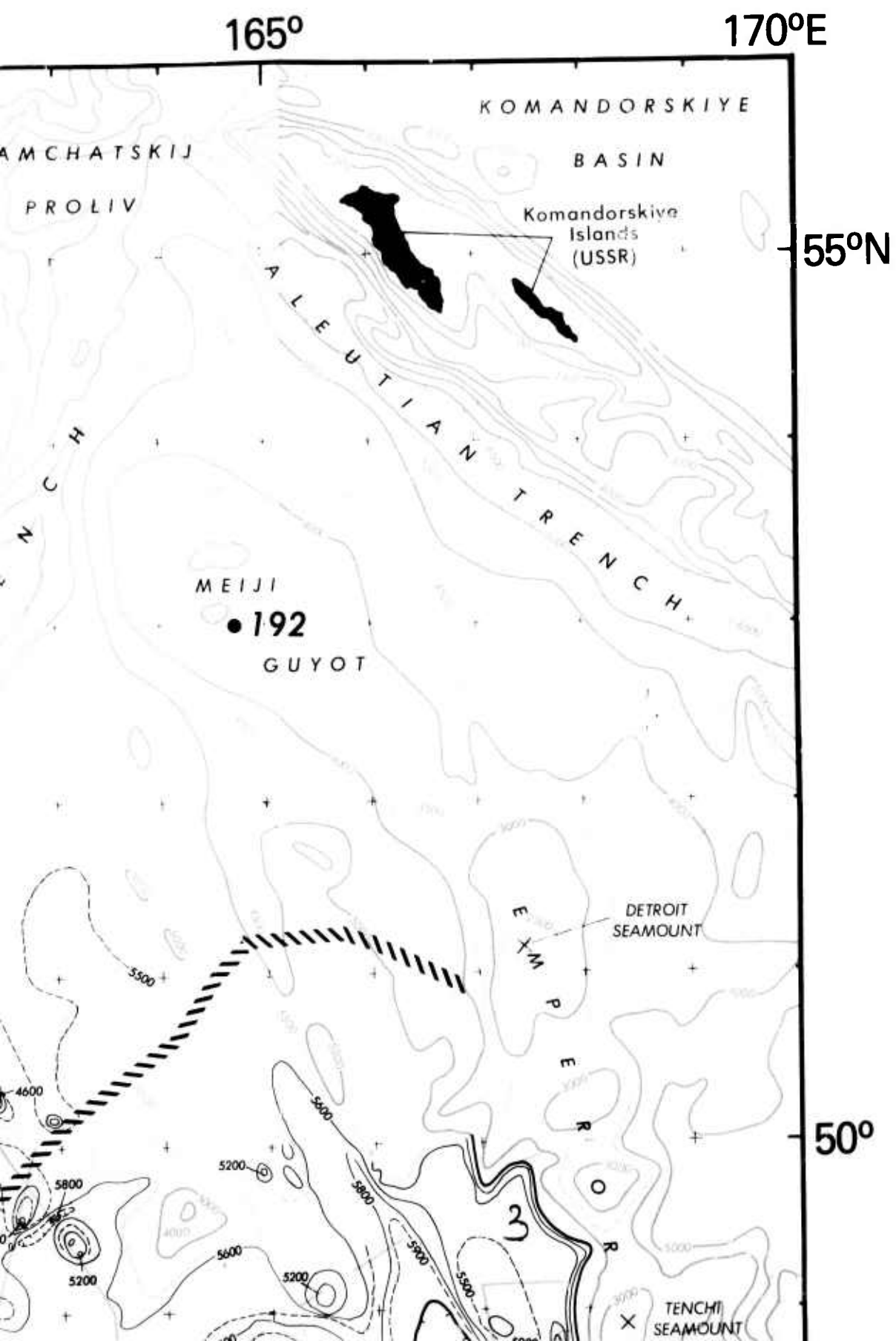
TRACKS

Track overlay includes all tracks used for compilation of the Northwest Pacific Basin. Bathymetry in bordering areas is taken from NAVOCEANO Pub. 1301 and revised by continuous seismic reflection profile depths. The bordering areas are contoured at 500 meter intervals and at 1000 meter intervals.



50°

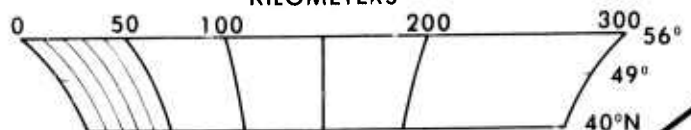




STANDARD MERCATOR PROJECTION

Scale at 49°N is 1: 3,000,000

KILOMETERS



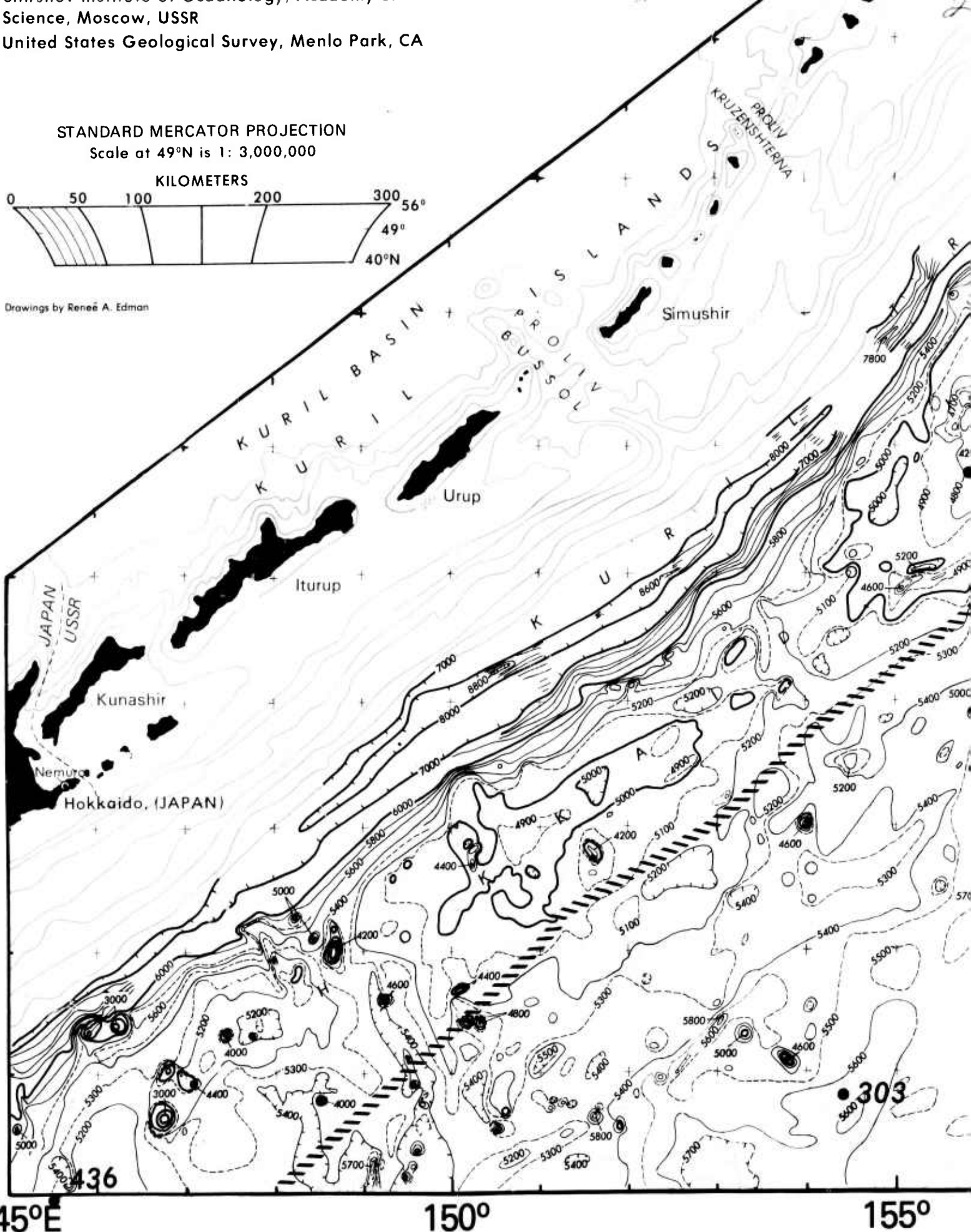
Drawings by Renée A. Edman

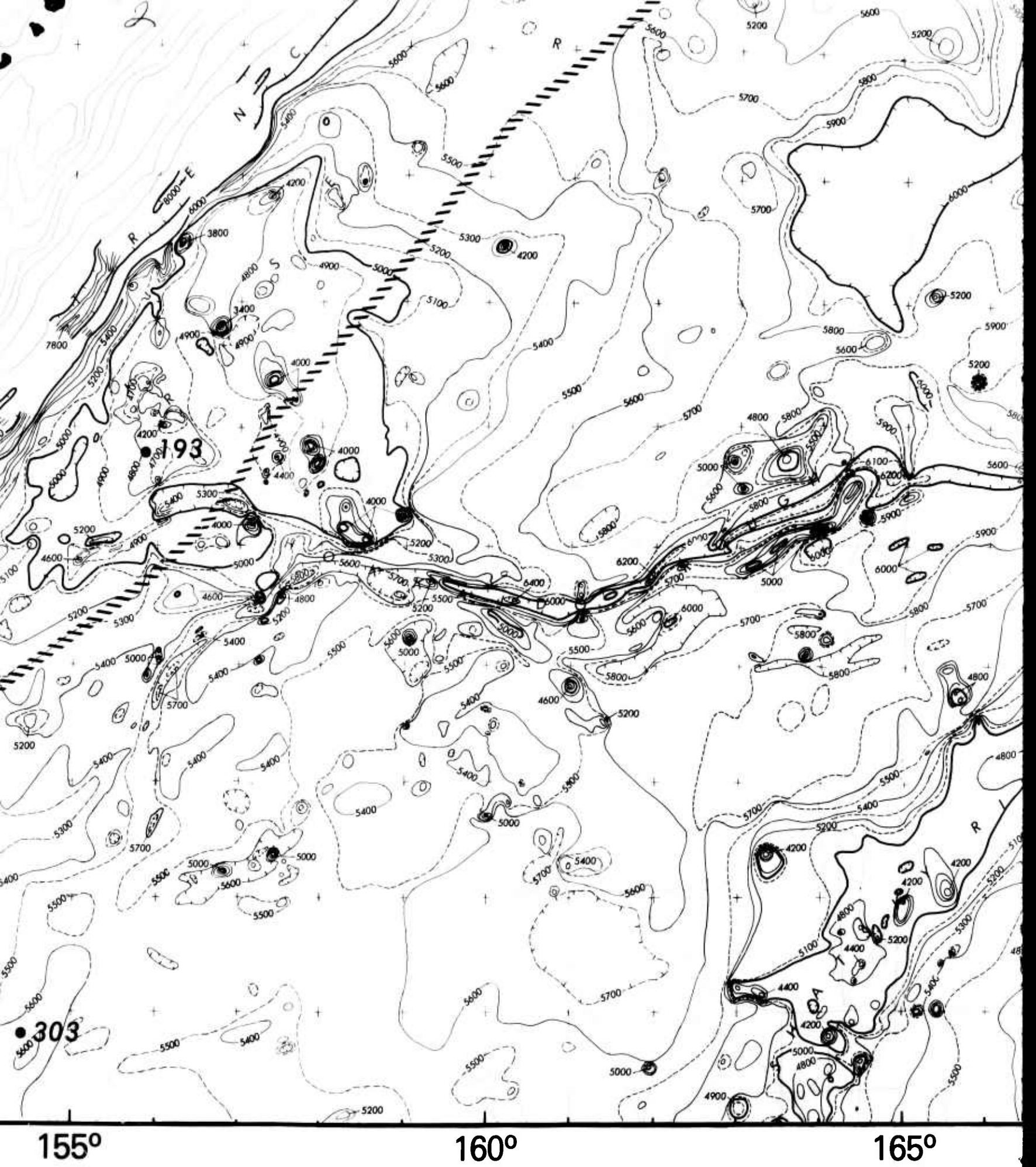
45°N

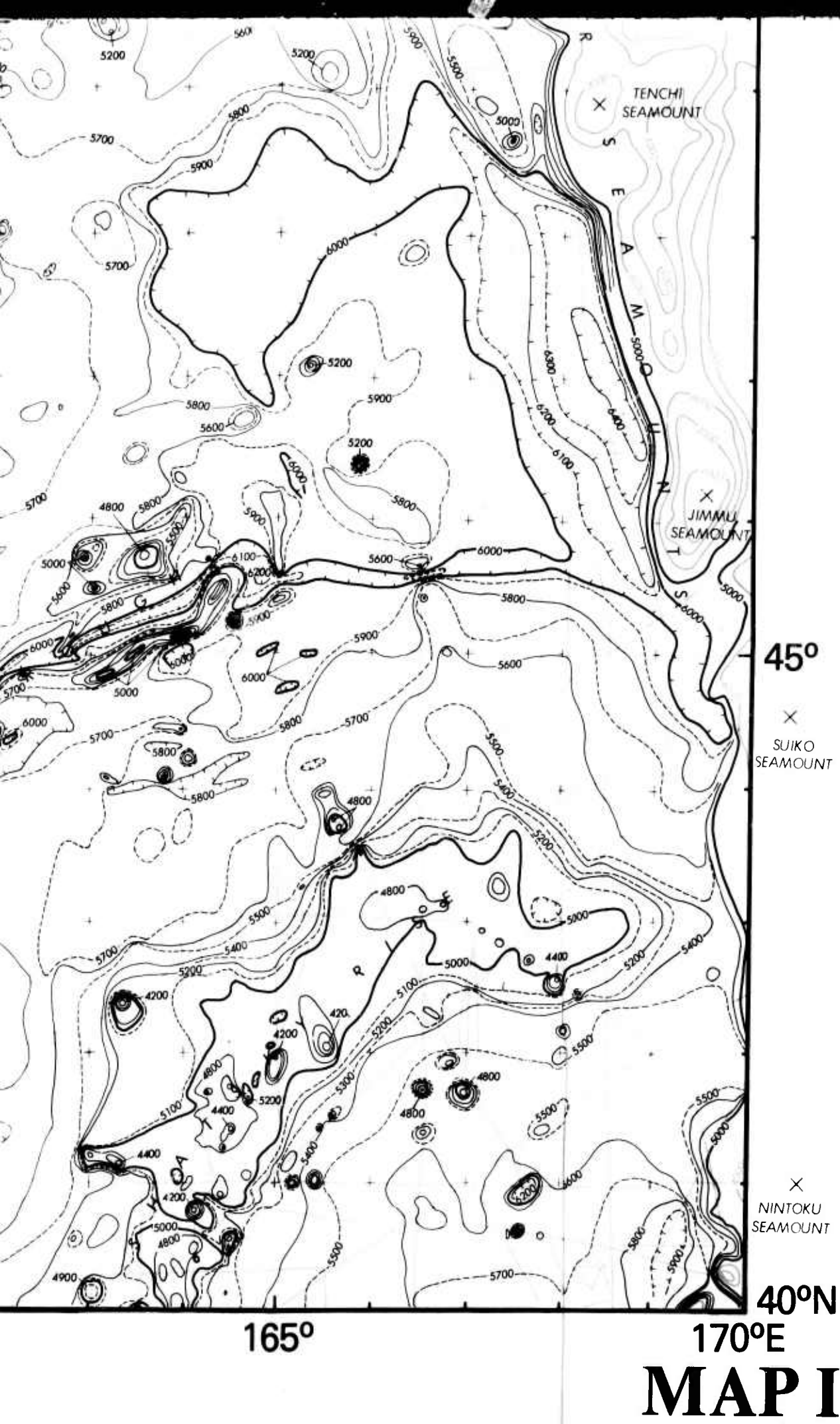
436

150°

155°







155

SEDIMENT ISOPACH MAP OF THE NORTHWEST PACIFIC OCEAN

55°N

Compiled by

James A. Green

Naval Ocean Research and Development Activity
NSTL Station, MS.

1980

Sediment isopachs are measured in seconds of two-way travel time from continuous seismic reflection profiles and represent the thickness at the upper transparent layer to the upper opaque layer (Ewing 1968) or to true basement.

CONTOURS - TWO-WAY TRAVEL TIME

- 1.0 — Whole second intervals
- 0.2 — Even 0.2 second intervals
- 0.1 — Odd two-tenths intervals

Unlabeled closed contours indicate thinner sediment except where implied by alternating solid and dashed 0.1 second contours.

Assuming an average velocity of 1700 meters/second (an average of Houtz and Ludwig (1979) and D.S.D.P. 303 and 192 measurements) the following thicknesses are calculated:

Seconds of two-way travel time	Actual calculated thickness in meters
0.1	85
0.2	170
0.4	340
0.6	510
0.8	680
1.0	850
1.2	1020
1.4	1190

Track control for sediment isopachs is less extensive than control for bathymetry. Sediment isopachs in sparsely surveyed areas can be inferred by overlaying the bathymetry.

• 303 D.S.D.P. Drill Sites

TRACKS

Track coverage includes all continuous seismic reflection profiles used to compile this map. Tracks are displayed according to the institute which collected the data.

- — — Lamont-Doherty Geological Observatory
Columbia University, Palisades, NY
- - - Naval Oceanographic Office, Bay St. Louis, MS
- - - Scripps Institute of Oceanography, La Jolla, CA
- - - Shirshov Institute of Oceanology, Moscow, USSR
- - - - United States Geological Survey, Menlo Park, CA

REFERENCES

Ewing, J., M. Ewing, T. Aiken, and W. J. Ludwig (1968). North Pacific Sediment Layers Measured by Seismic Profiling. American Geophys. Union Monograph 12, p. 147-173.

Houtz, R. E., and W. J. Ludwig (1979). Distribution of Reverberant Layers in the Southwest Pacific Basin. Journal of Geophys. Res., vol. 84, no. B7, p. 3497-3504.

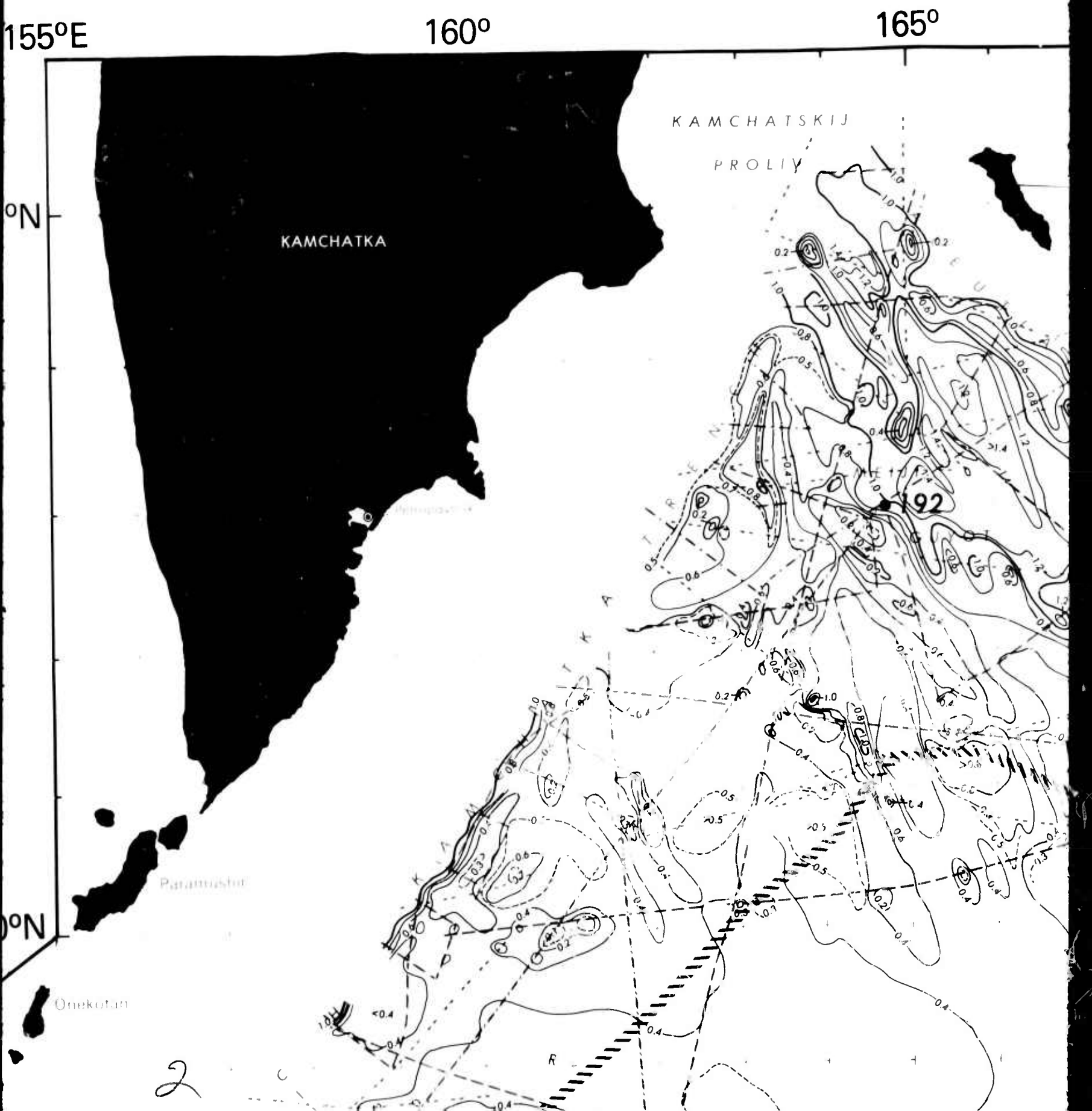
Creager, J. S., D. W. Scholl, et al. (1973). Initial Reports of the Deep Sea Drilling Project. Volume 19, Washington D. C. (U. S. Government Printing Office) p. 474

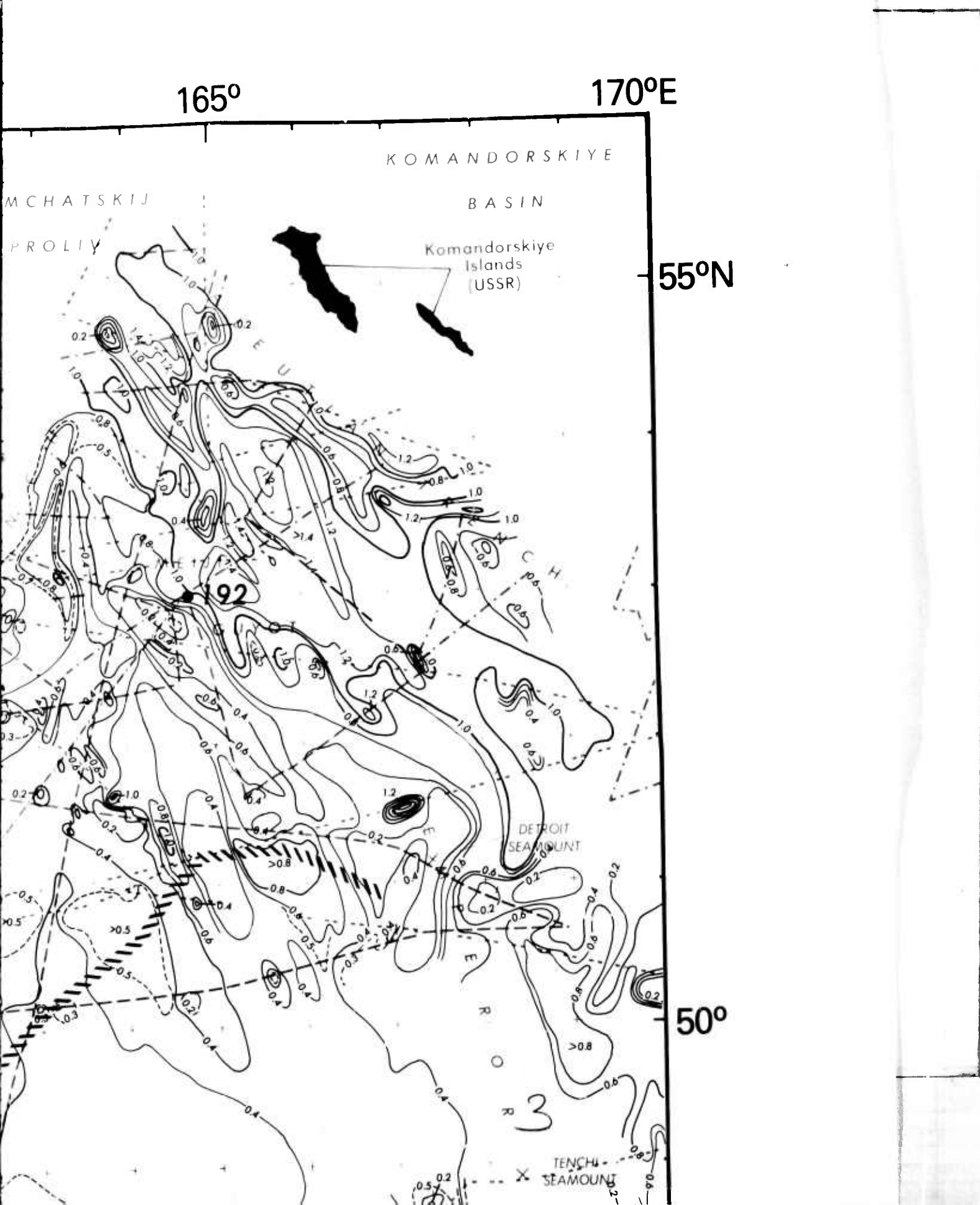
Larsen, R. L., R. Moberly, et al. (1975). Initial Reports of the Deep Sea Drilling Project. Vol. 32, Washington D. C. (U. S. Government Printing Office), p. 25

Drawings by Renée A. Edman

50°N

TRUE
PR





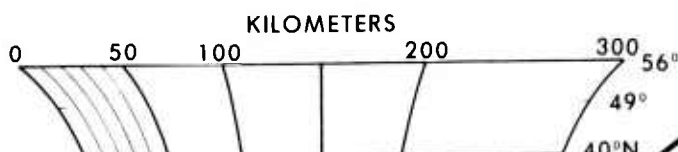
1.0 850
1.2 1020
1.4 1190

Drawings by Renée A. Edman

Track control for sediment isopachs is less extensive than control for bathymetry. Sediment isopachs in sparsely surveyed areas can be inferred by overlaying the bathymetry.

● 303 D.S.D.P. Drill Sites

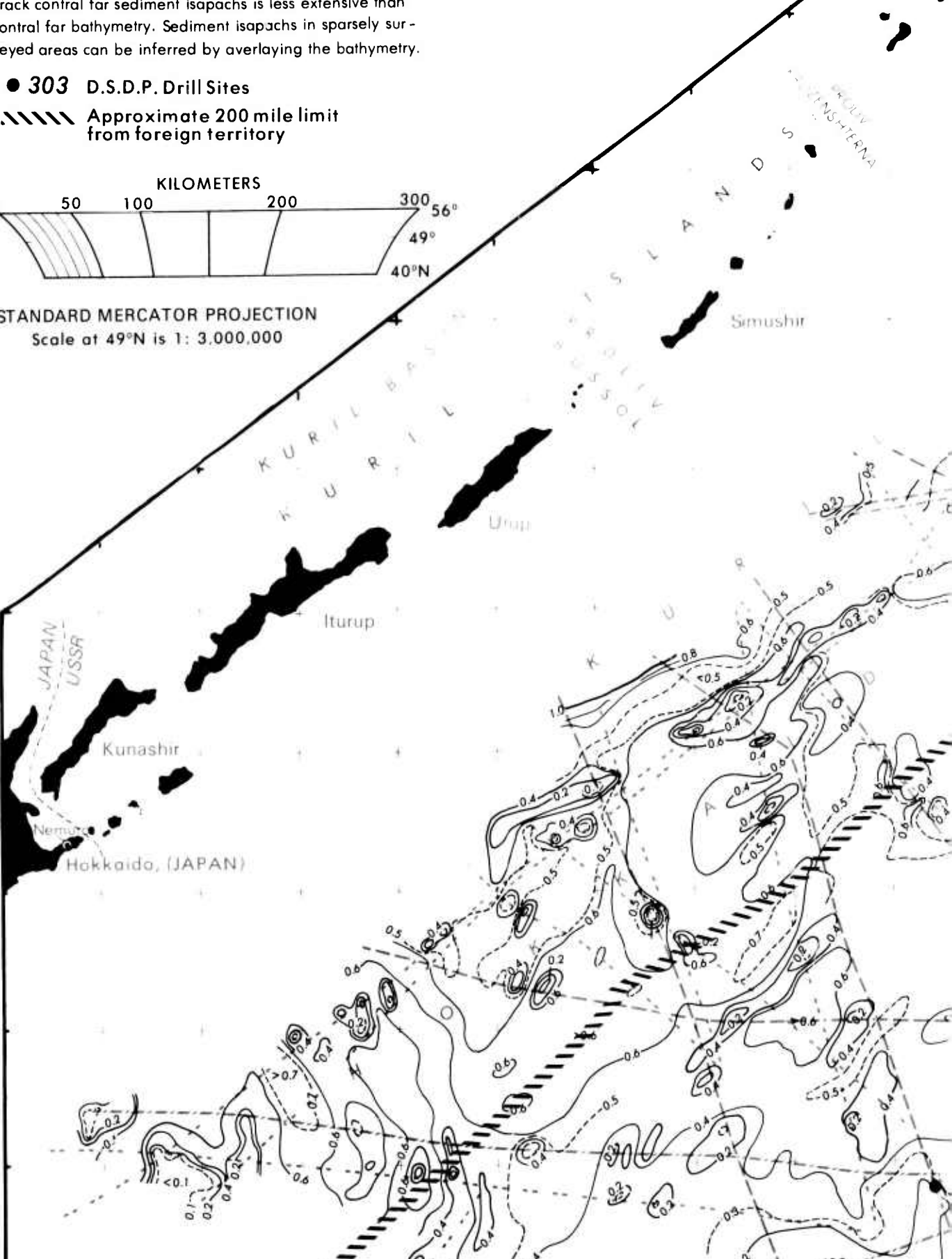
~~~~~ Approximate 200 mile limit from foreign territory

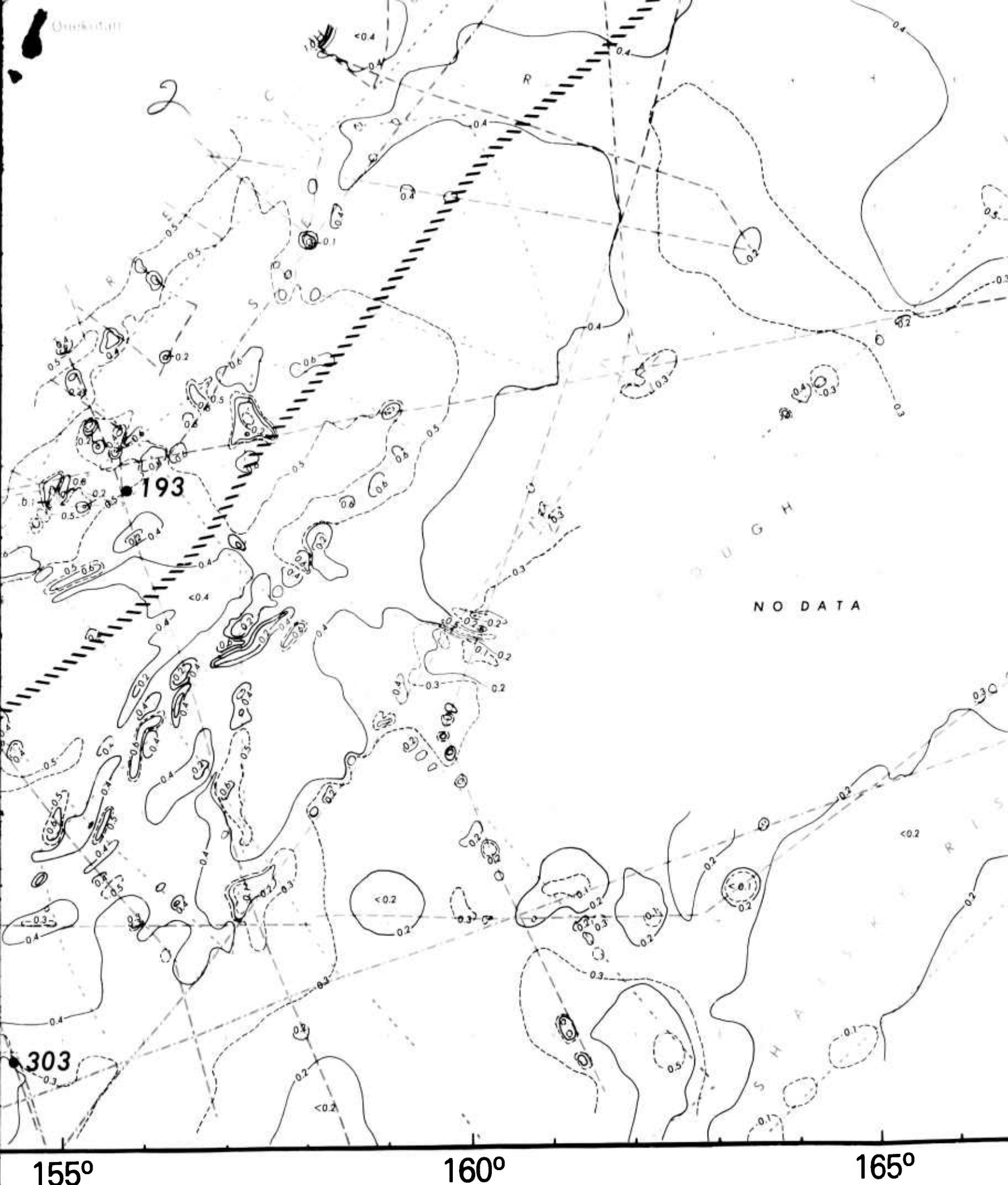


STANDARD MERCATOR PROJECTION  
Scale at 49°N is 1: 3,000,000

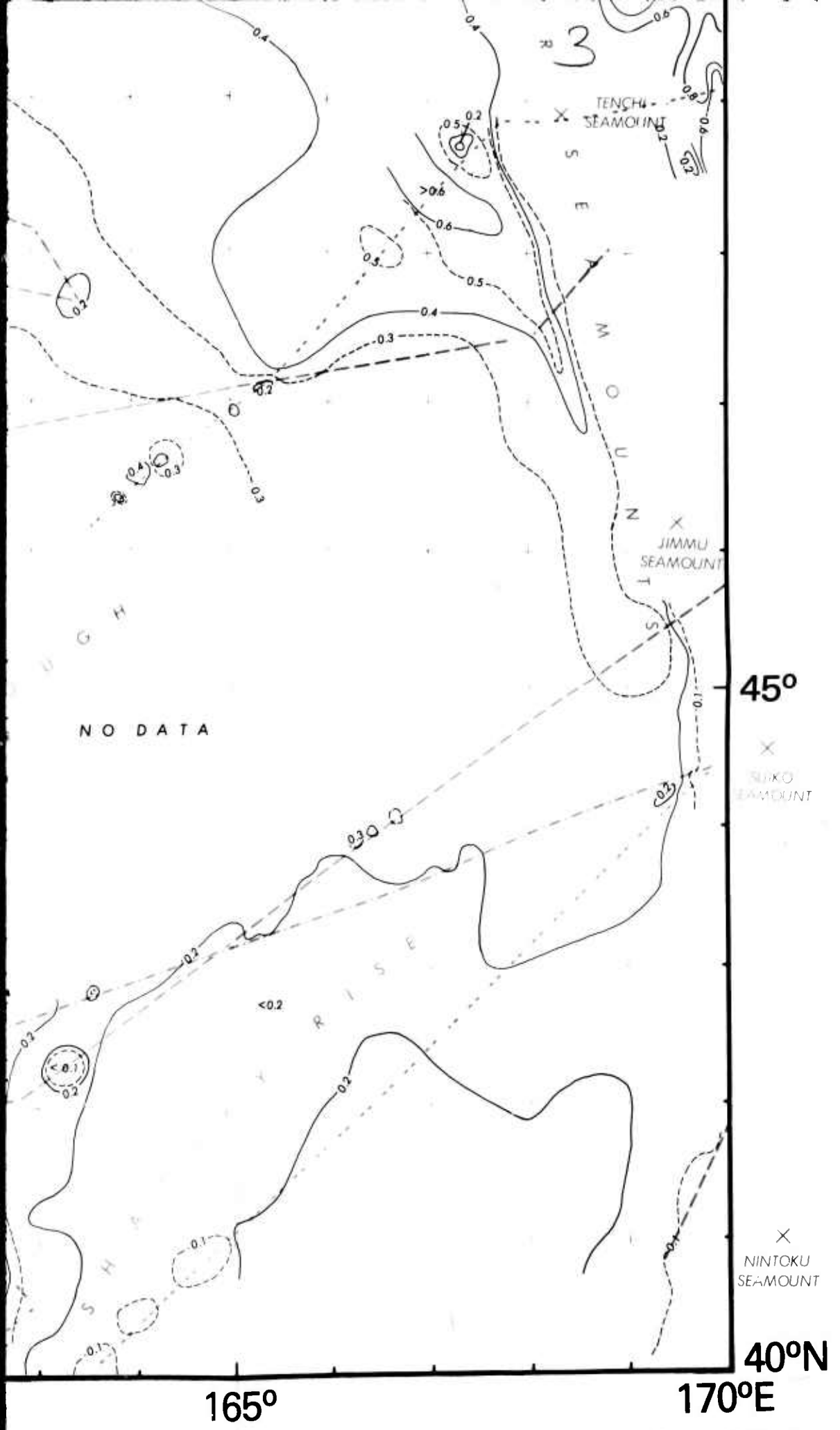
45°N

40°N 145°E 436 150°





5



# MAP II

# STRUCTURE CONTOUR MAP OF THE ACOUSTIC BASEMENT OF THE NORTHWEST PACIFIC OCEAN

55°N

Compiled by

James A. Green

Naval Ocean Research and Development Activity  
NSTL Station, Ms.

1980

Structure contours are measured in seconds of two-way travel time from continuous seismic reflection profiles and represent the depth from sea level to the upper opaque layer (Ewing et al., 1968) or to true basement.

## TRACKS

Track coverage includes all continuous seismic reflection profiles used to compile this map. Tracks are displayed according to the institute which collected the data.

- — Lamont-Doherty Geological Observatory  
Columbia University, Palisades, NY
- - - Naval Oceanographic Office, Bay St. Louis, MS.
- - - Scripps Institute of Oceanography, La Jolla, CA.
- - - Shirshov Institute of Oceanology, Moscow, USSR
- - - - United States Geological Survey, Menlo Park, CA.

## REFERENCES

- Ewing, J., M. Ewing, T. Aiken, and W.J. Ludwig (1968). North Pacific Sediment Layers Measured by Seismic Profiling. *American Geophys. Union Monograph* 12, p. 147-173.
- Houtz, R.E., and W.J. Ludwig (1979). Distribution of Reverberant Layers in the Southwest Pacific Basin. *Journal of Geophysical Res.*, vol. 84, no. B7, p. 3497-3504.
- Creager, J.S., D.W. Schall et al. (1973). Initial Reports of the Deep Sea Drilling Project. Vol 19, Washington, D.C. (U.S. Government Printing Office) p. 474.
- Larsen, R.L., R. Moberly, et al. (1975). Initial Reports of the Deep Sea Drilling Project. Vol. 32, Washington, D.C. (U.S. Government Printing Office) p. 25.

50°N

Depths from the bathymetry map added to the sediment isopach map thicknesses do not necessarily equal the structure contour depths since a more extensive data set was used to compile the bathymetry. Structure contours in sparsely surveyed areas can be inferred by overlaying the bathymetry.

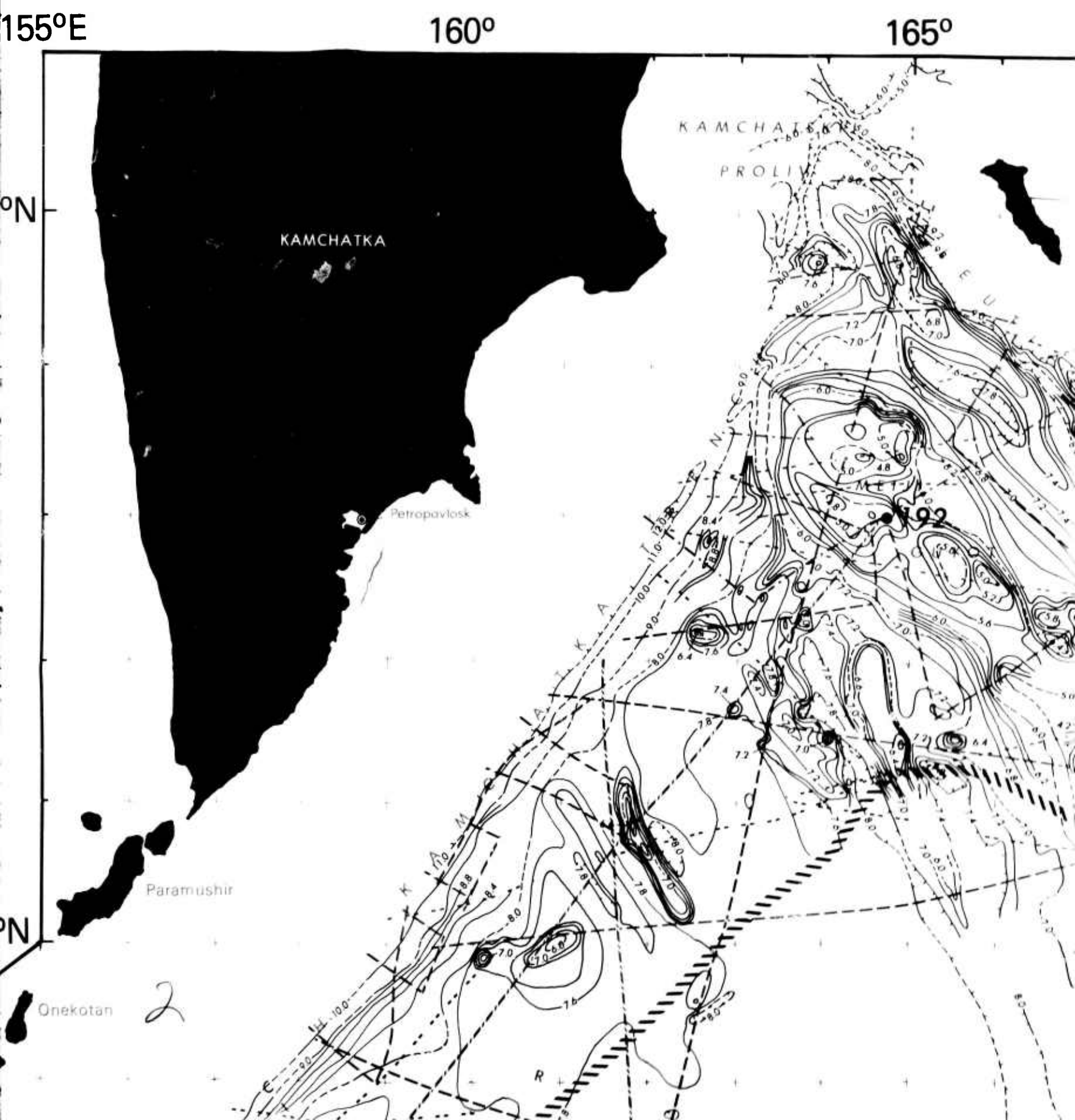
● 303 D.S.D.P. Drill Sites

VVVVV Approximate 200 mile limit  
from foreign territory

STANDARD MERCATOR PROJECTION

Scale at 49°N is 1: 3,000,000

KRUZENS  
PROF.

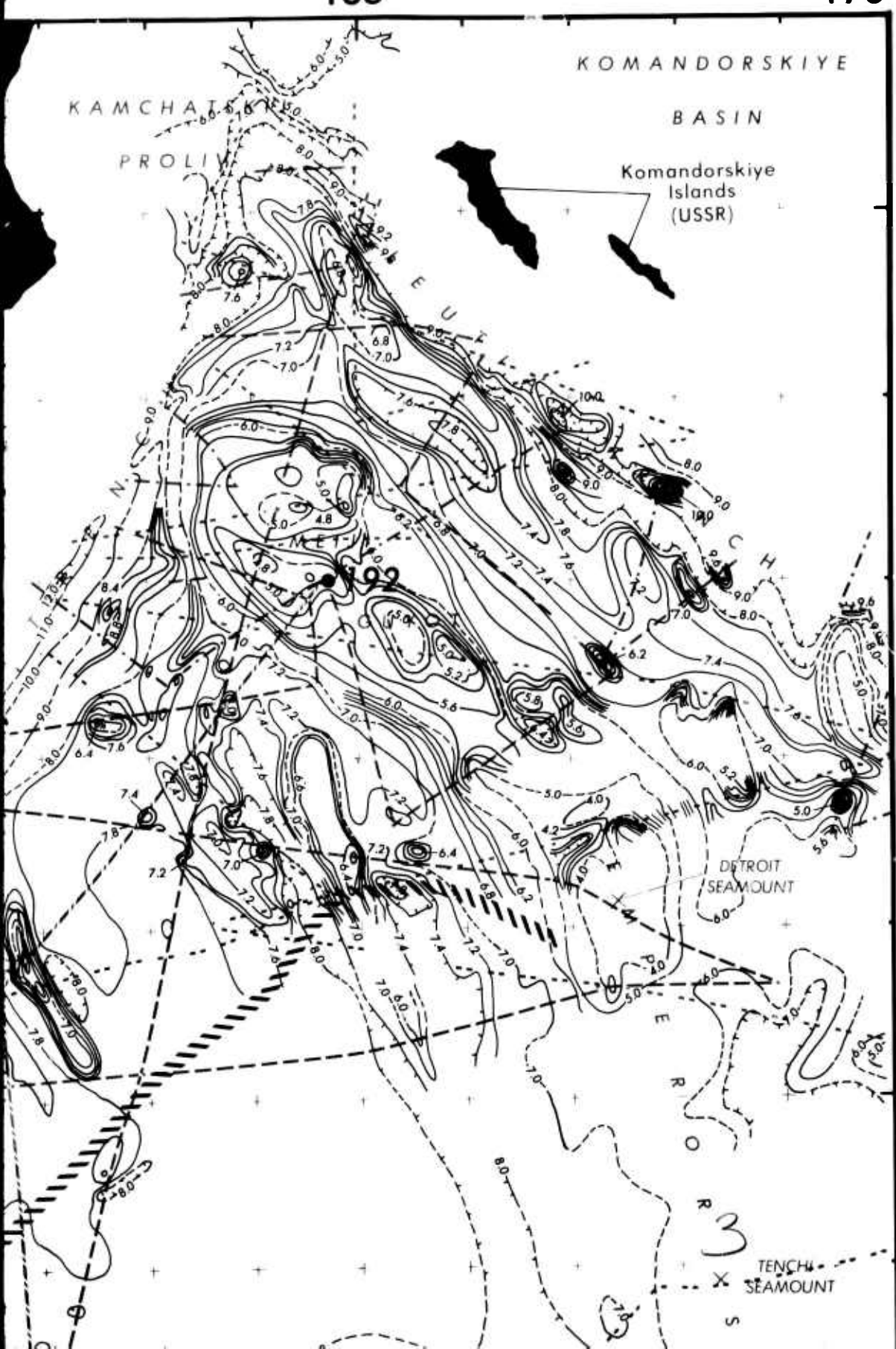


165°

170°E

55°N

50°



inferred by overlaying the barnymetry:

● 303 D.S.D.P. Drill Sites

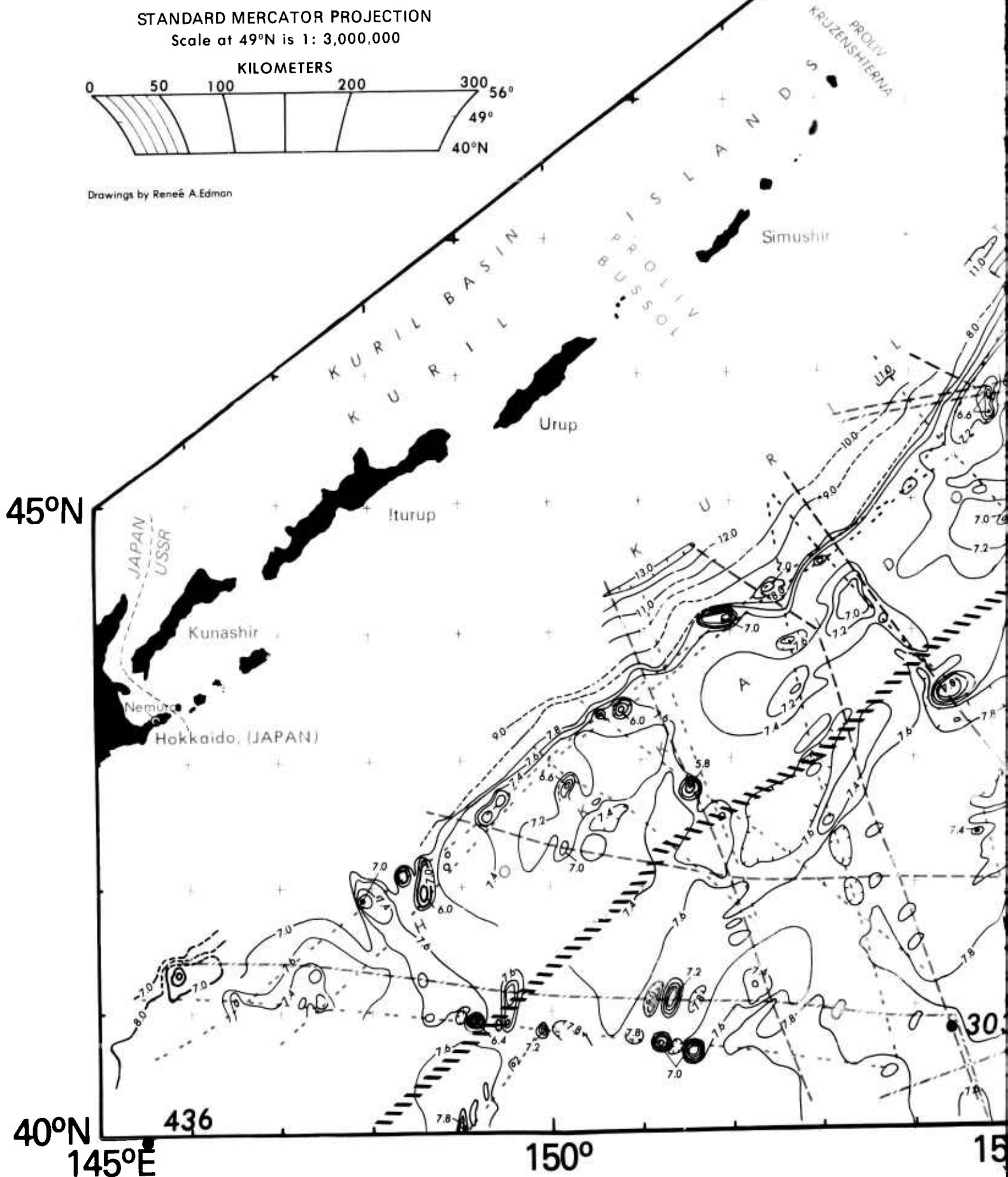
\\\\\\\\ Approximate 200 mile limit  
from foreign territory

## STANDARD MERCATOR PROJECTION

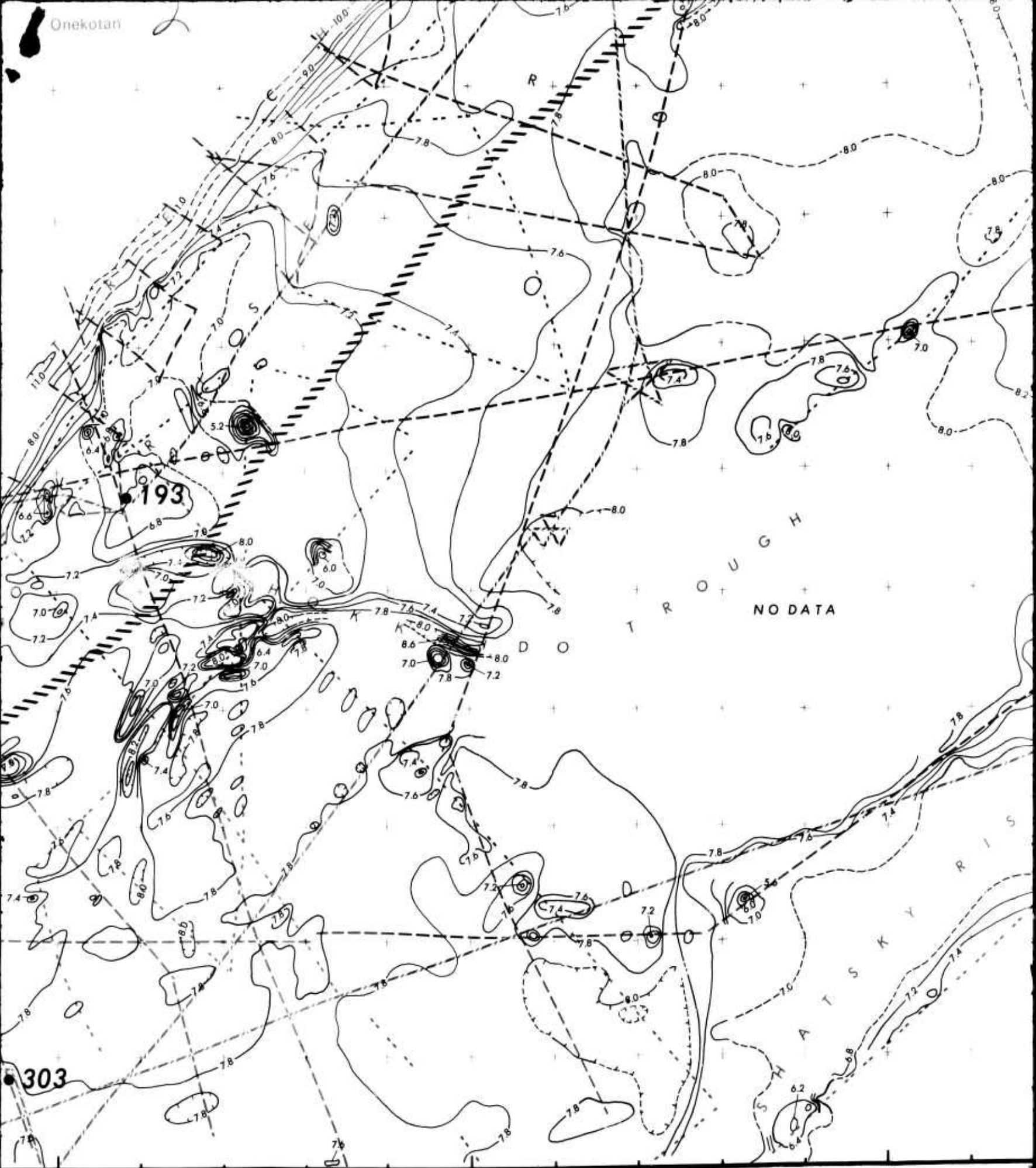
Scale at 49°N is 1: 3,000,000

## KILOMETERS

Drawings by Renée A. Edman



Onekotan

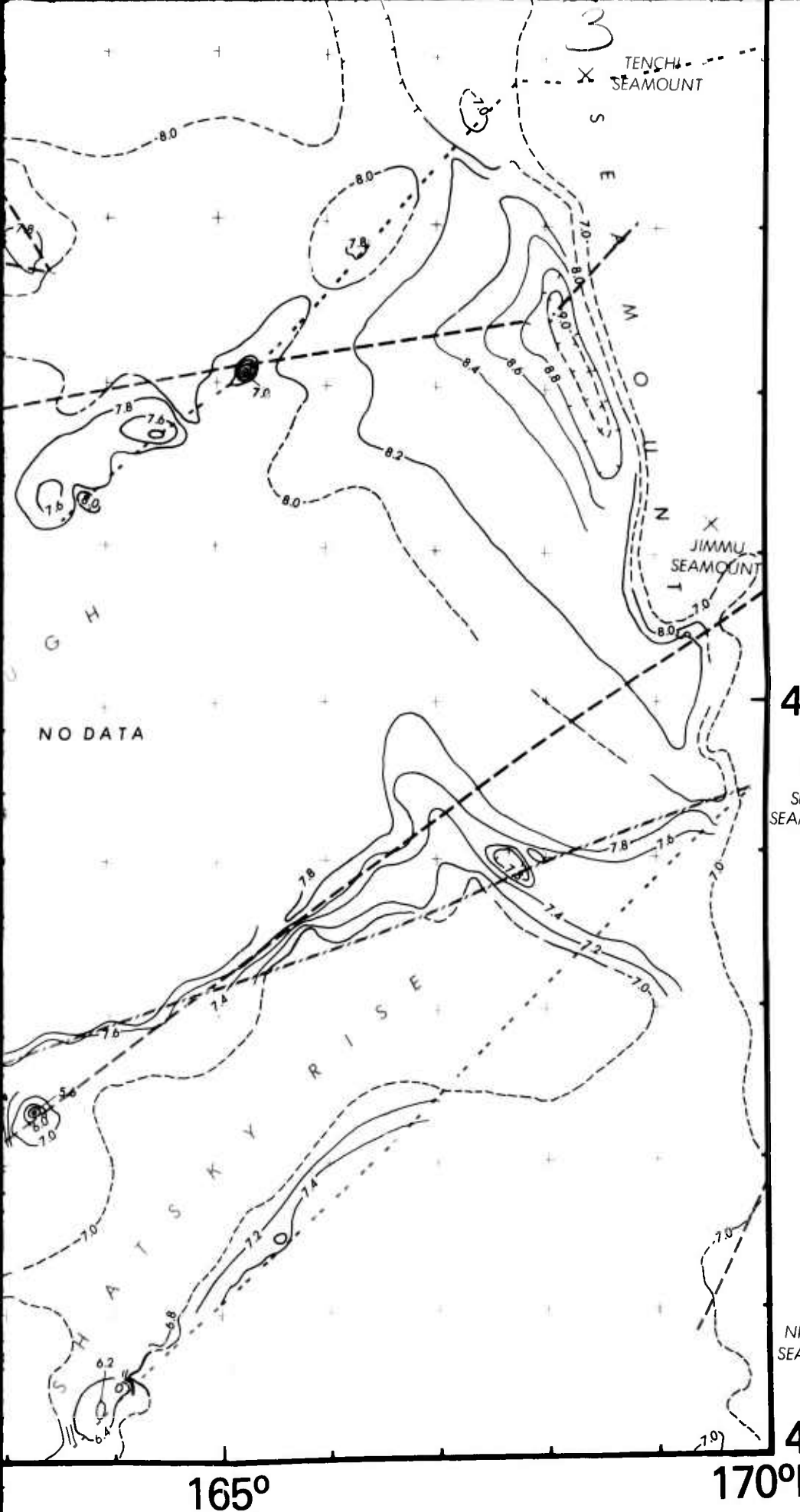


155°

160°

165°

5



165° 170°

45°

40°N

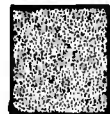
MAP III

# BOTTOM ROUGHNESS OF THE NORTHWEST PACIFIC OCEAN

Compiled by

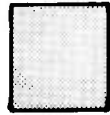
James A. Green  
Naval Ocean Research and Development Activity  
NSTL Station, Ms.  
1980

55°N



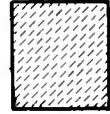
Smooth

Relief less than 200 meters in a 20KM span  
and/or slopes less than 3-4°



Intermediate

Intermediate relief and slopes of 3-10°



Rough

Relief greater than 200 meters in a 20KM span  
and/or slopes greater than 6-10°

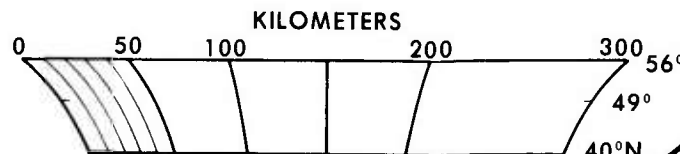
Roughness is based mainly upon digitized continuous seismic reflection profiles of the water/sediment interface. The bathymetry map is used to delineate rough areas where no seismic profiles exist.

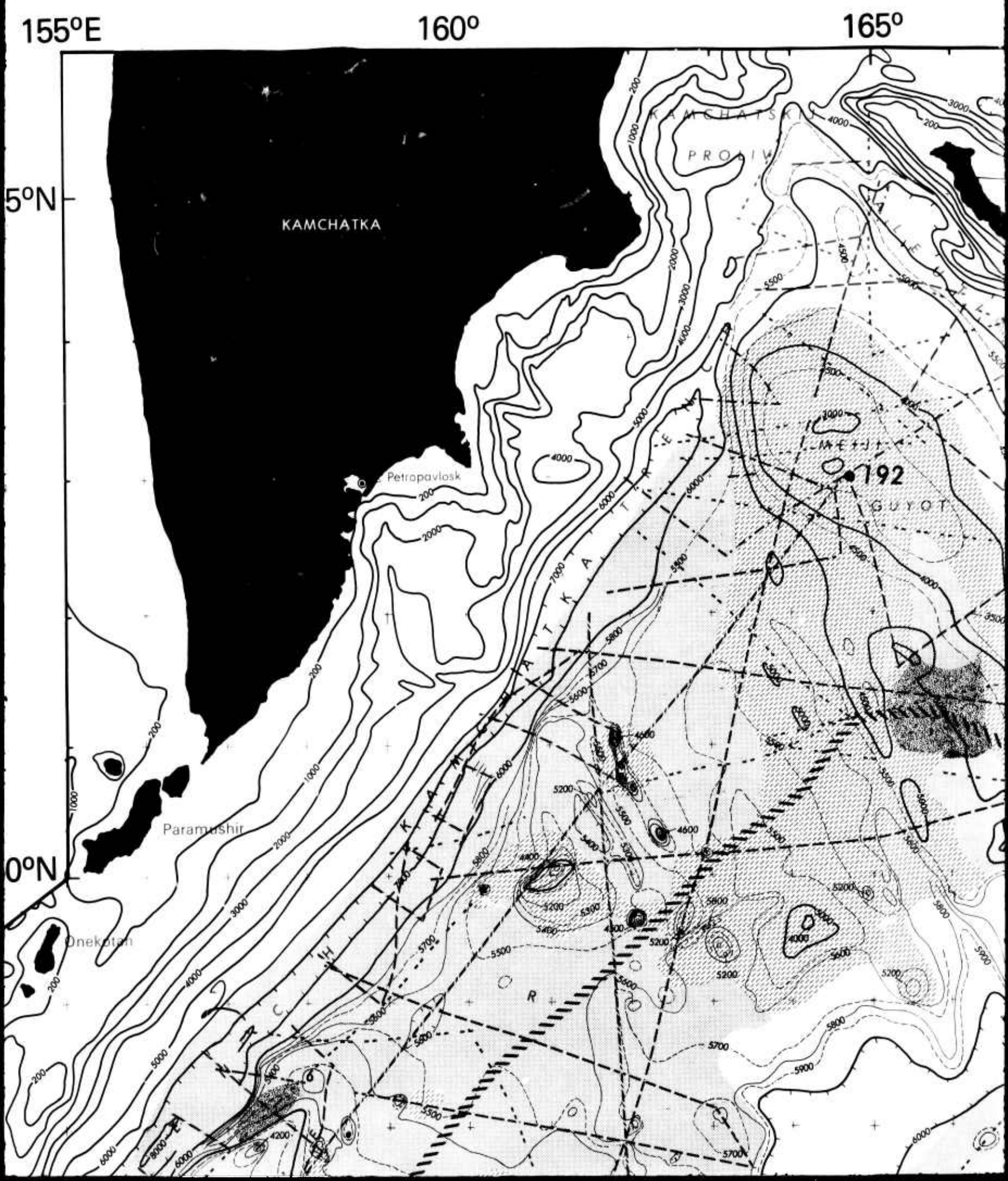
Overlays include:

1. Track coverage of continuous seismic reflection profiles.
2. Bathymetry map.

50°N

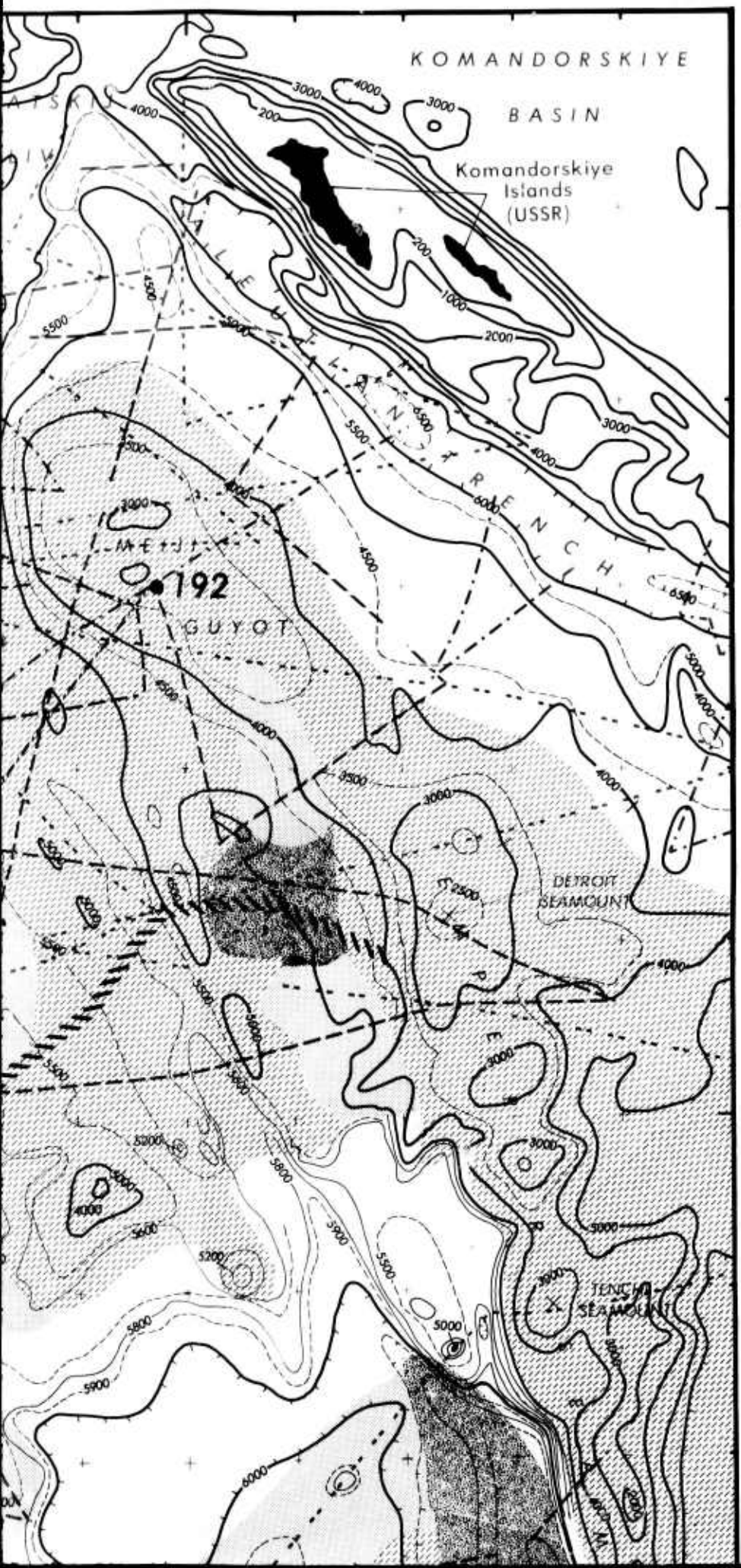
STANDARD MERCATOR PROJECTION  
Scale at 49°N is 1: 3,000,000





165°

170°E



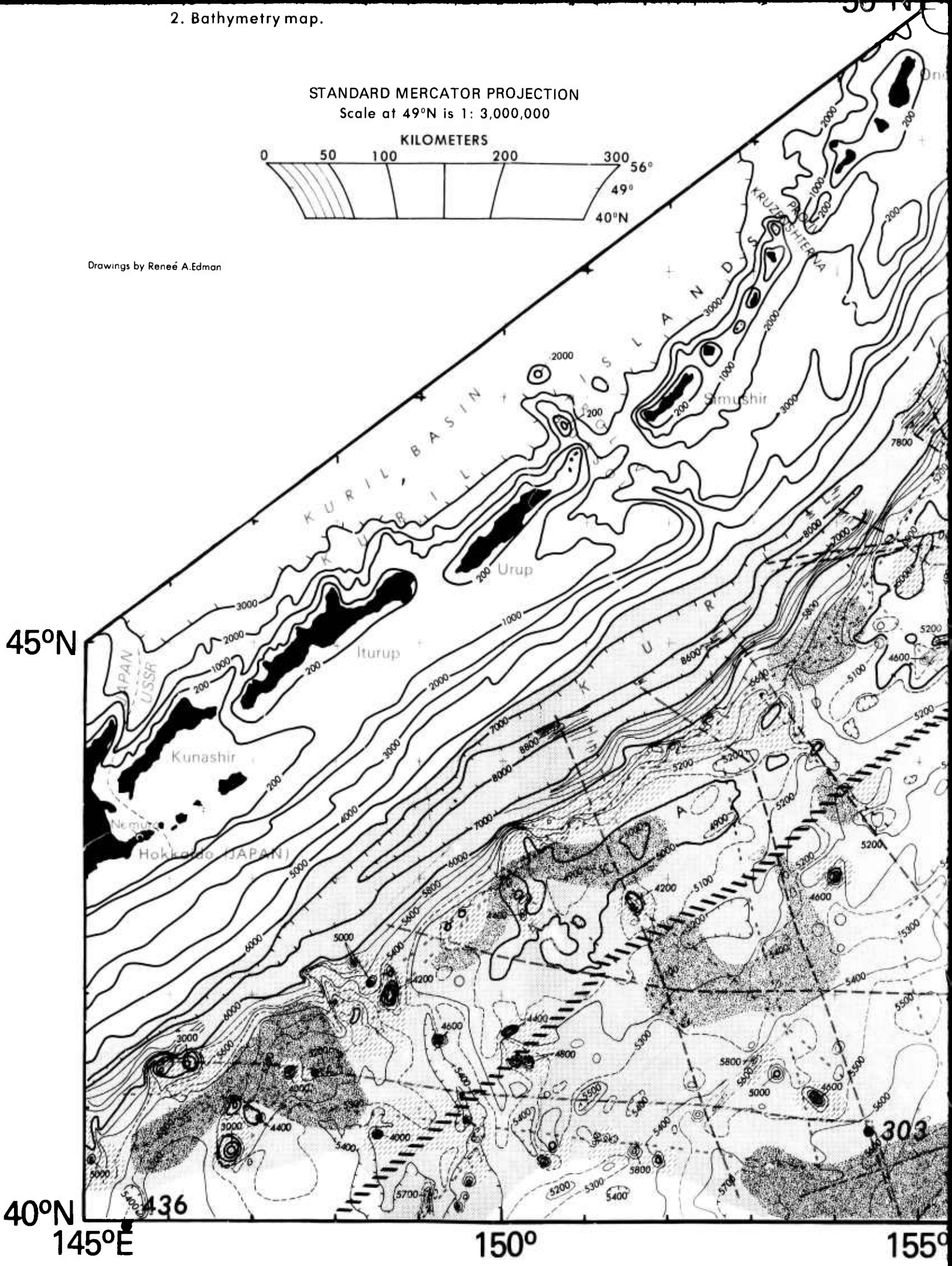
## 2. Bathymetry map.

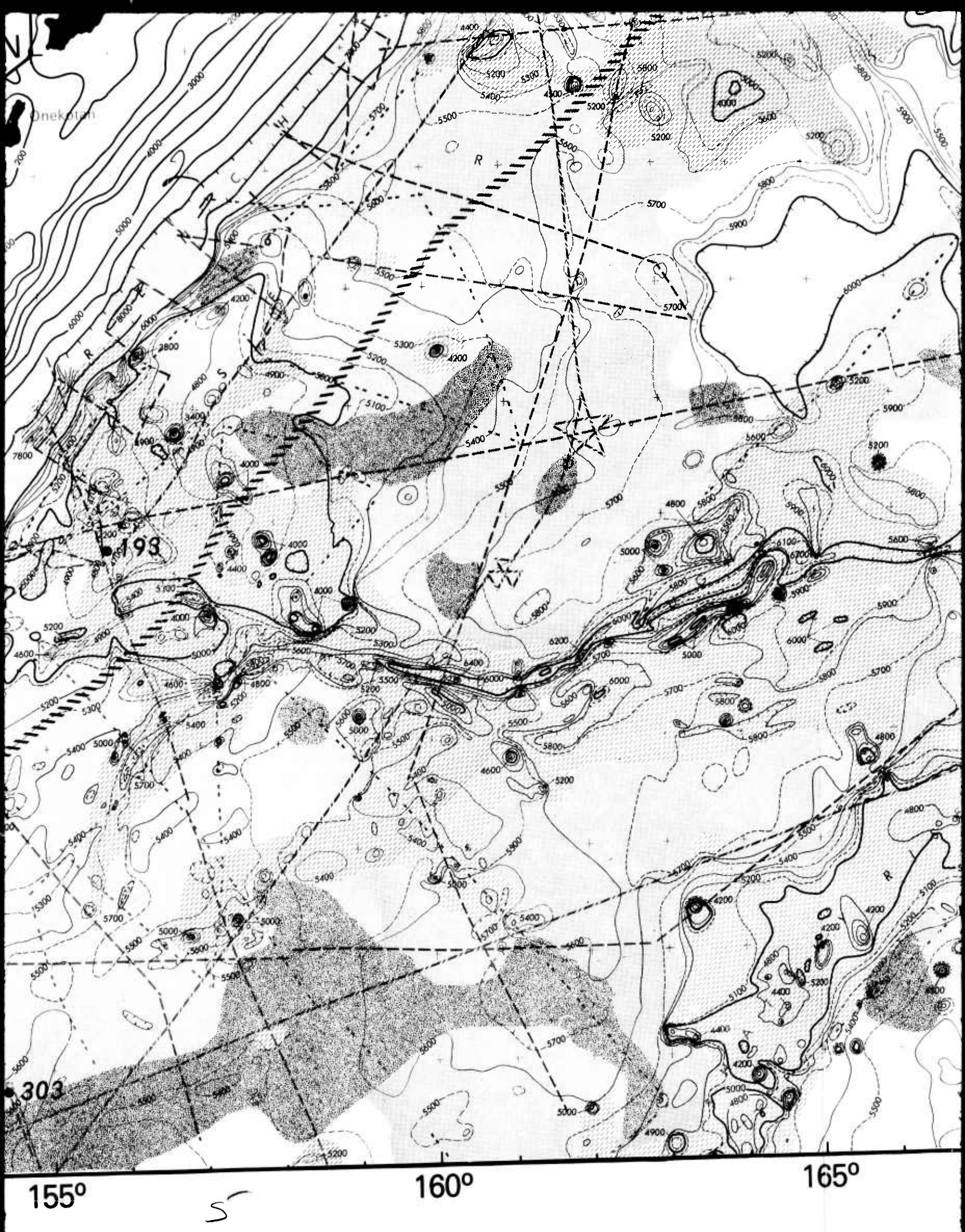
## STANDARD MERCATOR PROJECTION

Scale at 49°N is 1: 3,000,000

## KILOMETERS

Drawings by Renée A. Edman







50°

45°

X  
SUIKO  
SEAMOUNT

X  
NINTOKU  
SEAMOUNT

40°N

165°

170°E

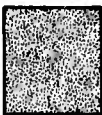
MAP IV

# ROUGHNESS OF ACOUSTIC BASEMENT OF THE NORTHWEST PACIFIC OCEAN

Compiled by

**James A. Green**  
Naval Ocean Research and Development Activity  
NSTL Station, Ms.  
1980

55°N



Smooth

Relief less than 200 meters in a 20 KM span  
and/or slopes less than 3-4°



Intermediate

Intermediate relief and slopes of 3-10°



Rough

Relief greater than 200 meters in a 20KM span  
and/or slopes greater than 6-10°

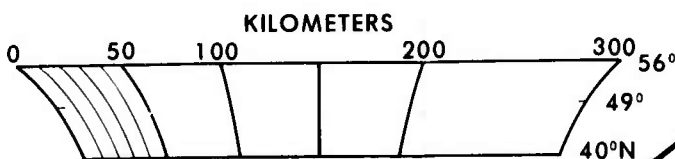
Roughness is based mainly upon digitized continuous seismic reflection profiles of the sediment/acoustic basement interface. The bathymetry map is used to delineate rough areas of suspected basement outcrop in areas where no seismic profiles exist.

Overlays include:

1. Track coverage of continuous seismic reflection profiles.
2. Depth to Acoustic Basement.

50°N

STANDARD MERCATOR PROJECTION  
Scale at 49°N is 1: 3,000,000

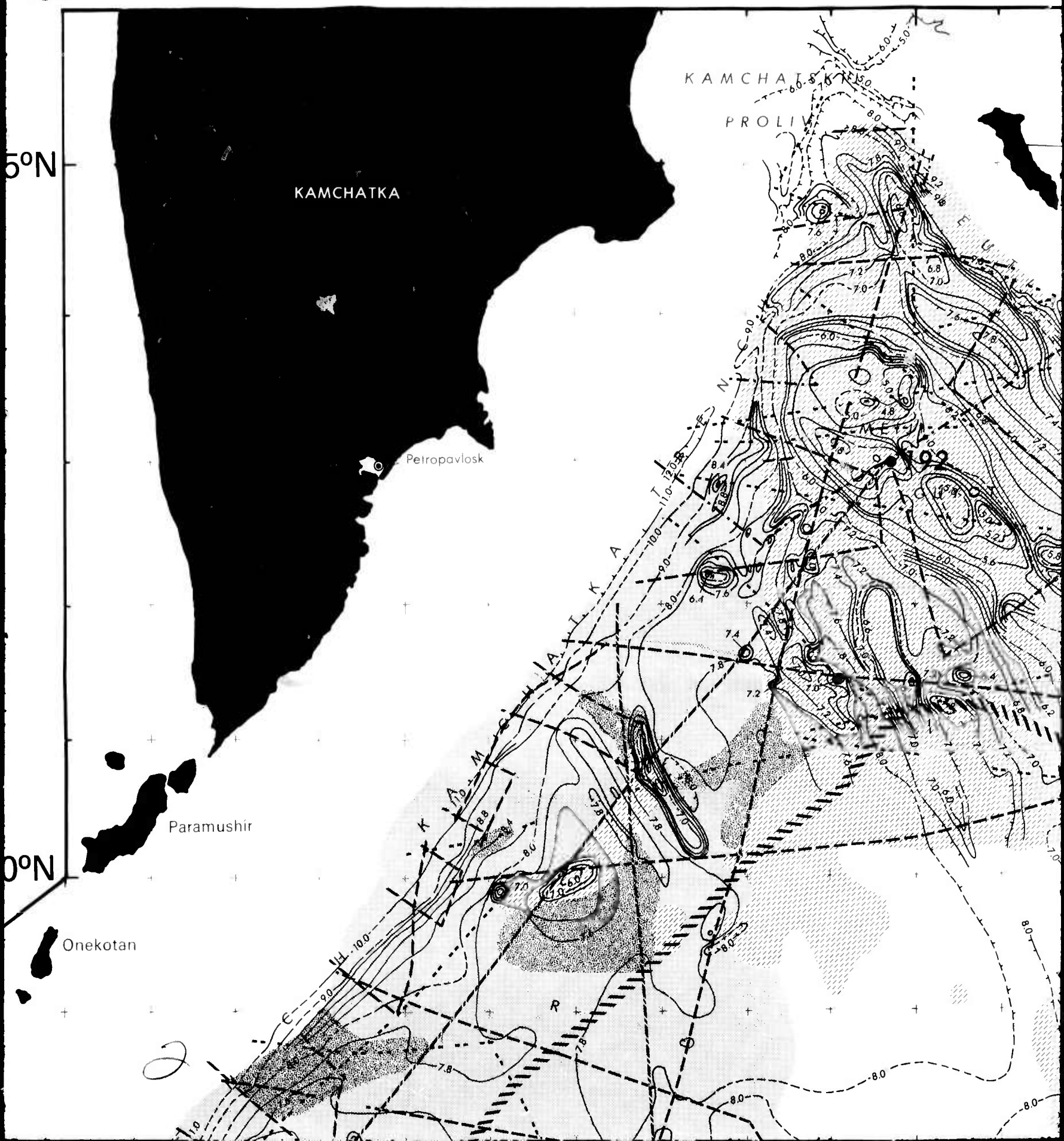


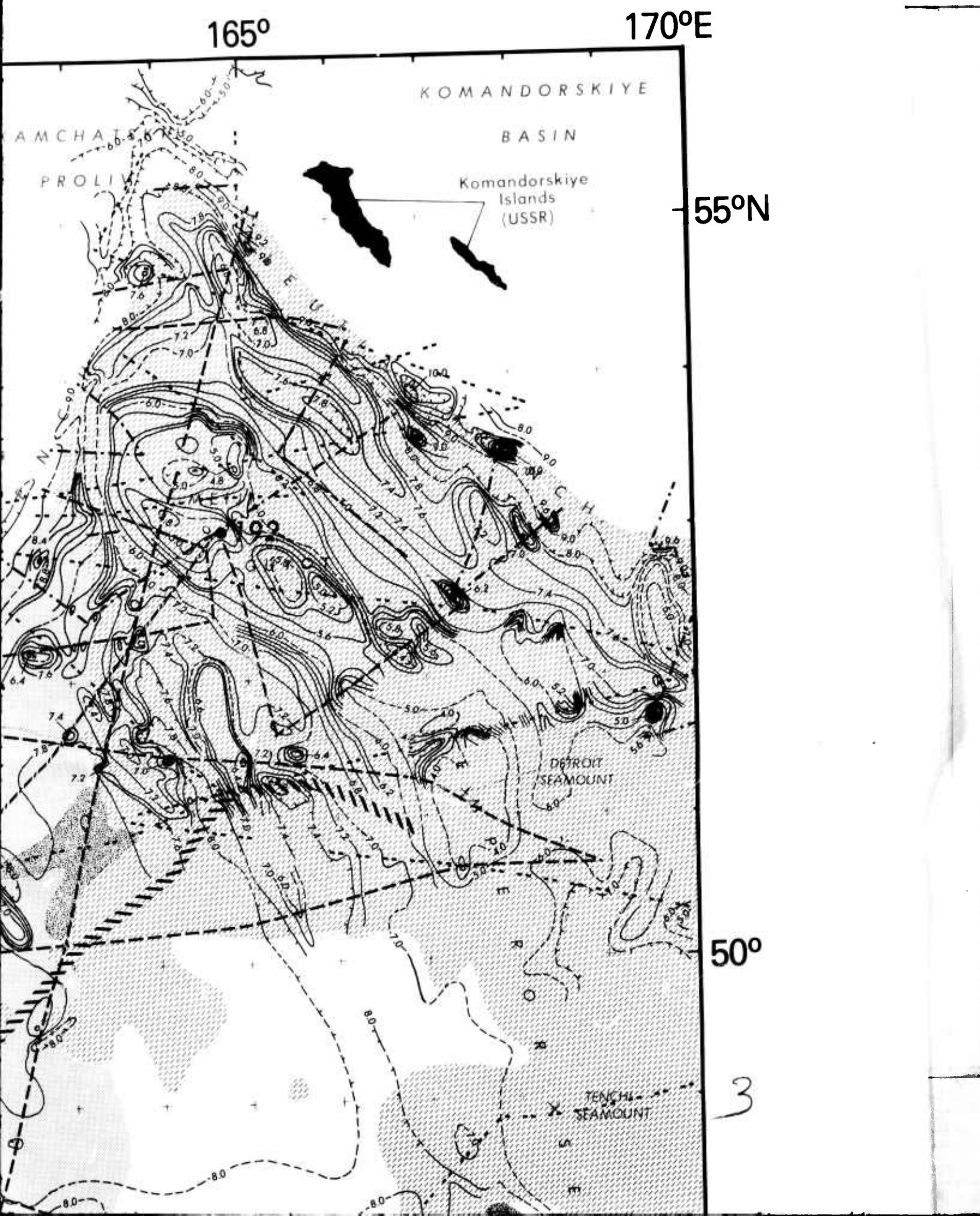
PROLIV  
KRUZENSHTERN  
S

155°E

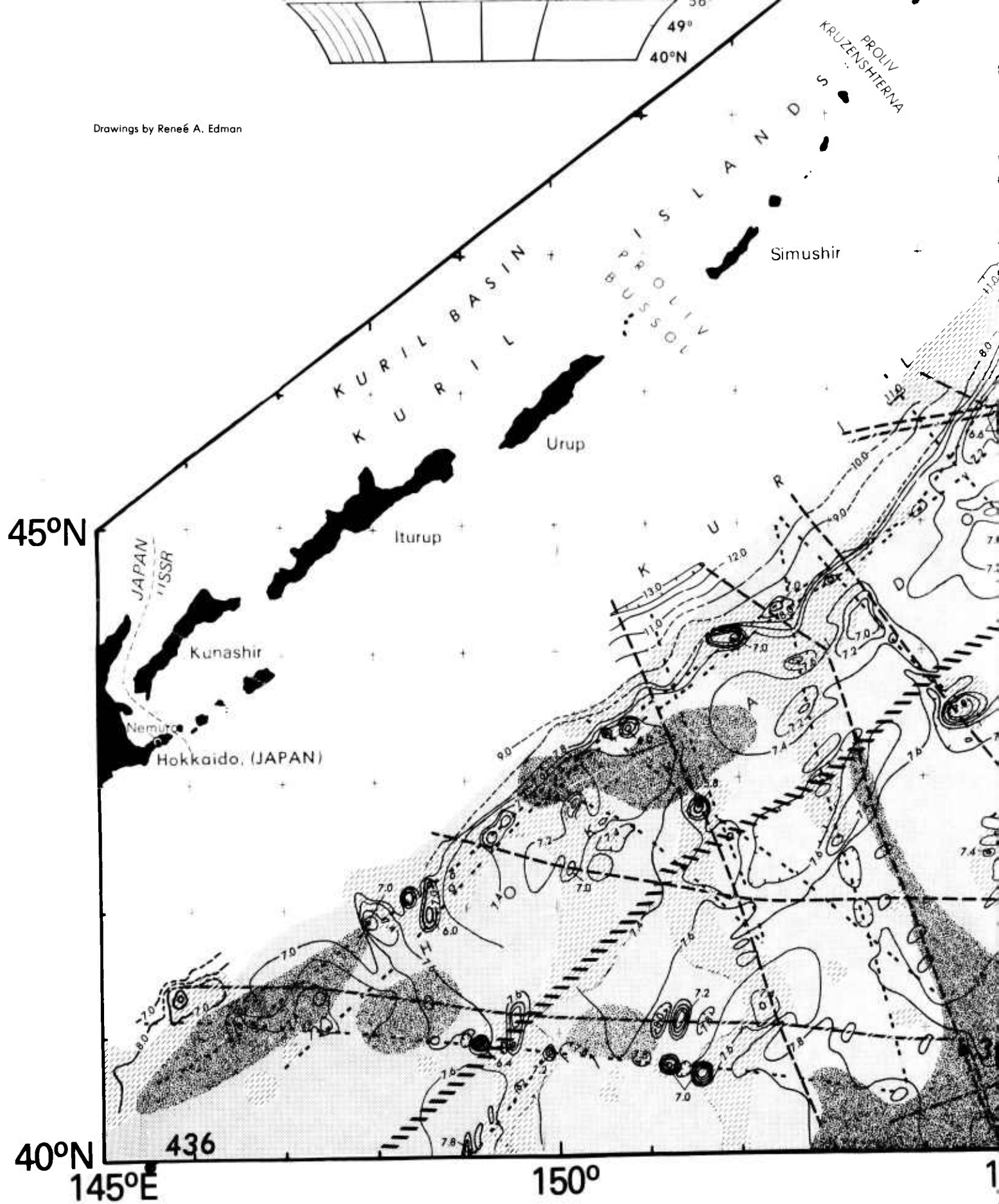
160°

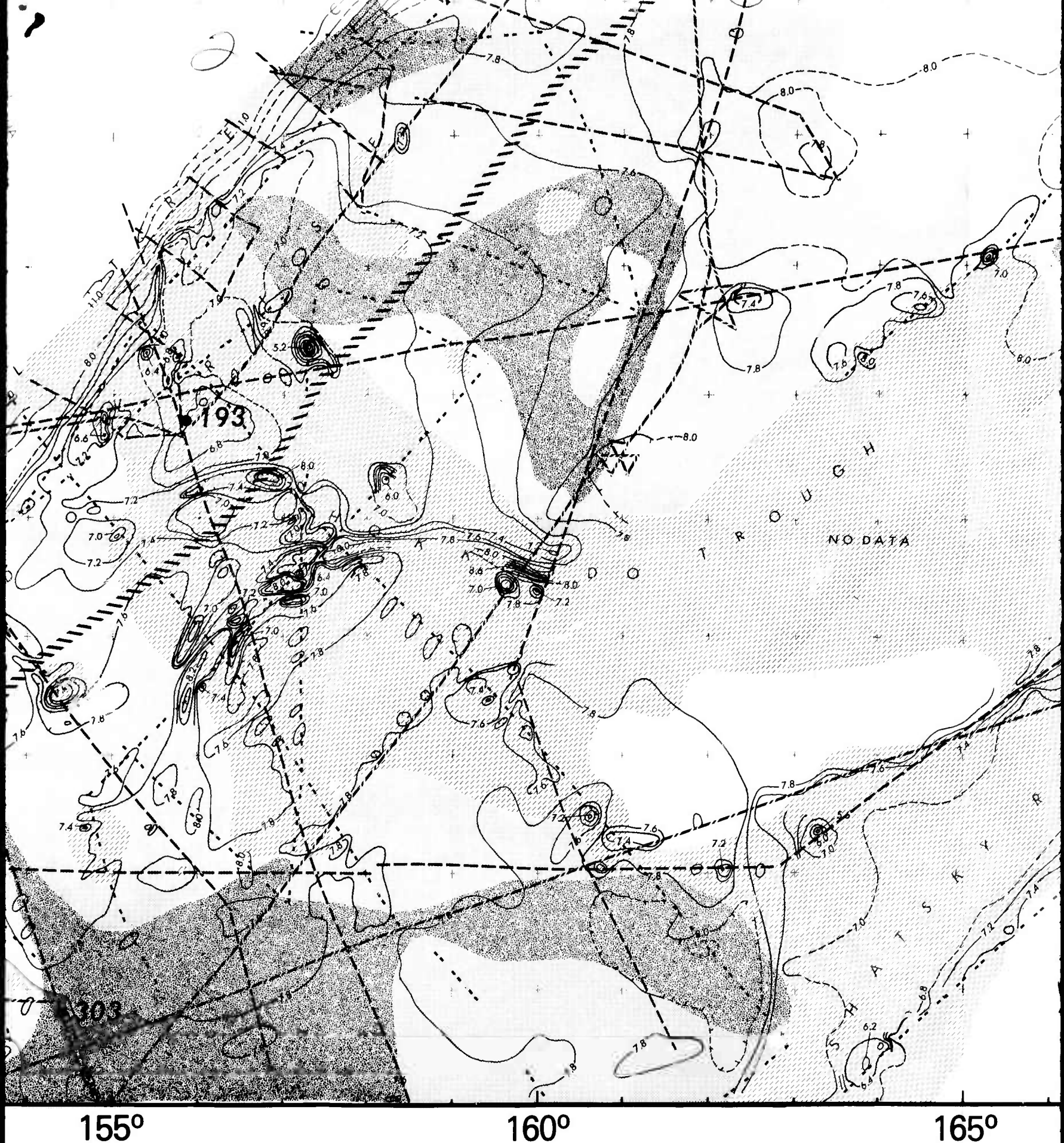
165°



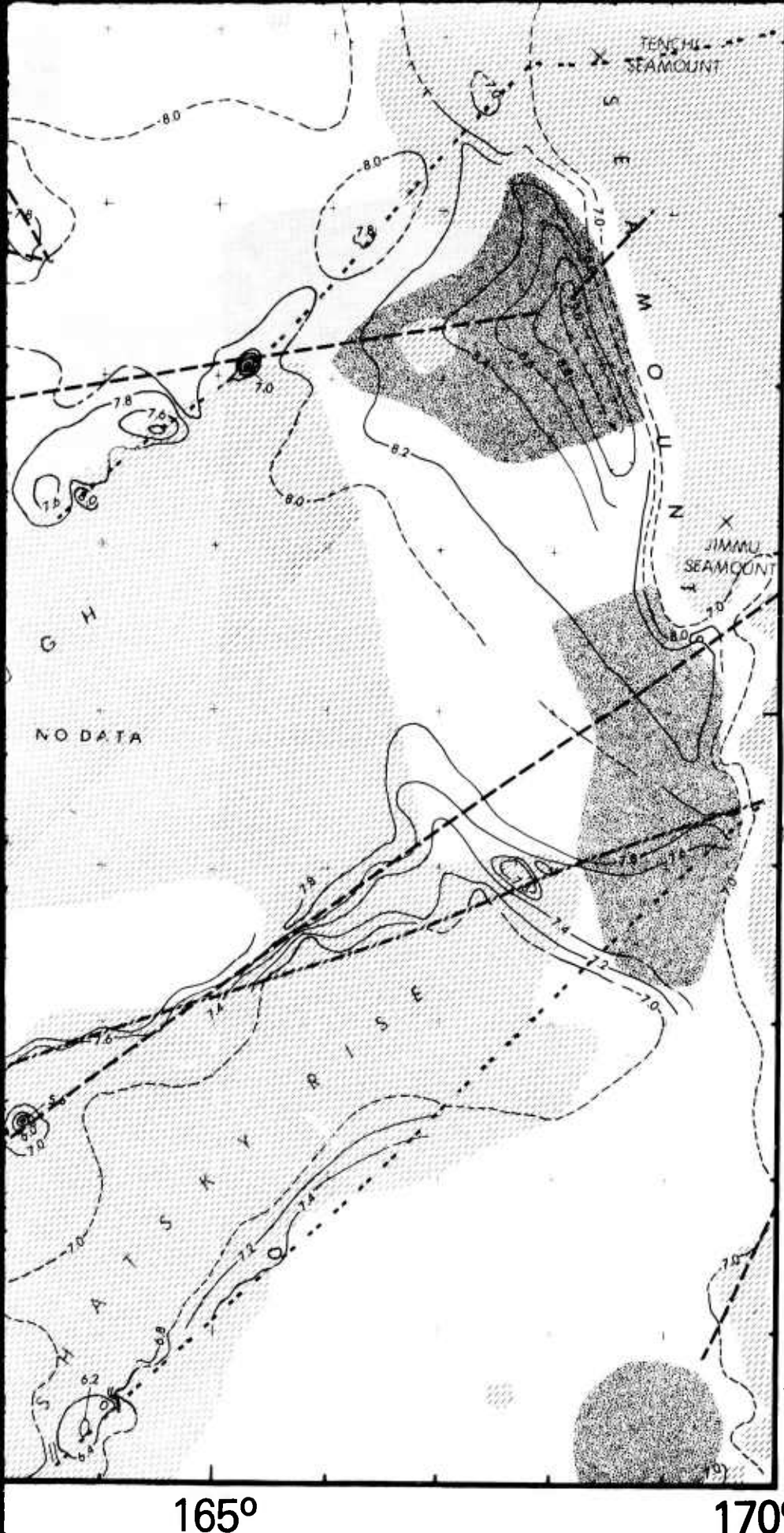


Drawings by Renée A. Edman





5-



**MAP V**

6

155°E

35°N

SEDIMENT ISOPACH, BOTTOM ROUGHNESS,  
AND  
BATHYMETRY  
ON THE  
NORTHWEST PACIFIC OCEAN

by

James A. Groot

Naval Ocean Research and Development Activity  
San Diego, Calif.

1960

BATHYMETRY ISOSURFACES.

46-maps-of-individual-isopachs-for-1000 fms.

STANDARD MERCATOR PROJECTION  
Scale in miles 1:1,000,000

KILOMETERS



160°

165°

KOMANDO

KAMCHATKA

Petropavlovsk

Paramushir

KAMCHATSKIJ

PROLIV

BAS

Komandor  
Islands  
(USSR)

192



65°

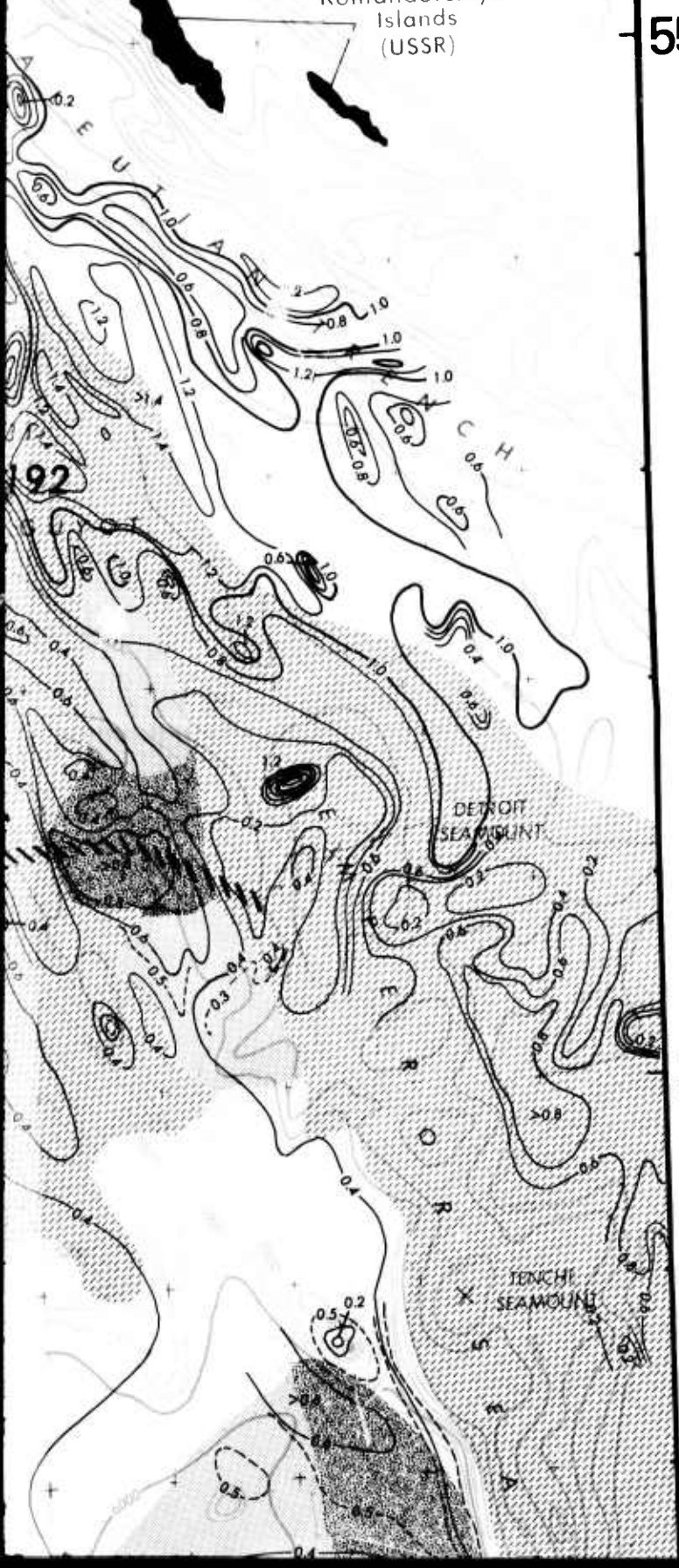
170°E

KOMANDORSKIYE

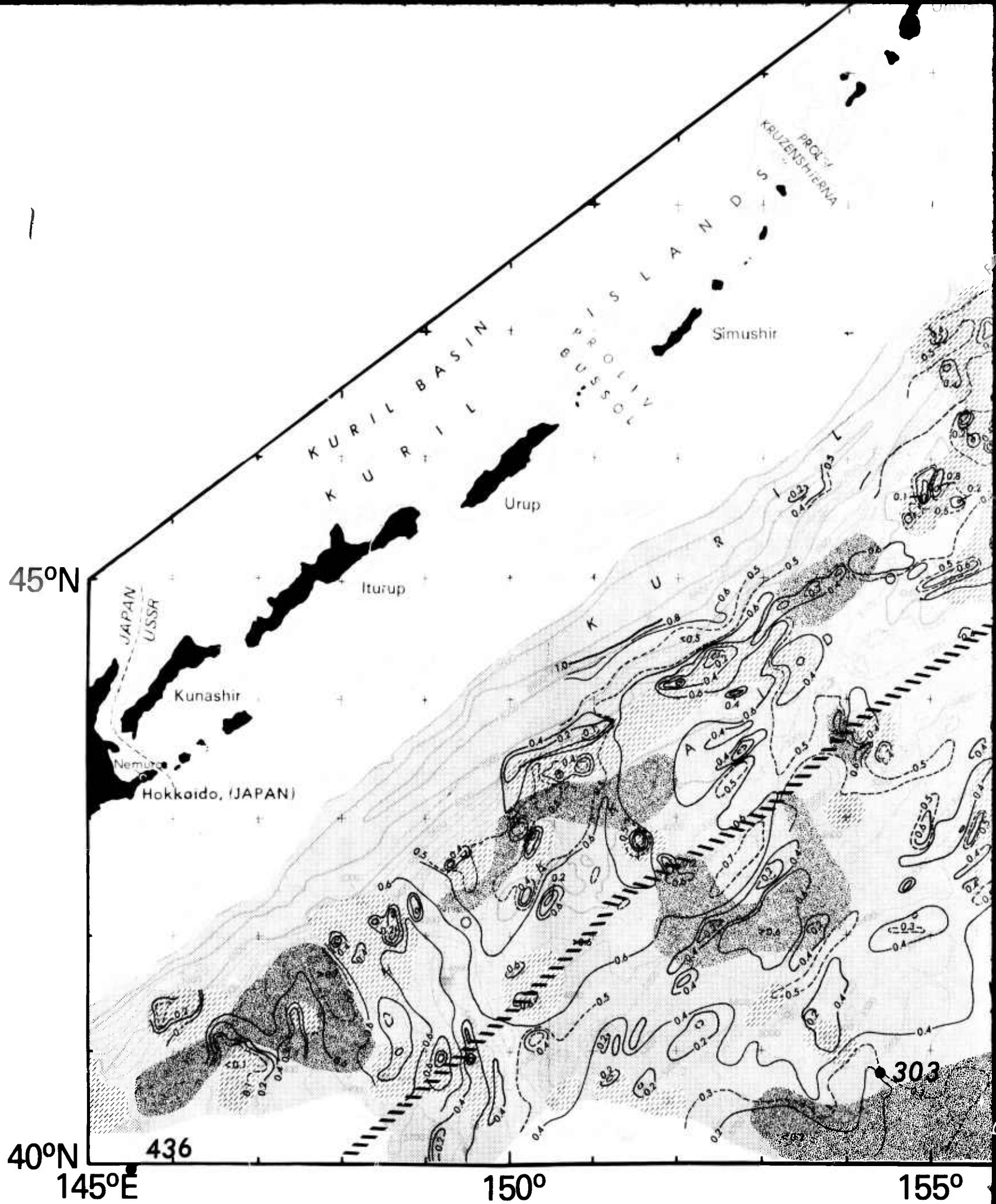
BASIN

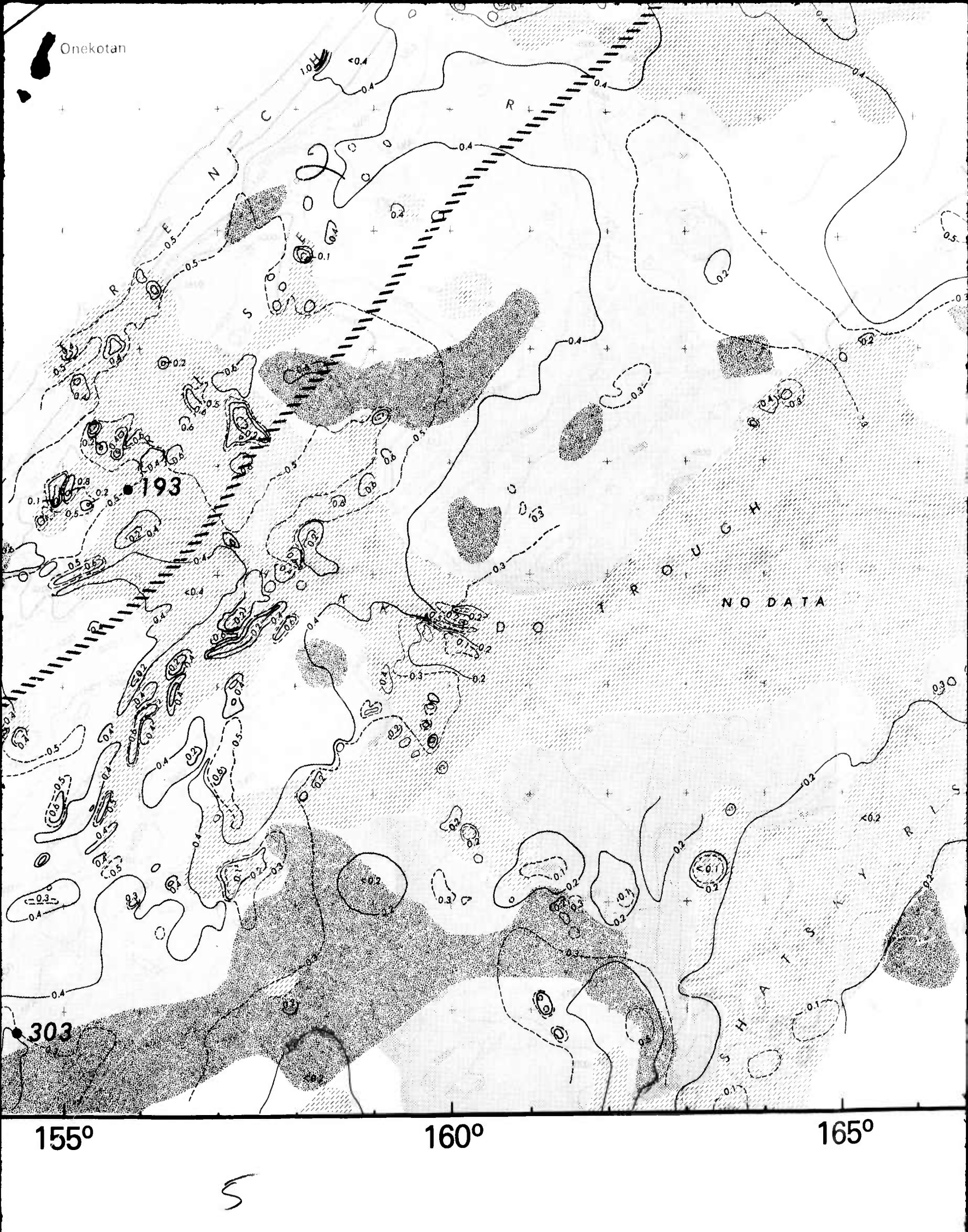
Komandorskiye  
Islands  
(USSR)

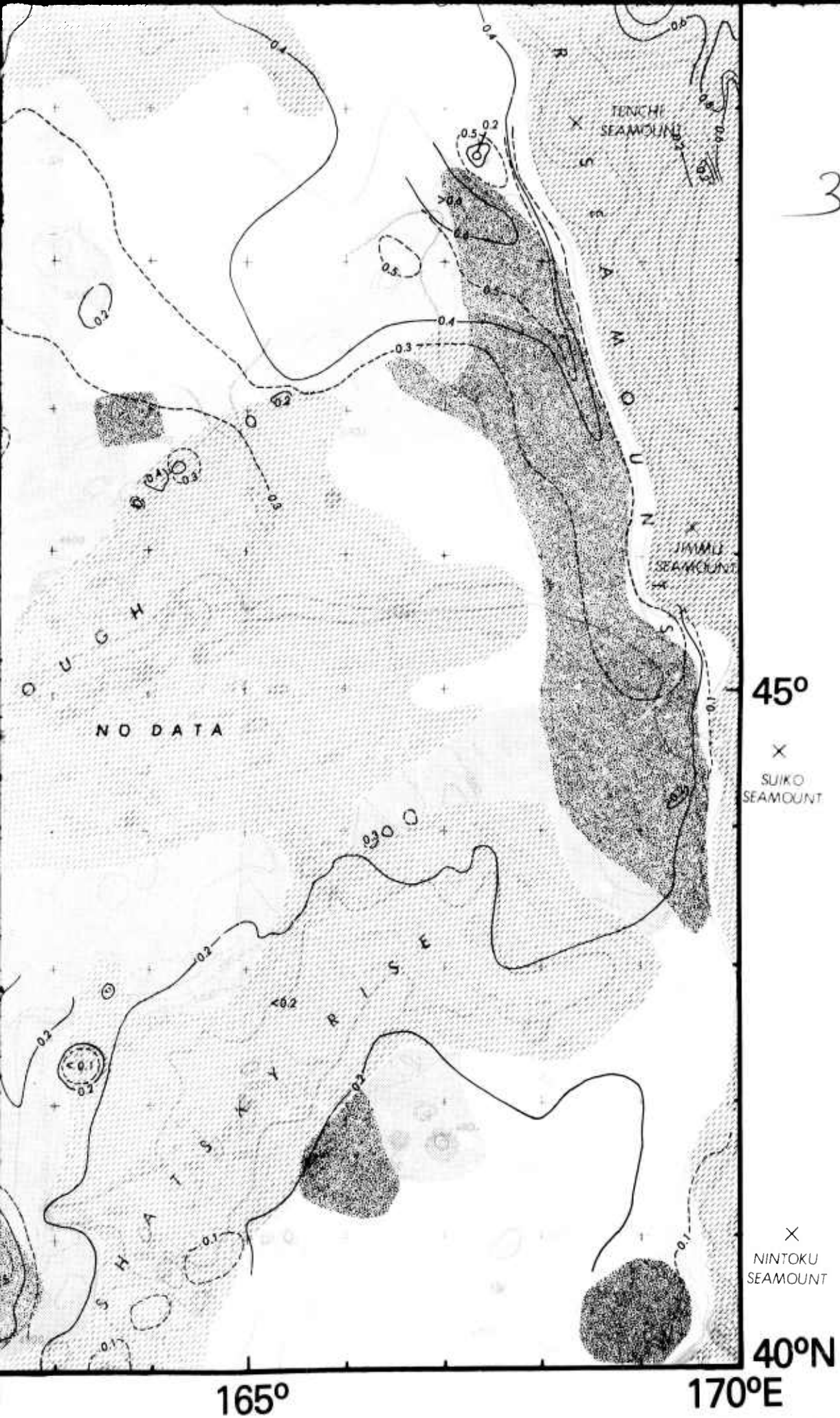
55°N



50°







6 MAP VI

# STRUCTURE CONTOUR MAP OF THE ACOUSTIC BASEMENT AND BATHYMETRY OF THE NORTHWEST PACIFIC OCEAN

Compiled by

James A. Green

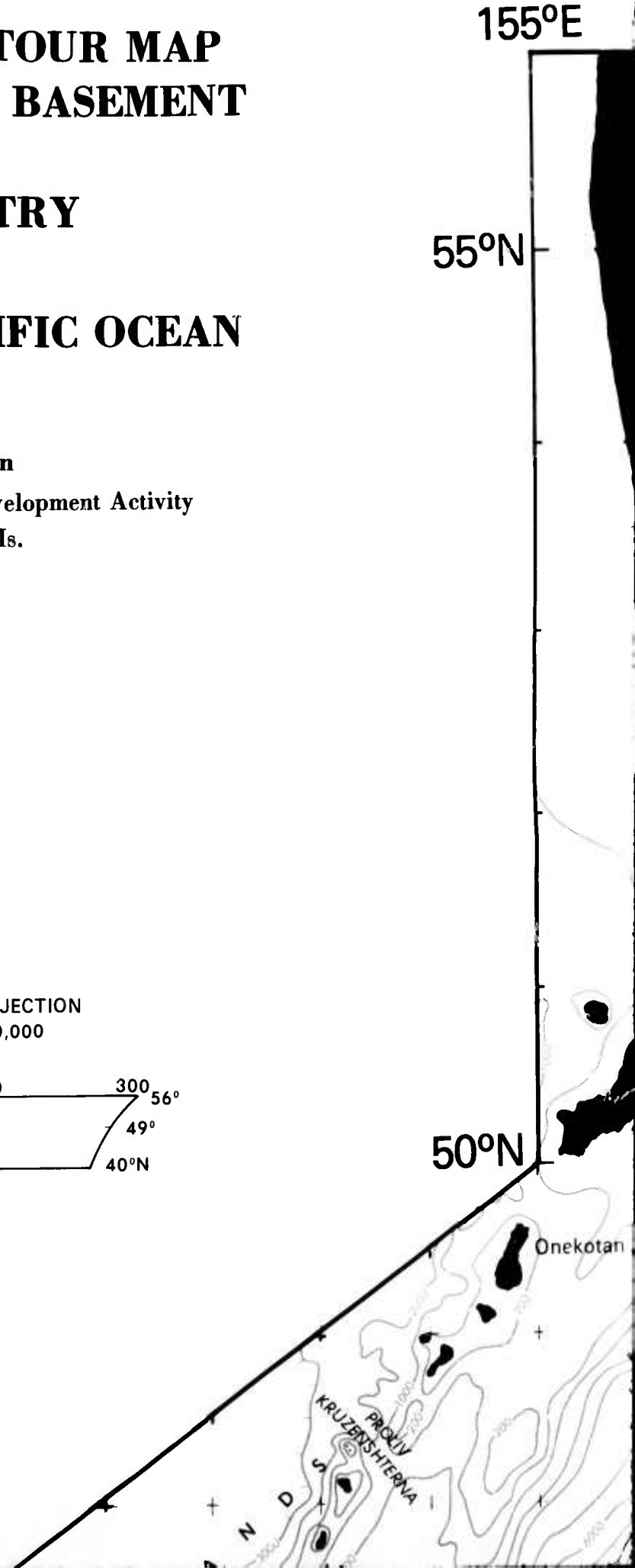
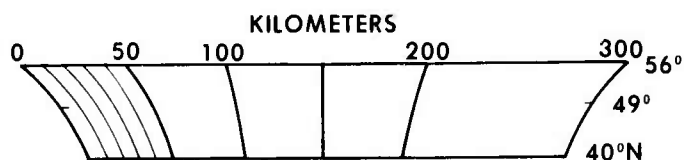
Naval Ocean Research and Development Activity  
NSTL Station, Ms.

1980

Bathymetry is screened.

See maps of individual subjects for legends.

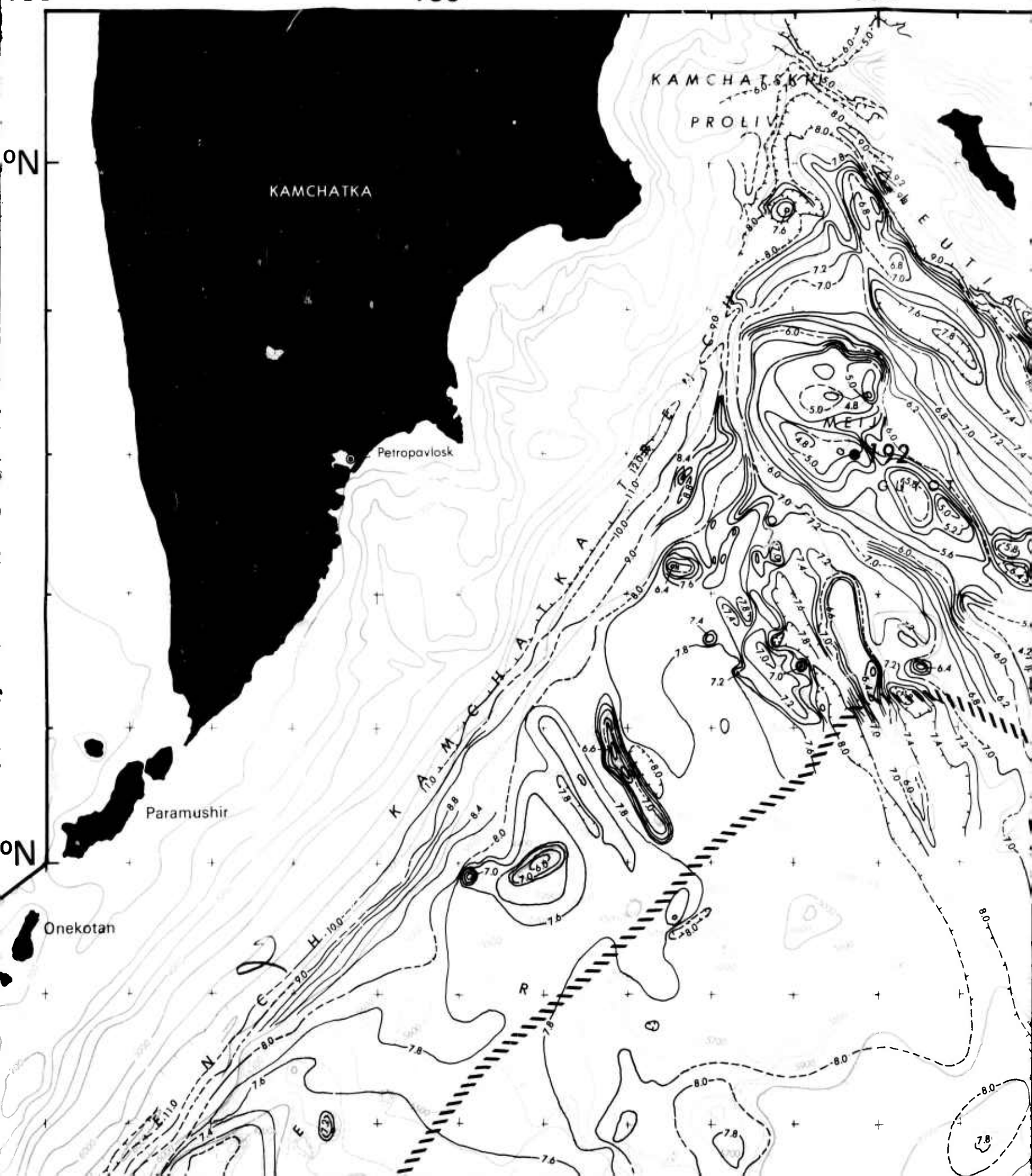
STANDARD MERCATOR PROJECTION  
Scale at 49°N is 1: 3,000,000



155°E

160°

165°



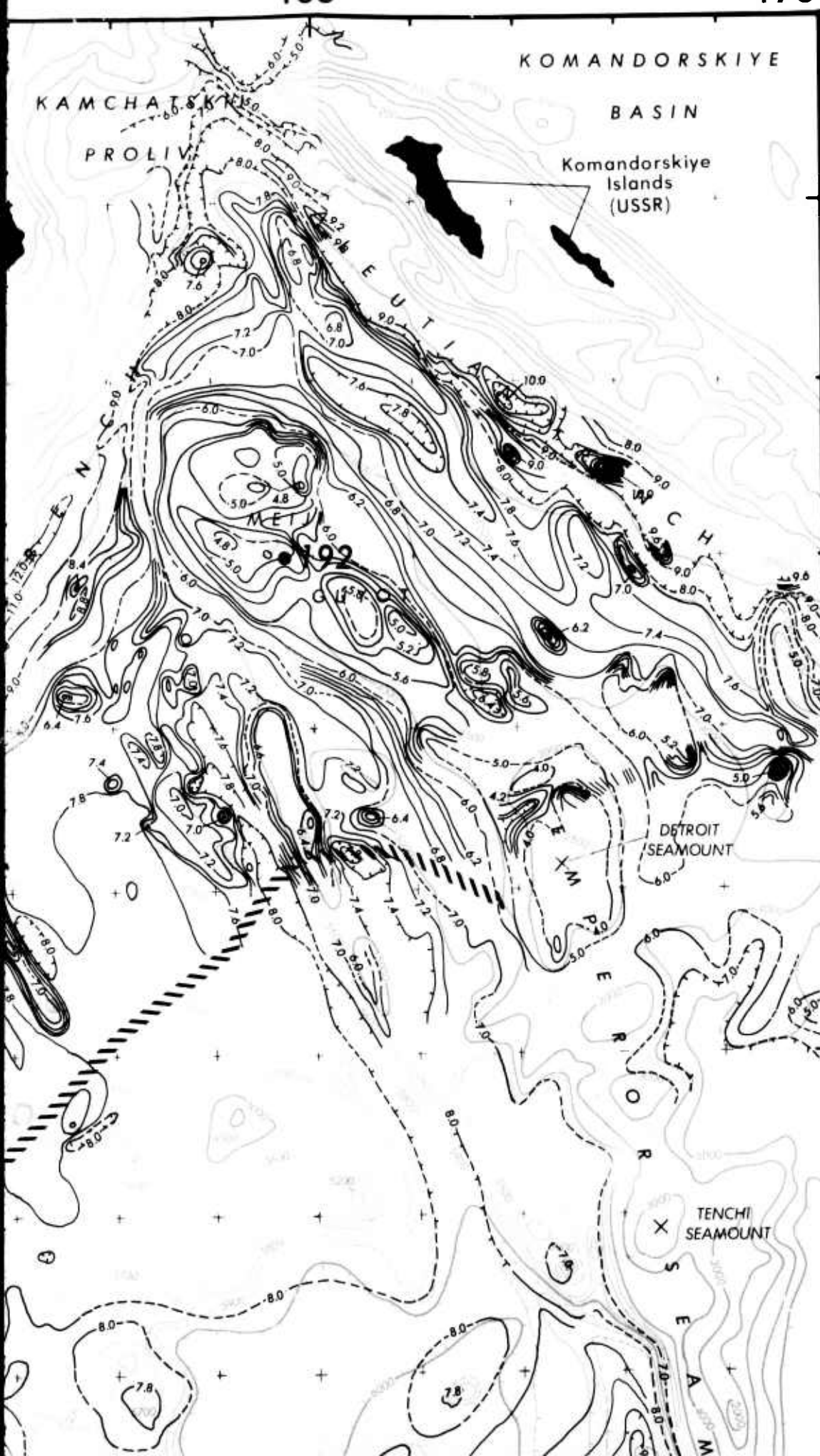
165°

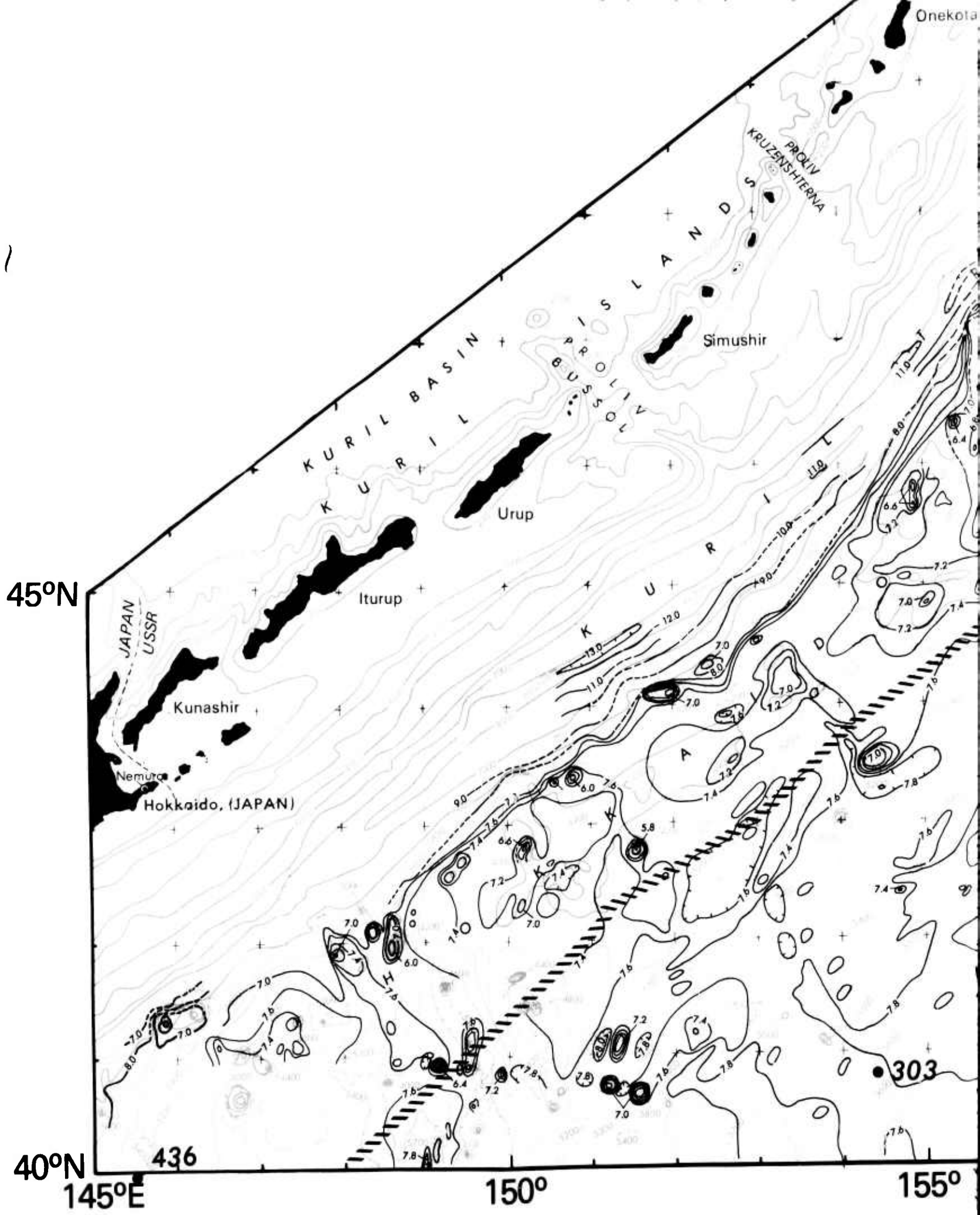
170°E

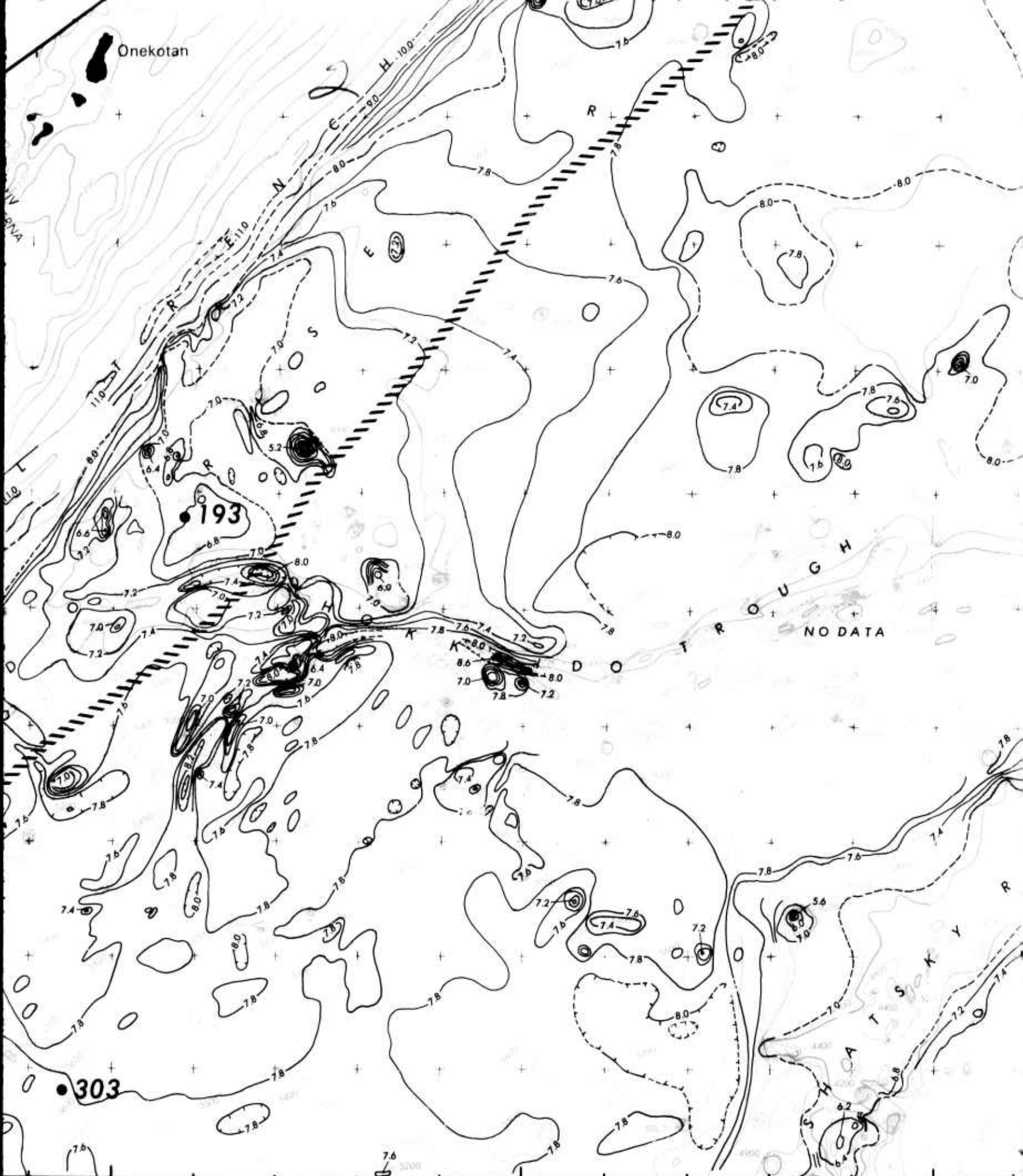
55°N

50°

3



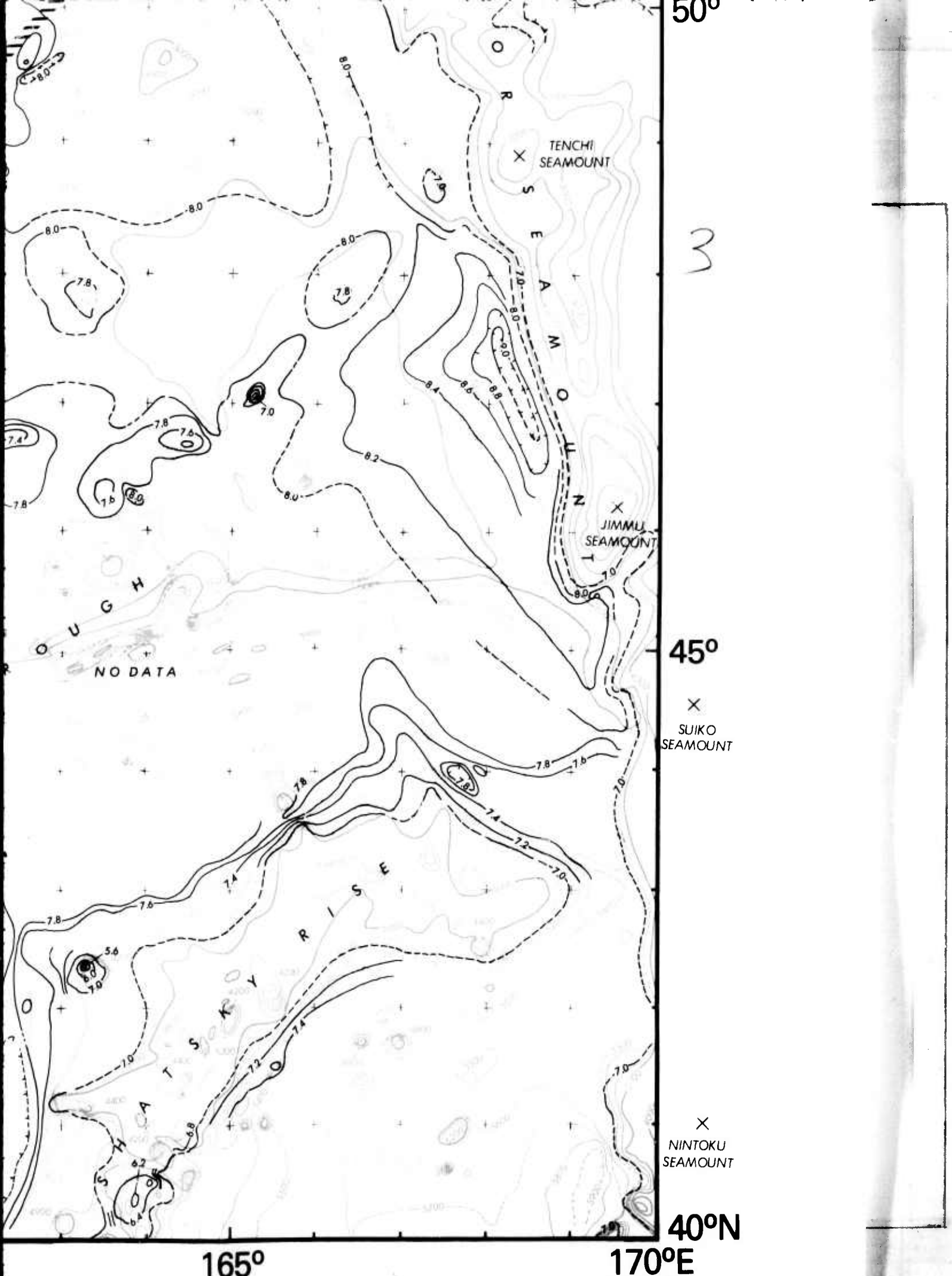




155°

160°

165°



6 MAP VII

**SEDIMENT ISOPACH,  
STRUCTURE CONTOUR MAP  
OF THE ACOUSTIC BASEMENT,  
AND  
ROUGHNESS OF ACOUSTIC BASEMENT  
OF THE  
NORTHWEST PACIFIC OCEAN**

Compiled by

**James A. Green**

Naval Ocean Research and Development Activity  
NSTL Station, Ms.

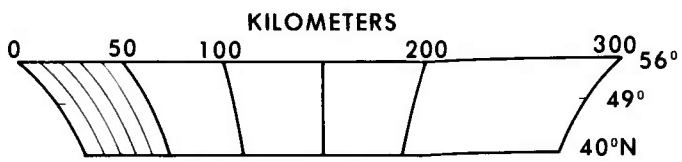
1980

Structure Contour Map of the Acoustic Basement is screened.

See maps of individual subjects for legends.

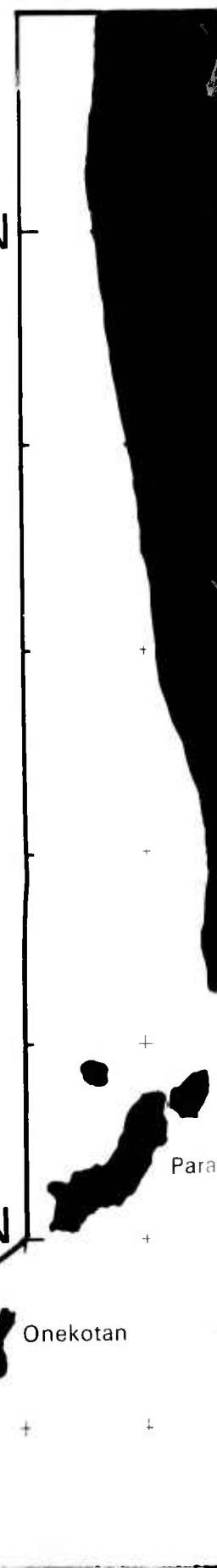
STANDARD MERCATOR PROJECTION

Scale at 49°N is 1: 3,000,000



155°E

55°N



Onekotan  
KRUZENSH  
PROVIN

5°E

160°

165°



165°

170°E

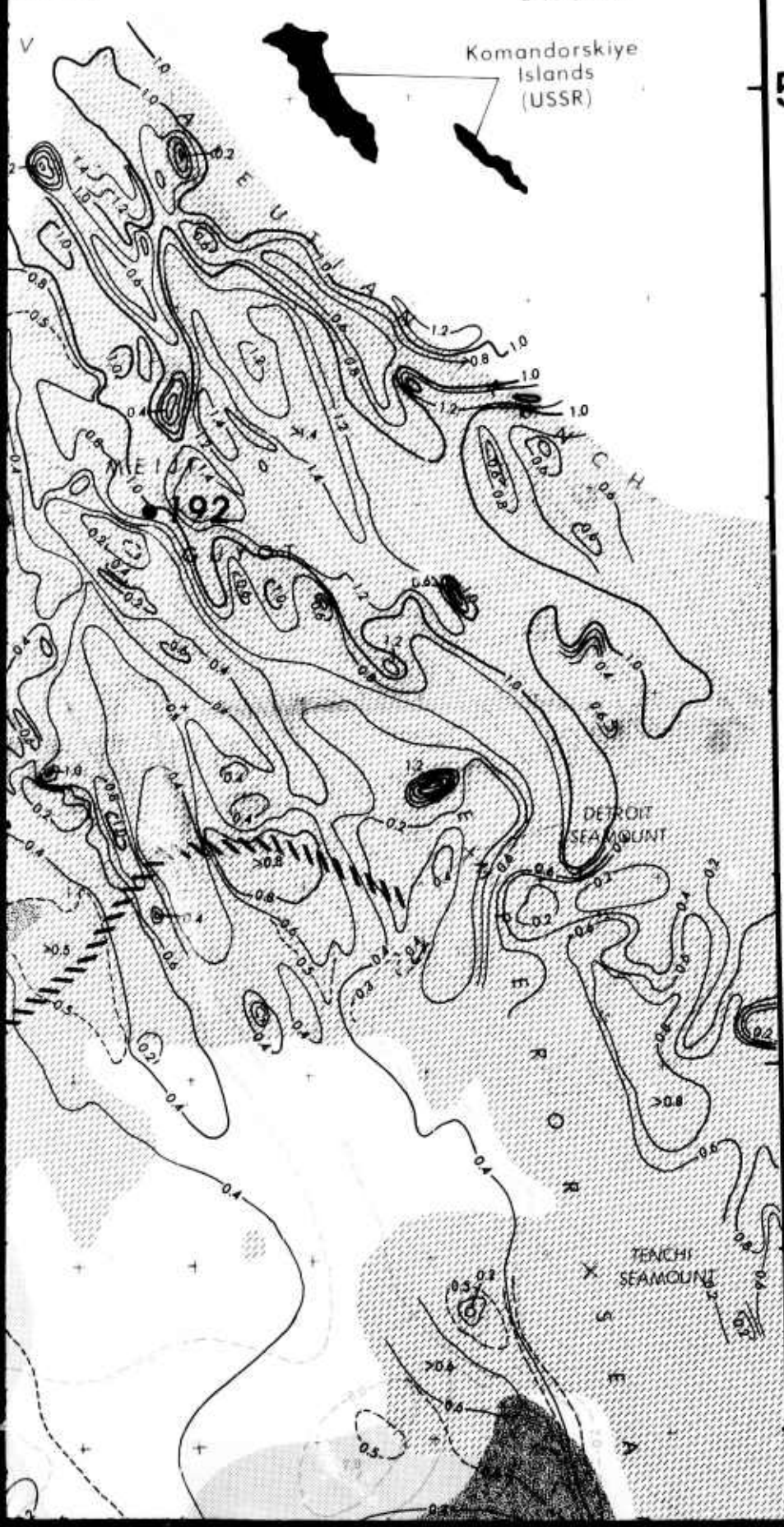
KOMANDORSKIYE

BASIN

Komandorskiye  
Islands  
(USSR)

55°N

50°



3

